9950-334
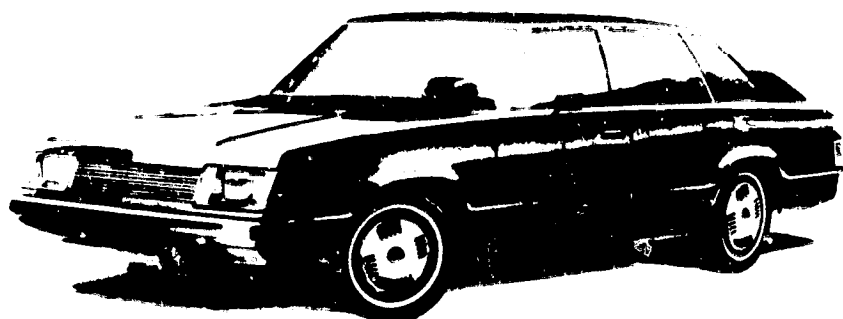
NEAR-TERM HYBRID VEHICLE PROGRAM

FINAL REPORT — PHASE I

Appendix C - Preliminary Design Data Package

Contract No. 955190

Submitted to

Jet Propulsion Laboratory
California Institute of Technology
4800 Oak Grove Drive
Pasadena, California 91103

Submitted by

General Electric Company
Corporate Research and Development
Schenectady, New York 12301

October 8, 1979

GENERAL 🔵 ELECTRIC

SRD-79-134/6

NEAR-TERM HYBRID VEHICLE PROGRAM

FINAL REPORT — PHASE I

Appendix C · Preliminary Design Data Package

Contract No. 955190

Submitted to

Jet Propulsion Laboratory
California Institute of Technology
4800 Oak Grove Drive
Pasadena, California 91103

Submitted by

General Electric Company
Corporate Research and Development
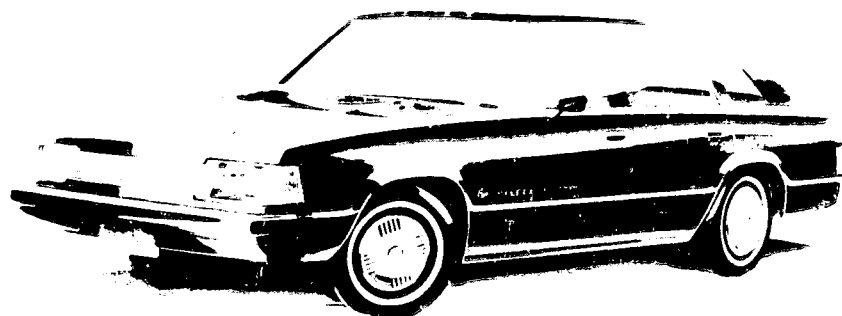Schenectady, New York 12301

October 8, 1979

GENERAL ⊛ ELECTRIC

FOREWORD

The Electric and Hybrid Vehicle (EHV) Program was established in DOE in response to the Electric and Hybrid Vehicle Research, Development, and Demonstration Act of 1976. Responsibility for the EHV Program resides in the Office of Electric and Hybrid Vehicle System of DOE. The Near-Term Hybrid Vehicle (NTHV) Program is an element of the EHV Program. DOE has assigned procurement and management responsibility for the Near-Term Hybrid Vehicle Program to California Institute of Technology, Jet Propulsion Laboratory (JPL).

The overall objective of the DOE EHV Program is to promote the development of electric and hybrid vehicle technologies and to demonstrate the validity of these systems as transportation options which are less dependent on petroleum resources.

As part of the NTHV Program, General Electric and its subcontractors have completed studies leading to the Preliminary Design of a hybrid passenger vehicle which is projected to have the maximum potential for reducing petroleum consumption in the near-term (commencing in 1985). This work has been done under JPL Contract 955190, Modification 3, of the Near-Term Hybrid Vehicle Program.

This volume is part of Deliverable Item 7 Final Report, of the Phase I studies. In accordance with Data Requirement Description 7 of the Contract, the following documents are submitted as appendices:

APPENDIX A is the Mission Analysis and Performance Specification Studies Report that constitutes Deliverable Item 7 and reports on the work of Task 1.

APPENDIX B is a three-volume set that constitutes Deliverable Item 2 and reports on the work of Task 2. The three volumes are:

- Volume I   -- Design Trade-Off Studies Report
- Volume II -- Supplement to Design Trade-Off Studies Report, Volume I
- Volume III -- Computer Program Listings

APPENDIX C is the Preliminary Design Data Package that constitutes Deliverable Item 3 and reports on the work of Task 3.

APPENDIX D is the Sensitivity Analysis Report that constitutes Deliverable Item 8 and reports on Task 4.

The three classifications - Appendix, Deliverable Item, and Task numbers - may be used interchangeably in these documents. The interrelationship is tabulated below:

PRECEDING PAGE BLANK NOT FILMED

Appendix	Deliverable Item	Task	Title
A	1	1	Mission Analysis and Performance Specification Studies Report
B	2	2	Vol. 1 - Design Trade-Off Studies Report
			Vol. II - Supplement to Design Trade-Off Studies Report
			Vol. III - Computer Program Listing
C	3	3	Preliminary Design Data Package
D	8	4	Sensitivity Analysis Report

This is Appendix C, Preliminary Design Data Package. It presents the design methodology, design decision rationale, vehicle preliminary design summary, and advanced technology developments.

TABLE OF CONTENTS

TABLE OF CONTENTS (Cont'd)

TABLE OF CONTENTS (Cont'd)

LIST OF ILLUSTRATIONS

LIST OF ILLUSTRATIONS (Cont'd)

LIST OF ILLUSTRATIONS (Cont'd)

GENERAL ⚡ ELECTRIC

LIST OF ILLUSTRATIONS (Cont'd)

LIST OF ILLUSTRATIONS (Cont'd)

LIST OF TABLES

Section 1

INTRODUCTION AND SUMMARY

Section 1

INTRODUCTION AND SUMMARY

1.1 INTRODUCTION

This is Appendix C, Preliminary Design Data Package (Deliverable Item 3). It reports on Task 3 and is part of Deliverable Item 7, Final Report, which is the summary report of a series which documents the results of Phase I of the Near-Term Hybrid Vehicle Program. This phase of the program was a study leading to the preliminary design of a hybrid vehicle utilizing two energy sources (electricity and gasoline/diesel fuel) to minimize petroleum usage on a fleet basis.

The program is sponsored by the U.S. Department of Energy (DOE) and the California Institute of Technology, Jet Propulsion Laboratory (JPL). Responsibility for this program at DOE resides in the Office of Electric and Hybrid Vehicle Systems. Work on this Phase I portion of the program was done by General Electric Corporate Research and Development and its subcontractors under JPL contract 955190.

This Appendix C presents the design methodology, the design decision rationale, the vehicle preliminary design summary, and the advanced technology developments. Included in this report are five appendices which present the detailed vehicle design; the vehicle ride and handling and front structural crashworthiness analysis; the microcomputer control of the propulsion system; the design study of the battery switching circuit, the field chopper, and the battery charger; and the recent HYVEC program refinements and computer results.

1.2 OBJECTIVES OF THE PRELIMINARY DESIGN (TASK 3)

The objective of the Preliminary Design (Task 3) is to develop a preliminary design of the hybrid vehicle concept identified as most promising from the Design Trade-off Studies (Task 2). This design will define vehicle external and internal dimensions, all power train components, material selected for body and chassis, weight breakdown by major subassemblies, projected production and life cycle costs, and all components required to satisfy the vehicle specifications produced in the conduct of Task 1 and reported in General Electric Report No. SRD-79-010. The report contains performance projections for individual power train components as well as for the total vehicle, measures of energy consumptions, and identification of technology development required to achieve the design.

This task has been broken down into the following areas:

- Simulation Refinement and Update
- Power Train Preliminary Design
- Vehicle Preliminary Design
- Advanced Technology Development Identification

Much of this work consisted of updating (where required) information already available from the Design Trade-Off Studies. However, significant new work was carried out in the areas of the power train and vehicle design.

The basic outline of the vehicle design concept was already known from the results of Task 2. The objective of Task 3 was to carry out additional and more detailed packaging and design studies of this design concept so as to arrive at power train and vehicle layouts which could be used to start the detailed design in Phase II. Results also include updated calculations of vehicle weight, performance, energy use, emissions, and initial and operating cost.

1.3 REPORT OUTLINE

This report is written to address all of the topics listed in Data Requirement Description, Deliverable Item 3, Preliminary Design Data Package, in the contract. Hence the report includes the following sections:

- Design Methodology
- Design Decision Rationale
- Vehicle Preliminary Design Summary
- Advanced Technology Developments

Technical details of the various studies undertaken in Task 3 are included in a number of Appendices dealing with the following areas:

- Vehicle Subsystem Preliminary Design
- System Control and Microcomputer Design
- Battery Switching, Field Chopper, and Battery Charger Circuits
- HYVEC Refinements and Simulation updates
- Use of a Continuously Variable Transmission in the Power Train

Section 2

DESIGN METHODOLOGY

Section 2

DESIGN METHODOLOGY

The progression of activity in the Near-Term Hybrid Vehicle Study (Phase I) is illustrated in Figure 2-1. As indicated in the figure, Task 1 (Mission Analysis and Performance Specifications) and Task 2 (Design Trade-Off Studies) were conducted such that they yielded the inputs needed to perform the preliminary design of the Near-Term Hybrid Vehicle (Task 3). The preliminary design activities were based almost completely on the work done in Task 1 and Task 2 with the goal being the detailed preliminary design of the hybrid vehicle. The specifications and characteristics developed are described in Section 9, Guidelines for the Preliminary Design Task and Vehicle Performance and Energy-Use Characteristics, of the Design Trade-Off Studies Report.[1] The primary activities undertaken in Task 3 were the following:

- Full-scale layouts of the power train package, and front suspension system

- Vehicle styling

- Vehicle handling and crashworthiness simulations.

- System microprocessor software study

- Battery switching, field chopper, and battery charger circuit design study

- Refinement of HYVEC simulation calculations

The results of the Task 3 activities are summarized in the appendices. In addition to the cited studies, further discussions were held with potential suppliers of the electric motor, heat engine, and batteries to ascertain that components having the characteristics being used in the Preliminary Design Task would be available for use in the Near-Term Hybrid Vehicle.

Task 1
Mission Analysis
and Performance
Specifications

Power Requirements

Electric Range

Driving Cycles/Patterns

Reference ICE Vehicle
1979 Chevrolet Malibu

Task 2
Design Trade-Off
Studies

Powertrain Configuration

Packaging Layout

Powertrain Component Sizes

Control Strategy

Task 3
Preliminary
Design

Full-Scale Vehicle Layouts

Vehicle Styling

Powertrain Component Identification

Microprocessor Software

Energy-Use Measures

→ Phase II Proposal

Figure 2-1. Hybrid Vehicle Design Methodology Flowchart

Section 3

DESIGN DECISION RATIONALE

Section 3

DESIGN DECISION RATIONALE

The rationale for most of the decisions made concerning the hybrid vehicle design is discussed in references 1 and 2. Those considerations are well-documented in the cited references and will not be repeated here. However, there are several design decisions which were either not discussed previously or were left unresolved (two or more possibilities indicated) in the previous reports. The rationale for the choices which have been made in the Preliminary Design Task are discussed in the paragraphs that follow.

As discussed in the Task 1 report,[2] the 1979 Chevrolet Malibu was selected as the Reference ICE Vehicle. Subsequent work has indicated that the Malibu would also be a good choice for a base vehicle from which to build/fabricate the Near-Term Hybrid Vehicle. Hence all the preliminary design layout work has been done using the 1979 Malibu as the starting point for the hybrid conversion. As will be discussed in detail in Section 4 and Appendix I, the Malibu has been extensively redesigned with only the interior, window and door mechanisms, front and side glass, and roof metal and door outlines being used essentially unchanged from the Stock Malibu. Hence, the interior dimensions of the hybrid vehicle will be the same as the Malibu, resulting in good comfort for five adult passengers. The exterior of the Malibu will be redesigned for improved aerodynamics (see Figure 4-2), and the power train and front and rear running gear will be replaced (see Figure 4-1). The conversion approach selected significantly reduces the cost of building/fabricating the hybrid vehicle with a minimal sacrifice in vehicle attractiveness and utility. Experience with the GE-100 Centennial and the DOE/GE Near-Term Electric Vehicle, which were essentially from-the-ground-up designs, has indicated that those parts of the vehicle being used from the stock malibu (ex. interior, window and door mechanisms, etc.) were particularly expensive and troublesome in the building of the new vehicles. Hence, the approach taken in the Near-Term Hybrid Vehicle Program is to redesign the power/train, running gear, load-carrying structural members and exterior styling of the vehicle and utilize the interior and windows/doors of the Stock Malibu. The introduction of GM front-wheel drive from downsized luxury cars, such as the Buick Riviera and Olds Toronado, has provided some of the mechanical components required in the hybrid vehicle (see table in Appendix I.2.2).

At the completion of the Design Trade-Off Studies,[1] options were still being considered for several of the hybrid power train components. These components and the options were:

- **Heat Engine** -- fuel-injected, naturally aspirated gasoline (VW 1.6 l) or a turbocharged diesel (VW 1.6 l)

- <u>Transmission</u> – multi-speed, automatically shifted gear-box or a steel-belt, traction drive, continuously vari-able transmission (CVT)

- <u>Torque Combination Unit</u> – single-shaft or power differential

- <u>Batteries</u> – 700 lb lead-acid or 500 lb Ni-Zn

In all cases it was decided to proceed in the Preliminary Design Task with the more readily available and more highly developed component and to include the alternative option in the advanced technology development category. Hence, the detailed vehicle lay-outs were prepared using a fuel-injected gasoline engine (1.6 l); a multi-speed, automatically shifted gearbox; a single-shaft (fixed speed ratios between input/output shafts) torque combina-tion unit; and 700 lb of ISOA lead-acid batteries. Further dis-cussions of the use of a turbocharged diesel engine, the steel-belt CVT, and Ni-Zn batteries in the hybrid/electric power train are included in Section 5, Advanced Technology Developments. The power differential torque combination was dropped from further consideration, because of the complexity of the control of such a unit and the belief that development of the single-shaft unit would permit adequate smoothness in power blending from the heat engine and electric motor. The advantages of the diesel engine, CVT, and Ni-Zn batteries are significant, and they would have been included in the design except for the following disadvantages for each of them: (1) diesel engine – NO_x and unregulated emis-sions (smoke and odor) and uncertainty regarding cold start in on/off operating mode, (2) steel-belt CVT – uncertainty regarding the availability of a unit with desired overall speed ratio and torque capability by mid-1981, (3) Ni-Zn batteries – uncertainty in performance, cycle life, and cost of cell available by 1981. The hybrid vehicle layout is such t'at the advanced-technology components could be substituted for their near-term counterparts if development progress on the advanced components indicates that is advisable. For example, the voltage and energy and power den-sities of the Ni-Zn batteries would be such that they could replace the lead-acid batteries with little or no change in the rest of the electric drive system.

Section 4

VEHICLE PRELIMINARY DESIGN SUMMARY

Section 4

VEHICLE PRELIMINARY DESIGN SUMMARY

4.1 INTRODUCTION

In this section, the preliminary design of the five-passenger hybrid/electric vehicle is summarized. Information/data for this section is taken from the Design Trade-Off Studies Report,[1] the Sensitivity Analysis Report,[3] and the appendices to this report. The material presented in the appendices was developed during the Preliminary Design Task and represents the status of the vehicle and component designs and HYVEC simulations from which the Phase II design effort would start.

4.2 GENERAL LAYOUT AND STYLING

The following are the general characteristics of the vehicle layout and chassis:

- Curb weight

    - 1786 kg (3930 lb)

- Body Style
    - Four-door hatchback
    - Drag coefficient - .40
    - Frontal area - 2.0m^2 (21.5 ft^2)
- Chassis/Power Train Arrangement
    - Front wheel drive
    - Complete power train, including the batteries, in front of firewall
    - Fuel tank under rear seat
- Baseline ICE Vehicle
    - 1979 Chevrolet Malibu

Full-scale drawings of the hybrid vehicle have been prepared and 1/5 scale reductions are included with this data package. The starting point in preparing the drawings presented was the 1979 Malibu. No changes were made in the seating package. A three-dimensional cutaway of the hybrid vehicle showing the placement of the power train is given in Figure 4-1. Note that the complete hybrid power train is located in front of the firewall with no intrusion into the passenger compartment. An artist's rendering of the vehicle styling is shown in Figure 4-2. A four-door hatch-back body type was selected because it maximizes the all-purpose character of the five-passenger vehicle.

PROPULSION BATTERY

HEATER

HEAT ENGINE
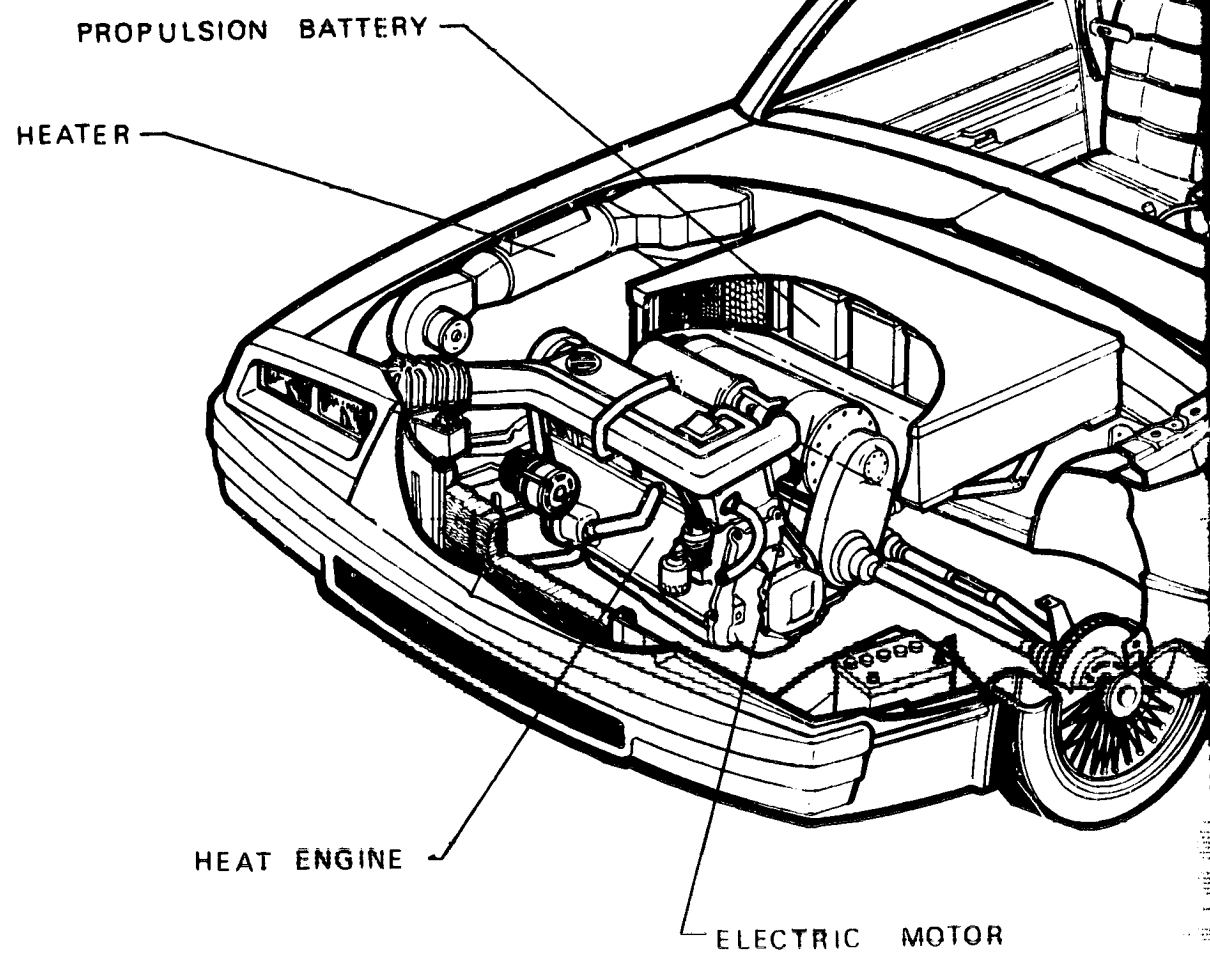
ELECTRIC MOTOR

Figure 4-1. Hybrid Vehicle, Thre
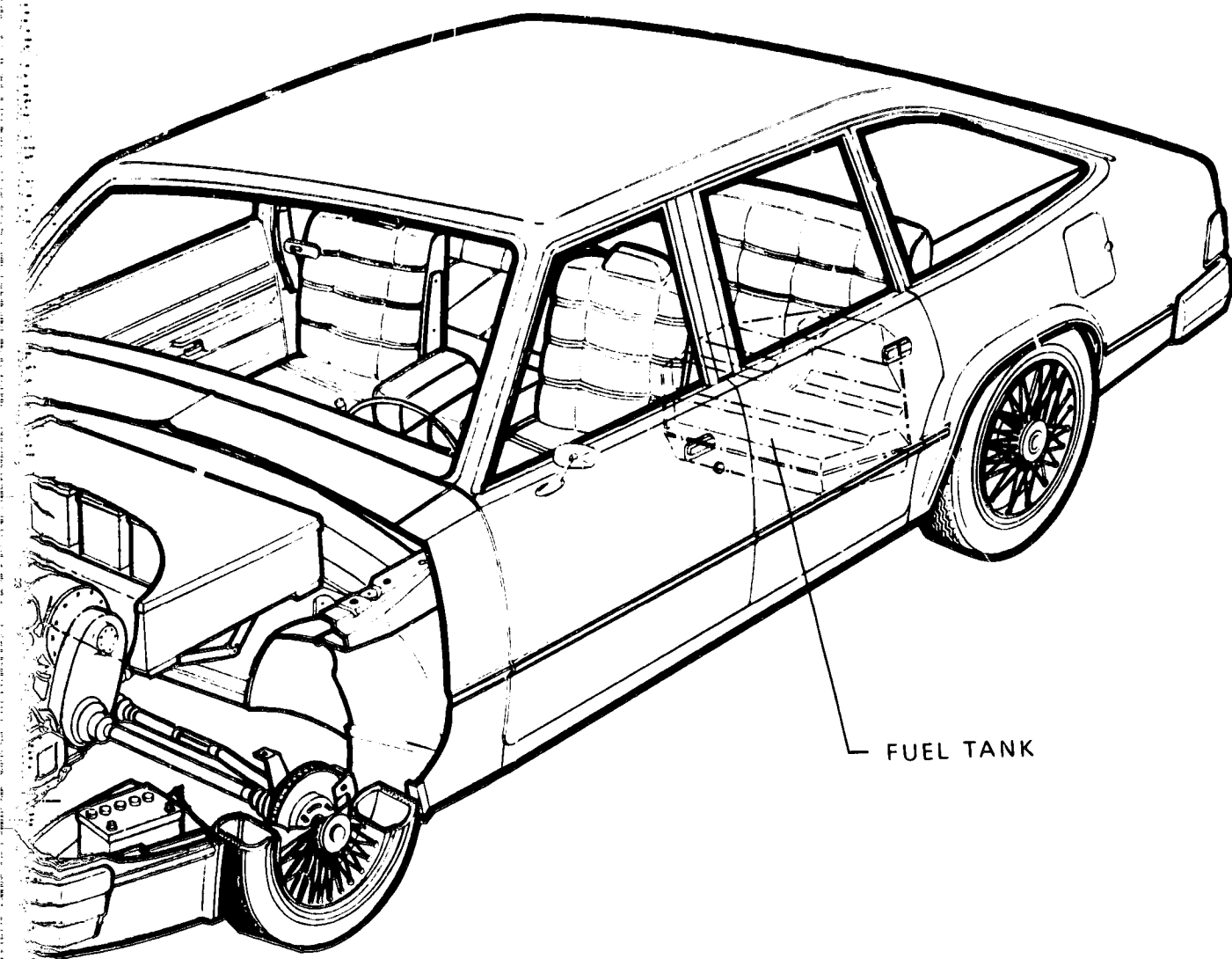
FUEL TANK

CTRIC MOTOR

Hybrid Vehicle, Three-Dimensional Cutaway
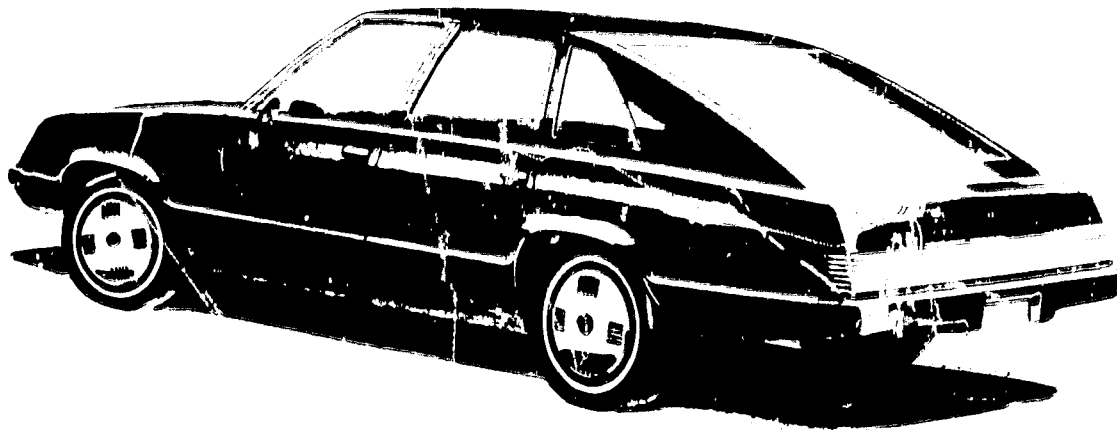
Left Rear Quarter View
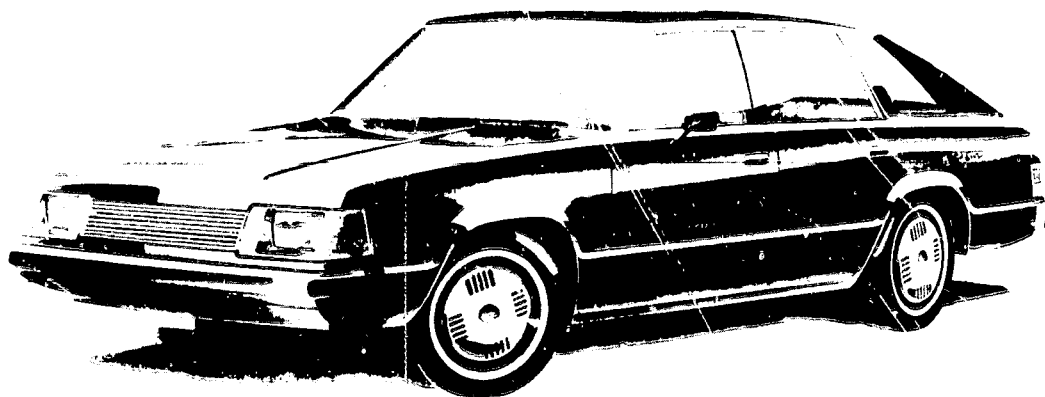
Left Front Quarter View

Figure 4-2.   Artist's Rendering of the Hybrid Vehicle

4-5

GENERAL ELECTRIC

4.3 POWER TRAIN SPECIFICATIONS AND WEIGHT BREAKDOWN

4.3.1 POWER TRAIN SPECIFICATIONS

Full-scale drawings of the hybrid power train have been pre-
pared and 1/5 scale reductions are included with this data pack-
age. A one-fifth scale drawing of the power train is shown in
Figure 4-3 for purposes of   scussion. As indicated in the figure,
the hybrid vehicle uses f .it-wheel drive with both the heat en-
gine and electric motor mounted in a transverse orientation above
the transaxle. This is clearly a parallel hybrid configuration.
Clutches are required as shown to permit decoupling the drive
system from the vehicle drive shaft and operating the heat engine
and electric motor in combination and separately. Drawings of
the components used in the transmission, clutch, and controls are
presented in Figures 4-4a, 4-4b, and 4-4c.

Specifications for each of the power train components are
discussed in the following sections.

4.3.1.1 Heat Engine

The heat engine used in the preliminary design of the hybrid
vehicle was the Volkswagen fuel-injected 4-cylinder, 1.6 liter
gasoline engine. This engine, equipped with the Bosch K-Jetronic
fuel injection system, is used in the VW Rabbit and Audi 4000. The
K-Jetronic system is often referred to as the CIS (Continuous
Injection System) and utilizes a mechanical airflow sensor and
distributing slots to control fuel flow to the engine (see Ref-
erence 4 for a description of the CIS system). The VW 1.6 liter
engine can also be equipped with the Bosch L-Jetronic system which
utilizes solenoid-operated injection valves associated with each
cylinder. The amount and timing of the fuel injection is controlled
by a microprocessor which requires inputs from measurements of
airflow, RPM, engine temperature, etc. (see Reference 5 for a
description of the L-Jetronic system). The L-Jetronic system is
a true electronically controlled fuel injection system and for
that reason is more compatible with the overall implementation of
the hybrid vehicle control strategy using a system microprocessor
as discussed in Appendix II. Volkswagen does not currently market
cars using the L-Jetronic fuel injection system. However, dis-
cussions with VW indicated they are currently fleet testing cars
using the L-Jetronic system and have done much laboratory testing
of engines using that system. Hence it is appropriate to use the
more advanced L-Jetronic system in the hybrid vehicle program.

As discussed in Reference 1, considerable fuel consumption and
emission data were available to characterize the electronically
fuel-injected (EFI), 1.6 liter engine. Those data were used in
the HYVEC simulation studies reported in Reference 1. The EFI
1.6 liter engine is rated at 80 hp at 5500 rpm with a maximum
torque of 84 ft-lb at 3200 rpm. Hence, the engine is sized al-
most exactly to meet the hybrid vehicle power requirement and is
an ideal choice for the hybrid application.

RADIATOR

1.6 LITER V.W. ENGINE

AIR CONDITIONING CONDENSER

PROPULS

MOTO LOW

Figure 4-3. Hybrid P

PROPULSION BATTERY

HYDRAULIC
BRAKE BOOSTER

MOTOR COOLING
BLOWER

ELECTRIC MOTOR

HYDRAULIC POWER
RACK & PINION
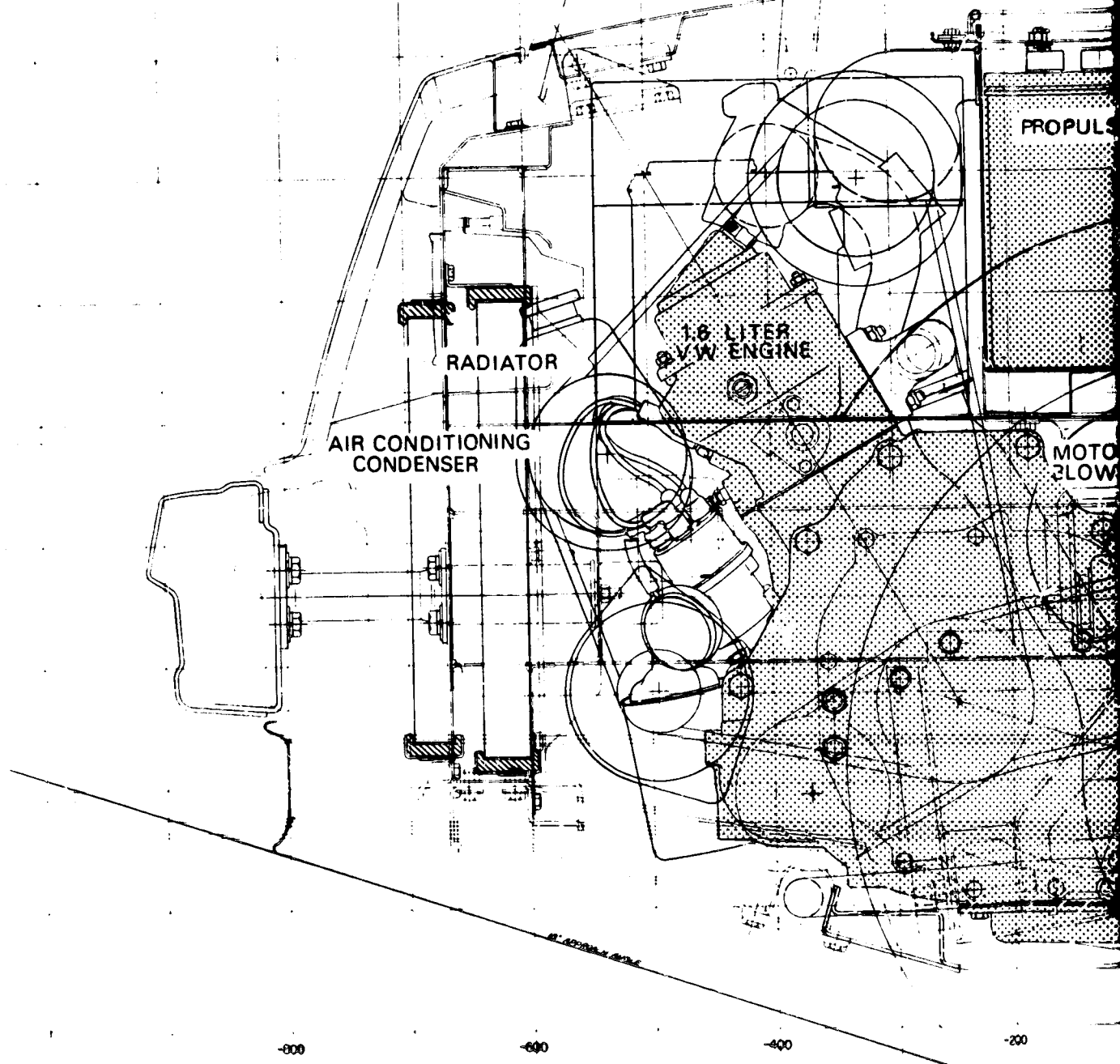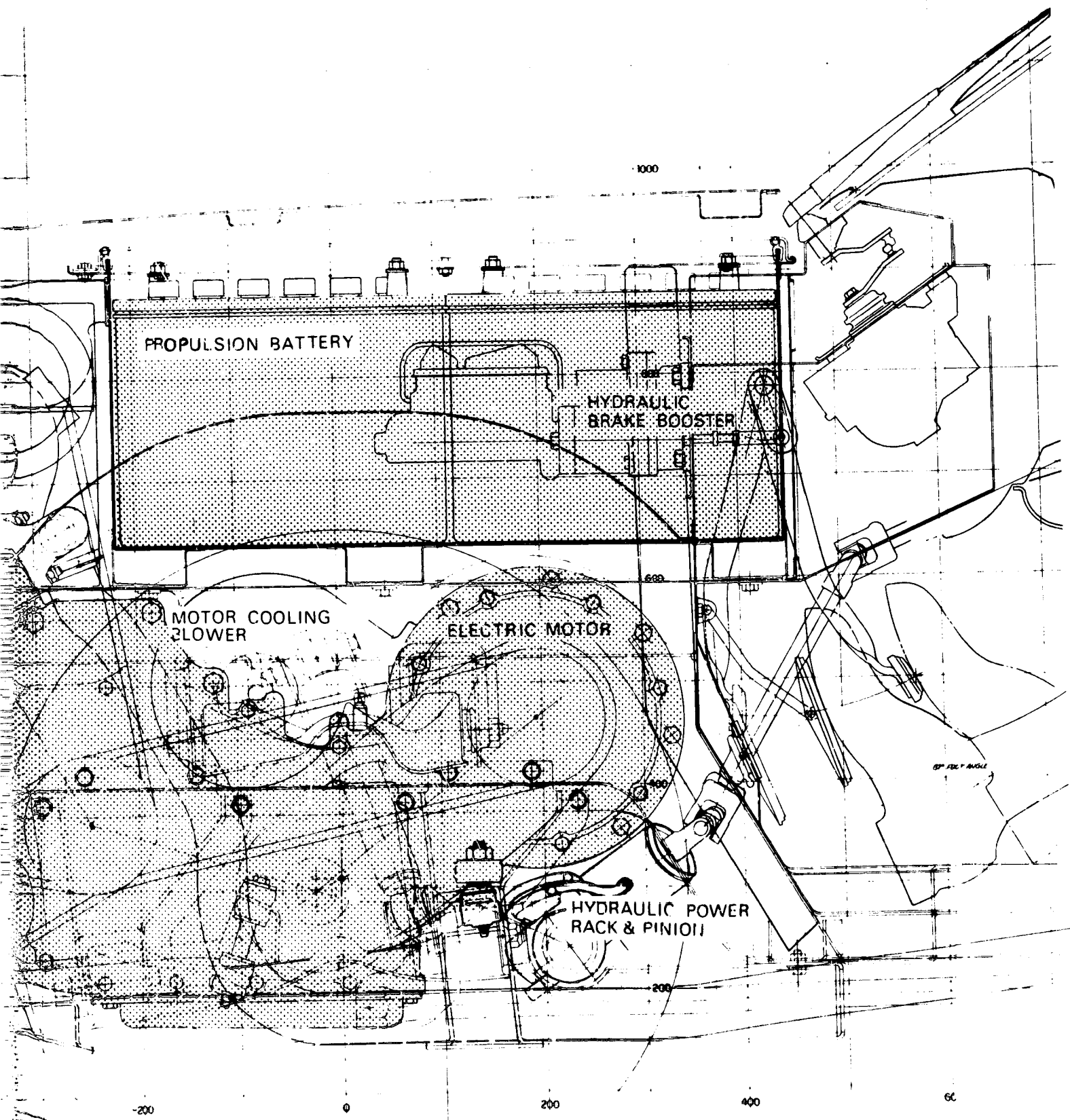
4-3. Hybrid Power Train
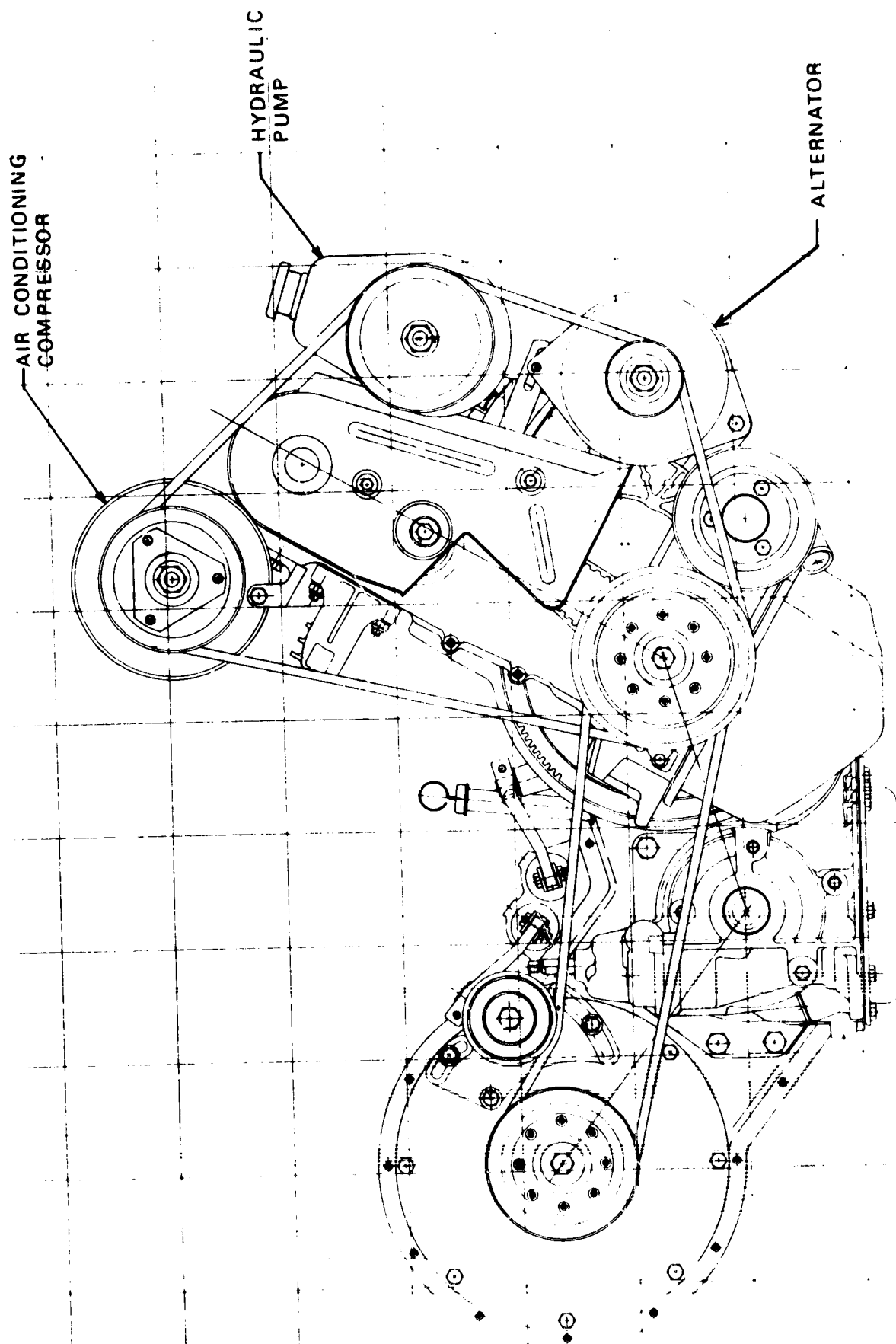
Figure 4-4a. Transmission, Clutch, and Controls, Right Side View

HYDRAULIC PUMP

ALTERNATOR

AIR CONDITIONING COMPRESSOR

PRECEDING PAGE BLANK NOT FILMED
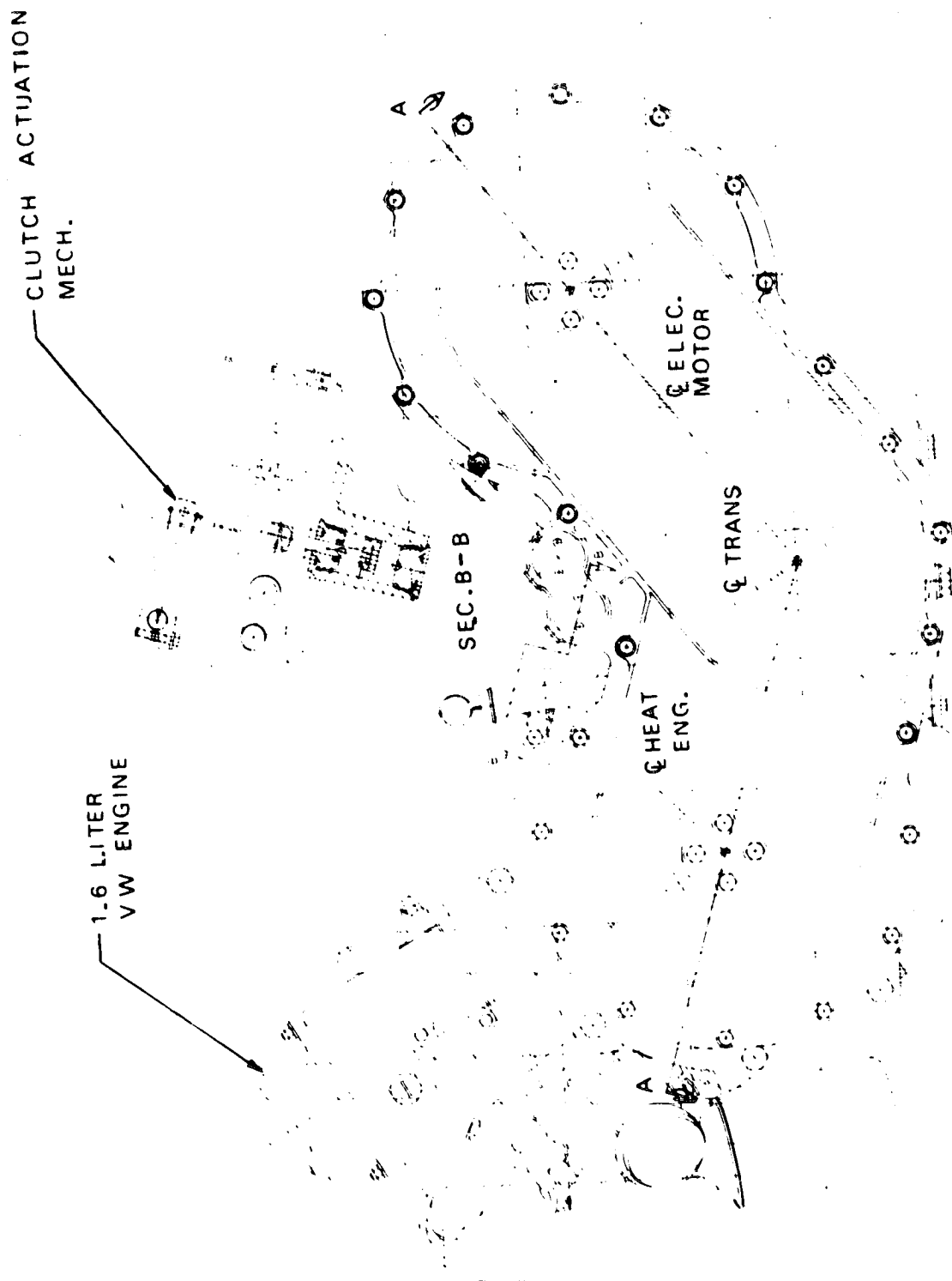
Figure 4-4b. Transmission, Clutch, and Controls, Left Side View

O/R CLUTCH

AUTOMATIC GEARBOX
3 SPEED

MOTOR PRIMARY
CLUTCH

MOTOR DRIVE CHAIN

O/R CLUTCH

ENGINE DRIVE CHAIN

ENGINE PRIMARY CLUTCH
SHOWN OVER-CENTER
MECH.)
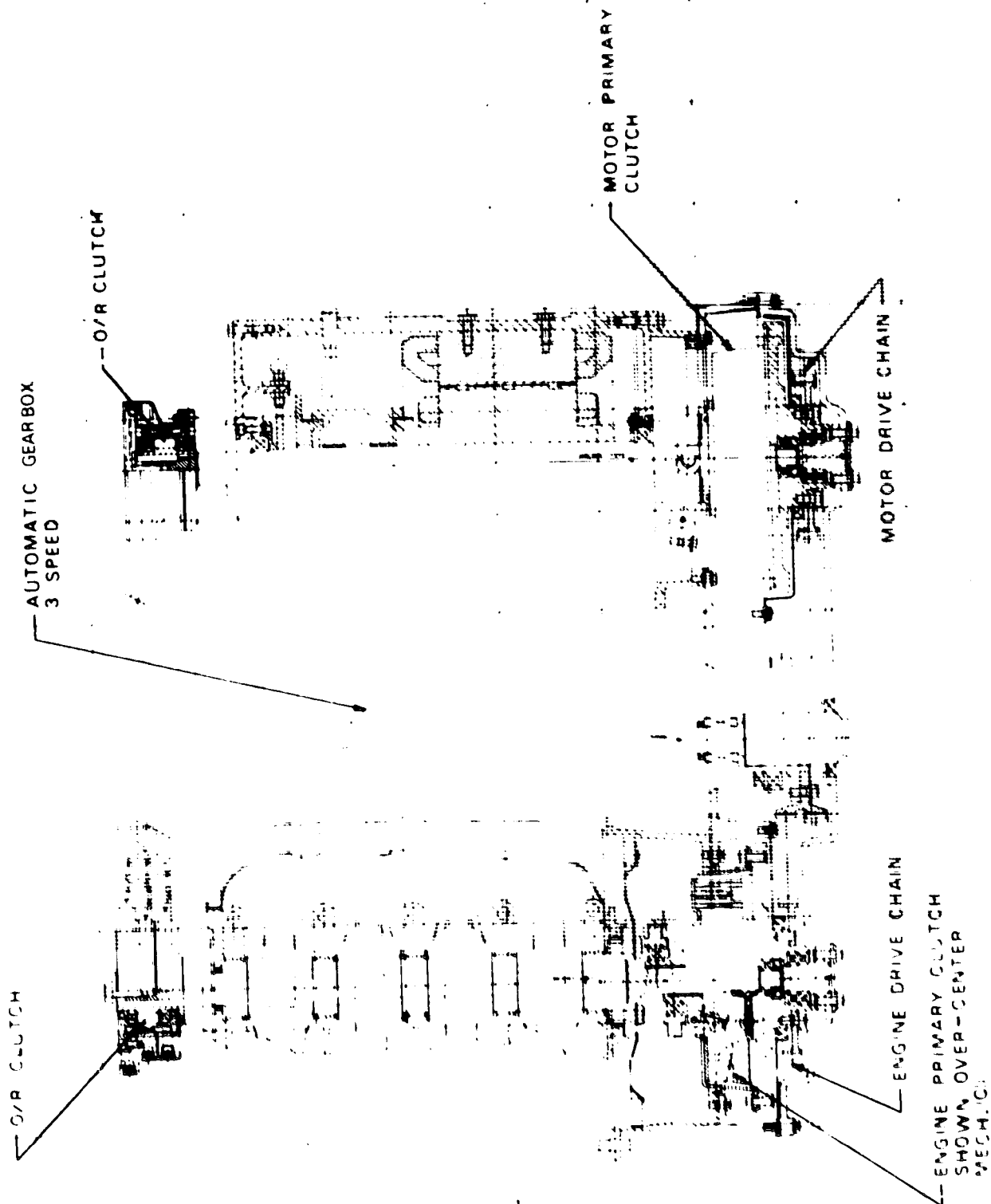
Figure 4-4c. Transmission, Clutch, and Controls, Section A-A

4-11

4.3.1.2 Electric Drive System

The electric drive system in the hybrid vehicle utilizes a dc separately excited motor with battery switching and field weakening to control motor speed and torque. The system uses a nominal voltage of 120 V with peak currents of about 400 A except during battery switching when the currents reach 500 A for a few seconds. The electric motor has a continuous rating (1-2 hours) of 18 kW (24 hp) and a peak rating (1-2 minutes) of 32.? kW. Discussions with the GE DC Motor and Generator Department in Erie, Pennsylvania, indicate that the dc motor for the hybrid vehicle can be developed from a modest redesign of the electric motor used in the Near-Term DOE/GE electric car. The resultant motor for the hybrid vehicle would be essentially the same size (length and diameter) and weight as the one for the DOE/GE electric car, but it would be worked harder, with slightly higher currents and flux, in the hybrid application. Testing of the original design has indicated this is possible without significantly reducing the reliability and lifetime of the motor.

The dc motor is controlled using field weakening and battery switching. The battery is arranged in two parallel banks so that it can be operated in parallel yielding 60 V or in series yielding 120 V. The base speed of the motor is 1100 rpm at 60 V and 2200 rpm at 120 V. A resistor is used when starting the motor and during short periods of battery switching. The battery switching circuit is discussed in Appendix III. Field weakening is accomplished using a transistorized field chopper in essentially the same way as in the DOE/GE electric car.

The motor rating may be summarized as follows:

Design No. 2366-2913

Frame	OD 12 1/4 inches
Name Plate Rating	24 hp, Peak Power 44 hp (1 minute)
Weight	220 lb
Rated Voltage	120 V
Rated Current	190 A
Rated Field	8.2 A
Rated Flux	0.84 Megalines
Base Speed	2200 rpm
Maximum Speed	6000 rpm

4.3.1.3 Batteries

The hybrid vehicle is designed to utilize 770 lb of Improved State-of-the-Art (ISOA) lead-acid batteries. The batteries are positioned under the hood in front of the firewall

as shown in Figure 4-3. The battery container has dimensions of 36" length, 26" width, and 13" height. The preferred battery module is 12 V, 105 AH/cell at the C/3 rate. The 770 lb battery pack stores 12.5 kWh at the C/3 rate for an energy density of 16.4 Wh/lb. The power characteristics of the battery are based on the voltage-current relationship for a 15-second pulse at 50% state-of-discharge during a C/3 rate discharge. The power characteristics specifications are the following:

Pulse Current, A	Volts/Cell	Volts/Module
210	1.82	10.9
315	1.71	10.3
420	1.61	9.6

For the maximum current pulse of 420 A, the corresponding power density is about 53 W/lb with a voltage droop of 20%. The lead-acid batteries used in the preliminary design of the hybrid vehicle have energy density and power characteristics comparable to those of the batteries developed by Globe-Union for the DOE/GE electric car. The cell capacity (AH) for the hybrid vehicle battery is considerably smaller, however, which means that new batteries must be designed and fabricated especially for the hybrid application.

4.3.1.4 Transmission and Axle Differential

For front-wheel drive vehicles, the transmission and axle differential are usually combined in a single unit termed the transaxle. Nevertheless, the speed change characteristics of the transmission and axle differential can be described separately. The transmission is an automatically shifted gearbox taken from a 3- or 4-speed automatic transmission. In the Design Trade-Off Studies,[1] a 4-speed transmission having an overall gear ratio of 3.46 was used. Such a gearbox would be part of a 4-speed, overdrive automatic transmission. Unfortunately, such a transmission in a transaxle unit is not currently being marketed by either a U.S. or a foreign auto manufacturer or supplier. It seems likely, however, that such a unit will become available in the next year or so as auto manufacturers seek to improve fuel economy. Three-speed automatic transmission gearboxes have a gear ratio of 2.5 - 2.85. HYVEC calculations have indicated that the use of smaller gear ratios (2.85 vs. 3.46) results in a 5% reduction in urban fuel economy and a 1.0 second increase in 0-100 km/hr acceleration time. Hence if an automatic transaxle gearbox with overdrive becomes available, it will be used. An axle ratio of 3.3 has been used in most of the HYVEC calculations. That value seems compatible with maximum motor and engine speeds of 6000 rpm and yields good fuel economy in both urban and highway driving.

4.3.1.5 Torque Combination

The outputs of the heat engine and the electric motor are combined using the single-shaft approach in which there are fixed ratios between the rotational speeds of the heat engine, electric motor, and vehicle drive shaft. HYVEC simulation studies have shown that the heat engine and electric motor can be operated near optimum efficiency by varying the power split in the neighborhood of 50%. This can be done using the system microprocessor and avoids the need for a power differential which would vary the shaft speed ratios as a function of desired power split between the heat engine and motor. The power differential is much more difficult to control than the single-shaft (fixed speed ratio) arrangement for torque combination.

4.3.1.6 Control Strategy and the System Microprocessor

A detailed control strategy for operating the heat engine and electric motor has been developed. The key features of the control strategy are:

- On/off engine operation

- Regenerative braking

- Electric motor idling when vehicle is at rest

- Electric drive system primary (battery state-of-discharge permitting) when vehicle speed is less than VMODE.

- Equal sharing of load between motor and engine when both are needed

- Batteries recharged by heat engine in narrow state-of-charge range ($0.7 < S < 0.8$)

- Electric motor dominant in determining shifting logic when it is operating

- Heat engine primary for highway driving

- Electric motor always used to initiate vehicle motion from rest and in low-speed maneuvers (e.g., parking)

- Vehicle operation controlled by a system microprocessor

As discussed in Appendix III, considerable work has been done to develop the microprocessor control logic (software) corresponding to the control strategy used in the HYVEC simulations. The general approach taken is to develop a system controller which receives inputs from the microprocessors governing the heat engine and electric motor and in turn sends control signals to those prime movers. Some aspects of the microprocessor hardware are discussed in Appendix III.

4.3.2 VEHICLE WEIGHT AND WEIGHT BREAKDOWN

A weight breakdown for the GE hybrid vehicle is given in Table 4-1. The weights shown in the table are based on the in-

formation given in Section 6 of Reference 1 adjusted to reflect
more refined powertrain weight inputs developed during the Pre-
liminary Design Task. A vehicle curb weight of 3928 lb is pro-
jected leading to an inertia test weight of 4228. This is 228 lb
greater than the 4000 lb used in the HYVEC calculations given in
the Design Trade-Off Study Report.[1] As discussed in Appendix V,
the hybrid vehicle simulations have been rerun using HYVEC to in-
clude the effects of the increased vehicle weight and other
changes in power train component characteristics made during the
Preliminary Design Task. The updated HYVEC results are used in
the discussions of vehicle characteristics presented in subsequent
sections.

Table 4-1

WEIGHT ANALYSIS - MALIBU BASED HYBRID

Chassis/Running gear		Weight (lb)	
Structure		806	
Bumpers		164	
Suspension		230	
Wheels and tires		254	
Brakes		128	
	Sub-Total		1582
Exterior/Interior/Control			
Seats		104	
Skins		153	
Human factor and control		484	
Air conditioner		113	
	Sub-Total		854
Power Train			
Gasoline engine (VW 1.6ℓ)		284	
Fuel system (incl. 10 gal. gasoline)		78	
Transaxle		90	
Electric motor		220	
Power electronics and controller		50	
Lead-acid batteries		770	
	Sub-Total		1492
Total curb weight			3928 lb (1785 kg)

4.4 VEHICLE PERFORMANCE

A format for presenting and discussing the performance spec-
ifications of the hybrid vehicle and how well the preliminary de-
sign meets or exceeds the minimum specifications is set forth in
Exhibit I of the RFP for the program. That format will be followed
in this and subsequent sections of this report, but for convenience
of discussion the complete list (P1 to P17) will be divided into
several parts. In this subsection, items P1 to P9 are considered.
These items deal directly with vehicle performance, operation,
and cost under normal (or routine) operating conditions and have
been studied in considerable detail in the Phase I effort. Some
of the other items in Exhibit I refer more to non-routine operation,
such as cold weather conditions, and have not been studied in as
great detail.

Vehicle performance characteristics of the preliminary de-
sign are given in Table 4-2 for items P1 through P9. In all
respects, the hybrid vehicle designed meets or exceeds the min-
imum requirements given in the RFP. This includes minimum require-
ments R1 through R6 and constraints C1 through C6. The values
given in Table 4-2 were taken from the updated HYVEC calcula-
tion given in Appendix V.

4.5 BATTERY CHARGING AND COLD/HOT WEATHER OPERATION

As discussed in Appendix IV, battery charger circuits es-
pecially tailored to the needs of the hybrid vehicle were designed.
In particular, the use of battery switching permitted efficient
battery charging from both 110 and 220 V services with the batteries
in parallel and series, respectively. Considerable attention was
given to battery charging in the DOE/GE Electric Car Program, Phase II,
and much of that work is directly applicable to the hybrid appli-
cation. For lead-acid batteries the charging voltage should be
limited to about 2.5 V/cell for routine charging in order to attain
long battery life. As shown in Figure 4-5, taken from Reference 6,
the voltage restriction limits the charging current to relatively
low values. The maximum charging current is proportional to the
cell capacity (AH) and thus would be much lower for the hybrid ve-
hicle batteries than for the electric vehicle batteries, which have
larger capacity cells. Hence, even though the hybrid vehicle bat-
tery stores less energy (ex. 12.5 kWh as compared to 18-20 kWh for
the electric vehicle), its charging time will be essentially the
same as that for the electric vehicle battery - that is, 5-7 hours
using either a constant voltage or a stepped-current charging
scheme.(6,7) Faster charging is possible, but it probably would
have an adverse effect on battery life unless careful attention
is given to heating effects. The charging voltages are 147 V in
series and 73 V in parallel. When possible, charging the batteries
in series is preferred because in that case there are no potential
problems with unequal currents in the two battery banks. However,
series charging would require a 220 V service, and that may not be
available at all locations.

Table 4-2

VEHICLE PERFORMANCE CHARACTERISTICS

P1	Minimum Nonrefueled Range		
	P1.1 FHDC (Gasoline - 10 gal. tank)	550 km [a]	
	P1.2 FUDC	120 km, [b]	400 km [a]
	P1.3 J227a(B) (all-electric operation)	80 km [a]	

P2	Cruise Speed	130 km/h

P3	Maximum Speed	
	P3.1 Maximum Speed	150 km/h
	P3.2 Length of Time Maximum Speed Can Be Maintained on Level Road	1 min

P4	Accelerations		
	P4.1 0-50 km/h (0-30 mph)	5.0 s	(6.0) [c]
	P4.2 0-90 km/h (0-56 mph)	12.6 s	(15.0) [c]
	P4.3 40-90 km/h (25-56 mph)	8.6 s	(12.0) [c]

P5	Gradability			
		Grade	Speed	Distance
	P5.1	3%	100 km/h (90) [c]	(Unlimited) [e]
	P5.2	5%	95 km/h	(Unlimited)
	P5.3	8%	80 km/h (50) [c]	(Unlimited)
	P5.4	15%	40 km/h (26) [c]	(Unlimited)
	P5.5 Maximum Grade	25%		

P6	Payload Capacity (including passengers)	535 kg

P7	Cargo Capacity	0.5 m^3

P8	Consumer Costs	
	P8.1 Consumer Purchase Price (1978 $)	$7600
	P8.2 Consumer Life Cycle Cost (1978 $)	0.11 $/km

P9	Emissions - Federal Test Procedure [d] (Gasoline Engine)	
	P9.1 Hydrocarbons (HC)	0.09 gm/km, 0.13 gm/km
	P9.2 Carbon Monoxide (CO)	0.62 gm/km, 0.79 gm/km
	P9.3 Nitrogen Oxides (NO$_x$)	0.48 gm/km, 0.57 gm/km

(a) Range at which the 10 gallon tank is empty.

(b) Range at which the battery is first recharged by the heat engine.

(c) JPL minimum specifications.

(d) The first number corresponds to first 50 km, second to 120 km.

(e) On heat engine alone.
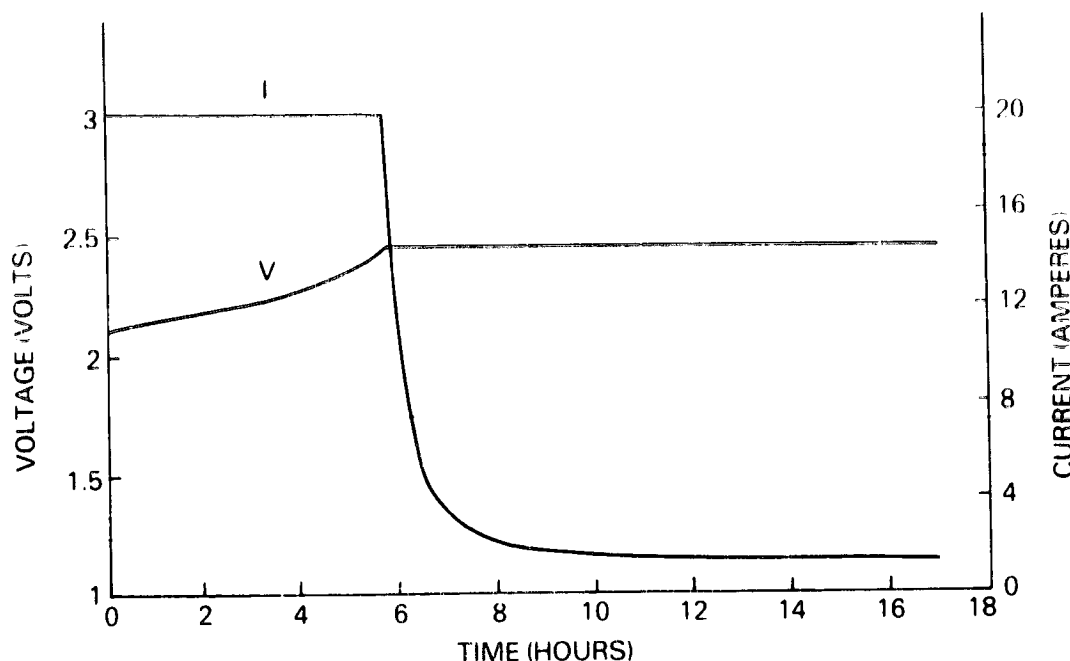
Figure 4-5.   Voltage and Current Profile During Constant-Voltage,
               20 A Current-Limited Charge of a Golf-Cart Battery
               at 80 °F (Prior Discharge - 80 % at 3 h Rate)

    Now consider the cold/hot weather operation of the hybrid ve-
hicle and in particular the effect of ambient temperature on the
batteries. It is well known that the internal resistance increases
and the AH capacity decreases (see Figure 4-6) significantly as the
temperature of the battery is decreased. These effects adversely
influence both the electric range and peak power of the hybrid
vehicle. Operation at high ambient temperatures (greater than
110°F) can adversely affect the life of both the battery and the
motor unless adequate ventilation is provided. Studies of bat-
tery insulation and warm-up at low ambient temperatures (down to
-20°F) and battery cooling at high ambient temperatures were
performed as part of the DOE/GE Near-Term Electric Vehicle Pro-
gram.(7) Those studies indicated that for cold storage at -20°F,
it takes about five days for the battery temperature to reach
the ambient value. The battery temperatures for shorter storage
periods are tabulated below.

Period of storage at -20°F (hrs)	Battery Temperature (F)
24	34
48	9
72	- 7
120	-20
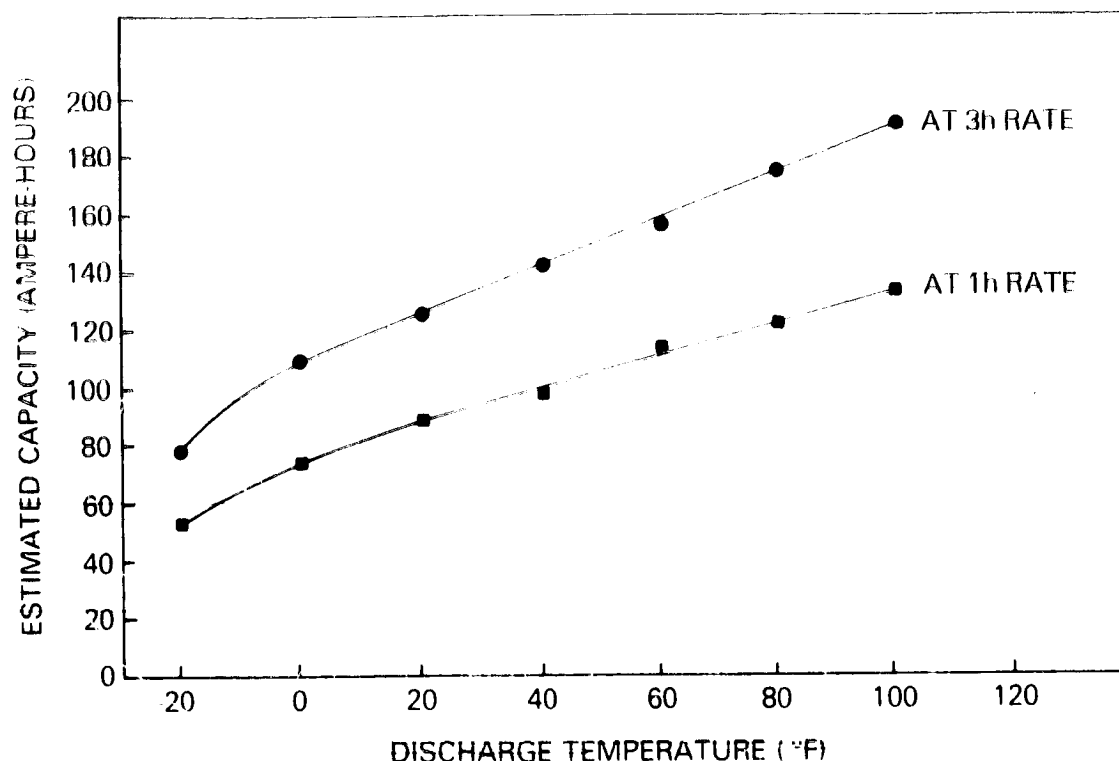
Figure 4-6.   Effect of Temperature on Capacity of an EV Battery

If a 30% reduction in battery capacity (AH) may occur without
significantly effecting vehicle performance, the battery temper-
ature should be maintained at or above 25°F during operation of
the vehicle.   If the temperature falls below 25°F during a cold-
soak period, it would be desirable to heat the battery.   Transfer
of heat from the outside to the inside of the batteries is equally
as slow as the cooling process (see the above table).   Hence,
increasing battery temperature solely by external heating has
been found to be unattractive.(7)   It may be possible to warm up
the lead-acid batteries by the so-called "boot-strapping" approach
which is used successfully by the General Electric Battery Business
Department for Ni-Cd aircraft engine starting batteries.   The
boot-strapping approach involves initially self-discharging the
battery and using the internal losses, which are high when the
battery is cold, to heat it.   After the battery is warmed up
somewhat, the discharge is continued using an external heating
tape to control discharge currents.   For the hybrid application,
the heat needed to raise the temperature of the battery from 0°F
to 25°F is only about 1 kWh, but distributing that energy through-
out the battery pack in 10 minutes could prove to be difficult
even when the battery is cold.   This problem has not been studied
to date for lead-acid batteries, but boot-strapping could prove
to be a means of attaining good performance after the vehicle has
soaked at low ambient temperatures for several days.   The hybrid
vehicle could be operated at reduced performance on the heat en-
gine alone even after prolonged inactivity at temperatures of
-20°C and lower.

Initial estimates of battery rechargeability and maintenance (P11, P12) and cold/hot temperature operation (P10, P13) are given in Table 4-3. Considerable work is needed in Phase II to refine the estimates given in the table, especially in the area of battery warm-up after long soak periods at sub-zero temperatures.

Table 4-3

VEHICLE PERFORMANCE CHARACTERISTICS

P10 Ambient Temperature Capability

Temperature range over which minimum
performance requirements can be met.

-20°C to 40°C

P11 Rechargeability

Maximum time to recharge from 80%
depth-of-discharge (routine charge
to 96% capacity).

6 hr

P12 Required Maintenance (Battery)

Routine maintenance required per
month.
    Watering (1 or less, depending   15 min/ea.
    on use).
    Equalization charge (2-4, de-   12-15 hr/ea.
    pending on use).

P13 Unserviced Storability

Unserviced storage over ambient
temperature range of -30°C to
+50°C

P13.1 Duration   ≥ 5 days

P13.2 Warm-up time required

    Battery heating (-20°F)   10-15 min.

    Engine starting   ‹30 sec.

4.6 MEASURES OF ENERGY CONSUMPTION

The energy use of the hybrid vehicle on the various driving cycles has been calculated using the HYVEC simulation program. The updated results are given in Figures 4-7 and 4-8. Additional energy-use results are given in Appendix V.

A format for summarizing the measures of energy consumption of the hybrid vehicle is given in Exhibit I of the RFP. Values for the various energy-use measures (El through E8) are given in Table 4-4. No values are given for E9, life cycle energy consumption per vehicle compared to the Reference ICE Vehicle, because information was not available concerning the energy required to fabricate and to dispose of the hybrid vehicle. Such information was not needed in the Design Trade-Off Studies and, thus, was not in hand at this stage of the hybrid vehicle study. Since the hybrid vehicle is about 1000 lb heavier than the Reference ICE Vehicle, it is reasonable to assume that the energy needed to fabricate the hybrid vehicle would be higher, but the net difference in fabrication energy would depend on the recycle pattern of those components which cause the weight difference between the vehicles. For example, much of the lead in the batteries and copper in the electric motor would be recycled with a significant favorable effect on the life cycle energy consumption of the hybrid vehicle. The material used to fabricate the exterior shell (doors, fenders, hood, etc.) of the vehicles will also have a strong influence on life cycle energy use. Life cycle energy use, including fabrication and disposal, will be considered in material selection in Phase II, but to date that subject has received only minimal attention.

4.7 INITIAL COST AND OWNERSHIP COST

The initial cost of the hybrid vehicle has been calculated using the same methodology used in References 1 and 3. A cost breakdown is shown in Table 4-5. The hybrid vehicle selling price is estimated to be $7667 compared with $5700 for the Reference ICE vehicle. The difference in power train costs is $1562. Both the vehicle selling price and the power train cost difference are somewhat higher than given in References 1 and 3. These differences are due primarily to the more detailed information that is now available concerning the size and cost of the power train components.

The ownership cost of the hybrid vehicle has also been calculated using the same methodology used in Reference 1. Results obtained in the references were corrected to account for the change in selling price of the hybrid vehicle. This was done by calculating the fixed capital recovery factor (FCRS) and applying it to the initial price difference. The change in ownership cost

UPDATED VEHICLE DESIGN
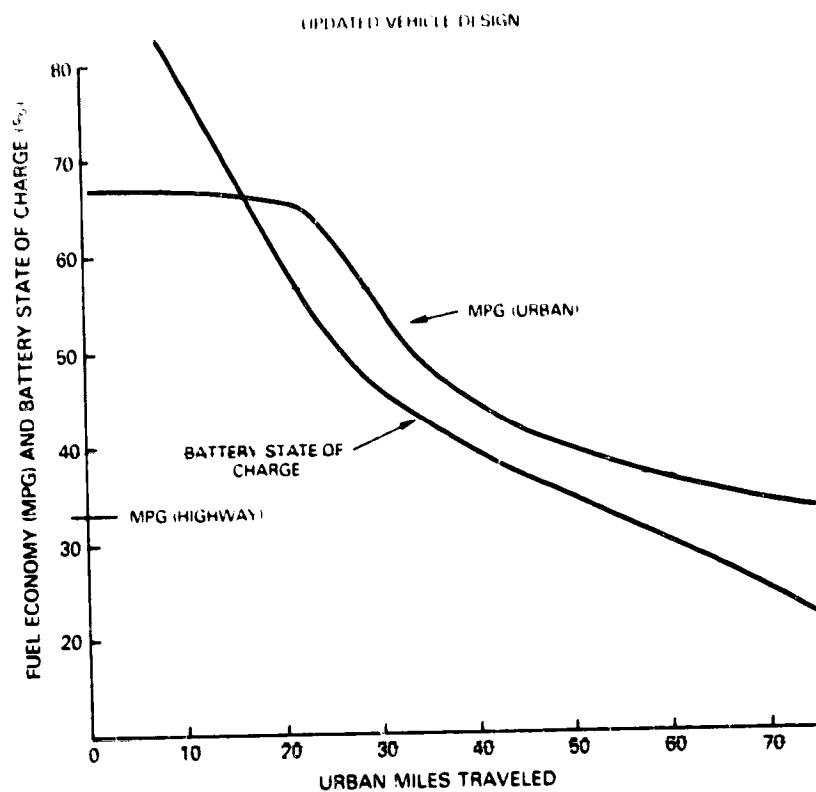
Figure 4-7. Battery State-of-Charge and Fuel Economy for Urban and Highway Driving

UPDATED VEHICLE DESIGN
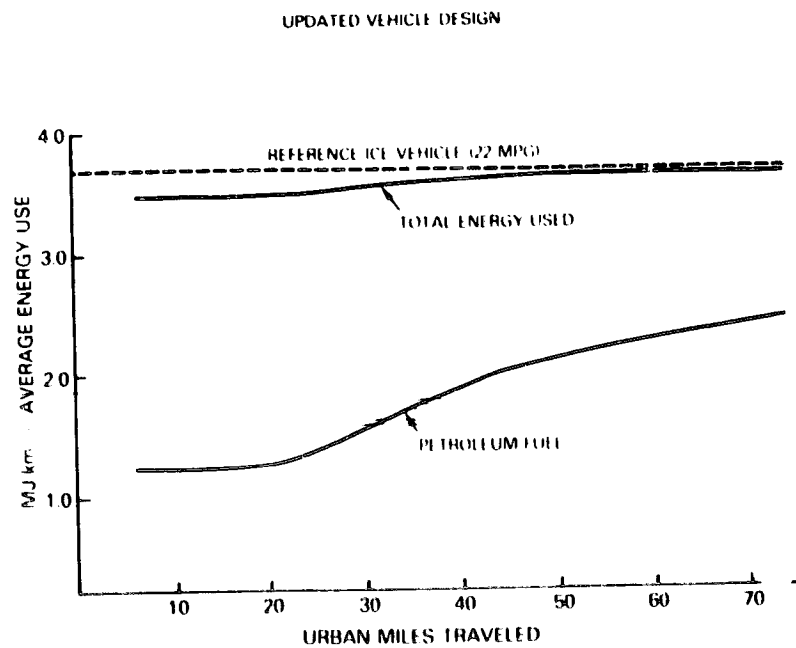
Figure 4-8. Total Energy and Petroleum Fuel Usage in Urban Driving

4-22

Table 4-4

ENERGY CONSUMPTION MEASURES

E1 Annual petroleum fuel energy consumption per vehicle
compared to reference vehicle over contractor-developed mission[a]
      25,710 MJ SAVED[b]

E2 Annual total energy consumption[c] per vehicle compared to reference
vehicle over contractor-developed mission[a]
      3,425 MJ SAVED[b]

E3 Potential annual fleet petroleum fuel energy savings compared
to reference vehicle over contractor-developed mission[c]
      25×10^9 MJ

E4 Potential annual fleet total energy consumption[c] compared to
reference vehicle over contractor-developed mission[d]
      3.4×10^9 MJ SAVED[b]

E5 Average energy consumption[c] over maximum nonrefueled range

    E5.1 FHDC (gasoline only)   2.45 MJ/km (32 mpg)

    E5.2 FUDC[e]   3.59 MJ/km, 3.68 MJ/km, 3.8 MJ/km

    E5.3 J227a (B) (electricity only)   2.45 MJ/km

E6 Average petroleum fuel energy consumption over
maximum nonrefueled range

    E6.1 FHDC   2.45 MJ/km (33 mpg)

    E6.2 FUDC[e]   1.5 MJ/km (54 mpg), 2.45 MJ/km (33 mpg), 3.4 MJ/km (23.5 mpg)

    E6.3 J227a (B)   0 MJ

E7 Total energy consumed[c] versus distance traveled starting
with full charge and full tank over the following cycles

    E7.1 FHDC   2.45 MJ/km (Not a Function of Distance)

    E7.2 FUDC   (See Figure 4-8)

    E7.3 J227a (B)   2.45 MJ/km (Not a Function of Distance)

E8 Petroleum fuel energy consumed versus distance traveled
starting with full charge and full tank over the follow-
ing cycles[f]

    E8.1 FHDC   2.45 MJ/km (Not a Function of Distance)

    E8.2 FUDC   (See Figure 4-7)

    E8.3 J227a (B)   0 MJ/km (Not a Function of Distance)

1 MJ = 0.278 kWh = 948 Btu = .00758 gal gasoline

10^9 MJ/yr = 452 barrels crude oil/day

(a) Mission is 11,852 mi/yr; 65% EPA urban cycle, 35% EPA highway cycle

(b) The annual fuel and energy usages of the Reference ICE Vehicle (1985 model)
are 456 gallons of gasoline and 60,158 MJ. A fleet of one million Reference
Vehicles would use 60×10^9 MJ.

(c) Includes energy needed to generate the electricity at the power plant
(35% efficiency)

(d) For one million hybrid vehicles replacing one million Reference Vehicles

(e) The first number corresponds to the first 50 km; the second number to
120 km; the third number to 425 km, at which the gasoline tank is empty

(f) Does not include petroleum consumption resulting from generation of wall
plug electricity used by the vehicle

Table 4-5

COST BREAKDOWN

Chassis/Shell/Pass. Compartment	OEM Price ($)	Dealer Sticker Price ($)
Base vehicle minus ICE power train	3482	
Additional weight	130	
Additional for extended life	182	
Subtotal	3794	4932
Hybrid Power Train*		
Heat engine	463	
Transmission	227	
Electric motor	365	
Controller (including microprocessor, field chopper, battery switching)	244	
Batteries (lead-acid)	688	
Battery charger	117	
Subtotal	2104	2735
Total Hybrid Vehicle Price (1978 Dollars)		7667**

*Cost of ICE power train (110 HP) is $1173 (dealer sticker price).
**Cost of Reference ICE Vehicle is $5700 (dealer sticker price - 1978 dollars).

was .63¢/mi for the nominal set of economic factors. The owner-
ship costs for the hybrid vehicle are shown in Figure 4-9 as a
function of the price of gasoline. A breakeven price of gasoline
of about $1/gal is indicated in the figure. At gas prices in ex-
cess of $1/gal, the hybrid vehicle has a lower ownership cost,
resulting in the net annual savings shown in Figure 4-10. The
sensitivity of the ownership costs to changes in the use pattern
and the price of electricity are discussed in detail in Refer-
ence 3.

4.8 MAINTENANCE AND RELIABILITY

Maintenance of the hybrid vehicle entails attention to the
same items as maintenance of the Reference ICE Vehicle. In ad-
dition, the electric drive system of the hybrid vehicle must also
be maintained. Considerable thought has been given to the mainte-
nance of the electric drive system as part of the DOE/GE Near-
term Electric Vehicle Program. Table 4-6, taken from the Opera-
tion and Maintenance Manual prepared for the DOE/GE Electric Car,
lists maintenance actions and frequency for the electric driveline.
Most of those items would also be required for the hybrid vehicle.
Routine maintenance and tune-ups for the heat engine should be
less frequent for the hybrid vehicle, because the engine would be
used only a fraction of the driving time (i.e., it would take
longer in calendar time to accumulate a fixed number of equivalent
miles or operating hours). The engine oil and coolant would have
to be selected such that they could function longer between changes.
One would expect that the brakes on the hybrid vehicle would last
more vehicle miles than the brakes on the Reference ICE Vehicle
because regenerative braking supplies much of the stopping torque
in stop-and-go urban driving. After the electric motor and elec-
tronics are fully developed and road tested for millions of miles,
it is reasonable to expect that they will have long life and a
minimum of routine maintenance. The batteries will, of course,
require continuing attention if they are to have a long life, but
most of that maintenance can be done by the car owner if the
battery charging (including equalization charging) and watering
systems are well designed.

In the calculations of ownership cost it was assumed that
paid-for maintenance of the hybrid vehicle would be 25% less
than for the Reference ICE Vehicle after the hybrid power train is
well developed and road-tested. This assumption is primarily
based on the less frequent need for engine maintenance/tune-ups
and the expectancy that the electric motor/electronics are rel-
atively maintenance free. It was also assumed that with proper
design of the non-propulsion components,* the effective lifetime
(miles or years) of the hybrid vehicle could be extended beyond
that of the Reference ICE Vehicle because of the expected longer
calendar life of the heat engine and the longevity of the electric
drive components. A hybrid vehicle life of 12 years or 120,000
miles was used in the cost calculations. It would, of course,
be necessary to replace the battery pack several times during the
hybrid vehicle lifetime, but that cost is included separate from
the routine or repair maintenance costs.

*Additional chassis and running gear cost (5%) has been included
 for the hybrid vehicle.
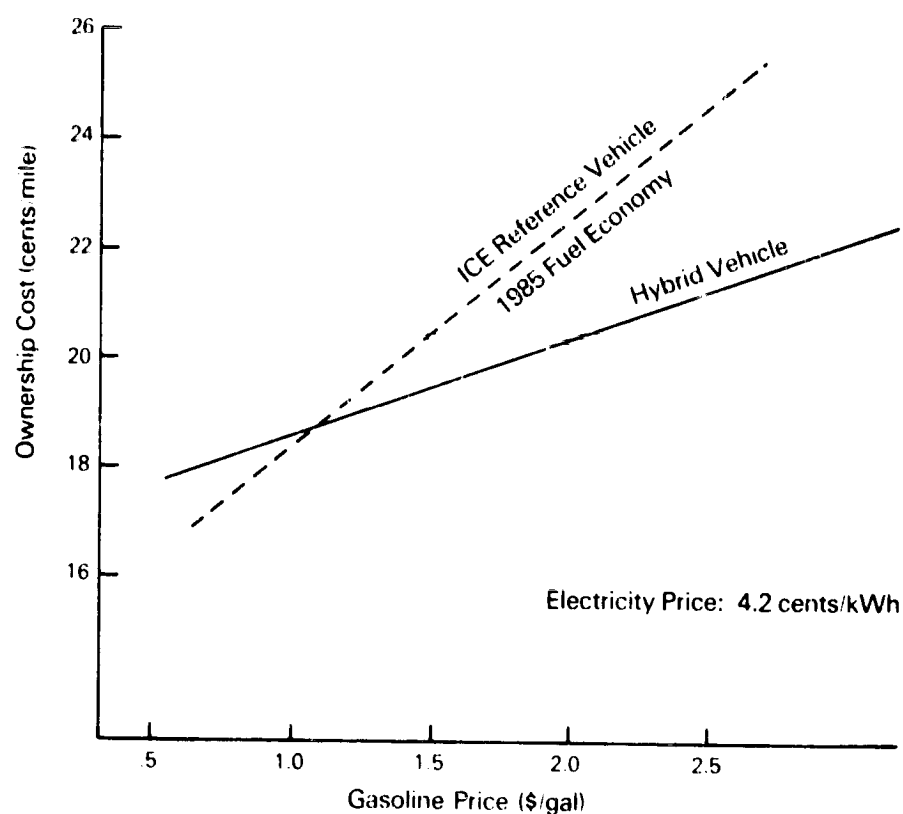
Figure 4-9. Ownership Cost as a Function of Gasoline Price
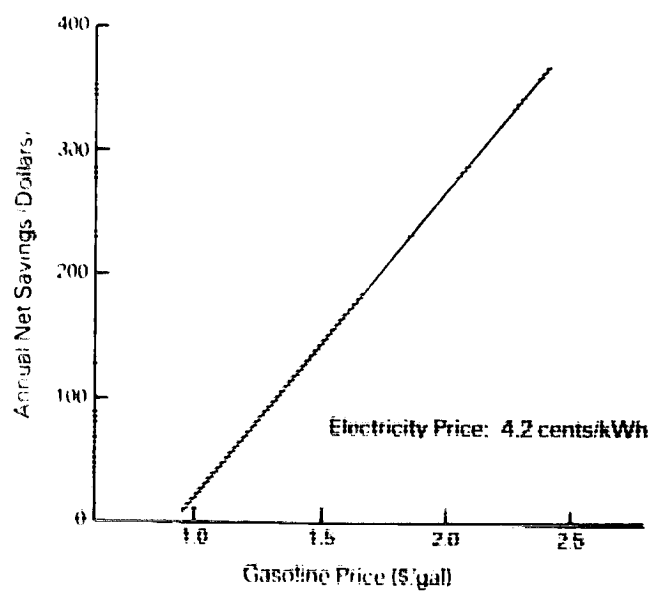
Figure 4-10. Annual Net Dollar Savings as a Function of Gasoline Price

Table 4-6

MAINTENANCE FOR DOE/GE NEAR-TERM ELECTRIC VEHICLE

Maintenance Item	Maintenance Action	Frequency
Propulsion Batteries	Perform Watering Procedure	Every 2 Months
	Check Operation of Watering/Vent Valves	Every 2 Months
	Check Watering/ Venting Tubing for Evidence of Cracks, Pinching, Looseness on Fitting	Every 6 Months and when battery compartment removed from vehicle
	Perform Equalization Procedure	Once every 7 Normal Charges
	Drop Battery Tray and Clean Battery Tray of Debris	Every 6 Months
	Check Specific Gravities or Open-Circuit Voltage	Every 6 Months
Flame Arresters	Inspect and Clean	Every 6 Months
	Replace Flame Arresters	Every 2 Years
Watering Tubing	Inspect and Move or Replace Flattened Section of Off-Board Watering Tubing	Every 12 Months
AC Power Cord	Inspect for Frayed or Broken Wires	Every 6 Months
108 Volt DC System	Validate Isolation of 108 Volt dc System from Chassis	Every 2 Months
Ground-Fault Current Interrupter	Check Normal Trip Mechanism via Test Button	Every 6 Months
High-Amperage Heavy Cabling	Inspect Cable from Battery to QD Switch to PCU and Motor	Every 6 Months
Drive Motor Brushes, Commutator Cleanliness	Inspect	Every 6 Months
Drive Motor Brushes	Replace	Every 2 Years

The reliability of the hybrid vehicle should be greater than that of the Reference ICE Vehicle, because the hybrid vehicle has two, rather than one, drive systems. Both systems would have to be inoperable for the vehicle to be stranded or totally unusable. The hybrid power train is designed such that the vehicle can operate on either of the drive systems alone, but at reduced performance.

It is difficult to assess quantitatively the vehicle maintenance and reliability factors (P14 through P16) in Exhibit J of the RFP. If the probability of a failure for each of the components in the power train is approximately the same, then it would be expected that system failures with the hybrid vehicle would be significantly more frequent than those with the Reference ICE Vehicle. Clearly, this cannot be permitted to be the case, or the hybrid vehicle could not be marketed in competition with the ICE vehicle. Hence a design goal for the hybrid vehicle (fully developed and tested) must be to maintain power train and vehicle failures to the same or lower frequency than that for the conventional ICE vehicle. Engine failures would be expected to be less frequent with the hybrid vehicle, because the engine is used less of the time. In addition, suitably designed electrical/electronic components have less frequent failures than mechanical components. Friction brake failures for the hybrid vehicle would be less frequent than for the conventional vehicle because the friction brakes are used less. Major repair of the electric drive system is expected to require less time than that of the engine, because the electrical components are smaller and lighter and it is feasible to replace the faulty component with a new or rebuilt one as is done with alternators, starter motors, and electronic ignition systems in conventional vehicles. In addition, it seems less difficult to engineer self-diagnostic capability into the electric drive system than into the engine system. Hence, it appears reasonable that repair of the electric drive system will take less time and exhibit less variability from case to case than repair of the conventional vehicle. It is, of course, assumed that the power train is assembled such that suitable access is provided to the electric drive components and electronics. The factors P14 through P16 are estimated qualitatively in Table 4-7 in relation to the Reference ICE Vehicle only after the hybrid vehicle is well-developed and road-tested. Hence, the maintenance/reliability factors are intended only as long-term design goals of any hybrid vehicle development program.

4.9 MARKET PENETRATION

In order for hybrid vehicles to have a significant impact on petroleum usage, they must be attractive to a relatively large fraction of potential new car buyers. As indicated in Table 4-8, a recent survey of new car buyers by Newsweek [8] shows that most cars are used to perform a number of missions and, thus, require all-purpose utility. Data is also available from the Newsweek survey regarding annual miles traveled by new cars in households

Table 4-7

VEHICLE MAINTENANCE AND RELIABILITY SPECIFICATIONS RELATIVE TO ICE

P14   Reliability

P14.1   Mean usage between failures - power train   same as or less frequent failures

P14.2   Mean usage between failures - friction brakes   less frequent failures

P14.3   Mean usage between failures - vehicle   same as or less frequent failures

P15   Maintainability*

P15.1   Time to repair - mean   smaller

P15.2   Time to repair - variance   smaller

P16   Availability*

Minimum expected utilization rate,   higher

[time in service ÷ (time in service + time under repair)]

---

*Compared with an ICE vehicle after the hybrid vehicle is well-developed and
road-tested

having one to three cars. That data (Figure 4-11) indicates that
to meet a large fraction of the potential market, a new vehicle
design must be suitable for use in excess of 10,000 miles per year.
The hybrid vehicle designed in this study is intended for all-
purpose use and as shown in the sensitivity study (3) is equally
attractive economically for a large range of use patterns (i.e.,
annual miles driven, fraction of driving in urban areas, etc.).
In particular, the hybrid vehicle design discussed in this report
would be attractive to new car buyers who need a reasonably large
(5-6 passenger capacity) car with all-purpose utility, and who
plan to use the car 10-15,000 miles annually. The hybrid vehicle
designed in this study is suitable for all potential buyers ex-
cept those who travel regularly more than 75 miles daily or do
considerable heavy hauling of such things as boats or trailers.

The various studies completed on the Near-Term Hybrid Vehicle
Program have shown no reasons why the market penetration of the
hybrid vehicle could not be significant - at least 50-75% in the
large car classes (5-6 passenger capacity).

Table 4-8

PERCENTAGE USAGE OF NEW CARS PURCHASED IN 1977

Mission	Large Cars [1]		Small Cars [2]	
	Principal Use [3]	Average Use [4]	Principle Use	Average Use
Commuting	38.9	31.7	57.4	41.6
Pleasure trips	15.7	21.2	8.7	17.3
Local Transportation	33.3	27.9	20.4	22.7
Business and School	12.0	19.2	13.5	18.4

(1) 5-6 passengers
(2) 4 passengers or less
(3) Percentage of owners for which this mission was dominant
(4) Percentage of time car used for this mission
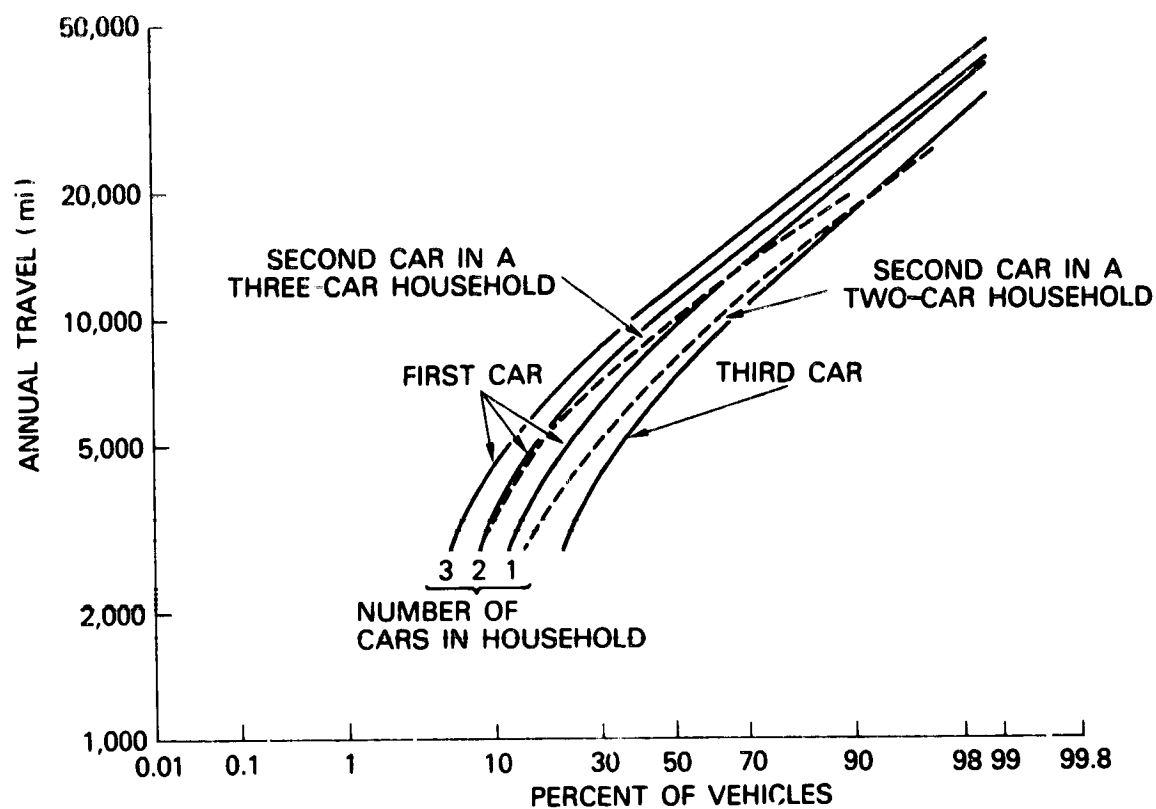
Figure 4-11. Annual Travel Characteristics for Multiple-Car Households

Section 5

ADVANCED TECHNOLOGY DEVELOPMENTS

Section 5

ADVANCED TECHNOLOGY DEVELOPMENTS

5.1 INTRODUCTION

The detailed preliminary design of the hybrid vehicle was performed using a gasoline engine, lead-acid batteries, and an automatically shifted gearbox that could be obtained in the near-term (mid-1981) with minimum uncertainty and technology risk. The hybrid vehicle which was designed meets or exceeds all the minimum vehicle specifications, but an even more attractive hybrid vehicle could be designed using one or more advanced technology components. These components include a turbocharged diesel engine, Ni-Zn batteries, and a steel belt continuously variable transmission (CVT) as identified in Section 3. The potential role of each of the advanced power train components is discussed in the following subsections.

5.2 TURBOCHARGED DIESEL ENGINE

HYVEC simulations[1] have shown that a hybrid vehicle utilizing a diesel engine would have about 25% better fuel economy than a similar vehicle using a gasoline engine. This comparison in fuel economy is shown in Figure 5-1. There is, however, considerable uncertainty regarding the ability of the diesel-powered hybrid
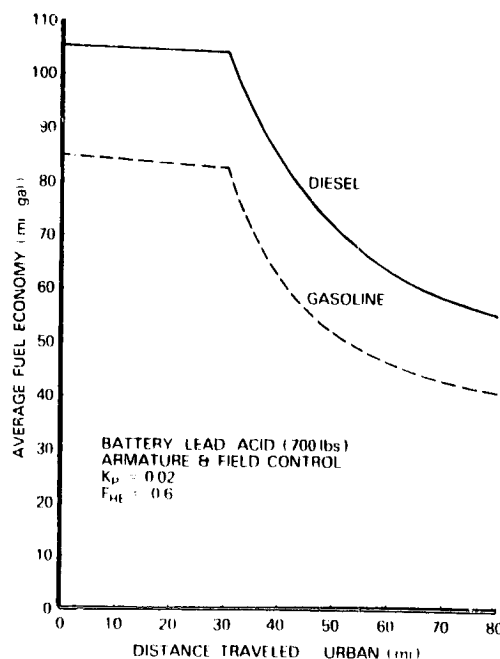
Figure 5-1.　Effect of Heat Engine Type on Average Fuel Economy

vehicle to meet potential EPA NO_x and particulate emission stan-
dards and to be used in the on/off engine operating mode which
would require very fast starts under a range of engine tempera-
ture conditions. Resolution of these uncertainties requires action
by EPA and additional test data for engine operating conditions
peculiar to the hybrid application. The test data could be ob-
tained in the early stages of the Phase II effort. The timing
of EPA decisions on the diesel emissions is more difficult to
predict.

5.3 NI-ZN BATTERIES

The use of 500 lb of Ni-Zn batteries in place of the 700 lb
of lead-acid batteries was studied in the Design Trade-Off Studies
(Ref. 1). A hybrid vehicle using the Ni-Zn batteries would weigh
about 400 lb less than one using the lead-acid batteries, and as
shown in Figure 5-2, would have better fuel economy for daily
ranges greater than 30 miles. There has been relatively little
operating experience to date with Ni-Zn batteries in electric
vehicles, and there is considerable uncertainty regarding their
performance, cycle life, and cost. Ni-Zn cells and batteries are
currently being developed for electric vehicles, but those cells
are much larger than would be needed for the hybrid application
(e.g., 250 AH compared with 115 AH). Thus, new cells would have
to be designed and fabricated for evaluation in the Phase II hy-
brid vehicle program. Discussions with Energy Research Corpora-
tion (ERC) indicated that this development could use essentially
the same plate/cell technology as used in the ongoing DOE Ni-Zn
battery programs. The characteristics (voltage and power) of the
Ni-Zn batteries would be such that they could be used in place of
the lead-acid batteries with a minimum change in the electric
drive system and battery charger.
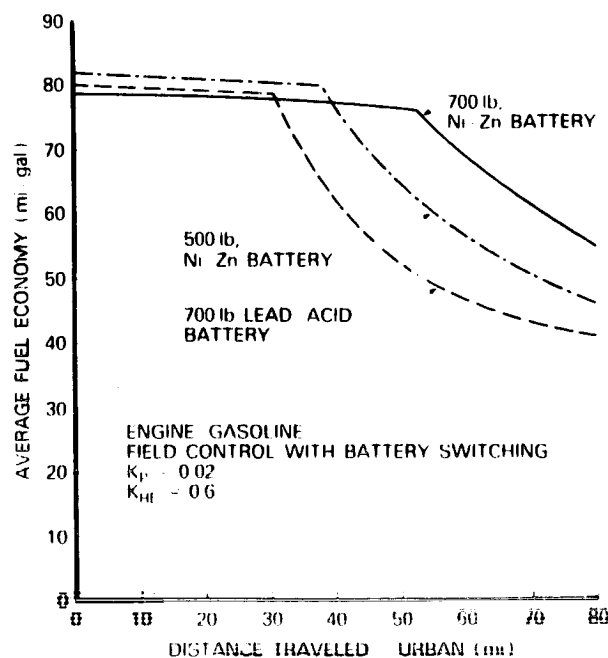
Figure 5-2. Effect of Battery Type
on Average Fuel Economy

GENERAL ELECTRIC

Cell and battery data provided to GE by ERC indicated that
Ni-Zn batteries could be fabricated which met the needs of the
hybrid vehicle program. That is energy density of about 27 Wh/lb
and power characteristics suitable for high-current, pulsed dis-
charge with tolerable voltage droop. However, these high expec-
tations were tempered considerably when the dissappointing recent
test results for a Ni-Zn battery pack delivered by ERC were dis-
covered. Subsequent discussions between Energy Research Corpora-
tion and General Electric indicated that ERC considered those
battery pack tests to be atypical and that the Ni-Zn battery data
sent to GE was more representative of present technology. Further
clarification of the discrepancy between the two test results is
needed.

The hybrid vehicle simulation results given in Figure 5-2
are based on the cell data sent to GE by ERC and are, of course,
dependent on meeting those specifications in practice. General
Electric has received a proposal from ERC for consideration in the
GF Phase II proposal stating that Ni-Zn batteries having the re-
quired energy density and power characteristics can be fabricated
by mid-1981. The attractiveness of such batteries from a vehicle
performance point of view is clearly evident.

5.4 STEEL BELT CVT

The use of a CVT in the hybrid power train would be advanta-
geous for several reasons:

- The effect of the transients on the system controller
  because of shifting of the automatic gearbox would be
  avoided.

- The electric motor and heat engine could be operated near
  maximum torque and efficiency for a wider range of vehicle
  speed and power conditions.

- The overall control logic (controller software) would be
  simpler.

As discussed in Appendix V, HYVEC calculations were made using a
CVT in the hybrid power train. The results indicated that accel-
eration performance and fuel economy, especially for urban driving
for distances less than the effective electric range of the ve-
hicle, were significantly better using a CVT than an automatic
gearbox of the same overall speed ratio. The fuel economy results
are summarized in Figure 5-3.

Discussions were held with Borg-Warner concerning the possible
availability of a steel-belt CVT by mid-1981 for use in the hybrid
vehicle. Borg-Warner is currently testing a CVT in a Ford Fiesta,
but GE was told by Borg-Warner that Borg-Warner's current plans
for marketing a CVT indicated a 1985 availability date. In addi-
tion, the torque capability of the unit being tested in the Fiesta
was only 100 ft-lb and development of a larger unit for the hy-
brid application would be required. Hence it was concluded that

5-3
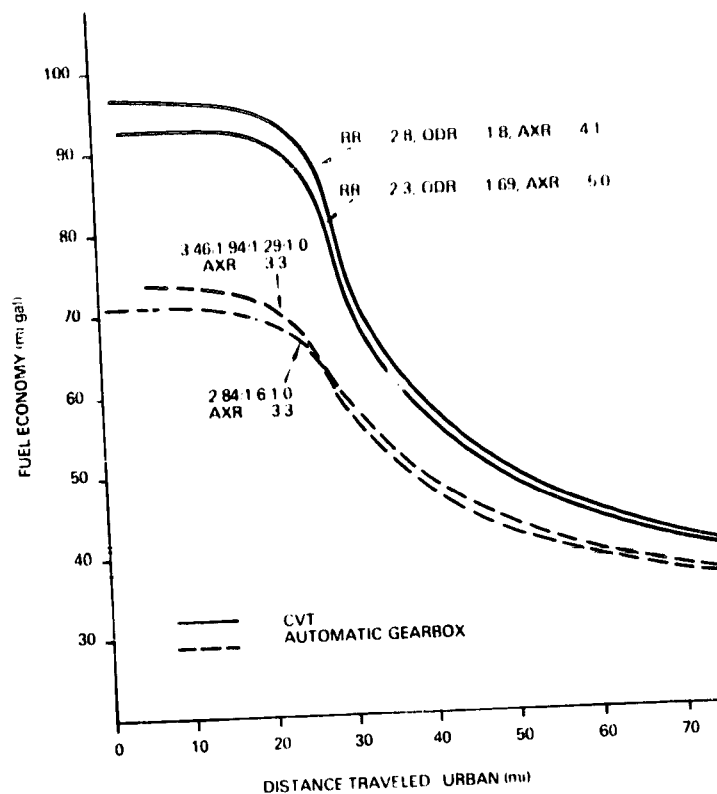
Figure 5-3.   Hybrid Vehicle Fuel Economy Using a Steel Belt Continuously Variable Transmission

even though a CVT has significant advantages in the hybrid power train, it was not possible to consider it for use in the Near-Term Hybrid Vehicle Program.

Section 6

REFERENCES

Section 6

REFERENCES

1. Design Trade-Off Studies Report, Near-Term Hybrid Vehicle Program; Contract No. 955190; General Electric Company Report SRD-79-075, June 8, 1979

2. Mission Analysis and Performance Specification Studies Report, Near-Term Hybrid Vehicle Program; Contract No. 955190; General Electric Company Report SRD-79-010, February 6, 1979.

3. Sensitivity Analysis Report, Near-Term Hybrid Vehicle Program; Contract No. 955190, General Electric Company Report SRD-79-093, June 8, 1979

4. Technical Instruction, Fuel Injection, Continuous Injection System (CIS); Robert Bosch Gmbh, Stuttgart, Federal Republic of Germany, Publication No. VDT-VBP 741/1B, 1974.

5. Technical Instruction, Electronically Controlled Fuel Injection; Robert Bosch Gmbh, Stuttgart, Federal Republic of Germany, Publication No. VDT-VBP 751/1B.

6. Near-Term Electric Vehicle, Phase II, Mid-Term Summary Report; Contract No. E4-76-C-03-1294, General Electric Company, July 1, 1978.

7. Electric Car Design, Interim Summary Report, Phase I - Deliverable Item 9, Contract No. E4-76-03-0294, SRD-77-078, General Electric Company, May 9, 1977.

8. The Study of American Markets - Automotive, U.S. News and World Report, 1977.

Appendix I

DETAILED VEHICLE DESIGN

Appendix I

DETAILED VEHICLE DESIGN

I.1 DESIGN METHODOLOGY

Foremost in the design of the hybrid vehicle was the desire to minimize the time spent on those elements of the car whose function and design are not affected by the hybrid nature of the propulsion system. This philosophy will maximize the effort expended in solving the hybrid vehicle related problems, and minimize the total cost of the Phase II program. It was decided to utilize as many appropriate, standard automotive components as possible in the preliminary design, and, in fact, to employ as many components from the Chevrolet Malibu (Reference ICE Vehicle) as practical in order to maintain equivalent value to the customer.

I.2 GENERAL HYBRID VEHICLE SPECIFICATIONS

The general specifications of the hybrid vehicle, as determined in the Preliminary Design Task, are discussed in this Appendix. The drawings presented at the end of this Appendix represent graphic illustrations of the elements considered.

Those components which are not critical to the hybrid nature of the vehicle will be presented without discussion. However, it should be noted that appropriate calculations regarding function, load carrying capability, etc. were carried out in their selection. Maximum effort was made to utilize components which are presently available from automotive manufacturers or their suppliers.

Elements are categorized according to Uniform Parts Classification (UPC) groups which are commonly utilized by major automotive manufacturers. The system utilized is that of General Motors.

I.2.1 GENERAL VEHICLE DESCRIPTION

Figures I-1a, I-1b, I-1c, and I-1d are layout drawings of the hybrid vehicle as outlined in the Design Trade-Off Studies Report.[1] The drive, battery, and fuel systems are clearly shown in the phantom views. A three-dimensional cutaway artist's rendering of the vehicle showing these features is depicted in Figure I-2.

The following is a general description of the vehicle and its subsystems:

(1) Body Configuration - 5 passenger (2 front, 3 rear) - identical with the 1979 Chevrolet Malibu, 4-door hatchback sedan.

(2) Structural Configuration - Body frame integral with resil-
     iently mounted front sub-frame.

(3) Front Suspension - Independent short and long arm (SLA) with
     torsion bars.

(4) Rear Suspension - Linkage controlled solid axle.

(5) Brakes - Hydraulically power-assisted front disc and rear
     drum brakes with proportioning and diagonal split.

(6a) Engine - 4-cylinder, 1.6 liter gasoline with electronic fuel
     injection.

(6b) Electric Motor - Shunt-wound dc motor with separately con-
     trolled field and soft-start armature control.

(7) Transmission, Clutch and Controls - Three-speed, automatically
     shifted microprocessor controlled transmission driven through
     toggling dry friction clutches from transversely mounted en-
     gine and electric motor. Concentric differential drives
     through half-axle shafts to front wheels (see Figures I-3a,
     I-3b, and I-3c).

(8a) Fuel System - Ten gallon sealed fuel tank mounted under
     rear seat with vacuum relief fuel cap and charcoal canister
     for vapor absorption and storage.

(8b) Exhaust System - Centrally routed exhaust system with 3-way
     catalyst. Muffler mounted longitudinally in rear.

(9) Steering System - Closed center hydraulically assisted rack
     and pinion steering system.

(10) Wheels and Tires - Steel 15-inch wheels with radial tires.
     Spare rear-mounted.

(11) Front End Sheet Metal - Re-styled components with fiberglass
     reinforced outer fender panels and steel inner reinforcements.

(12) Electrical System - 60/120 volt lead-acid battery mounted for-
     ward of the cowl in an enclosed, lined container. Blower ven-
     tilated. 12 volt accessory electrical system with alternator.

(13) Engine Cooling - Front mounted water radiator with electric
     fan.

(14) Bumpers - Body-colored, steel-face bars with hydraulic energy
     absorbers and bumperettes.

(15) Accessories
     (a) Heater/Ventilator/Air Conditioning package consisting
          of a cycling clutch vapor compression air conditioning

system, and a hot water heater augmented by a gasoline burner (see Figures I-4a and I-4b).

(b) Radio

(c) Power Windows

(d) Power Bucket Seats

I.2.2 DETAILED COMPONENT SPECIFICATION

Specific components which have been employed in the preliminary design are discussed in this section. A brief description is presented when custom fabricated components are utilized/required.

UPC#**	NAME	DESCRIPTION
1	BODY	
1A1A	Underbody	New fabricated unit structures employing high strength steel members
1A1B	Front Hood	New styling. Steel construction.
1A1C	Rear Lid	New styling. Hatch with tempered glass and steel frame
1A1D	Front Fenders	New styling. Fiberglass outer and steel inner panels.
1A1E	Rear Quarters	New styling. Fiberglass construction.
1A1F	Doors	1979 Malibu
1A1G	Roof & Pillars	1979 Malibu
1A1H	Glazing	1979 Malibu
1A1J	Front Seats	1979 Malibu
1A1S	Rear Seat	1980 Citation (modified)
1A2A	Floor & Sill	New. Steel fabrication.
1A2B	Instrument Panel	1979 Malibu except instrumentation
1A2D	Windshield Wiper & Washer	1979 Malibu re-located
1A2E	Miscellaneous Body Hardware	1979 Malibu
1A2F	Exterior Body Ornamentation	New styling.

**General Motors Unified Parts Classification

UPC	NAME	DESCRIPTION
1A2H	HVAC	*
	Heater Core	1979 Chevette
	Evaporator	1979 Chevette
	Gasoline Heater	Vespak
	Condensor	1979 Chevette
	Compressor	GM Rotary Piston
	HVAC Control	1979 Malibu (modified)
1A2R	Restraint System	1979 VW Rabbit
2	FRAME	New front subframe
3	FRONT SUSPENSION	1979 GM "E" Body complete
4	REAR SUSPENSION	1980 GM "X" Body modified for additional load.
5	BRAKES	
5A	Front Brakes	1979 GM "E" Body
5B	Rear Brakes	1979 GM "E" Body
5C	Service Brake Pedal	1979 Malibu (modified)
5D	Parking Brake Mechanism	1979 Malibu
5E	Hydraulic Master Cylinder	1979 GM "E" Body
5F	Hydraulic Plumbing	New
5H	Hydraulic Brake Booster	*Bendix Hydro-Boost (modified)

* Items so marked will require significant development.

UPC	NAME	DESCRIPTION
6	ENGINE	
6A1	Engine	1.6 liter VW (EFI-L Jetronic). Modified for on/off operation.
6O	Flywheel	Flex plate with ring gear
6E	Oil Pan	Modified shape
6F	Oil Pump	Modified pick-up
6L	Inlet & Exhaust Manifolds	Modified outlets
6M1	Induction System	
6M3	Air Cleaner	Remote mount
6Q	Engine Mounting	*New
6Y	Accessory Drive	*New - over/running clutches
6Y2	Starting Motor	VW modified
6Z	Electric Motor	GE. Shunt wound, double-ended output
7	TRANSMISSION CLUTCH & CONTROLS	
7A	Transmission External Controls	*Servo-actuated
7B	Transmission Case and Gearing	*GM "X" Body with modifications
7B1A	Engine Clutch	*Borg-Warner Overcenter 8 in.
7B1B	Motor Clutch	*Borg-Warner Overcenter 8 in.
7B1F	Clutch Control	*Modulated Servo Control
7C	Transfer Case	New housing with Hy-Vo chain drive
8	FUEL AND EXHAUST	
8A	Fuel Tank Mounting & Gauge	Modified GM "X" Body

UPC	NAME	DESCRIPTION
8B	Fuel Lines	New
8C	Exhaust Pipe and Muffler	
8C-1A	Catalytic Converter	VW. 3-way catalyst
8C-1B	Exhaust Pipes	New
8C-1C	Muffler	VW Rabbit
8D	Evaporative Emission Control	1980 GM "X" Body
9	STEERING	
9A	Steering Gear	Power rack and pinion
9B	Steering Wheel	1979 Malibu
9C	Steering Column and Support	1979 Malibu
9D	Steering Linkage	GM "E" Body modified
9E	Power Steering	*Citröen CX modified with cycling
10	WHEELS AND TIRES	P-225/70R15 on 6J Rim
10E	Spare Tire	Full sized
11	FRONT END SHEET METAL	New
11A	Front Fenders	Fiberglass - new styling
11B	Hood	New styling - steel
11E	Reinforcements and Attachments	New - steel

GENERAL **GE** ELECTRIC

UPC	NAME	DESCRIPTION
12	ELECTRICAL	
12A	Batteries - Propulsion	*Globe-Union - 12 volt units
12B	Battery Box & Supports	Stainless steel with internal reinforcements
12B1A	Ventilation	Forced
12C	Accessory Electrical	Globe-Union - 12 volt
12C1A	Charging Control	GM 60 amp alternator
12C1B	Lamps	1979 Malibu
12F	Electric Radiator Fan and Controls	VW Rabbit
12G	Horn, Switch and Mounting	1979 Malibu
12H	Wiring Harness	New
12J	Instrumentation	New
12K	Electrical/ Electronic Sensors & Control	*New. Microprocessor
13	RADIATOR ASSEMBLY	VW Rabbit
13A	Radiator Mounting	New
14	BUMPERS	
14A	Face Bars	New
14B	Energy Absorbers	GM "E" Body

UPC	NAME	DESCRIPTION
34	ACCESSORIES	
	Radio	GE
	Power Seats	1979 Malibu
	Power Windows	1979 Malibu

Those items marked with an (*) will require significant development work.

I.3 STYLING

Styling changes have been made to reduce the aerodynamic drag coefficient and to lend a new identity to the hybrid vehicle. Since the roof, glass, and side doors of a Malibu are employed in the vehicle design (see Figure I-5), appearance changes have been limited to the front and rear areas of the vehicle. Additionally, the vehicle has been re-configured to incorporate a hatchback design to reflect future market trends in family sedans. Figures I-6 and I-7 are artists' concepts of the hybrid passenger car.

I.4 STRUCTURAL DESIGN

The structural design approach centers on the utilization of the basic body shell (roof, doors, pillars, and cowl) from the Chevrolet Malibu. This is a significant step because much of the body engineering work which would be required for a new vehicle would be expended on these components. The underbody, which must support the hybrid power train components, will be new from bumper to bumper. Consistent with contemporary practice, it will be fabricated in steel, making use of high strength alloys where required. The Chevrolet Malibu, which has a separate frame, will be converted to an internal frame construction for reduced weight without sacrificing structural rigidity.

Figure I-5 is an illustration of the body structure depicting the underbody, front structure with upper fender reinforcements, and integral rear wheelhouses. All components, with the exception of the basic body shell, will be designed and fabricated specifically for the hybrid vehicle.

I.5 POWER TRAIN COMPONENT ARRANGEMENT

The power train consists of the following elements:

● Heat Engine

● Electric Motor

- Transmission
- Wheel Differential
- Drive Axles
- Clutches
- Clutch Actuation Mechanisms
- Transmission Shifting Controls
- Accessory Drives
- Engine Starting System

The Design Trade-Off Study[1] showed that the vehicle should be front-wheel driven. Hence, all of the preliminary design activity was on front-wheel drive configurations.

I.5.1 SYSTEM FUNCTIONAL REQUIREMENTS

In order to develop a viable power train arrangement, primary consideration must be given to the functional requirements demanded by the control strategy. Hence, the power train accommodates the following operating modes:

- Idle the electric motor with accessories operational and vehicle at rest with transmission in gear.
- Idle the heat engine with the accessories operational and vehicle at rest with transmission in gear.
- Accelerate from rest with the electric motor only.
- Accelerate from rest with the heat engine only (for emergency situations).
- Deliver power to the wheels from both prime movers simultaneously.
- Transmit power from the wheels to the electric motor for regeneration.
- Allow the electric motor to be electrically and mechanically removed from the system for prolonged high speed cruising.
- Start the heat engine rapidly while the vehicle is in motion.
- Start the heat engine from the electric motor while the vehicle is at re..
- Start the heat engine with the vehicle at rest without the assistance of the electric motor (for emergency situations).
- Charge the batteries from the heat engine even when the vehicle is at rest.
- Turn off the heat engine while the vehicle is in motion.
- Shift gears in the transmission automatically in response to system microprocessor commands.

I.5.2   CANDIDATE CONFIGURATIONS

I.5.2.1   Clutching

It becomes clear immediately that at least two clutches are required to have the ability to mechanically disconnect either of the prime movers. Additionally, there must be at least one energy dissipative clutching member between the transmission input shaft and the prime movers. Another conclusion which can be drawn is that the clutching members at both the engine and the motor must be active (as opposed to passive or overrunning) since torque must be transmitted in both directions to each member at various times.

It seems, therefore, that the simplest system would be to have one active, energy-dissipating clutch mounted on each prime mover. Since both of these clutches are active, they can perform both the "switching" as well as the starting functions. Of all of the candidate configurations analyzed, this system proved to be the simplest and easiest to package.

Accessories pose additional problems as discussed in the Trade-Off Studies Report. The need to drive the accessories from either prime mover requires some interconnection between them. The further requirement that the accessories be driven with the transmission in gear and the vehicle at rest requires that this interconnection cannot be shared with the primary driveline unless an additional driveline clutch capable of transmitting the sum of both powerplant torques is inserted between the interconnecting member and the transmission. Since this torque is about ten times the accessory torque, it seems more reasonable to drive the accessories independent of the transmission drive. A simple "back to back" overrunning clutch mechanism between the motor and engine will accomplish the desired result of sharing the accessory load between the two prime movers. This clutching mechanism is passive and requires no outside control.

Consideration of the two driveline clutches reveals two important points regarding clutch actuation. First, these clutches must be modulated on application, and their rate of application is dependent on the desired rate of acceleration of the vehicle. Second, contrary to most energy dissipative automotive clutches, the actuating mechanism must be capable of operation in both the applied and released mode for extended periods. This requirement led to the selection of a clutch with a "toggle" or "over-center" actuation mechanism similar to those employed on implements and power take-offs.

I.5.2.2   Transmission Type

It was decided at the outset that the development of an all-new transmission was beyond the scope of this project and that only available transmissions, albeit re-packaged or modified, would be considered. Although this is not unnecessarily restrictive, it does limit such things as the overall ratio availability.

For the purposes of this section, a transmission is considered that unit in the mechanical drive which includes the final drive gears, the axle differential, the individual gearsets and their associated clutching elements, and the housing to contain all of these components. An automatically shifted transmission is defined as one which can be shifted under power. Contemporary automatic transmissions are of the planetary gear type and have their input and output shafts on the same line. The choices were restricted to this type.

There are five basic types of transmissions which were studied. These are listed below with examples of vehicles which utilize them:

- Straight through types (GM Toronado)

- Through-and-back types with hypoid final drive (Audi, Dasher)

- Through-and-back types with spiral bevel final drive (Renault)

- Through-and-back types with helical final drive (Omni/ Horizon)

- Concentric differential (GM "X" Body)

Of these five basic types, only two of them yield drive packages which fit within the envelope established. These were a longitudinal arrangement employing the through-and-back type with hypoid final drive, and a transverse arrangement utilizing the concentric differential.

As shown in Figure I-1a, the heat engine and electric motor are mounted transversely in the hybrid design. Computer analysis indicated that insufficient frontal crush space was available with a longitudinal arrangement of the engine and motor mandating the transverse arrangement. With the transverse motor/engine arrangement, the concentric differential type transmission followed as the logical choice. The gear ratios of the 3-speed GM "X" body gearbox are 2.84/1.6/1.0:1 in first, second, and third gear, respectively. The overall gear ratio of 2.84:1 is less than optimum, but it seems to be the best choice of transmissions currently available.

I.5.3 SYSTEM OPERATION

Figure I-8 is a schematic representation of the final drive package. Table I-1 illustrates the operational status of all major elements related to the list of power train operating modes listed in Section I.5.1.

I.5.4 SYSTEM LAYOUTS AND DRAWINGS

Figure I-1a is a layout of driveline components depicting the major functional elements. The major components are labelled to correspond to the schematic (Figure I-8).

Table I-1

MAJOR ELEMENT OPERATIONAL STATUS

OPERATING MODE	C1	C2	O/R1	O/R2	HE	EM	TRANS
1	Open	Open	Free	Driving	Off	Base RPM	Any
2	Open	Open	Driving	Free	Idle	Off	Any
3	Open	Activated	Free	Driving	Off	Various	Forward
4	Activated	Open	Driving	Free	Various	Off	Forward
5	Closed	Closed	Driving	Driving	Various	Various	Forward
6	Open	Closed	Free	Driving	Off	Above Base RPM	Forward
7	Closed	Open	Driving	Free	High	Off	Forward
8	Activated	Closed	Free	Driving	Starting	Above Base RPM	Forward
9	Activated	Closed	Free	Driving	Starting	Base	Neutral
10	Open	Open	Driving	Free	Starting	Off	Any
11	Closed	Closed	Driving	Driving	Various	Above Base RPM	Neutral
12	Open	Closed	Free	Driving	Off	Any	Any
13	Closed	Closed	Driving	Driving	Any	Any	Any

I.6 FURTHER DEVELOPMENT OF HARDWARE

Even though every effort was made to minimize the hardware development tasks which would be needed in Phase II, there are several areas in the vehicle system which will require development of mechanical hardware which is not readily available from conventional ICE automotive use. These elements are discussed briefly below.

I.6.1 PRIME MOVER CLUTCHES AND ACTUATORS

Two over-center or toggling dry friction clutches with automatically modulated application mechanisms and thermal protection or control must be developed to perform the function of smoothly starting the vehicle from rest and of starting the gasoline engine when the vehicle is in motion (see Figure I-3c).

I.6.2 CLOSED CENTER CENTRAL HYDRAULIC SYSTEM

A complete closed center hydraulic system to provide power steering and power brake boosting must be developed including cycling clutch hydraulic pump, control, priority valve, steering valve, and brake booster modifications. This system will be built employing as much available hardware as possible. However, the total system function will require some development work.

I.6.3 ACCESSORY DRIVE SYSTEM

An accessory drive system (Figure I-3a) capable of powering the accessories from either the motor or engine must be developed. This drive will also include the hydraulic pump required for transmission shifting.

I.6.4 NOISE AND VIBRATION

The control scheme requires the intermittent operation of the heat engine at relatively high loads and speeds. This could prove to be annoying because the engine will not seem to be operating in concert with the driver's demand. Some considerable effort might be required to minimize, by using noise insulation techniques, the noise and vibration entering the passenger compartment from the forward power train package.

I.7 SUMMARY LIST OF DRAWINGS AND ILLUSTRATIONS

The Preliminary Design Data Package drawings are all included at the end of this appendix. A summary of the drawing content and the figure number for each are given below:

Subject	Figure Number
Transmission, clutch, and controls, right side view	I-3a
Transmission, clutch, and controls, left side view	I-3b
Transmission, clutch, and controls, Section A-A	I-3c
Heating, ventilating, and air conditioning package, plan view	I-4a
Heating, ventilating, and air conditioning package, left side view	I-4b
Hybrid vehicle body structure, exploded view	I-5
Artist's rendering of the hybrid vehicle	I-6 and I-7
Schematic of drive package	I-8
Hybrid vehicle layout, left elevation, 1/5 th scale	I-1a
Hybrid vehicle layout, plan view, 1/5 th scale	I-1b

GENERAL ⚙ ELECTRIC

1200

1000

800

600

400

200

-800

-600

-400

-200

PROPULSI

RADIATOR

1.6 LITER
VW ENGINE

AIR CONDITIONING
CONDENSER

MOTOR
BLOWER

-800

-600

-400

-200

PROPULSION BATTERY

HYDRAULIC
BRAKE BOOSTER

1.6 LITER
VW ENGINE

MOTOR COOLING
BLOWER

ELECTRIC MOTOR

HYDRAULIC POWER
RACK & PINION
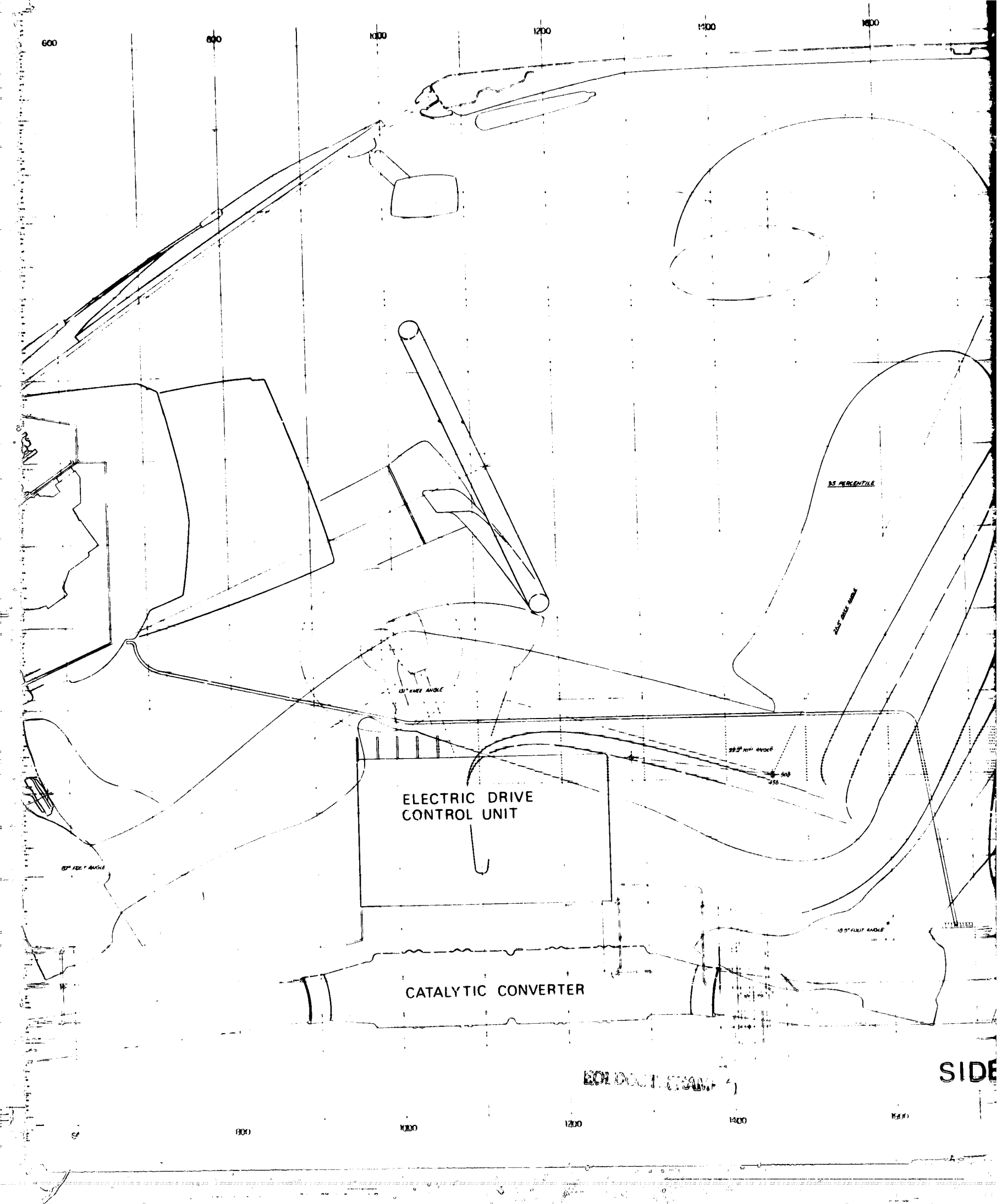
ELECTRIC DRIVE
CONTROL UNIT

CATALYTIC CONVERTER

SIDE

95 PERCENTILE

MALIBU SEATING

FOLD-DOWN
REAR SEAT

95 PERCENTILE

FUEL TANK

SIDE VIEW

FOLDOUT FRAME

FOLD-DOWN
REAR SEAT

MUFFLER

SPARE TIRE

FOLDOUT

3600

1200

1000

800

600

400

200

Figure I-1a. Hybrid
Vehicle Layout, Left
Elevation, 1/5 Scale

I-15
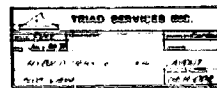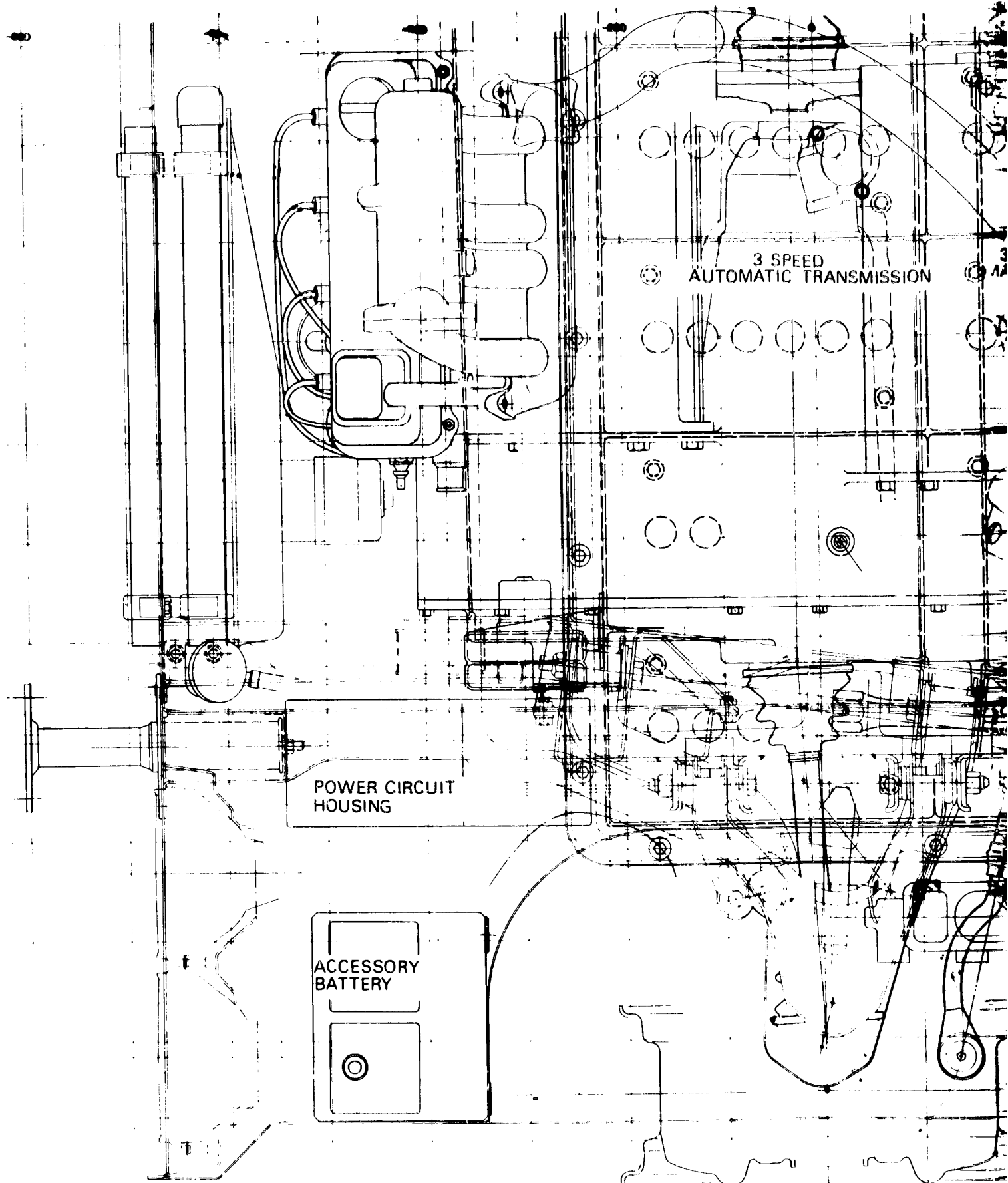
3600

3 SPEED
AUTOMATIC TRANSMISSION

POWER CIRCUIT
HOUSING

ACCESSORY
BATTERY

FOLDOUT FRAME

-800   -600   -400   -200
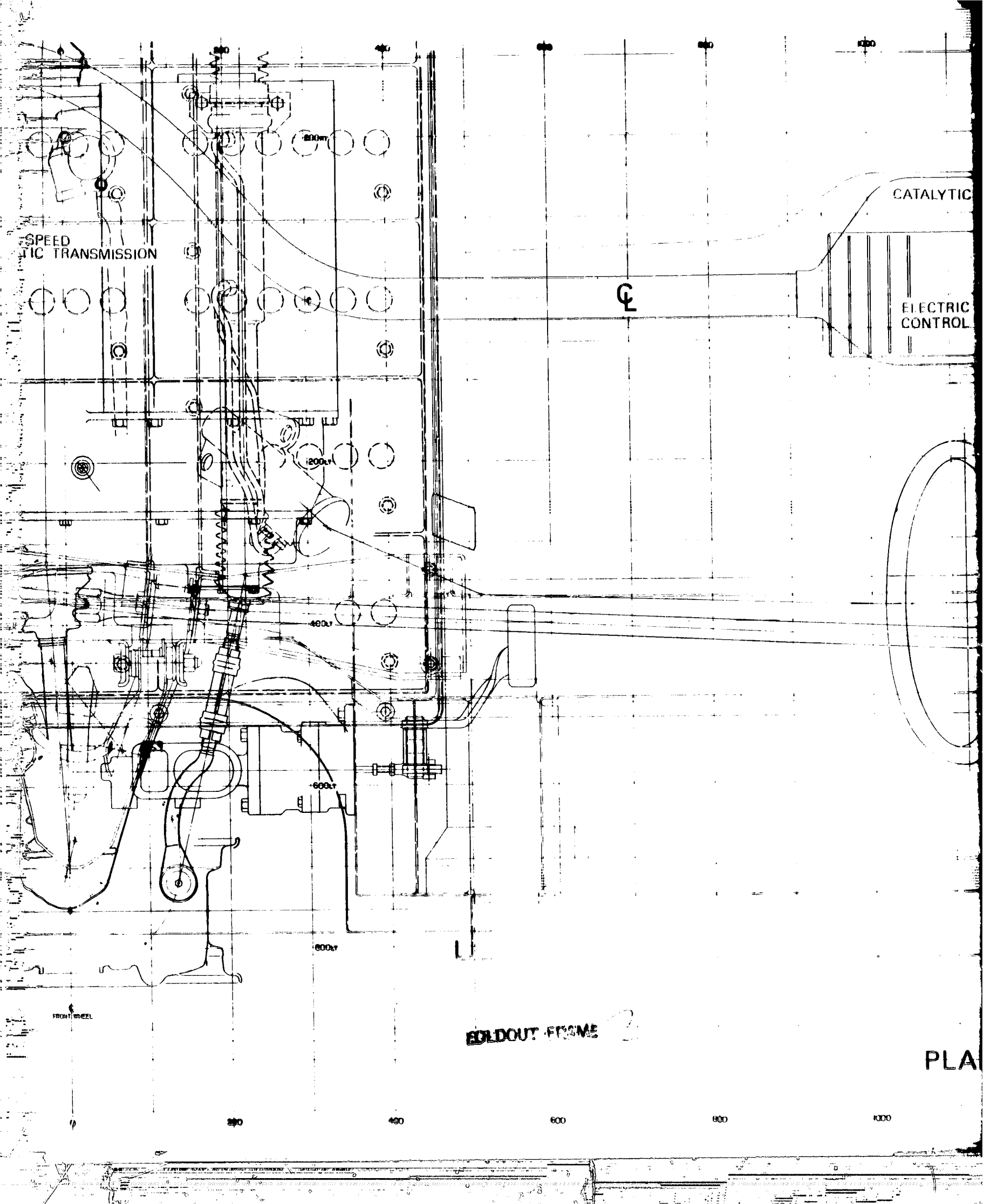
SPEED
TIC TRANSMISSION

CATALYTIC

ELECTRIC
CONTROL

$\mathcal{C}_{L}$

200RT

200LT

400LT

600LT

600RT

FRONT WHEEL

PLA

200

400

600

800

1000

CATALYTIC CONVERTER

ELECTRIC DRIVE
CONTROL UNIT

PLAN VIEW

FUEL TANK

SOLID AXLE
REAR SUSPENSION

FOLDOUT FRAME

SPARE TIRE

ION

FRAME

C_L

Figure I-1b. Hybrid Vehicle Layout, Plan View, 1/5 Scale

I-17

GENERAL ELECTRIC

PROPULSION BATTERY

ELECTRIC DRIVE
CONTROL UNIT

FRONT VIEW

I-19

Figure I-1c. Hybrid Vehicle Layout, F

BATTERY

POWER CIRCUIT HOUSING

ACCESSORY BATTERY

ELECTRIC DRIVE CONTROL UNIT

1979 G.M. E BODY SUSPENSION

FRONT DISC BRAKE

FRONT VIEW

Vehicle Layout, Front View, 1/5th Scale

OF POOR QUALITY

REAR DRUM
BRAKE

SPARE TIRE

SOLID AXLE

REAR VIEW

I-21

Figure I-1d. Hybrid Vehicle Layout

1200

1000

800

600

SPARE TIRE

400

MUFFLER

200

REAR VIEW

0 RV   200 RV   400 RV   600 RV   800 RV
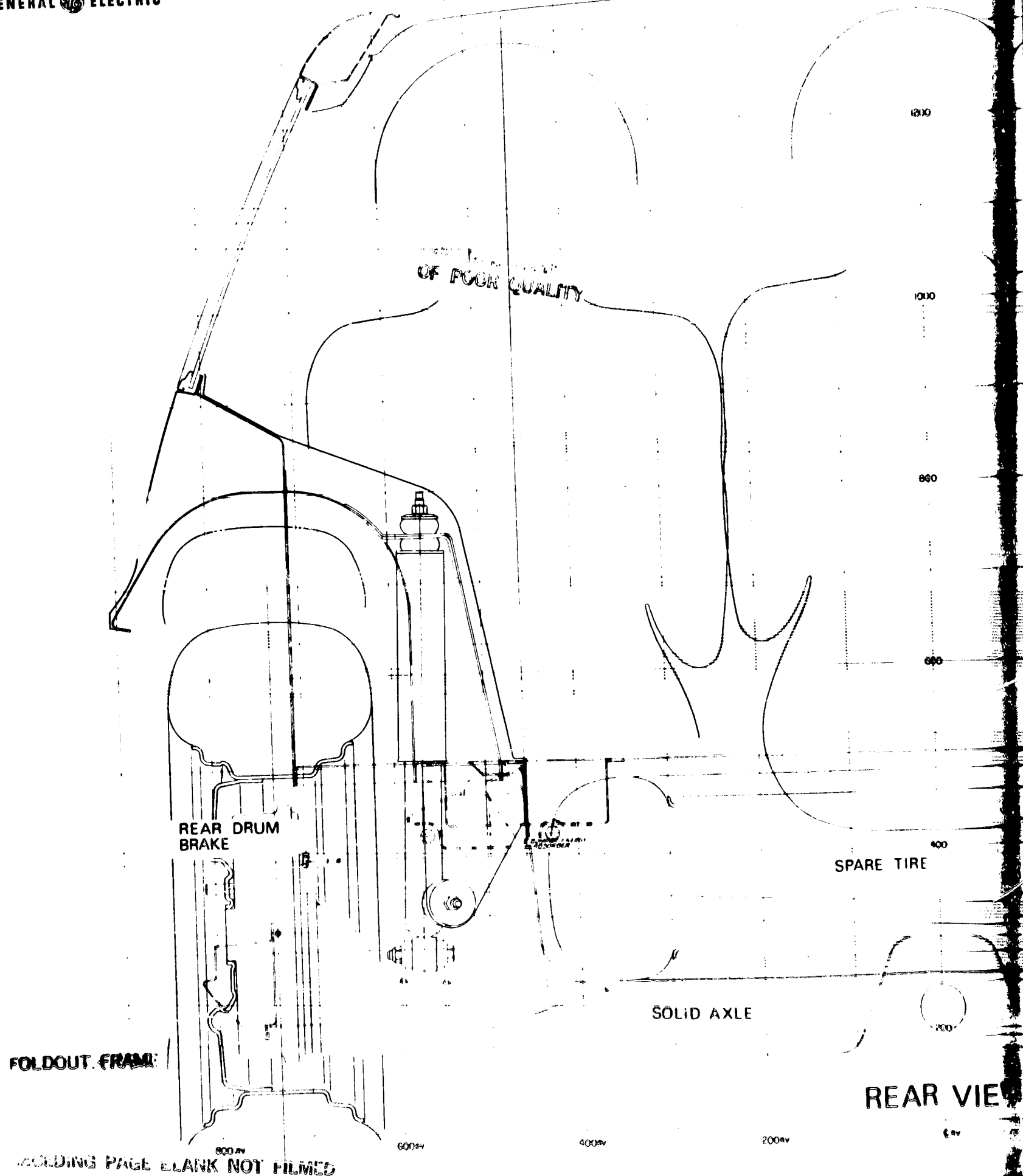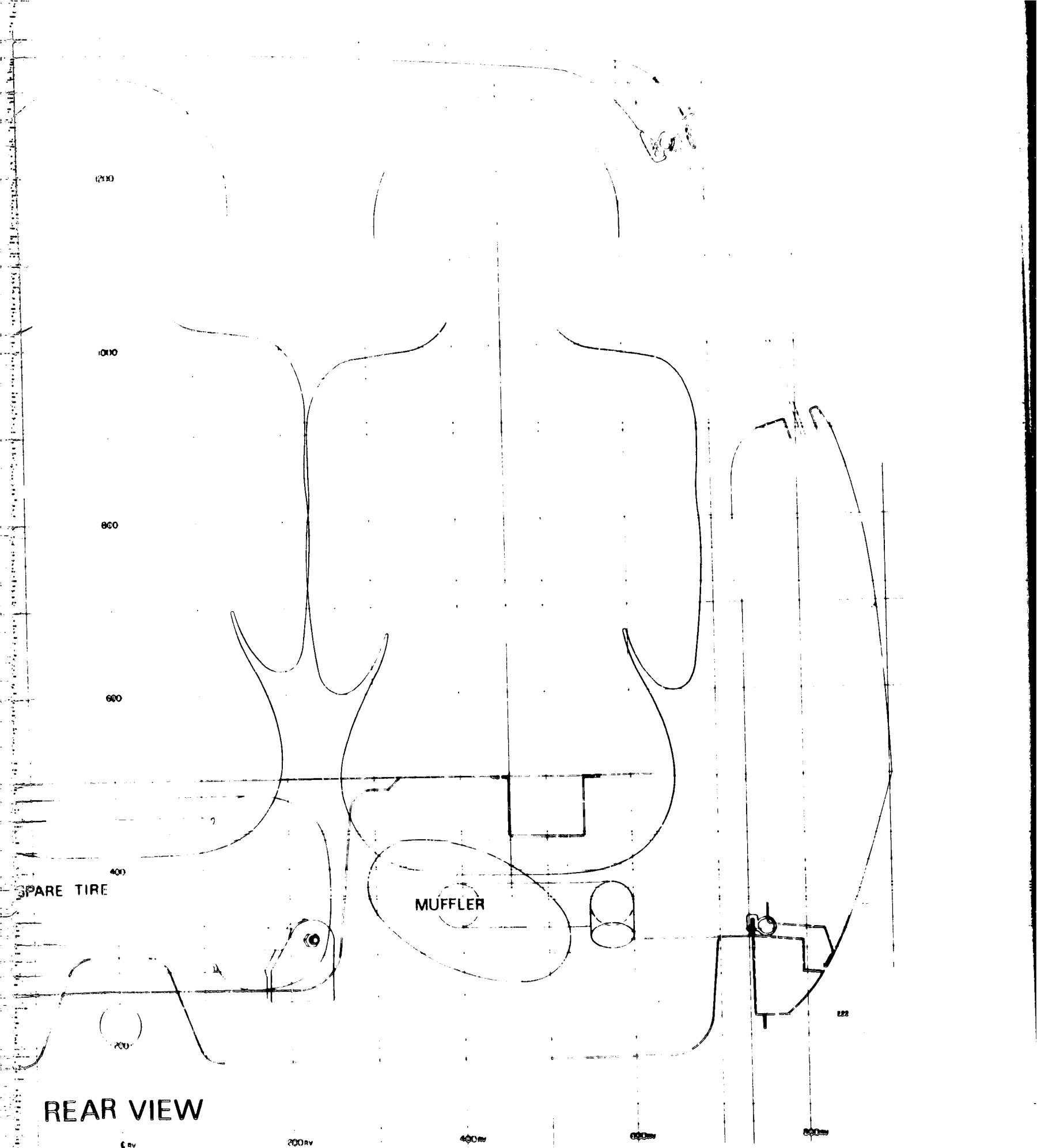
Vehicle Layout, Rear View, 1/5th Scale

PROPULSION BATTERY

HEATER

HEAT ENGINE

ELECTRIC MOTOR
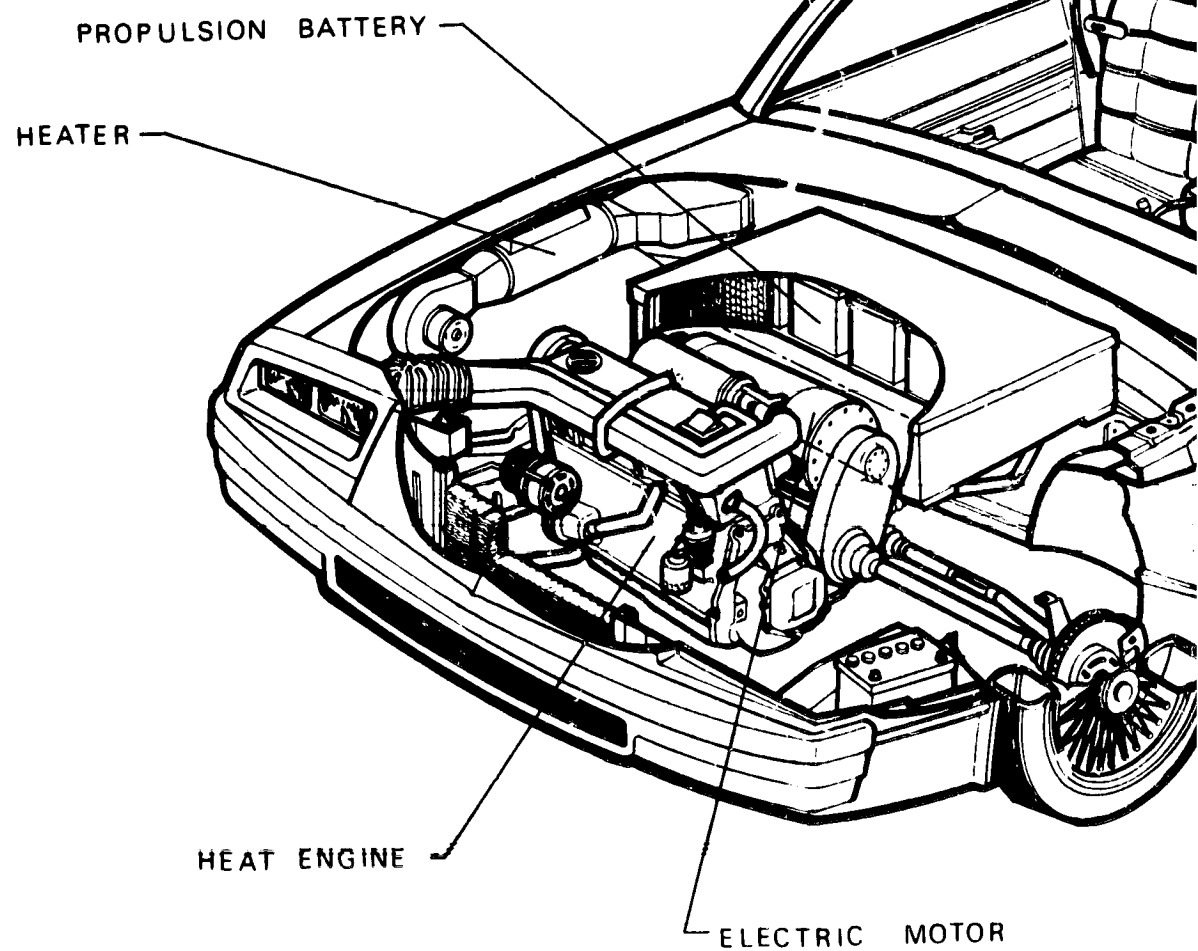
Figure I-2. Hybrid Vehicle, Thre

I-23
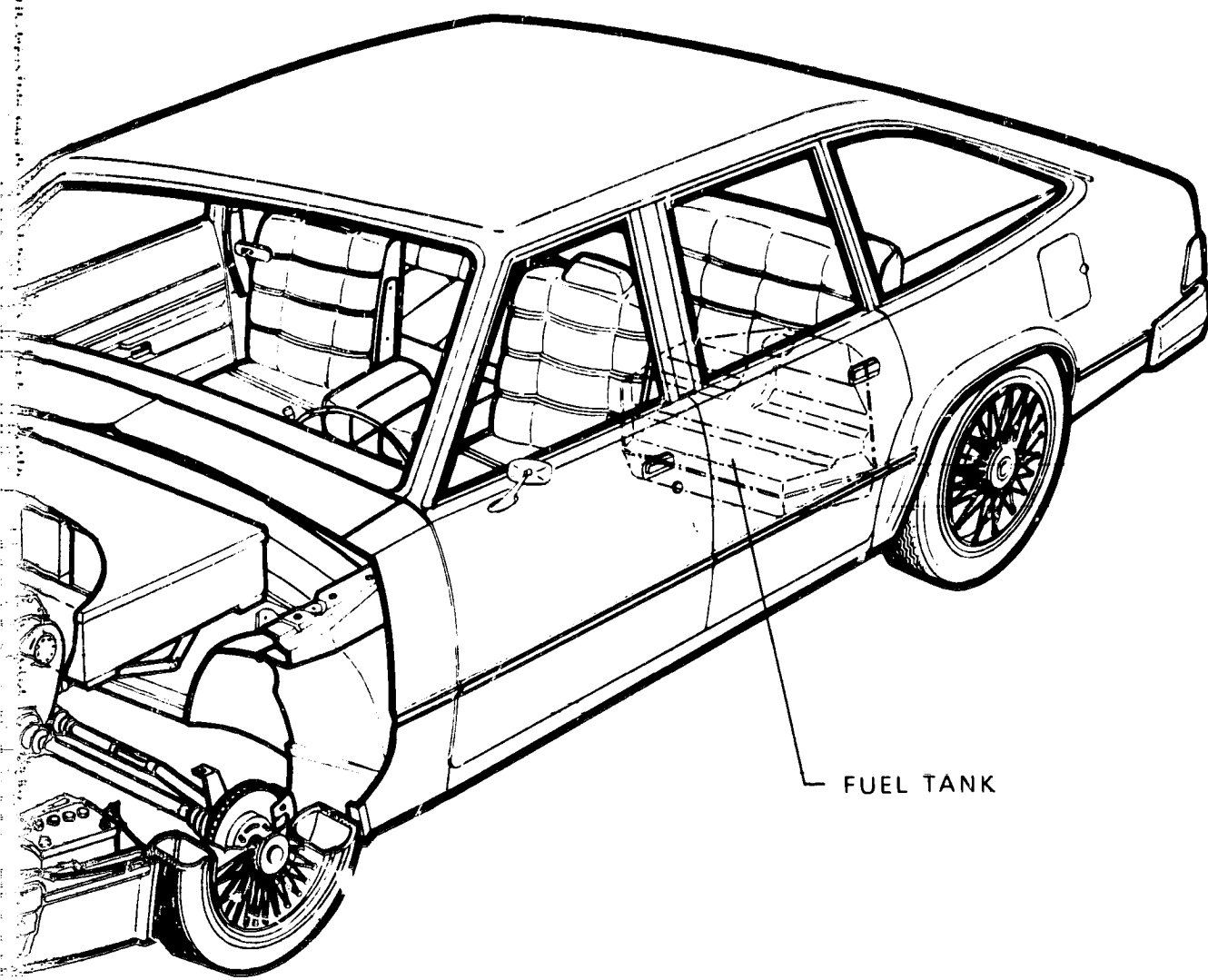
FUEL TANK

MOTOR

brid Vehicle, Three-Dimensional Cutaway
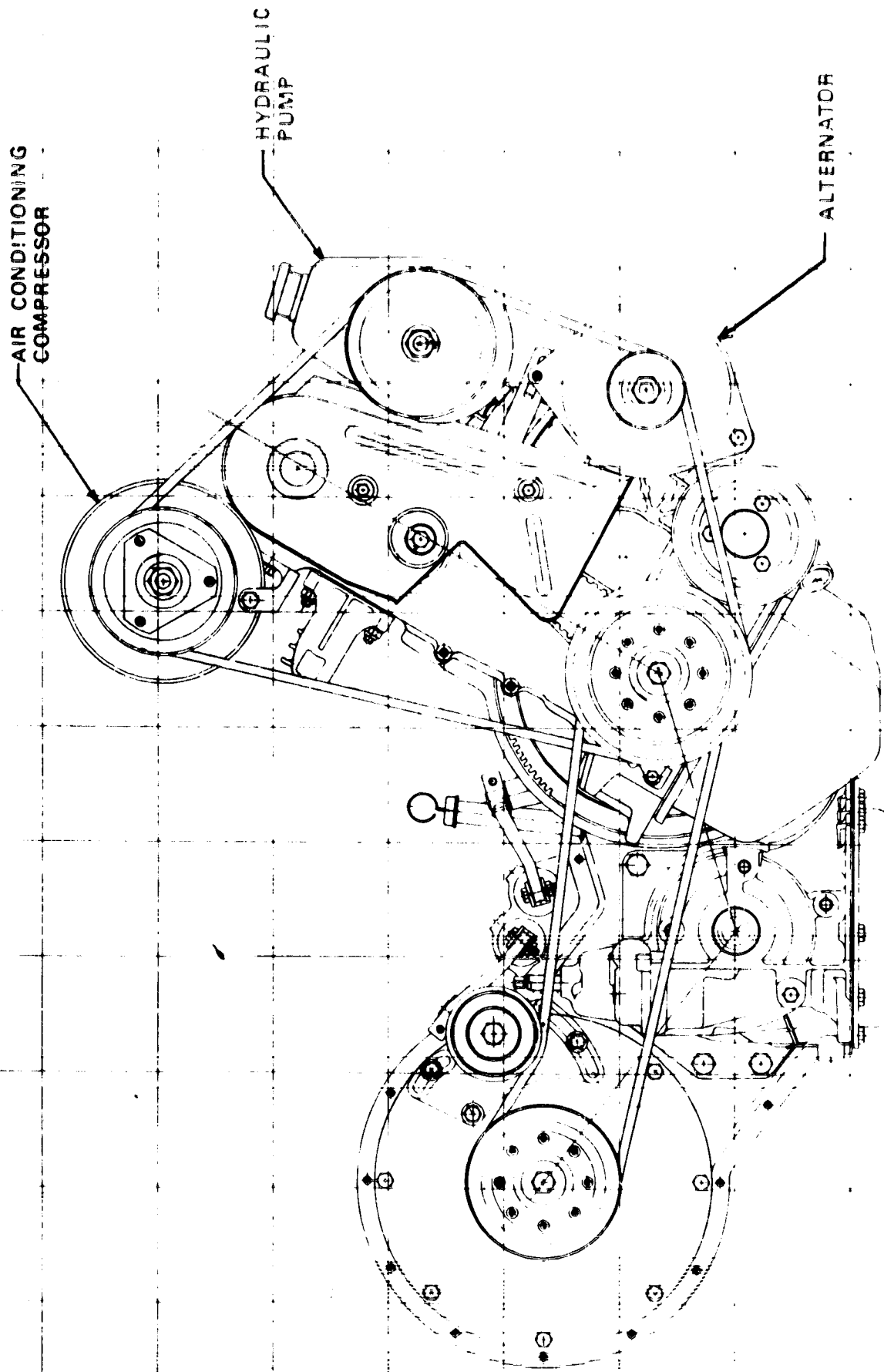
Figure I-3a. Transmission, Clutch, and Controls, Right Side View

AIR CONDITIONING COMPRESSOR

HYDRAULIC PUMP

ALTERNATOR

CLUTCH ACTUATION MECH.

1.6 LITER VW ENGINE

SEC. B-B

℄ HEAT ENG.

℄ TRANS

℄ ELEC. MOTOR

A
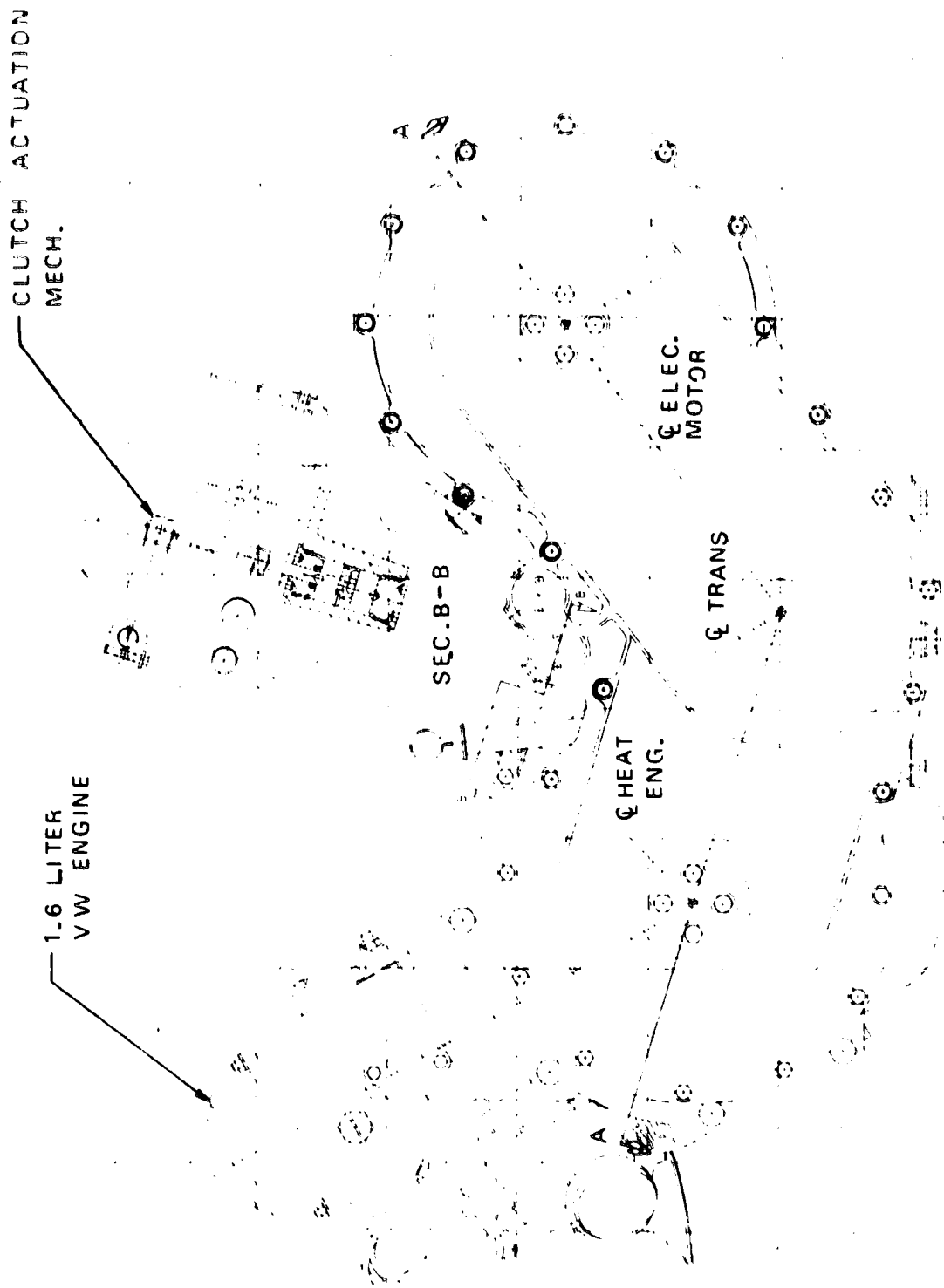
Figure I-3b. Transmission, Clutch, and Controls, Left Side View

GENERAL ELECTRIC
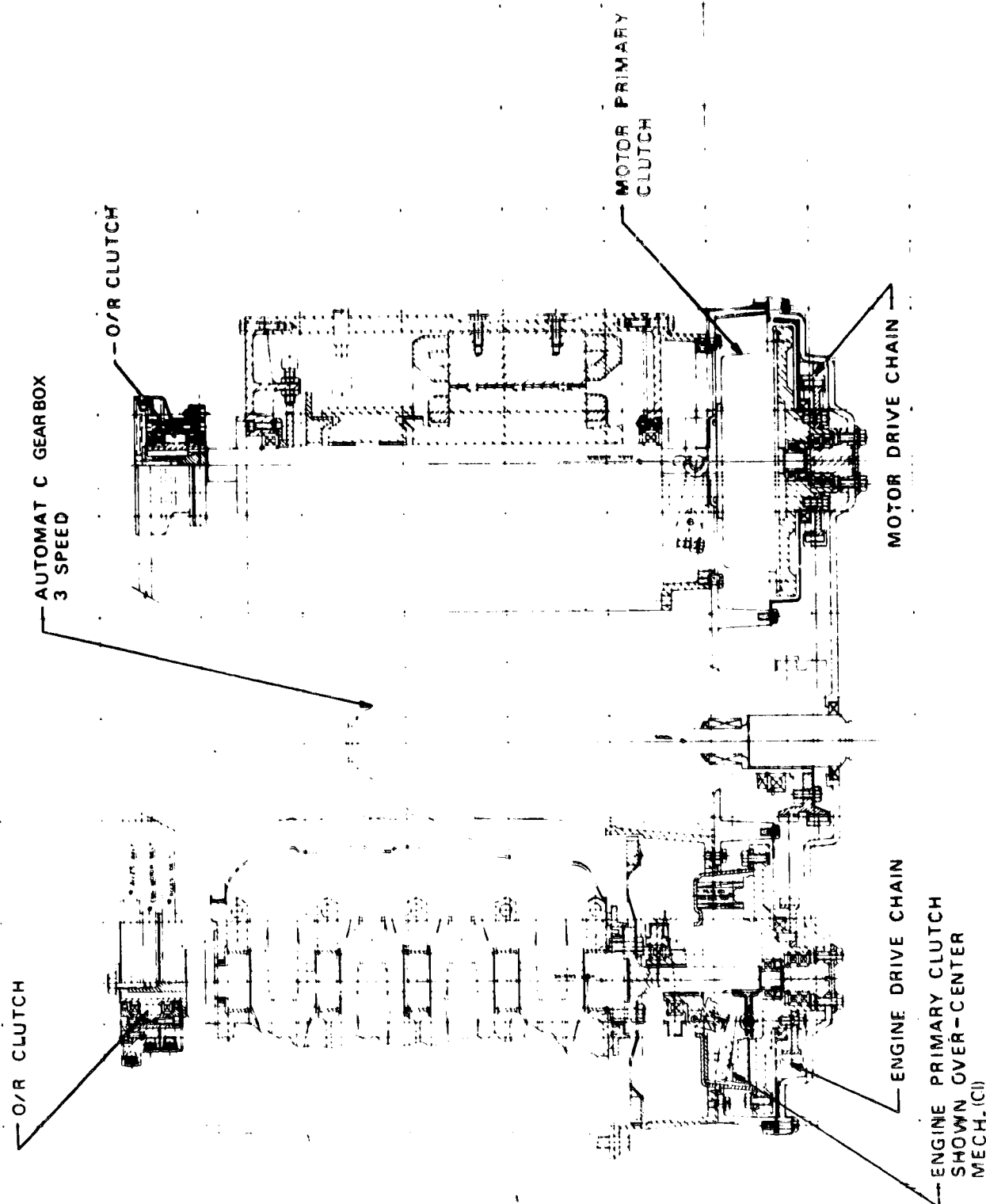
Figure I-3c. Transmission, Clutch, and Controls, Section A-A

I-27

WATER/AIR
HEAT EXCHANGER

GASOLINE BURNING
HEATER

EVAPORATOR

BLOWER

COMPRESSOR
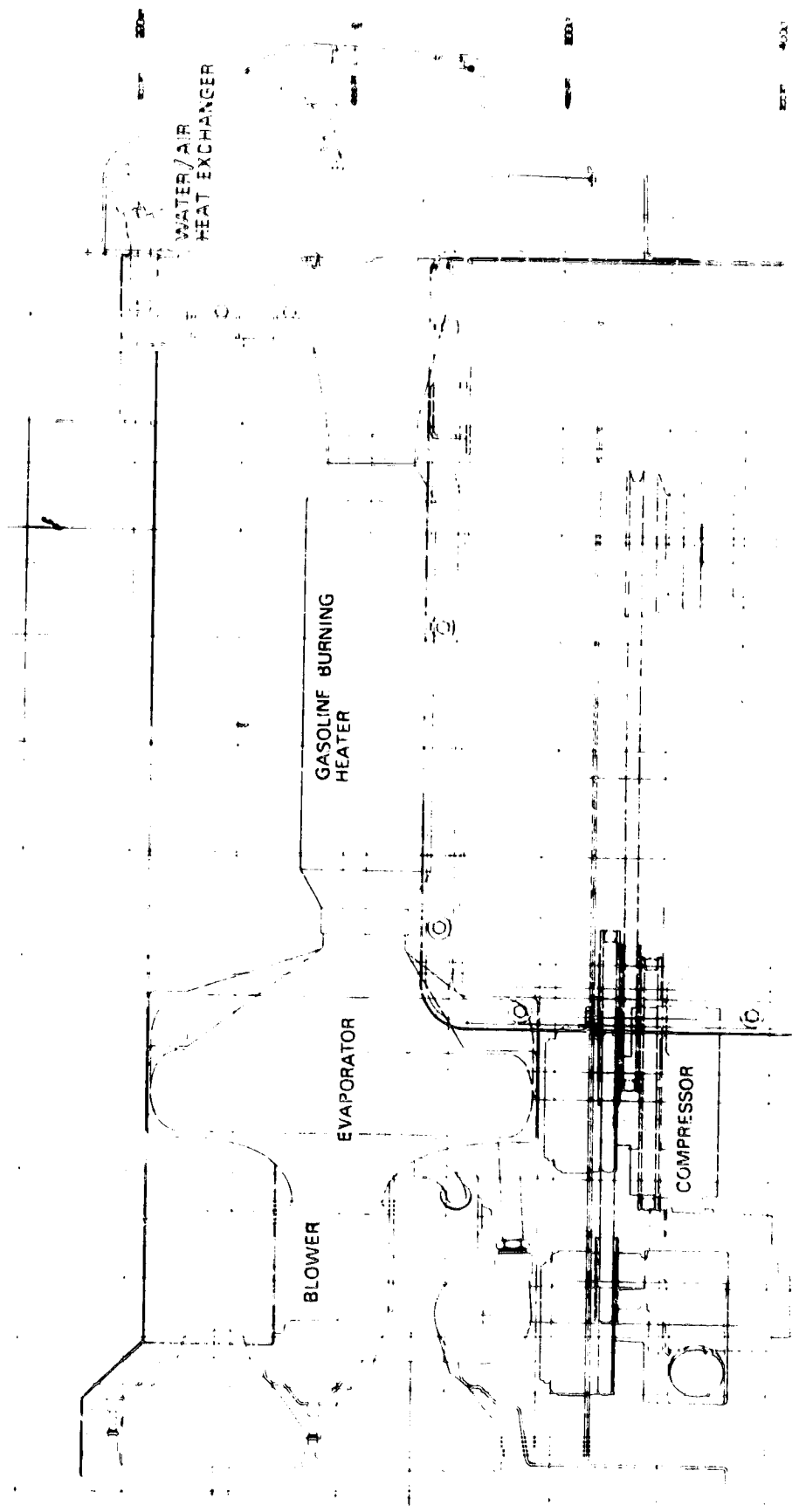
Figure i-4a. Heating, Ventilating, and Air-Conditioning Package, Plan View

HVAC SYSTEM

GASOLINE BURNING
HEATER

EVAPORATOR

BLOWER
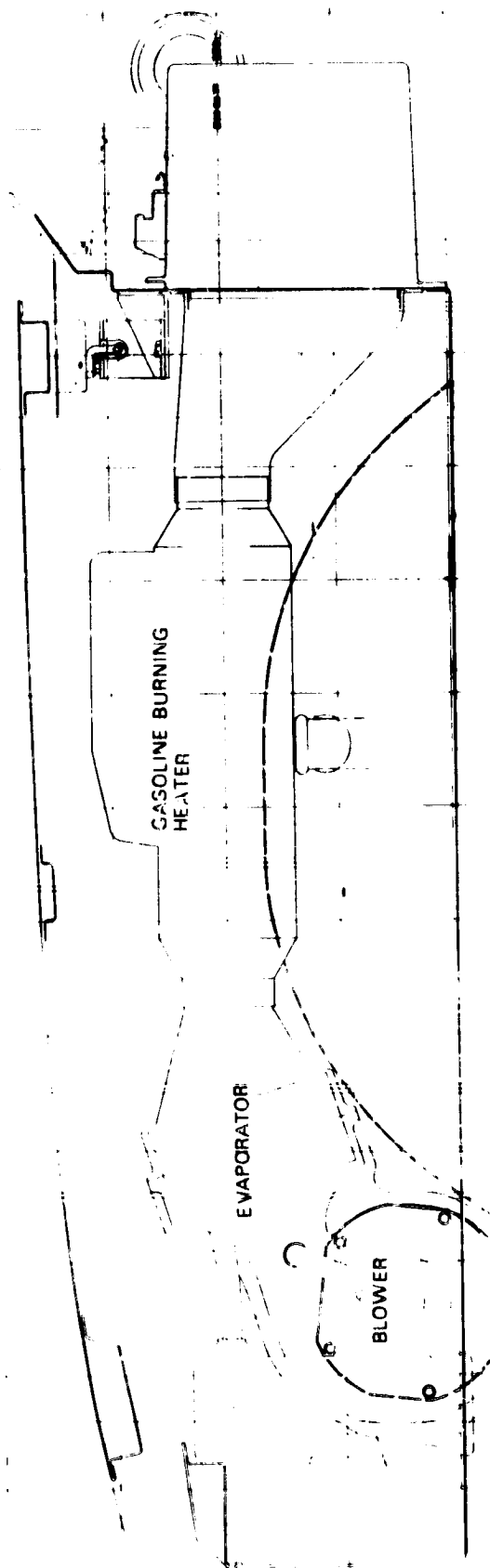
Figure I-4b. Heating, Ventilating, and Air-Conditioning Package, Left Side View

CHEVROLET MALIBU

NEWLY STYLED NOSE

NEW FRONT STRUCTURE
WITH CATWALK

FOLDOUT FRAME
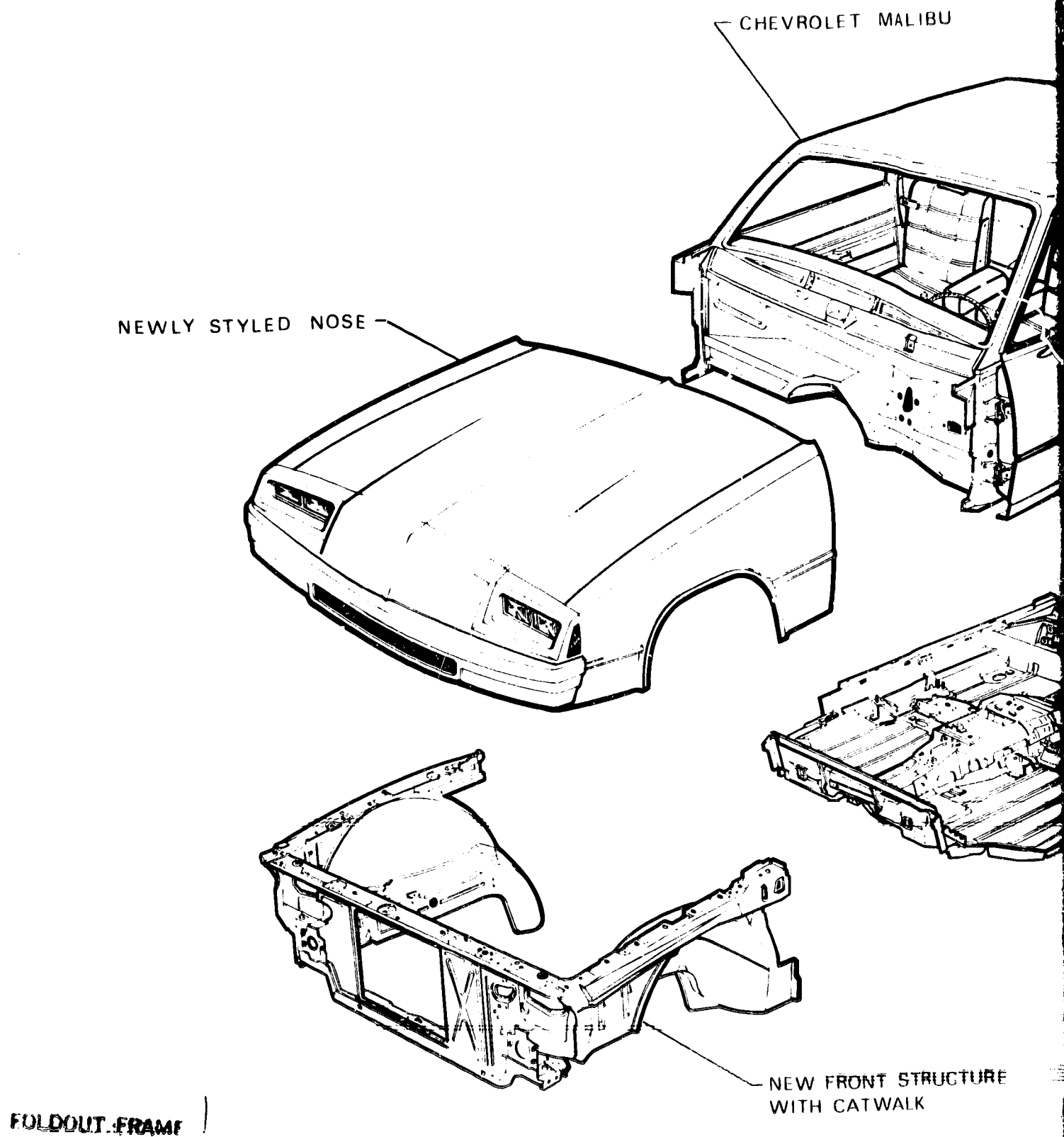
Figure I-5. Hybrid Vehicle Body Struct

VROLET MALIBU

NEW REAR
HATCHBACK
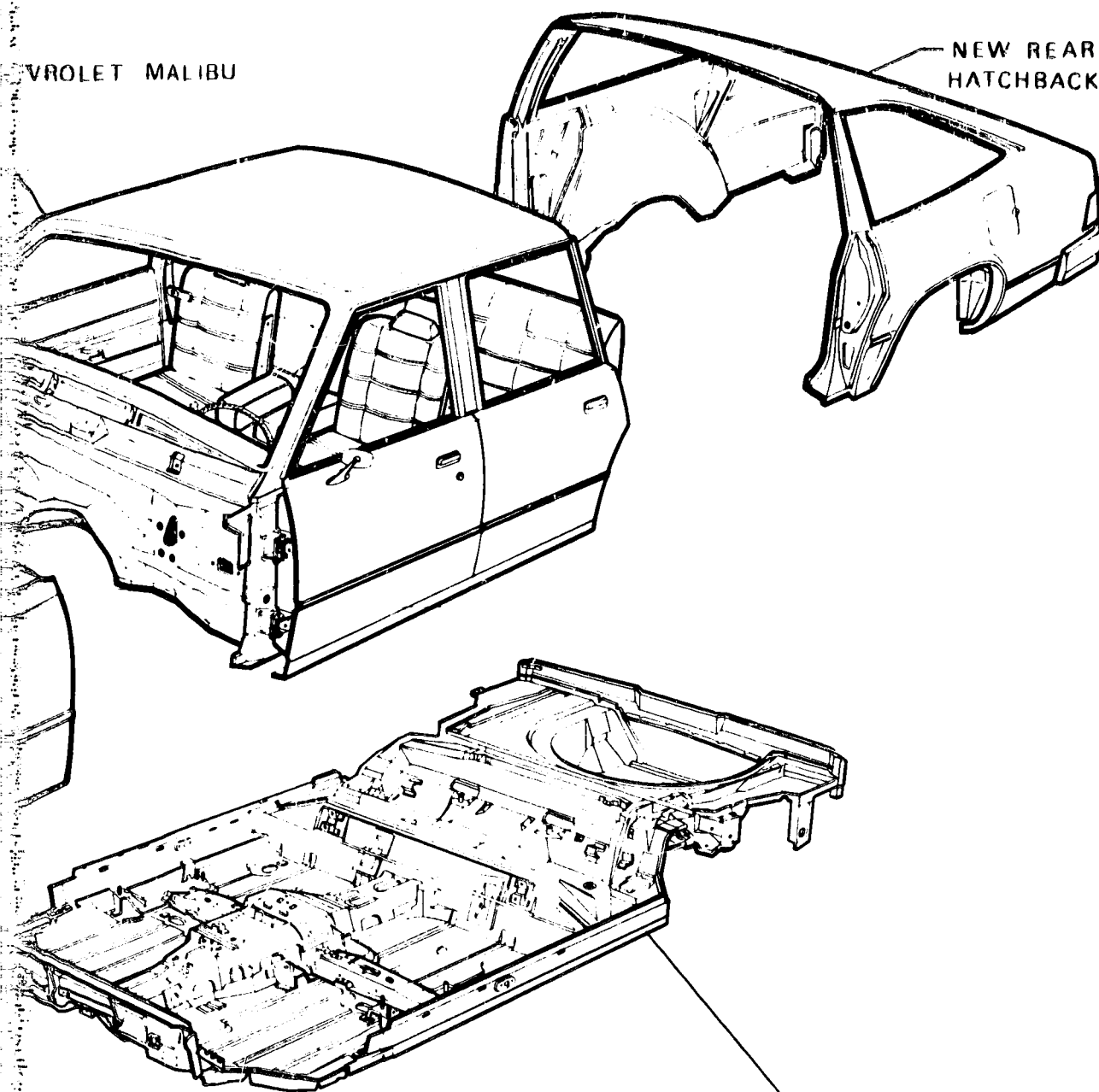
NEW UNDERBODY

FRONT STRUCTURE
CATWALK

Vehicle Body Structure, Exploded View
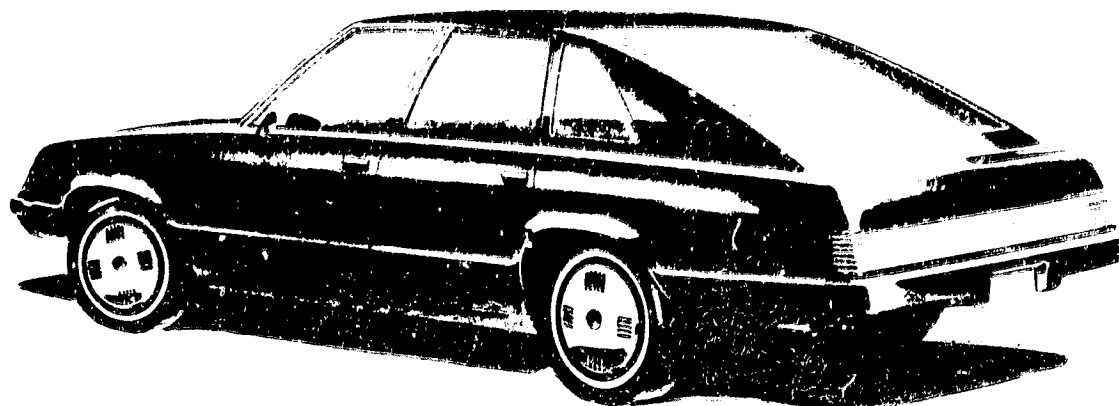
Figure I-6.   Artist's Rendering of the Hybrid Vehicle -
               Left Rear Quarter View
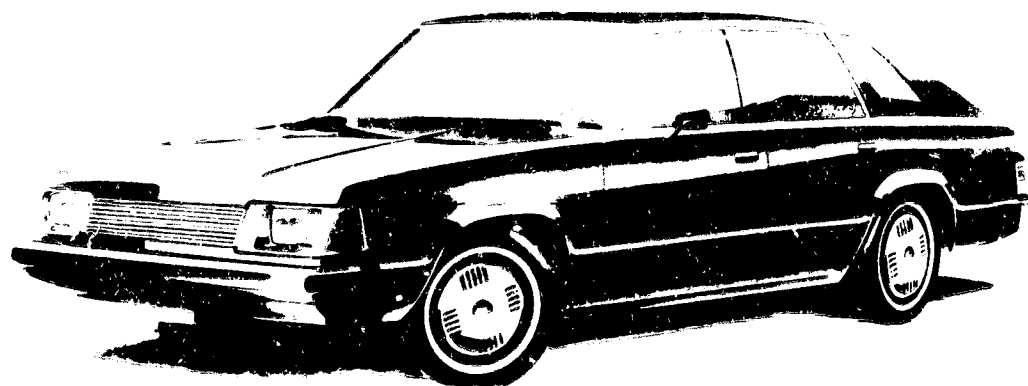
Figure I-7.   Artist's Rendering of the Hybrid Vehicle -
               Left Front Quarter View
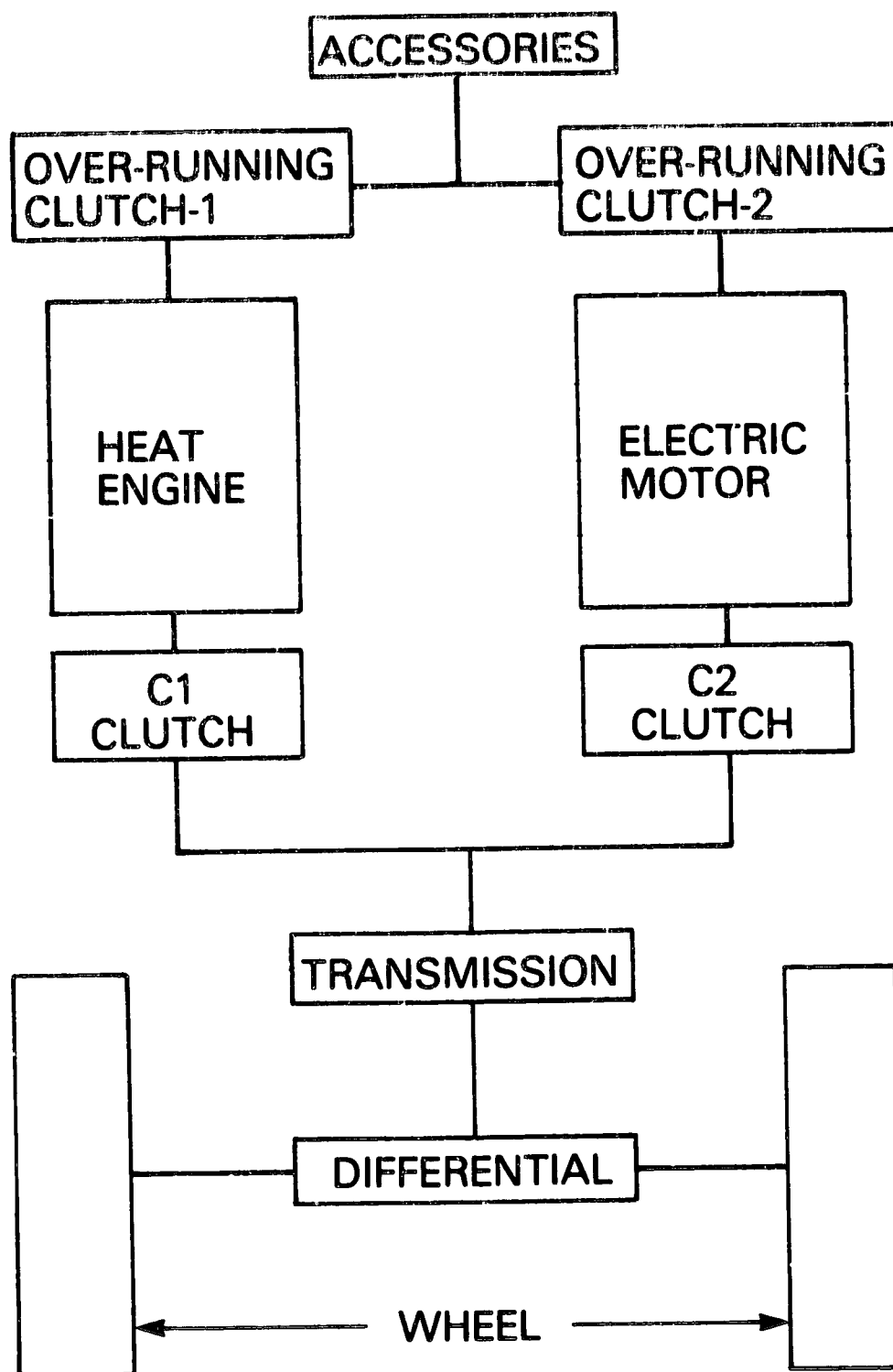
Figure I-8.   Schematic of Drive Package

Appendix II

VEHICLE RIDE AND HANDLING AND FRONT STRUCTURAL CRASHWORTHINESS ANALYSIS

Appendix II

**VEHICLE RIDE AND HANDLING AND FRONT
STRUCTURAL CRASHWORTHINESS ANALYSIS**

II.1 INTRODUCTION

Preliminary vehicle ride calculations were made in conjunction with a linear range handling analysis in order to verify that the hybrid vehicle would exhibit response characteristics similar to those of contemporary ICE vehicles. A computer study was conducted to provide a preliminary assessment of the crashworthiness potential of the hybrid vehicle frontal structure.

II.2 RIDE RATES

Ride character is established by the ride frequency. In an attempt to match the ride character of the Chevrolet Malibu (the Reference ICE Vehicle), the front and rear ride frequencies were measured and determined to be 1.16 Hz and 1.35 Hz, respectively.

The front frequency was matched exactly as a starting point. Since the vehicle has a different pitch inertia, the rear ride frequency for the hybrid was calculated by obtaining a similar pitch response. This calculation resulted in a rear ride frequency for the hybrid of 1.9 Hz. The large difference in rear ride frequency to attain the same vehicle ride as the Malibu is due to the more forward location of the vehicle's center of gravity and the differences in the pitch inertia.

II.3 HANDLING ANALYSIS

An analysis of the line ~ range handling characteristics of the hybrid vehicle was made in order to determine its steady state and transient responses to a steer input. The model utilized includes all suspension geometry and compliance effects. The inertial properties of the vehicle, as well as the linear range properties of the tires, were also included.

At this stage of the design process, all of the suspension parameters (bushing rates, for example) are not known exactly, and some estimates must be made based on measurements of suspension parameters from vehicles with similar suspension systems. Additionally, the tire characteristics, which alone are one of the most critical variables in the system, can only be estimated because the tires to be utilized on the final vehicle have not yet been determined. The results of this analysis, however, proved to be very significant because they illustrated that the hybrid vehicle as proposed herein will exhibit handling responses similar to those of other vehicles in its class.

II.3.1 RESULTS

The results of the handling analysis are summarized below in tabular form. The input data for the handling calculations are listed in Table II-1 and are shown graphically in Figures II-1 and II-2.

PARAMETER	DRIVER ONLY	FULL RATED LOAD
Roll Gain, Deg/g	7.05	8.01
Control Sensitivity @ 60 mph, $Ft/Sec^2/Deg$	2.99	2.97
Vehicle Total Understeer, Deg/g	8.61	8.70
Characteristic Speed, mph	29.9	29.7
Yaw Velocity Response Time, Sec	.101	.098
Lateral Acceleration Response Time, Sec	.304	.329
Sideslip Response Time, Sec	.338	.356

II.3.2 INTERPRETATION OF RESULTS

The usual range of roll gain for American passenger cars is 6 to 10 degrees per g., while control sensitivities usually fall between 2 and 7 ft/sec²/deg at 60 mph. Characteristic speeds for passenger cars are normally in the range of 25 to 40 miles per hour. At 60 miles per hour, yaw velocity response times are usually less than 0.2 second with lateral acceleration and sideslip responses usually below 0.5 second. Low response times are desirable since the vehicle will tend to feel more stable with little driver tendency to overcontrol.

All the handling parameters for the hybrid vehicle fall into the normal ranges cited for American passenger cars. Hence, the handling of the hybrid vehicle should be satisfactory.

II.4 FRONT STRUCTURAL CRASHWORTHINESS ANALYSIS

In order to provide a preliminary assessment of the crashworthiness of the hybrid vehicle's frontal structure and drive component placement, a computer study was conducted. Utilizing the preliminary design package configuration, a series of vehicle collision simulations were made to evaluate the vehicle crash environment for a 30 mile per hour frontal barrier impact. The computer study was done by MGA Research Corporation using their lumped mass vehicle collision simulation program (SMDYN) which is described in Section II.5.

Table II-1

INPUT DATA FOR HANDLING ANALYSIS

Variable	Definition	Units	Magnitude
W_f	Total weight on front wheels of the vehicle	lb	2704
W_r	Total weight on rear wheels of the vehicle	lb	1306
W_{uf}	Front unsprung weight	lb	309
W_{ur}	Rear unsprung weight	lb	274
L	Wheelbase	in.	108
h_f	Front roll center height above road plane	in.	1.67
h_r	Rear roll center height above road plane	in.	12.89
h_{uf}	Front unsprung weight cg height above road plane	in.	12.58
h_{ur}	Rear unsprung weight cg height above road plane	in.	12.98
h_t	Total vehicle cg height above road plane	in.	23.18
I_{xx}^s	Sprung mass roll inertia about origin on roll axis below cg of total vehicle	$lb\text{-}sec^2\text{-}ft$	805.3
I_{zz}^s	Sprung mass yaw inertia about origin on roll axis below cg of total vehicle,	$lb\text{-}sec^2\text{-}ft$	1561.7
I_{zz}^u	Unsprung mass yaw inertia about origin on roll axis below cg of total vehicle	$lb\text{-}sec^2\text{-}ft$	478.4
I_{xz}^s	Sprung mass product of inertia about origin of roll axis below cg of total vehicle	$lb\text{-}sec^2\text{-}ft$	0
D_f	Front roll damping coefficient	ft-lb-sec/deg	23
D_r	Rear roll damping coefficient	ft-lb-sec/deg	9.8
K_f	Front roll stiffness	ft-lb/deg	5.70
K_r	Rear roll stiffness	ft-lb/deg	375
$\Gamma_{\phi f}$	Front roll camber coefficient (+ understeer)		+.91
$\Gamma_{\phi r}$	Rear roll camber coefficient (+ understeer)		0
$E_{\phi f}$	Front roll steer coefficient (+ understeer)		+.06
$E_{\phi r}$	Rear roll steer coefficient (+ understeer)		0
E_{Nf}	Front aligning torque deflection steer per wheel (+ understeer)	deg/100 ft-lb	+1.5
E_{Yf}	Front lateral force deflection steer per wheel (+ understeer)	deg/1000 lb	+.6
Γ_{Nf}	Front aligning torque deflection camber per wheel (+ understeer)	deg/100 ft-lb	+.02
Γ_{Yf}	Front lateral force deflection camber per wheel (+ understeer)	deg/1000 lb	+1.2
E_{Nr}	Rear aligning torque deflection steer per wheel (+ understeer)	deg/1000 ft-lb	=.3
E_{Yr}	Rear lateral force deflection steer per wheel (+ understeer)	deg/100 ft-lb	-.1
Γ_{Nr}	Rear aligning torque deflection camber wheel (+ understeer)	deg/1000 ft-lb	-.1
Γ_{Yr}	Rear lateral force deflection camber per wheel (+ understeer)	deg/1000 lb	-2.0
$C_{\alpha f}$	Front tire cornering stiffness for one tire (always positive)	lb/deg	293

Table II-1 (continued)

Variable	Definition		
$c_{\alpha r}$	Rear tire cornering stiffness for one tire (always positive)	lb/deg	180
$c_{\gamma f}$	Front tire camber stiffness for one tire (positive)	lb/deg	40
$c_{\gamma r}$	Rear tire camber stiffness for one tire (positive)	lb/deg	23
$N_{\alpha f}$	Aligning torque per unit slip angle for one front tire (positive)	ft-lb/deg	56
$N_{\alpha r}$	Aligning torque per unit slip angle for one rear tire (positive)	ft-lb/deg	11
$N_{\gamma f}$	Aligning torque per unit camber angle for one front tire (positive)	ft-lb/deg	3
$N_{\gamma r}$	Aligning torque per unit camber angle for one rear tire (positive)	ft-lb/deg	3
$L_{\alpha f}$	Overturning moment per unit slip angle for one front tire (positive)	ft-lb/deg	32
$L_{\alpha r}$	Overturning moment per unit slip angle for one rear tire (positive)	ft-lb/deg	30
$L_{\gamma f}$	Overturning moment per unit camber angle for one front tire (positive)	ft-lb/deg	24
$L_{\gamma r}$	Overturning moment per unit camber angle for one rear tire (positive)	ft-lb/deg	21
A_{Yss}	Steady state lateral acceleration selected by user (should not exceed 10 ft/sec^2)	ft/sec^2	10.0
x	Distance from front wheel center to lateral acceleration measurement point (positive for points behind wheel center)	in.	57.3
z	Distance from road plane to lateral acceleration measurement point (positive for points above road plane)	in.	19.8
u	Forward velocity	mph	60
Δt	Printing time increment for transient response (not to exceed .1 sec)	sec	.05
t_{max}	Total time interval for transient response	sec	1.25
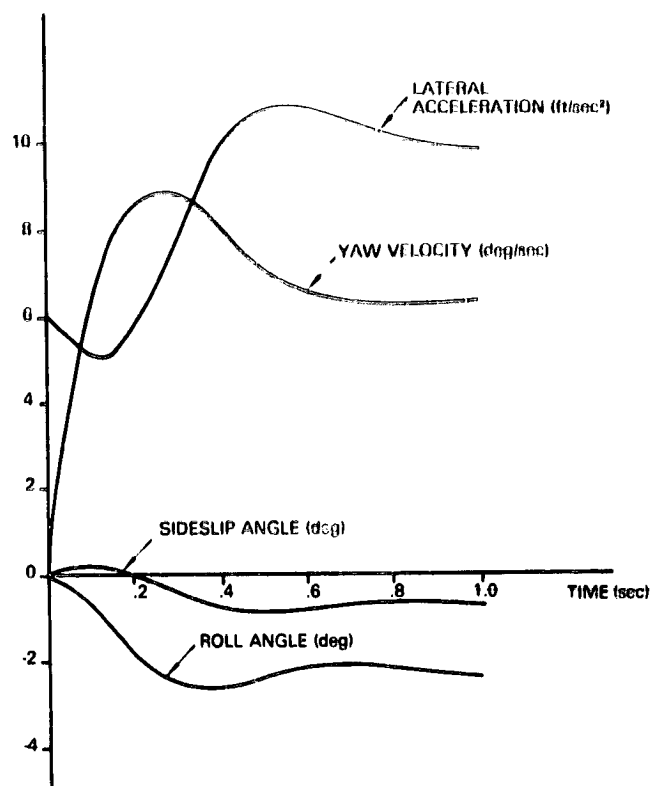
Figure II-1. Transient Response to Steer Input Hybrid Vehicle - Driver Only
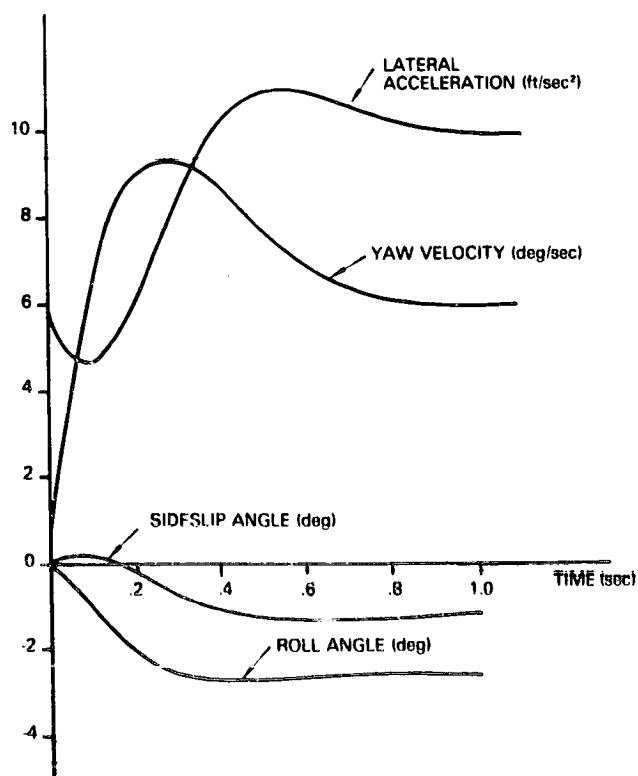
Figure II-2. Transient Response to a Steer Input Hybrid Vehicle - Full Load

II-5

GENERAL ⊛ ELECTRIC

The methodology used was based on the assumptions that the hybrid's occupant compartment would be identical to that of the 1978 Chevrolet Malibu and that occupant survivability in the hybrid configuration could be insured if the hybrid's crash environment was found comparable to that of the Malibu compliance test crash data results. The following approach was used. First, compliance test crash data was obtained for a 1978 Chevrolet Malibu. This data provided the basis of comparison for evaluating the proposed hybrid configuration. Second, since static crash data was not available for the base car structure, data from similar sized vehicles was employed in the SMDYN model in order to duplicate the known vehicle collision performance. Modifications were made on the crash data based on engineering judgments to achieve a match between simulation results and the known base car deceleration pulse.

The front structural elements used in the simulations are representative of existing automotive designs and represent structural elements which can be packaged into the hybrid. Further investigations are necessary to determine the actual structural design; however, the slight modifications necessary to fine-tune the elements should not create problems within the constraints of the hybrid's front structure.

Once the base simulation was completed, a series of calculations were made to study the following component configurations as variables:

- Longitudinal and transverse heat engine package, without a battery pack
- Both engine configurations with battery pack installed behind the heat engine
- Various battery pack crash characteristics
- Structural component changes
- Variations in vehicle weight

From the analysis results, it was found that a transverse heat engine layout can result in crash performance similar to that currently provided by the Chevrolet Malibu. However. the longitudinal heat engine package cannot achieve this objective within the dimensional constraints of the preliminary design.

II.4.1 CONCLUSIONS

The following conclusions were derived from the study based on data/information available at the time of the study. In some cases the data is not directly applicable to the proposed hybrid. However, trends shown as a result of the study are valid.

1. The Transverse Drive System (TDS) package shows much greater promise of affording crash protection comparable to that of the conventional car than does the Longitudinal Drive System (LDS). The

LDS could afford similar levels of protection, but would require a major redesign to obtain more structural crush space.

2. For both drive configurations, the maximum intrusion into the passenger compartment occurred in the tunnel area as a result of the heat engine and associated drive components. This area of the body structure should receive a high level of emphasis during Phase II.

3. Increasing the structural resistance (while maintaining reasonable values within the state-of-the-art automotive technology) reduces passenger compartment intrusion without significantly affecting the peak deceleration levels of the TDS Hybrid.

4. Battery pack intrusion into the passenger compartment was not a serious problem. It appears that the TDS layout can achieve a desired objective of preventing such intrusion. However, further test information is required for the interaction between the transverse heat engine and battery pack.

5. Although occupant response was not addressed directly in this study, it seems likely that a hybrid vehicle design which paid careful attention to crashworthiness would satisfy FMVSS 208 injury criteria for fully restrained occupants. This conclusion is based on the reasonably similar passenger compartment decelerations for the Chevrolet Malibu and the TDS strengthened structure, and on the occupant injury levels recorded in the G.M. "A" Body tests.

Trends resulting from the computer simulation runs become very apparent when the maximum deceleration is plotted against maximum intrusion (Figure II-3). Most evident is the clear separation of the LDS and TDS configurations, with the LDS results tending toward both higher intrusion and higher peak decelerations. Irrespective of the absolute validity of these results, it is clear that the longitudinal drive system will be much more difficult to package for crash protection than the transverse system unless significantly greater crushing space is made available.

II.4.2 ANALYSIS RESULTS

Vehicle crash test information was obtained by MGA which summarizes the results of 30 mph frontal barrier collisions of a 1978 Malibu four-door coupe and a 1978 Oldsmobile Cutlass Salon two-door coupe. Both tests were conducted with belted part 572 dummies in the front outboard seating position.

The average passenger compartment decelerations are shown in Figure II-4 and the injury criteria along with other significant measurements are shown in Table II-2. Note that all established injury criteria for FMVSS 208 are satisfied in both baseline tests. The maximum dynamic crush of the Malibu was 27.8 inches, and of the Cutlass, approximately 30.0 inches. The corresponding reduction in compartment space (intrusion) was 2.9 inches in the driver's toe board area for the Malibu and 6.0 inches in the passenger's toe board area for the Cutlass.
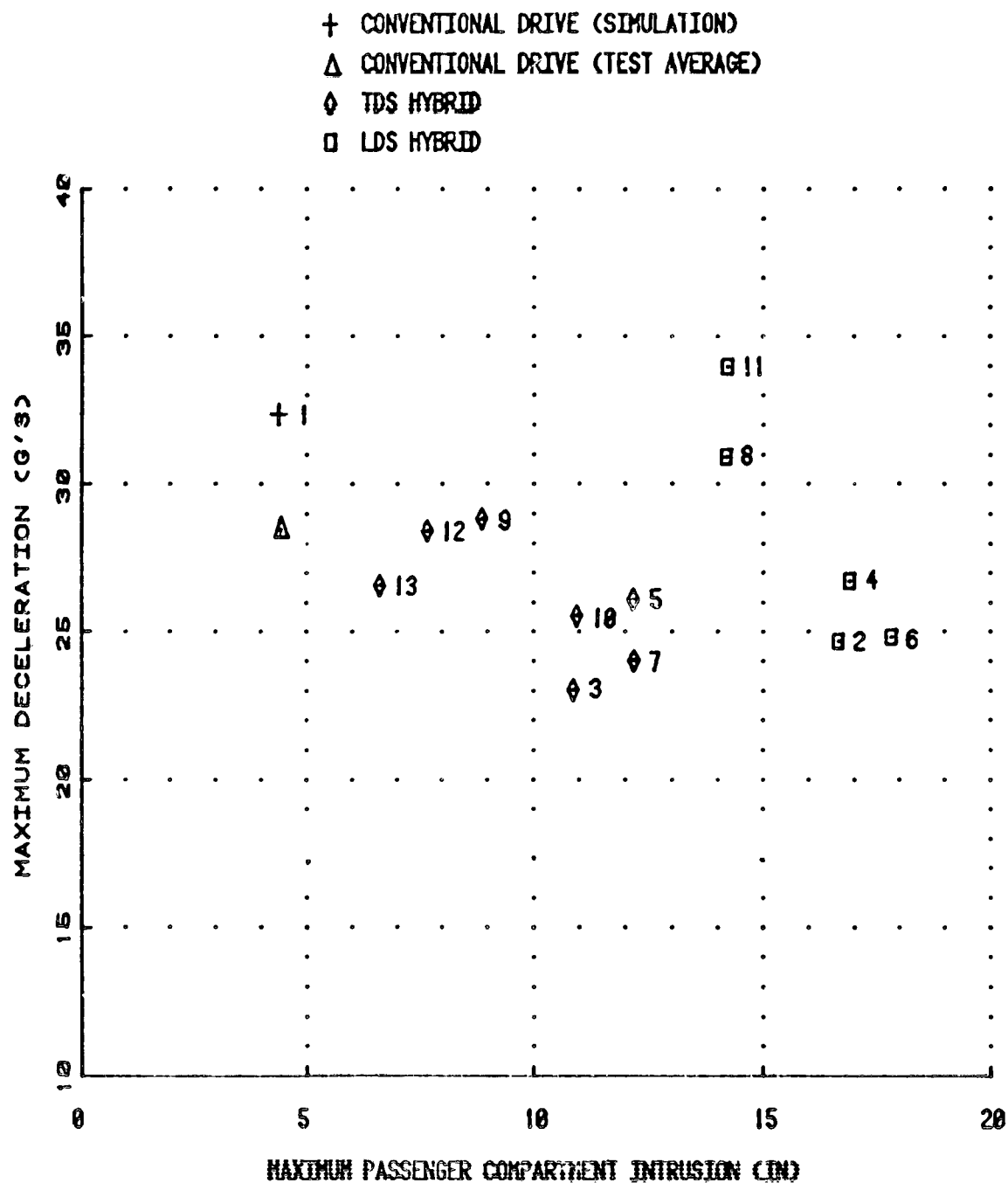
Figure II-3. Maximum Deceleration as a Function
of Maximum Intrusion (Refer to
Table II-3 for Run Identification)
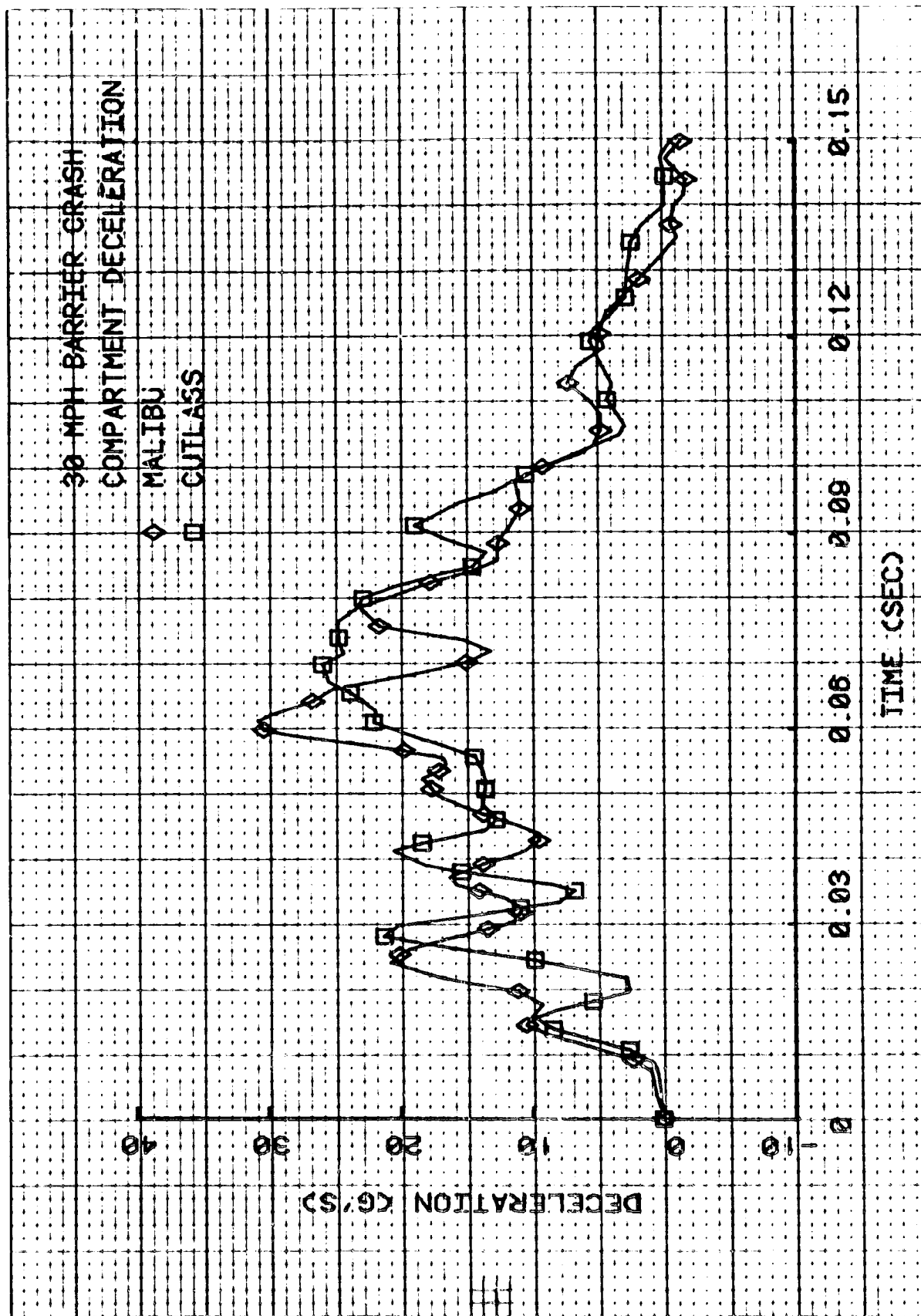
Figure II-4. G.M. "A" Body Crash Test Results

Table II-2

SUMMARY OF INJURY CRITERIA

	1978 Chevrolet Malibu		1978 Oldsmobile Cutlass	
	Driver	Passenger	Driver	Passenger
Peak Resultant Head Acceleration (g)	102.9	54.0	115.3	68.5
Peak Resultant Chest Acceleration (g)	41.4	31.1	39.2	39.4
Head Injury Criteria (HIC)	931.0	588.6	759.5	828.2
Gadd Severity Index (GSI)	392.8	236.7	289.5	316.2
Peak Femur Loads: Left (lb)	538.6	239.6	233.6	185.8
Right (lb)	452.2	537.6	307.8	585.3
Peak Belt Loads: Lap (lb)	1684.5	1375.2	1709.	1736.
Torso (lb)	1356.0	1377.7	1320.	1739.

Since the proposed hybrid design will be based on a Malibu occupant compartment, the vehicle should meet applicable standards if the deceleration waveform and intrusion levels do not exceed those observed in these test results.

Utilization of the SMDYN mathematical model requires structural strength data as input. Crush test data was not available for a G.M. "A" Body car, so estimates were used based on static data from a 1974 Ford Torino.

A schematic diagram of the baseline Malibu model is shown in Figure II-5. The basic structural force-deflection profiles used are plotted as Figure II-6. Some structural properties were adjusted to provide a better agreement between the predicted and measured compartment deceleration values. These adjustments consisted of a 20% reduction of the rear rail force level and a decrease in an early spike in the front frame from 49,000 lb to 29,000 lb at 4.0 inches of deformation. A comparison of the final predictions with the test results for the Malibu is shown in Figure II-7. The maximum dynamic crush predicted by the simulation was 28.8 inches with a firewall crush of 4.4 inches.

Data was available for a VW Rabbit radiator and engine frontal structure (Figure II-8). This data was used as input in the TDS Model with the appropriate clearances for the hybrid package.

In order to provide for the battery crush characteristics, a single 6 volt lead-acid battery was statically crushed (Figure II-9). Since the battery layout included two banks of individual batteries, one in front of the other, an optimum condition was hypothesized in which the front and rear batteries crushed simultaneously at the same force levels. This was designated the soft battery condition and results in the same force level at twice the deflections of the single battery crush.

Twelve SMDYN simulations were run of hybrid vehicle configurations. Five of these were of the LDS (longitudinal) and seven of the TDS (transverse) configurations. Table II-3 identifies the runs made and lists some significant results obtained from each run.

From a crashworthiness point of view, there are two functions that a vehicle structure serves:

- Protecting the occupants of the vehicle from excessive deformation of the passenger compartment.

- Protecting the occupants of the vehicle from excessive deceleration levels.

If we consider the base Malibu configuration results to be the goal for the proposed hybrid design, the TDS configuration shows great promise and with additional effort would probably be successful.
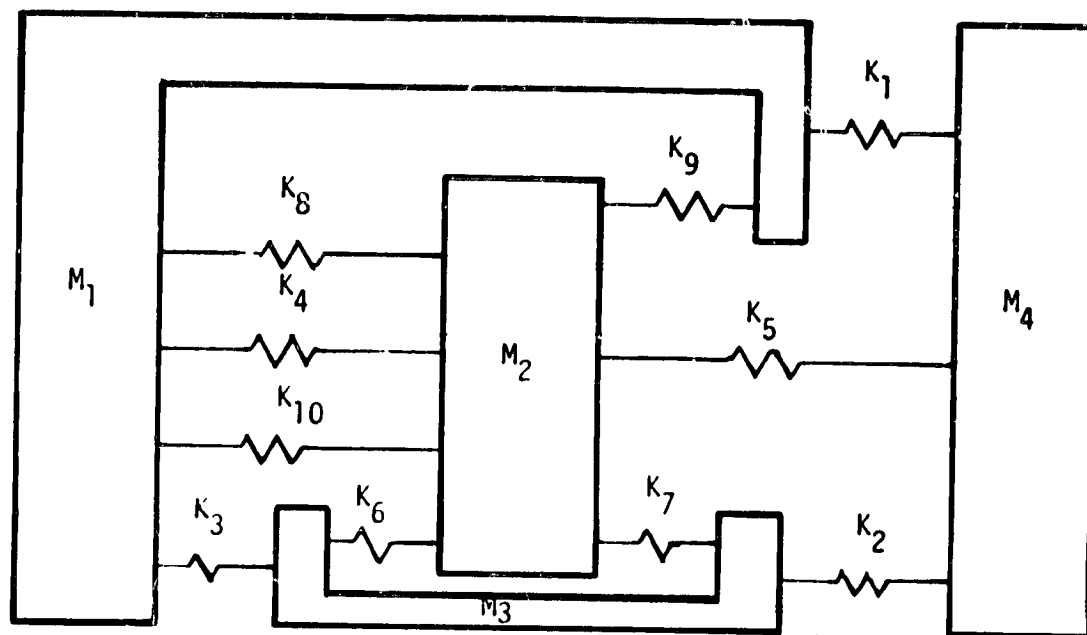
M_1	-	body
M_2	-	engine
M_3	-	cross member
M_4	-	barrier
K_1	-	upper sheet metal
K_2	-	front frame rails
K_3	-	rear frame rails
K_4	-	firewall
K_5	-	radiator/engine front
K_6	-	engine mount (forward)
K_7	-	engine mount (rearward)
K_8	-	transmission mount (forward)
K_9	-	transmission mount (rearward)
K_{10}	-	drive line

Figure II-5. Schematic of Conventional Vehicle Model
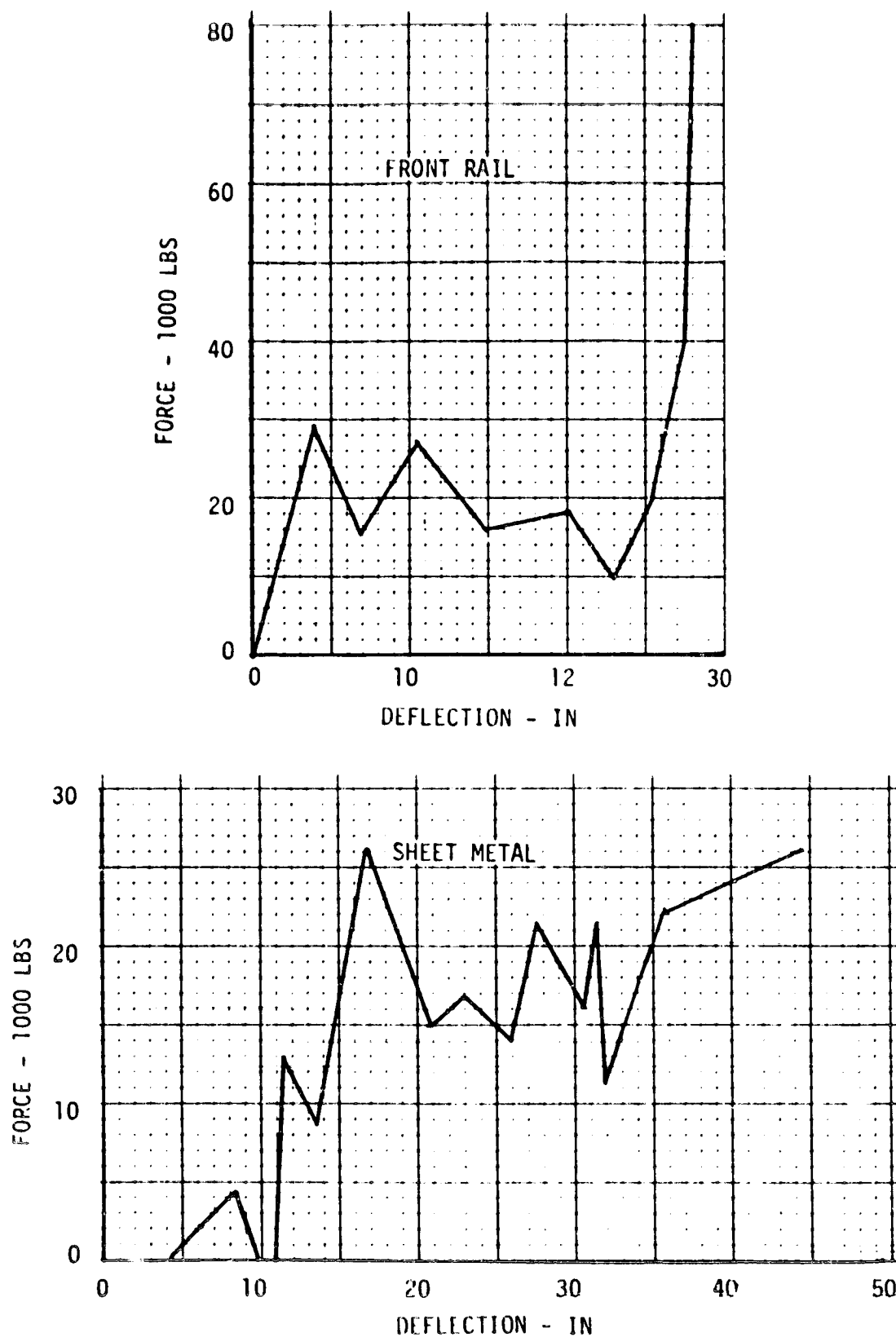
Figure II-6a. Baseline Structural Characteristics
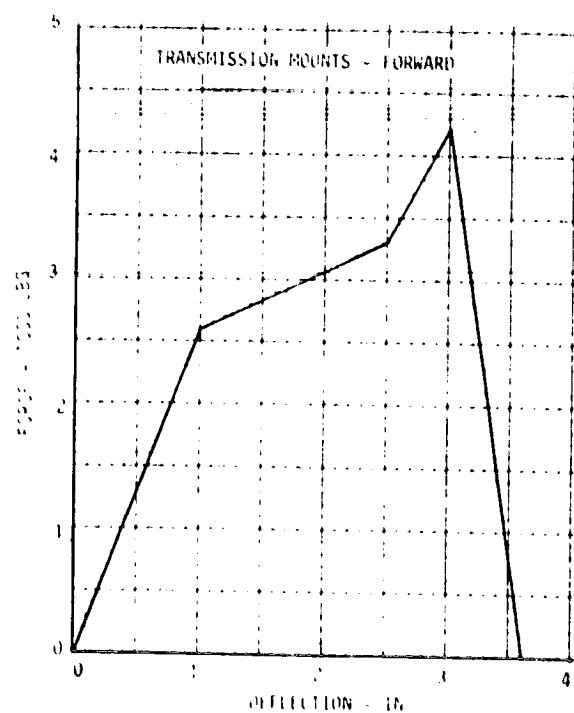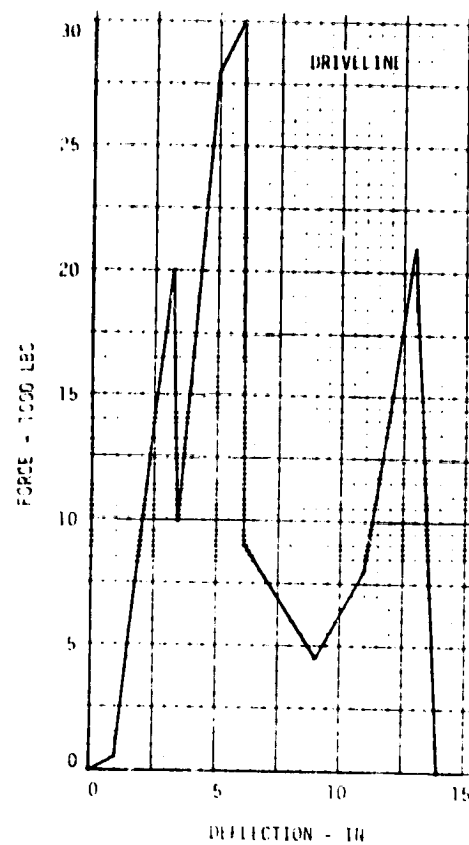
Figure II-6b.   Baseline Structural Characteristics

GENERAL ELECTRIC
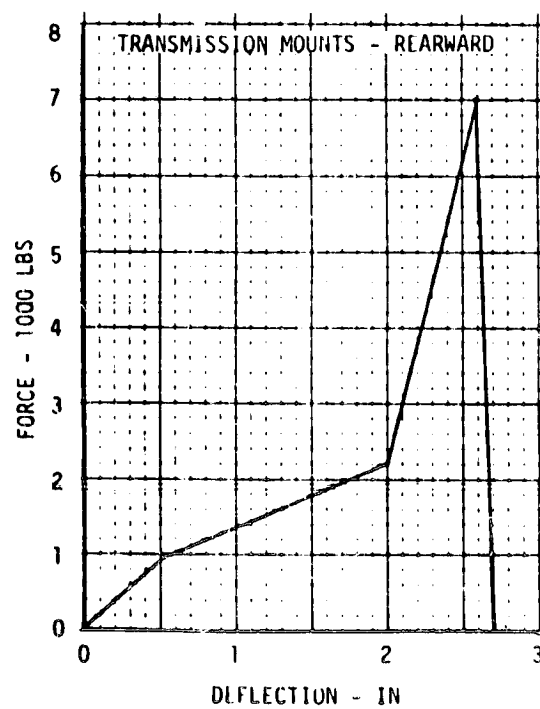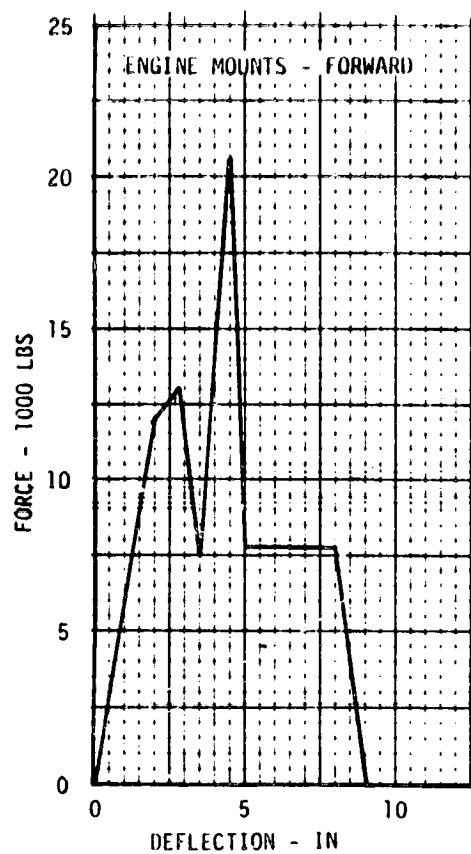
Figure II-6c.   Baseline Structural Characteristics

II-15
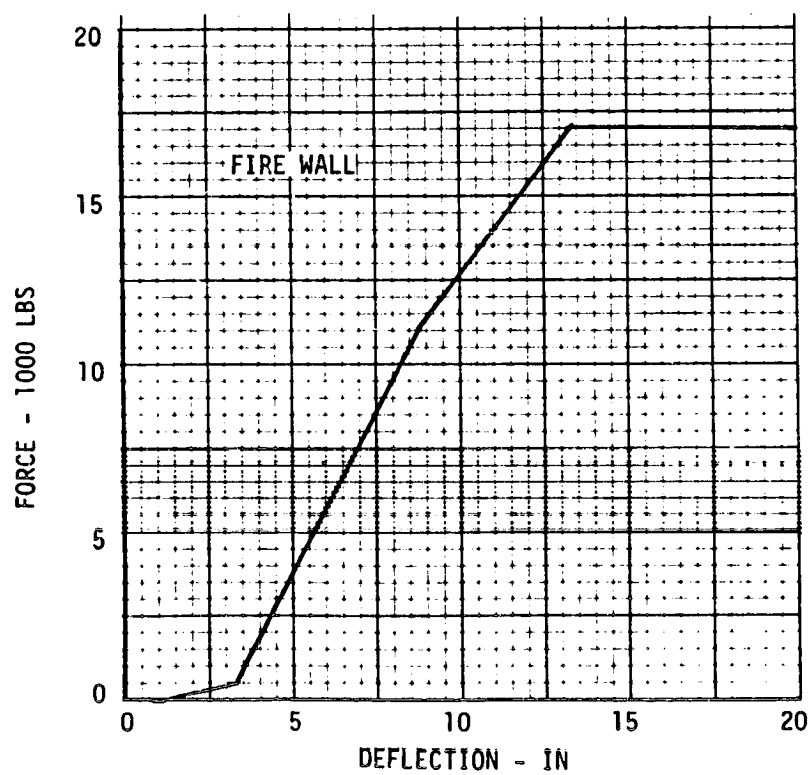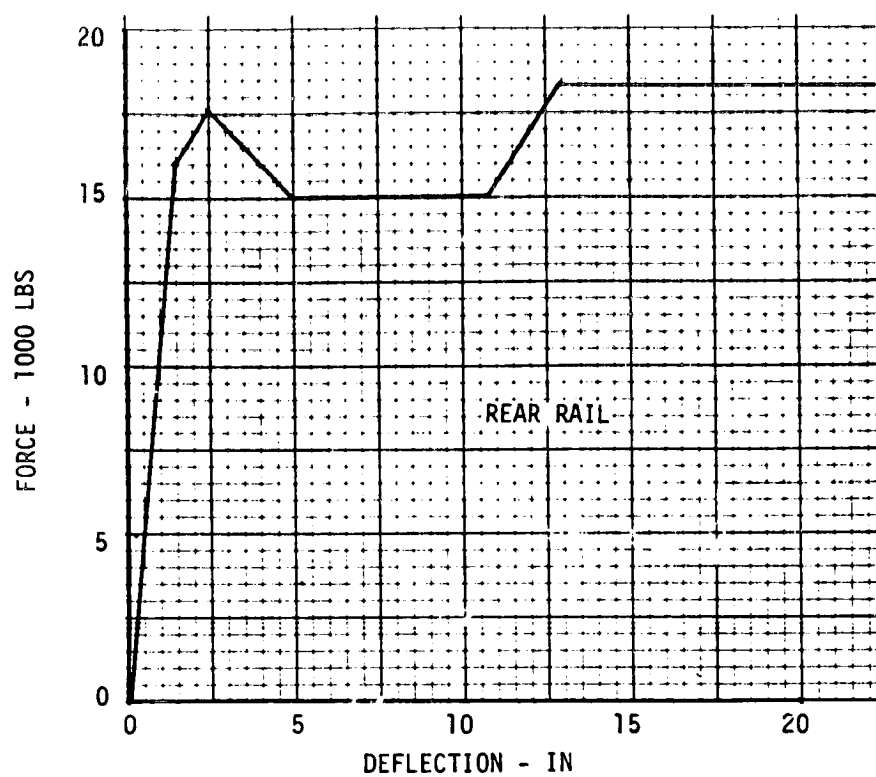
Figure II-6d.   Baseline Structural Characteristics
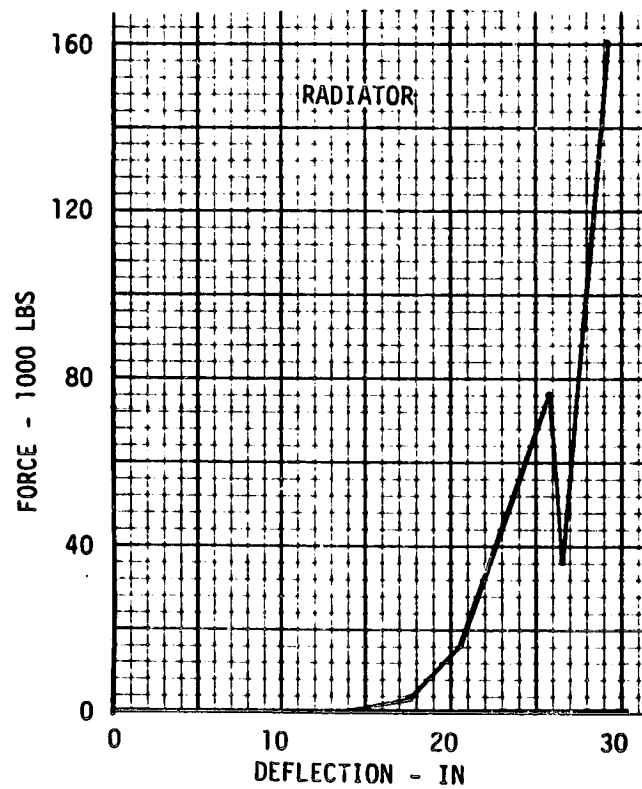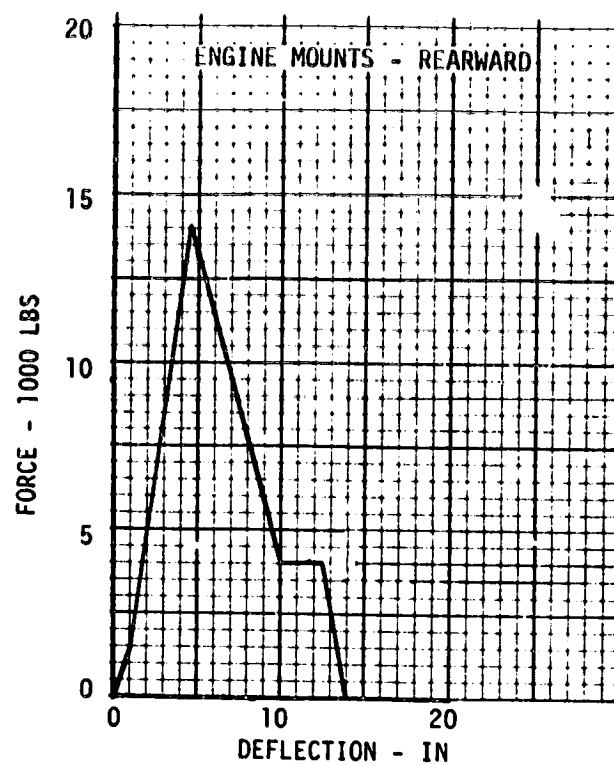
Figure II-6e. Baseline Structural Characteristics
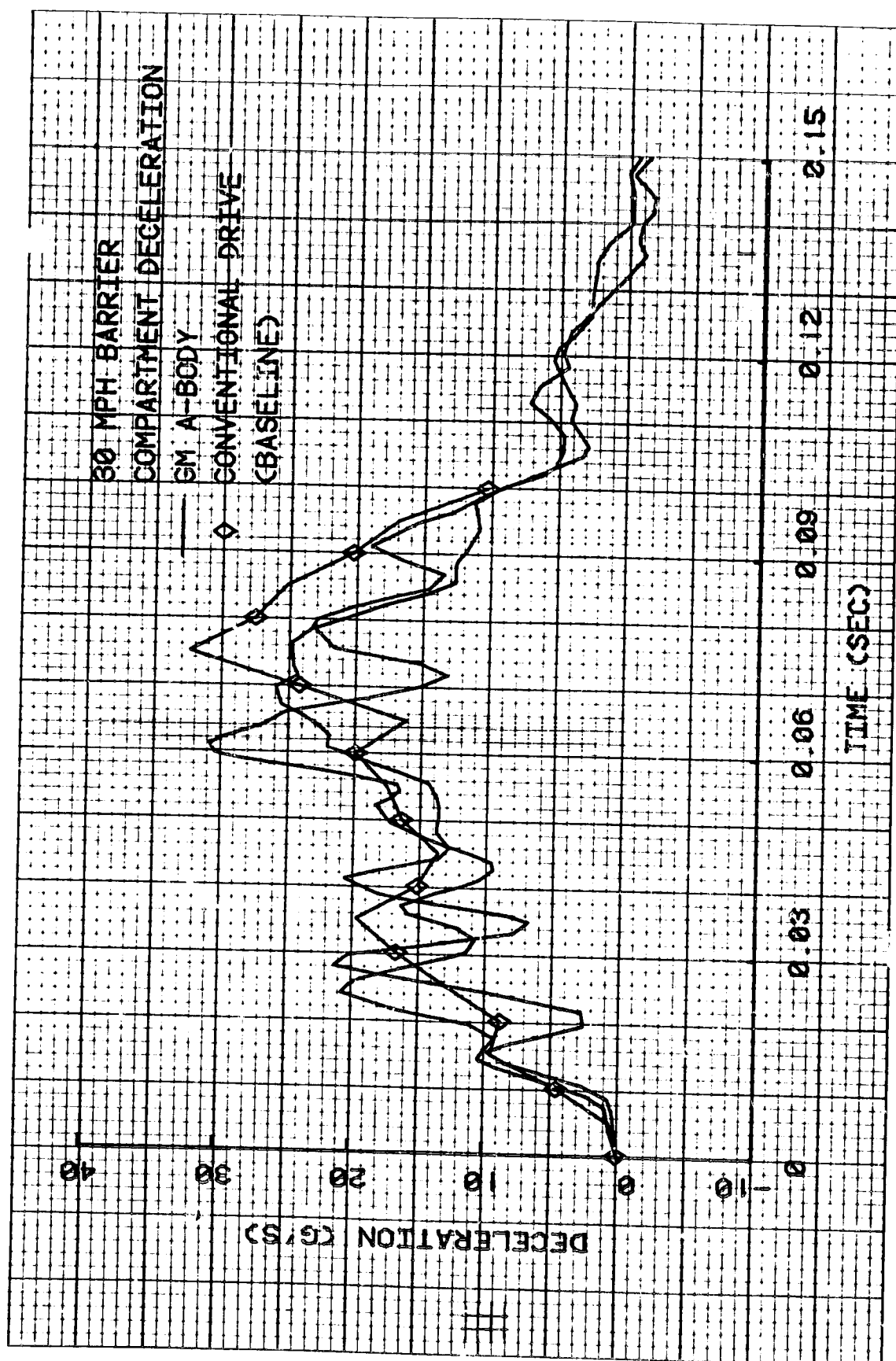
Figure II-7.   Comparison of Conventional Drive Baseline Run and Test Results
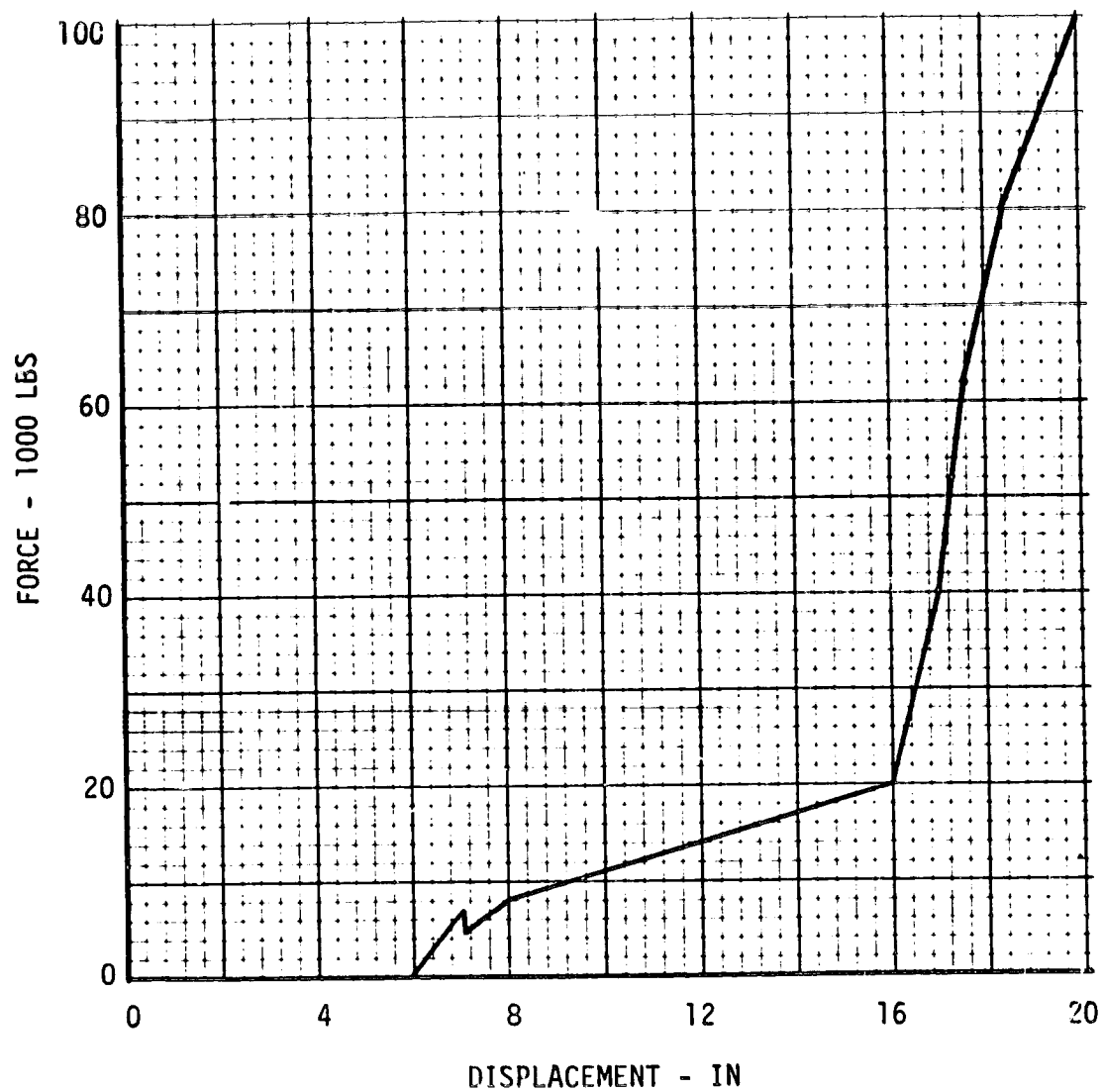
Figure II-8.   VW Rabbit Radiator/Engine Crush Data

GENERAL ELECTRIC
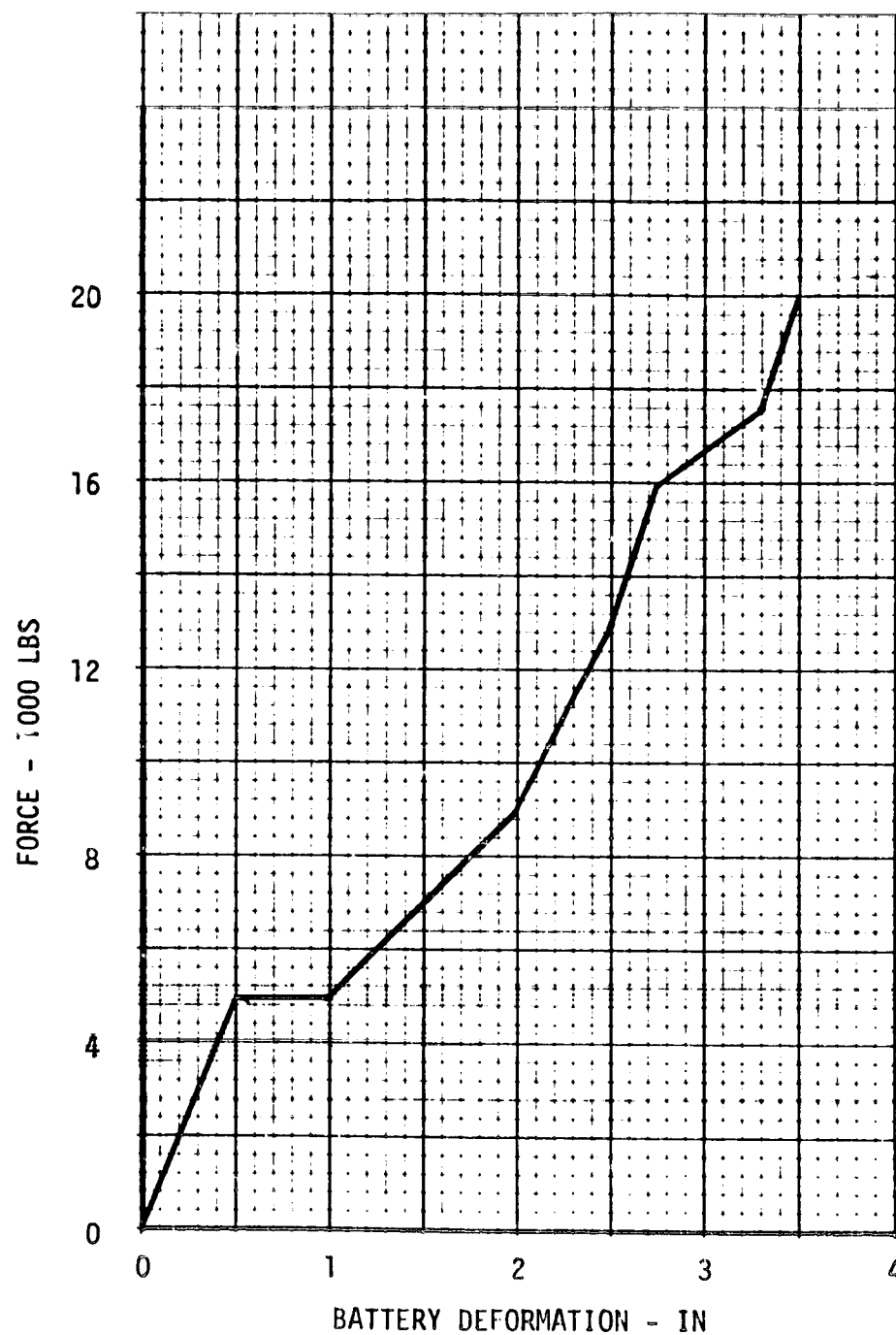
Figure II-9. Single Battery Crush Data

II-20

Table II-3

SUMMARY OF SIMULATION RESULTS

RUN NO.		Maximum Deceleration (G)	Maximum Crush (in.)	Drive System Intrusion (in.)	Battery Intrusion (in.)
1	Conventional Drive	32.35	28.76	4.38	----
2	LDS Hybrid - No Batteries	24.67	25.82	16.64	----
3	TDS Hybrid - No Batteries	23.01	28.99	10.87	----
4	LDS Hybrid - STD Batteries	26.72	26.90	16.9	7.46
5	TDS Hybrid - STD Batteries	26.09	30.88	12.17	4.97
6	LDS Hybrid - Soft Batteries	24.81	27.00	17.82	3.45
7	TDS Hybrid - Soft Batteries	24.01	30.94	12.18	1.52
8	Light LDS Hybrid	30.90	23.81	14.18	4.46
9	Light TDS Hybrid	28.83	27.68	8.86	1.43
10	TDS Hybrid - Strengthened Frame	25.53	29.96	10.94	3.65
11	Light LDS Hybrid Strengthened Frame	33.97	22.82	14.21	2.02
12	Light LDS Hybrid Strengthened Frame	28.42	26.27	7.66	0.2
13	Light TDS Hybrid Strengthened Structure	26.58	24.80	6.61	0.0

Figure II-10 is a schematic representation of the hybrid model. Included are plots of the representative simulation runs. A comparison of the deceleration waveforms with and without battery packs for the longitudinal and transverse driveline arrangements is shown in Figures II-11a and II-11b. A preliminary indication of the effect of battery crush characteristics is illustrated in Figures II-12a and II-12b. riation in battery crush strength does not result in a signific. _ change in compartment deceleration for either driveline configuration.

In an effort to reduce the passenger compartment intrusion levels, additional runs were made increasing the strength levels of the frontal structure. This strengthened structure included a 20% increase in the front sheet metal and frame elements. The effect of this change is shown in Figures II-13a and II-13b for the lightweight vehicle (4000 lb) and Figure II-14 for the 470ᵤ lb configuration.

Of the hybrid vehicle configurations simulated, the most promising in achieving the same level of crash protection (judged by deceleration waveform and compartment intrusion) as provided by the baseline Chevrolet Malibu was the transverse drive system arrangement with frame rails and sheet metal crush strength increased 20% above that shown in Figure II-15. A direct comparison of deceleration waveforms achieved with this configuration and with the baseline G.M. "A" Body is shown in Figure II-16.

II.5 SPRING-MASS SIMULATION (SMDYN)

SMDYN is a rather simple (in concept) computer program that treats a physical automobile structure as a one-dimensional representation, idealized in the form of discrete (lumped) masses interconnected by massless, deformable elements characterized by force-deflection properties. The model is general in nature allowing a large number of discrete masses with totally flexible connectivity. Each specific application requires the definition of lumped masses and resistive elements to approximate the physical characteristics of the structural system under consideration. Figure II-17, for example, illustrates a typical modeling approach for simulation of an automobile impacting a rigid barrier.

The program is implemented in the BASIC computer language and inputs required include the magnitude, initial displacement, and velocity of each discrete mass, and a definition of the connectivity and force-deflection properties (for both loading and unloading) of each resistive element. Schematic diagrams of various collision models typically studied are shown in Figure II-18.

Force-deflection properties of specific resistive elements can be obtained by static crush testing of the corresponding physical structures. Crush testing techniques have been developed that facilitate isolation, proper collapse mode control, and measurement of the force-deflection properties of various automotive structural elements.
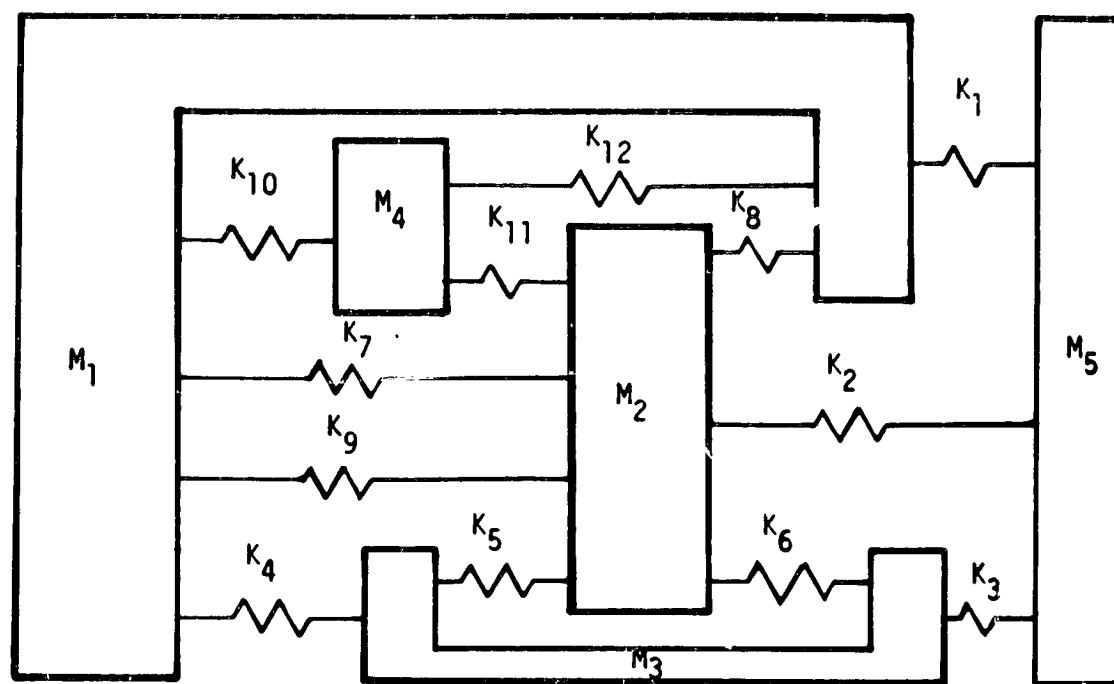
M_1	–	body	K_4	–	rear frame rails
M_2	–	engine/drive system	K_5	–	engine mount (rearward)
M_3	–	cross member/unsprung mass	K_6	–	engine mount (forward)
M_4	–	battery	K_7	–	transmission mount (rearward)
M_5	–	barrier	K_8	–	transmission mount (forward)
K_1	–	upper sheet metal	K_9	–	drive system/firewall
K_2	–	radiator/engine front	K_{10}	–	battery/firewall
K_3	–	front frame rails	K_{11}	–	engine/battery
			K_{12}	–	battery containment structure

Figure II-10.   Schematic of Hybrid Drive Models
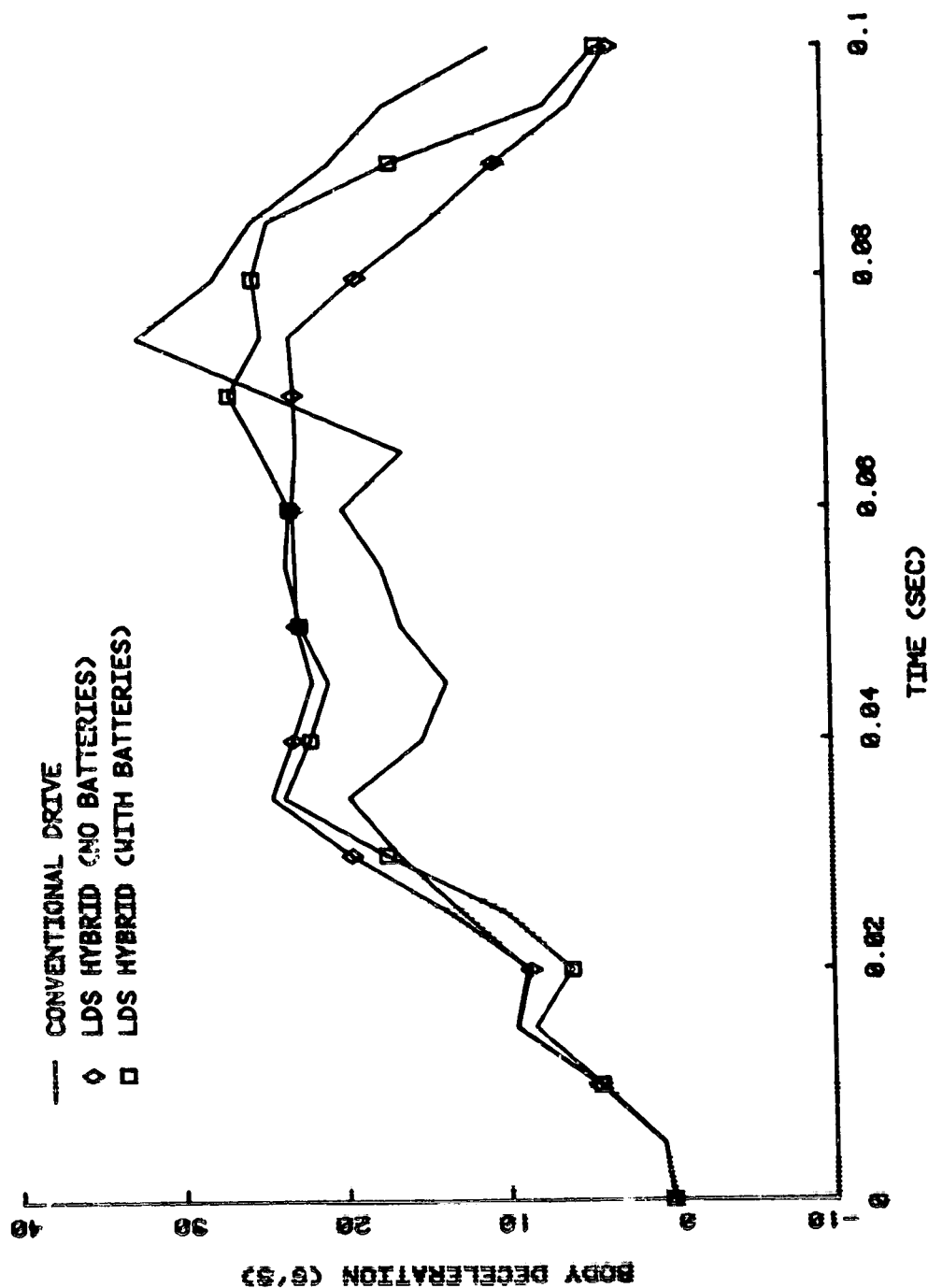
Figure II-11a. Influence of Battery Presence on Body Deceleration
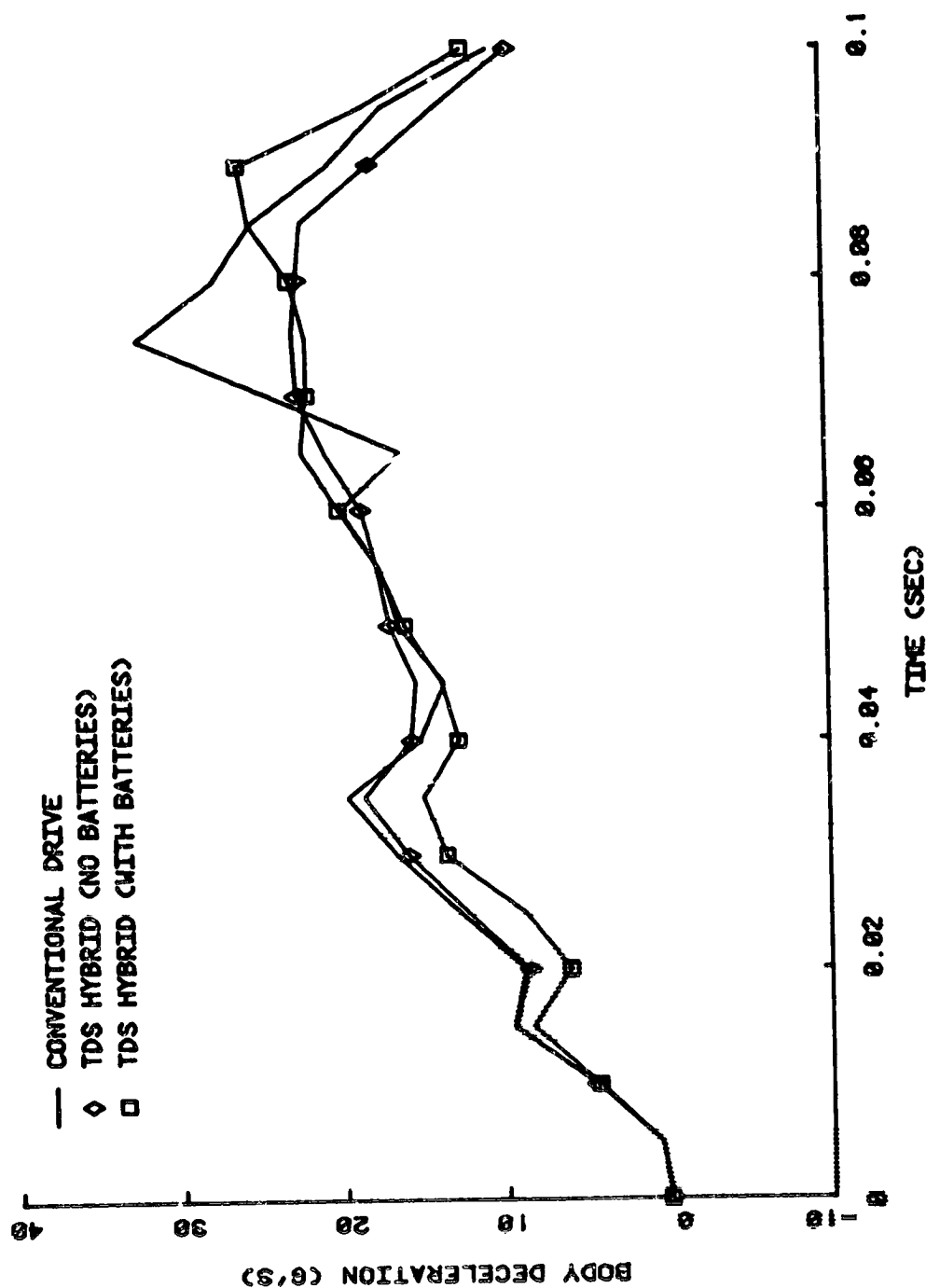
Figure II-11b. Influence of Battery Presence on Body Deceleration
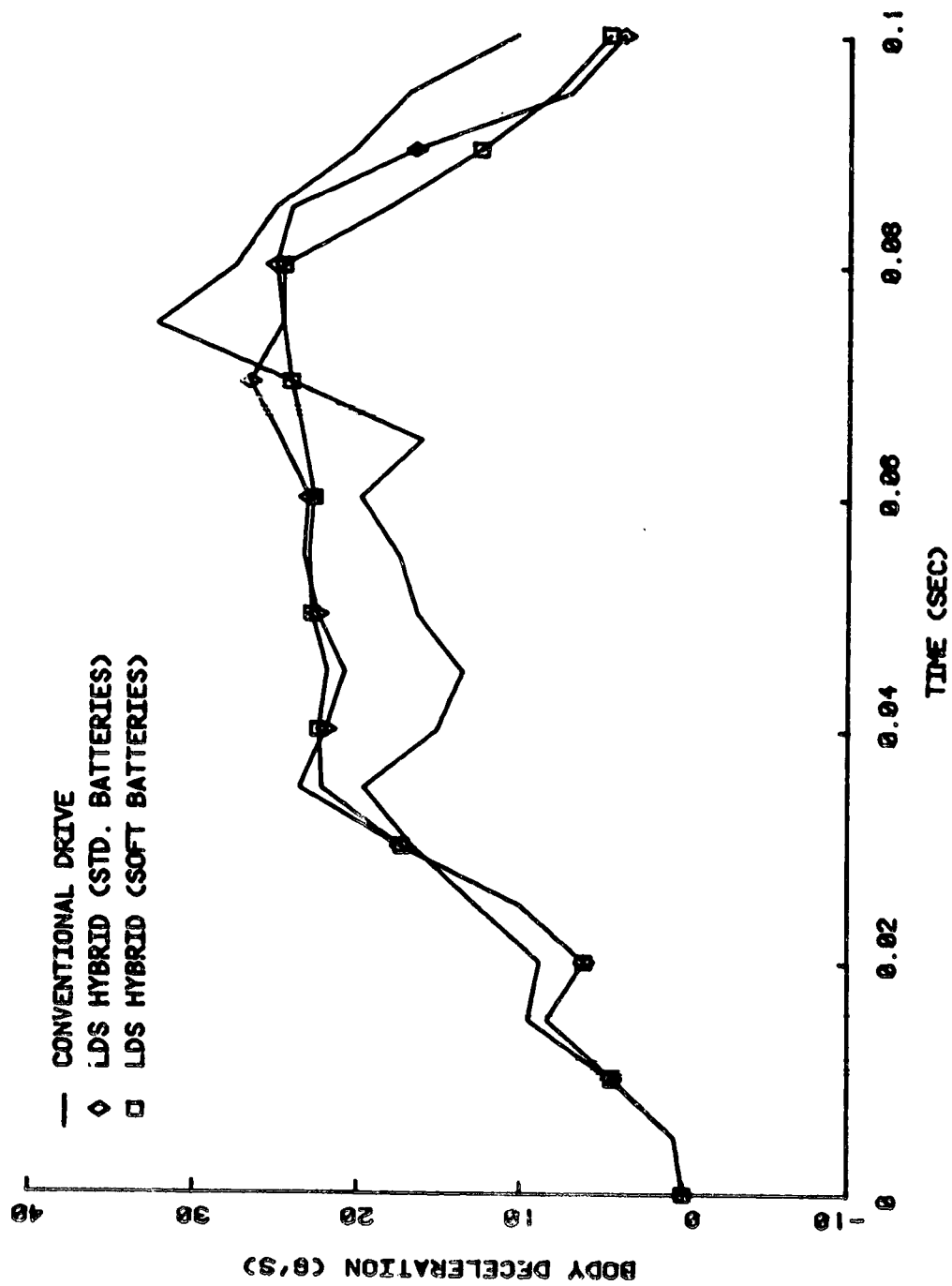
Figure II-12a.   Influence of Battery Stiffness on Body Deceleration
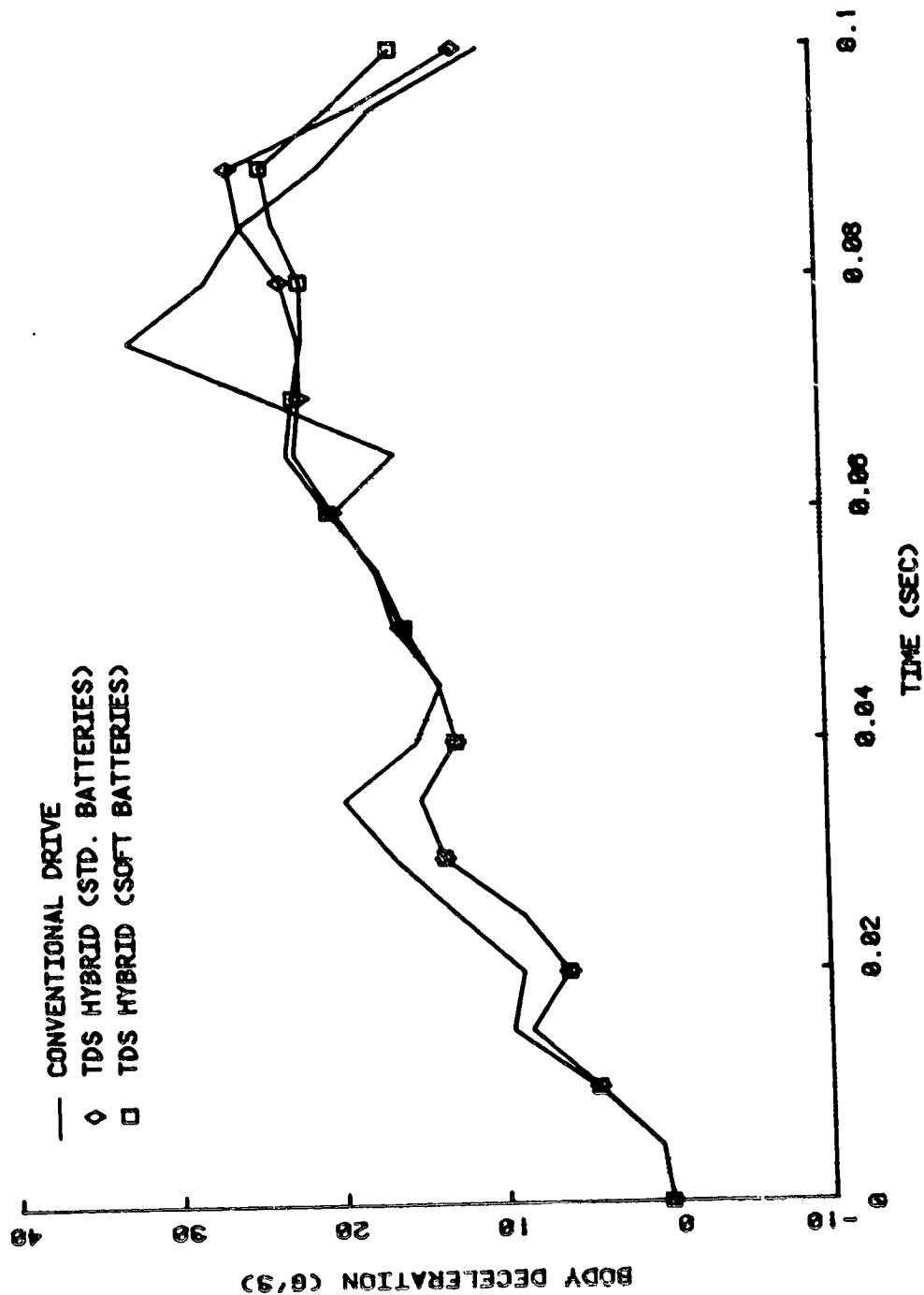
Figure II-12b. Influence of Battery Stiffness on Body Deceleration

II-27
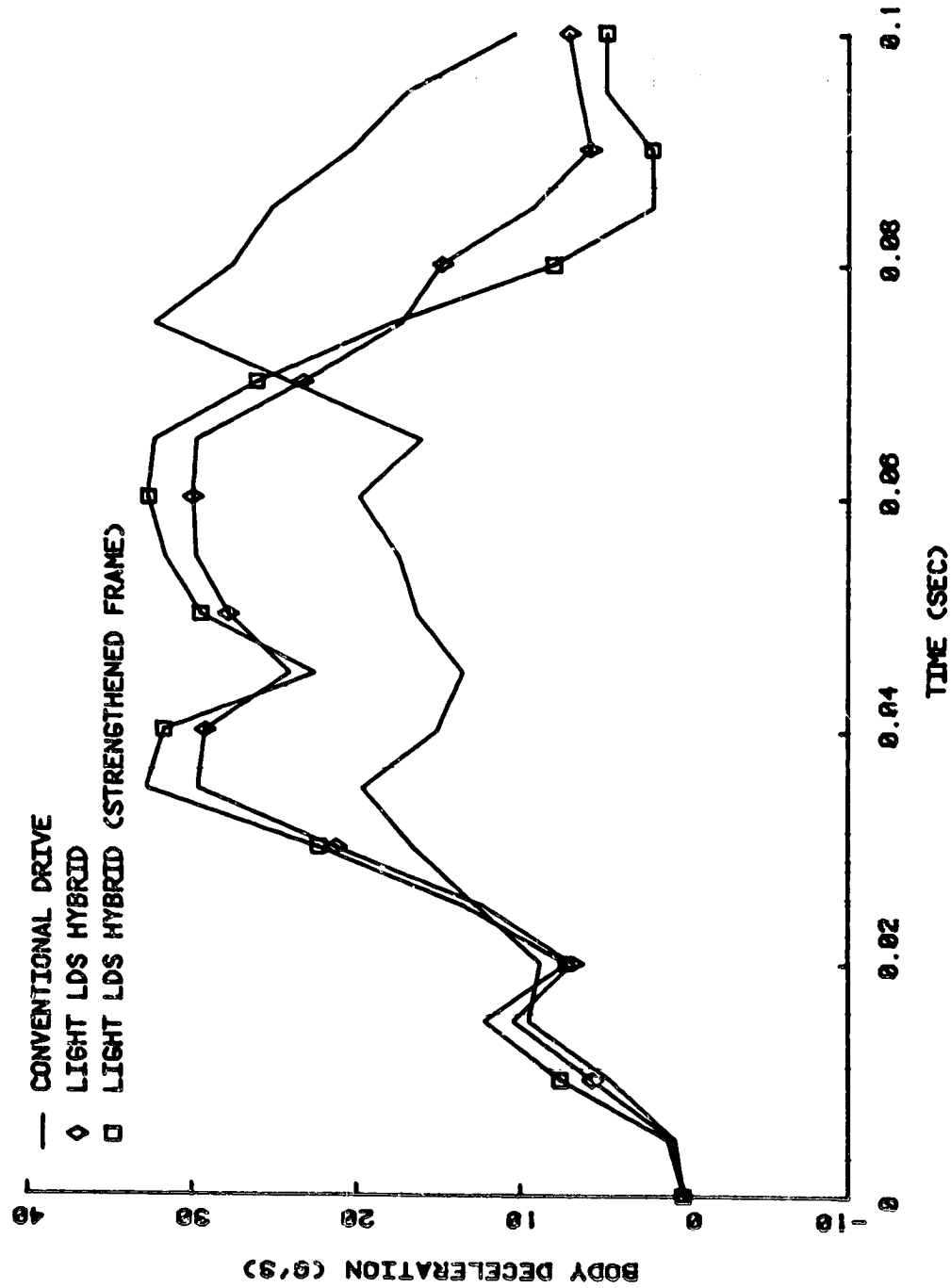
Figure II-13a. Influence of Frame Strength on Body Deceleration
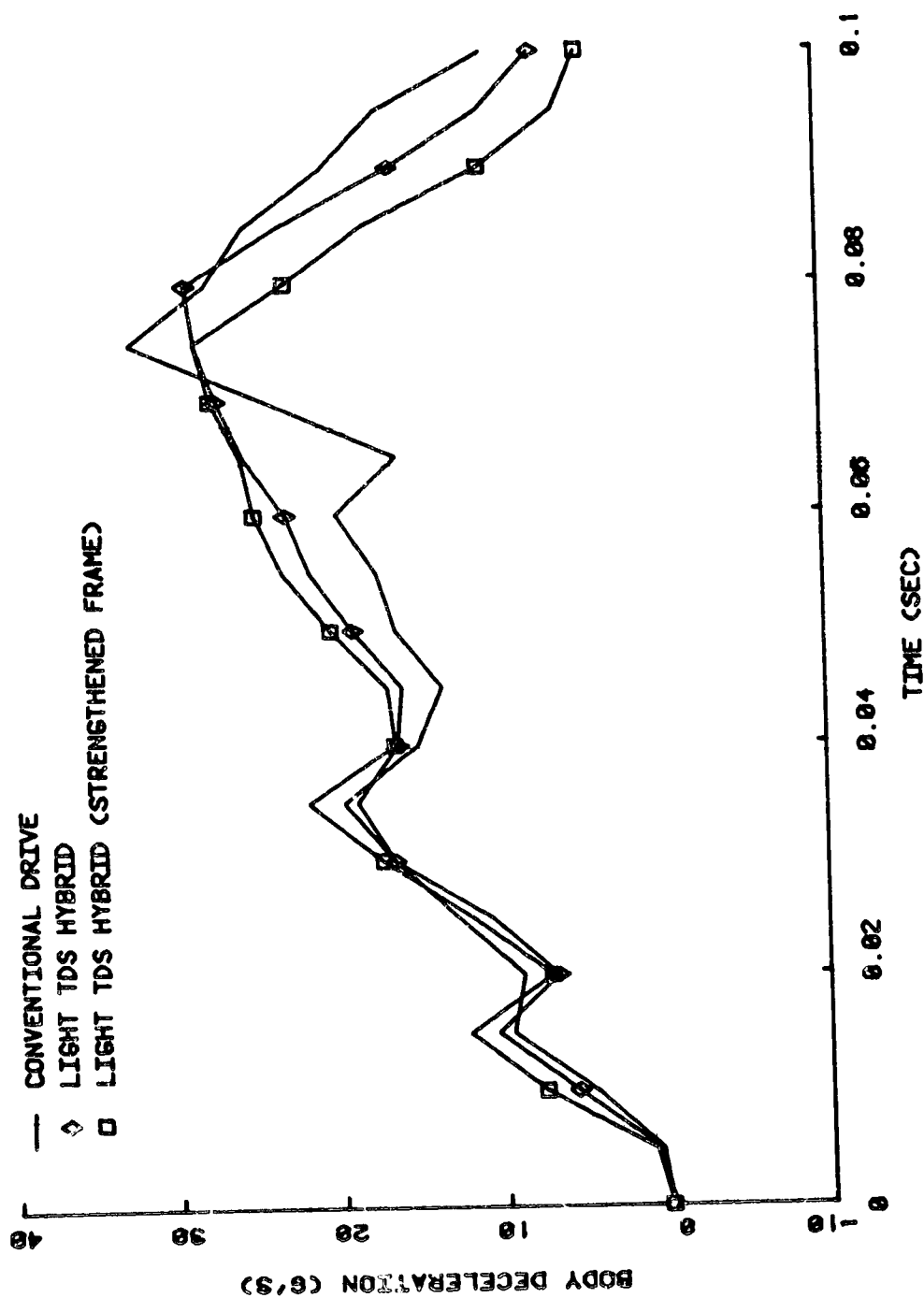
Figure II-13b. Influence of Frame Strength on Body Deceleration
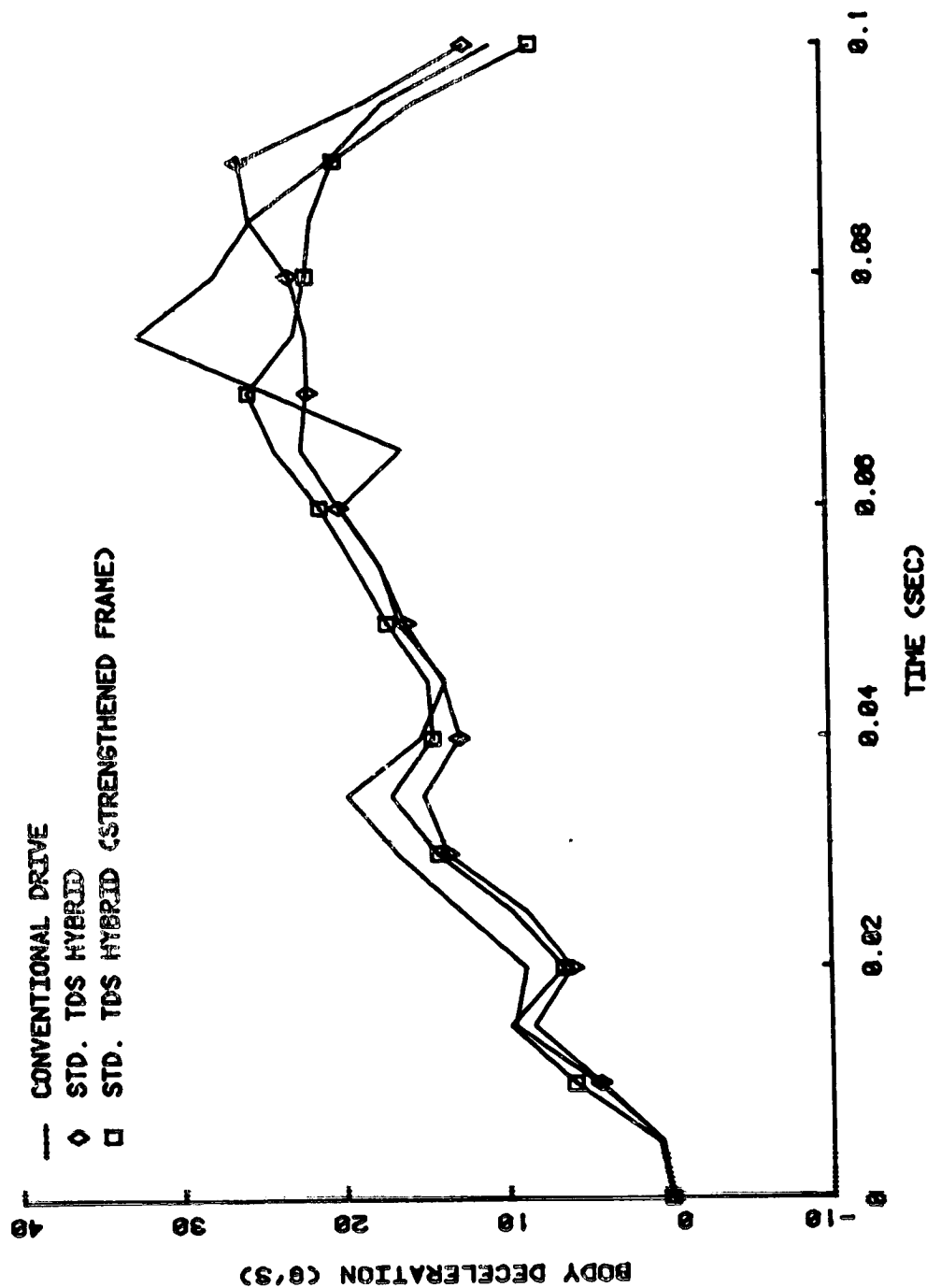
Figure II-14. Influence of Frame Strength on Standard TDS Body Deceleration
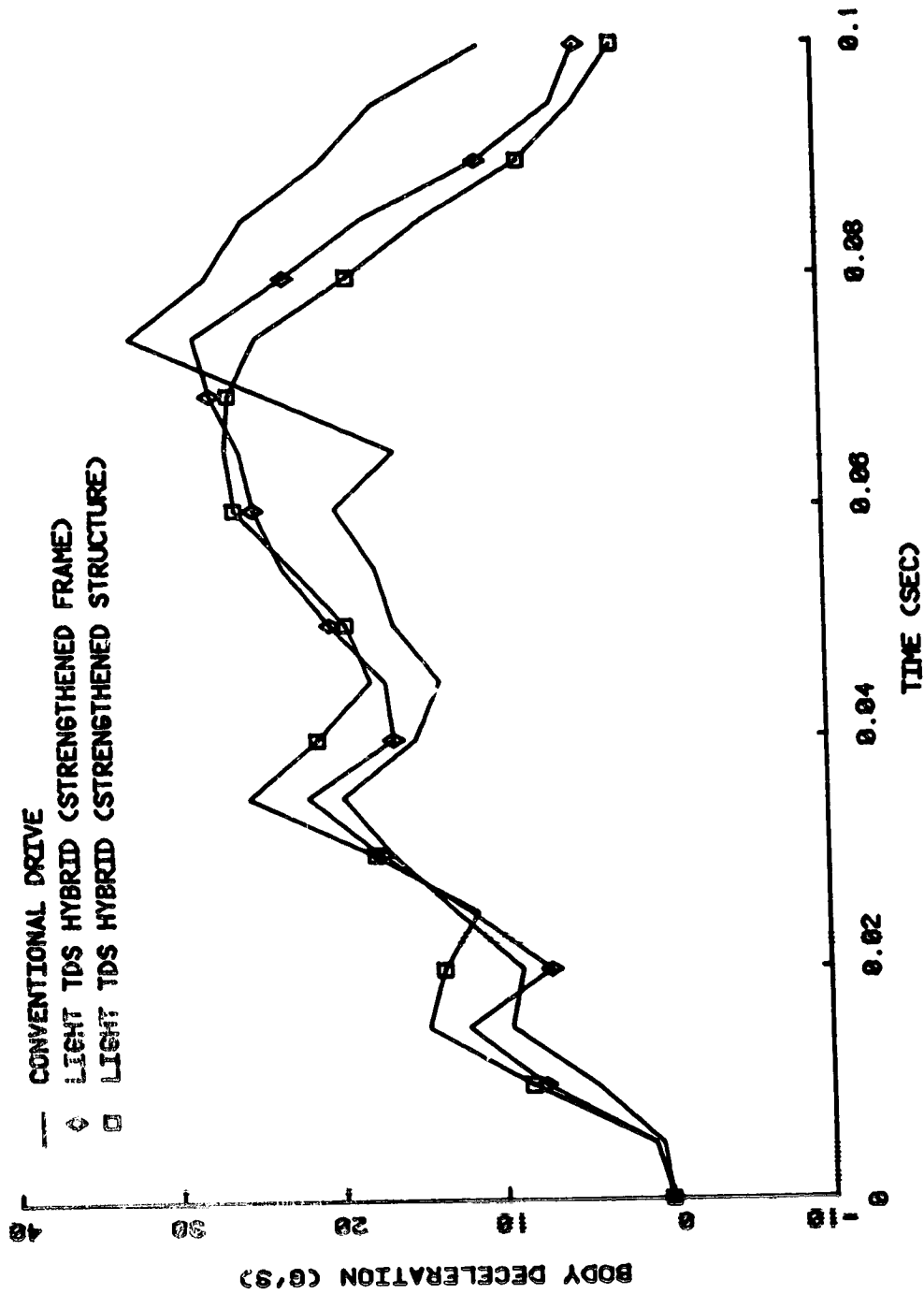
Figure II-15.   Influence of Front Structural Strength on Light TDS Hybrid Deceleration
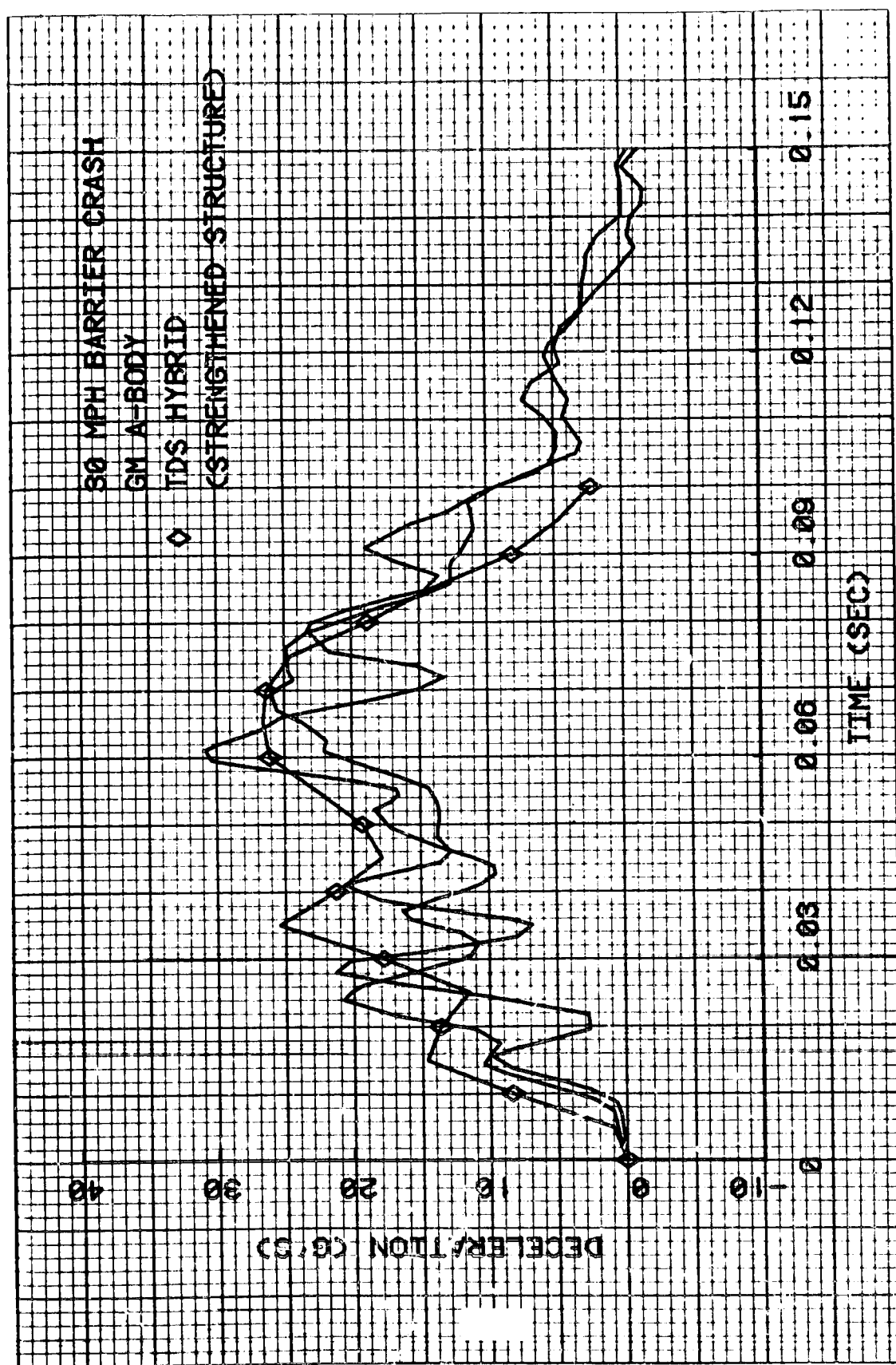
Figure II-16. Comparison of TDS Hybrid and Crash Test Results

MASSES

M1 - TOTAL CAR LESS M2 AND M3
M2 - ENGINE AND TRANSMISSION
M3 - FRONT CROSSMEMBER, TIRES, SUSPENSION, AND WHEELS

1 - FRONT OF RAILS
2 - REAR OF RAILS
3 - FRONT SHEETMETAL
4 - DRIVELINE
5 - DASH
6 - RADIATOR
7 - ENGINE MOUNTS - FWD.
8 - ENGINE MOUNTS - RWD.
9 - TRANS. MOUNTS - FWD.
10 - TRANS. MOUNTS - RWD.
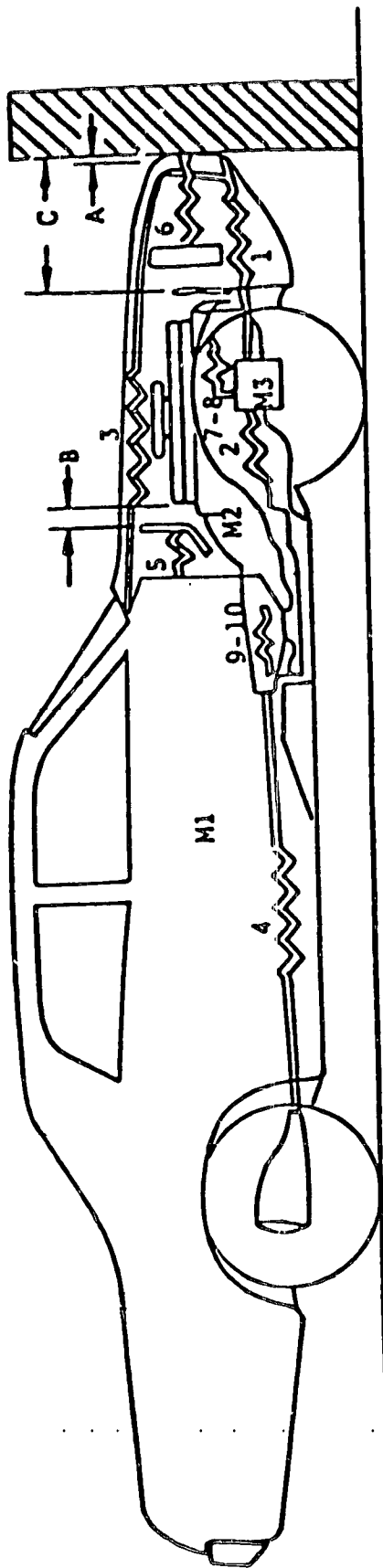
DIMENSIONS

A - FRONT SHEETMETAL TO BARRIER
B - REAR OF ENGINE TO DASH PANEL
C - FRONT OF ENGINE TO BARRIER

Figure II-17. Schematic of Front Structural Model
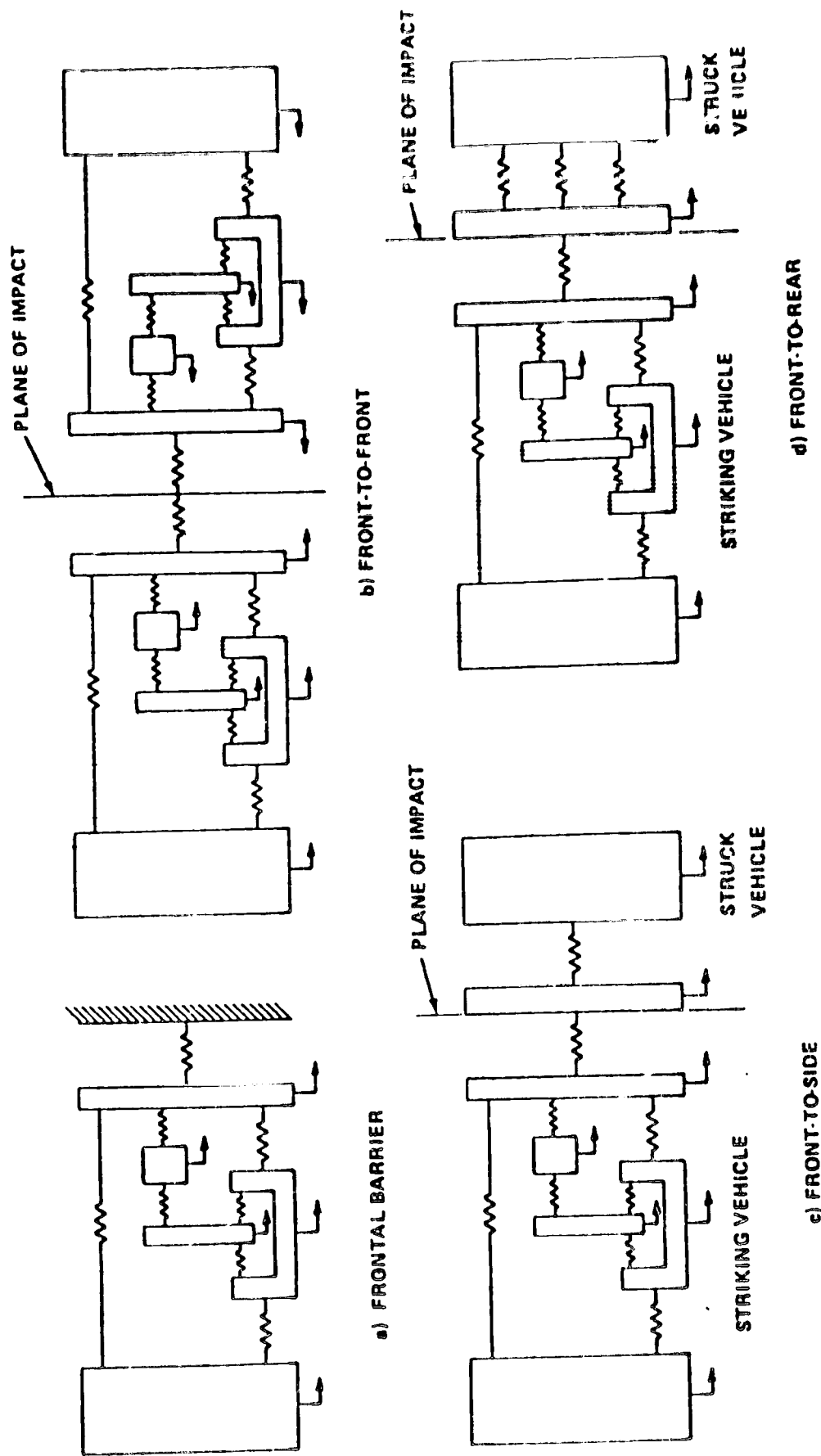
Figure II-18.   Schematic of One-Dimensional Vehicle Structure of Collision Models

GENERAL ⚡ ELECTRIC

The program itself accepts such empirically developed force-deformation characteristics in a tabular format, thus allowing a general loading curve consisting of a number of force-deflection coordinates. An unloading curve is also specified for each resistive element in the form of three unloading slopes (Figure II-19). The unloading path is automatically constructed based on the point at which unloading is initiated. If re-loading takes place, the unloading curve is retraced back to the primary loading curve which is then used thereafter. Cyclical loading/unloading is also considered. If this does occur, the unloading path shifts parallel to the deflection axis consistent with the most recent point of zero deflection rate. The general nature of the unloading path allows consideration of elements that allow only compression (e.g. the bumper structure) or elements that are physically capable of developing tension forces (e.g., the frame rails).
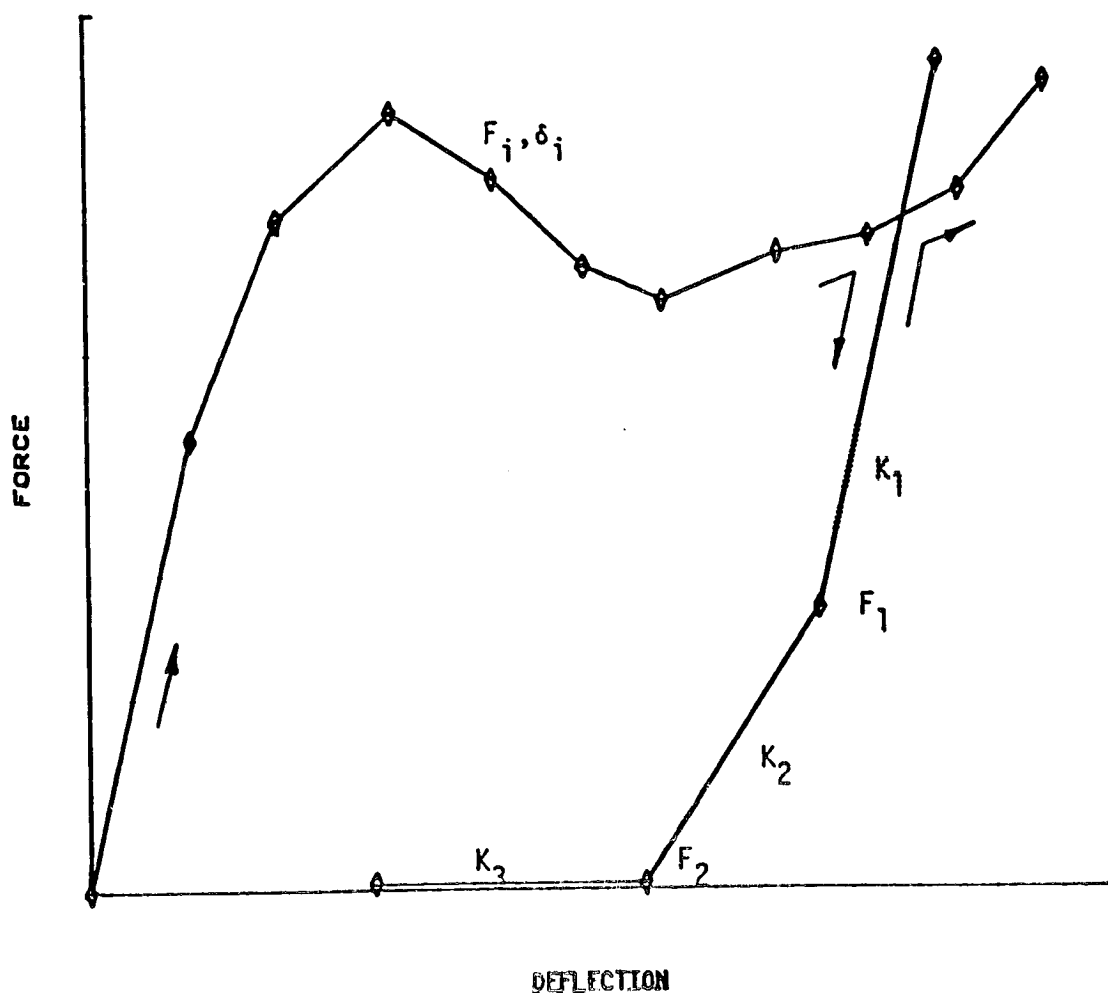
Figure II-19. Illustration of Resistive Element Input Properties

II-35

Since automobile collisions are obviously dynamic events and automotive structural materials are known to be strain rate sensitive, a method of accounting for dynamic overstress is incorporated into the model. Based on the work of Kamal and others, an overstress (rate) factor in the neighborhood of 1.3 or 1.4 has been found to produce reasonable correlation between static and dynamic test data for collision velocities around 30 mph. Within SMDYN, a logarithmic rate factor, as shown in Figure II-20 is employed consistent with the nominal overstress magnitudes indicated above and also providing the additional advantage of producing static load values as the deflection rate approaches zero.

Output from the simulation consists of: a) a concise listing of all input parameters, b) acceleration, velocity, and displacement time histories for each discrete mass, c) force and deflection time histories for each resistive element, d) maximum value of acceleration for each mass, and e) maximum value of deflection for each resistive element.

$$DMF = \begin{cases} 1.0 \text{ for } \dot{X}=0 \\ 1.2728+.01971 \ln(\dot{X}) \text{ for } \dot{X}>0 \end{cases}$$
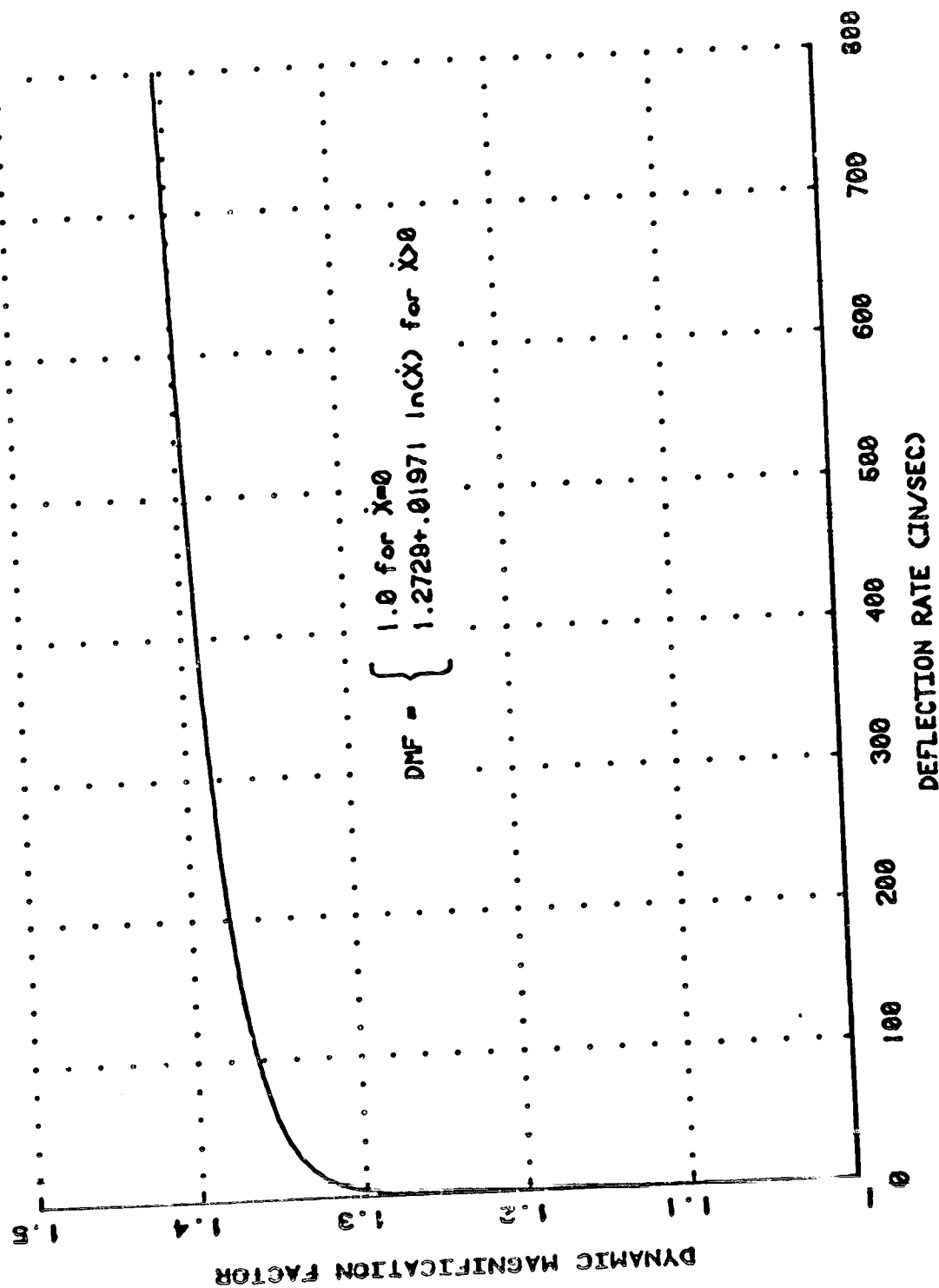
Figure II-20. Dynamic Overstress Factor Used in Model

Appendix III

MICROCOMPUTER CONTROL
OF PROPULSION SYSTEM

Appendix III

MICROCOMPUTER CONTROL
OF PROPULSION SYSTEM

III.1 INTRODUCTION

The main function of the hybrid vehicle propulsion control subsystem is to translate the driver commands to the vehicle into a controlled response of the heat engine, motor, and other components of the propulsion system. This complex control function must be carried out in an optimal manner taking into consideration the limitations and constraints imposed by the various components of the propulsion system. The complexity of the control function necessitates the use of a microcompute. whose major functions are summarized as follows:

- Vehicle Drive Train Sequencing
  - Startup sequencing
  - Selection of propulsion source
  - Propulsion source sequencing
  - Optimum torque/power distribution for combined electric motor and heat engine operation
  - Gear selection
  - Clutch and contactor status selection and control

- Feedback Control of Heat Engine Torque

- Feedback Control of Electric Motor Torque

- Operation Interface

- Battery Charging/Gauging

- System Monitoring, Warning, Operator Displays, and Diagnostics.

The most complex of these functions is the vehicle drive train sequencing. The control strategy developed will be executed by the microcomputer in order to accomplish the functions listed above.

The vehicle drive train sequencing includes sensing the need for switching from one mode of operation to another mode and includes controlling the blending of the heat engine and electric motor outputs so as to minimize jerking and provide optimum performance. The operation of the heat engine and motor are controlled in order to obtain as high an efficiency as possible and to minimize the amount of emissions to the extent practicable for the given conditions of operation. Details of the overall control strategy are given in the next section. The control strategy to be discussed is an improvement on the earlier control strategy used in the Design Trade-Off Studies. Modifications were made to:

- Improve fuel economy

- Reduce emissions

- Operate the electric motor as near to its theoretical
  maximum efficiency as possible.

The basic principles of the control strategy are the same if a
fuel-injected gasoline engine or a diesel engine is used. The
characteristics of the engine used in the torque-speeds curves
are those of a diesel engine. For the Phase II project however,
detailed data on the 1.6 ℓ EFI-L engine will be used which will
be supplied by VW. Figure III-1 shows a block diagram of the hy-
brid vehicle propulsion system. The combined vehicle controller
block contains the microcomputer that forms the decision making
system. Several vehicle, electric motor, battery, and heat engine
parameters are measured and sent to the microcomputer as inputs.
The output of the microcomputer is converted by the appropriate
transducers and sent to the various propulsion system components.

III.2 CONTROL STRATEGY

III.2.1 PROPULSION WITH ELECTRIC MOTOR ONLY

The propulsion battery state-of-charge permitting, the elec-
tric motor will be the primary source of power in city driving
where the speed will be normally limited to less than 30 mph.
This mode of operation will be valid also when the vehicle is pro-
viding regenerative braking or is moving in reverse. The state-
of-discharge diagram of the battery with operation states is shown
in Figure III-2 for the zone $0.7 > S > 0$, where S is the battery
state of discharge. The motor is the primary power source in the
city, but the heat engine takes over if S goes above 0.7. The
region $.75 > S > .7$ is used for load leveling by the motor. If
$S > 0.75$, the heat engine starts charging the battery until S = 0.7.
The battery will not be allowed to discharge above S = 0.8.

The battery modules can be connected all in series, giving a
nominal voltage of 120 V or connected as two series packs in paral-
lel giving a nominal voltage of 60 V. This approach is used to
reduce motor base speed during starting. The full voltage (120 V)
operation and the half voltage (60 V) operation are referred to
later in the text as E_b and $.5 E_b$ operation, respectively. The
motor can be operated in either mode with or without the starting
resistor (R_s).

III.2.1.1 Motor Performance Characteristics

The motor operates so that it will be started by battery
switching until the speed reaches the base value. Then as the
motor enters into the constant hp region, the developed torque is
controlled by the field current. The motor is permitted to oper-
ate in steady state either with half battery voltage $(0.5 E_b)$ or
with full battery voltage (E_b). Correspondingly, there are two
base speeds of the motor, i.e., 1000 rpm and 2000 rmp, respec-
tively. Note: In the Preliminary Design the rpm values are 1100
and 2200 but calculations were done for 1000 and 2000 rpm.

Operator Commands AP,BP

Operator Displays
Fuel (S)

120V 16 20A
240V 60A

AC DC Converter

Battery Charger

Battery

Combined Vehicle Controller

Field Regulator

Armature Contactors & Starters

DC Motor

Field

BPC,PC,SC,MPC

BPA, PA, SA, MPA

Heat Engine

Torque Transfer Unit

4 Sp Automatic Transmission

Tach

Final Drive Ratio

Clutch
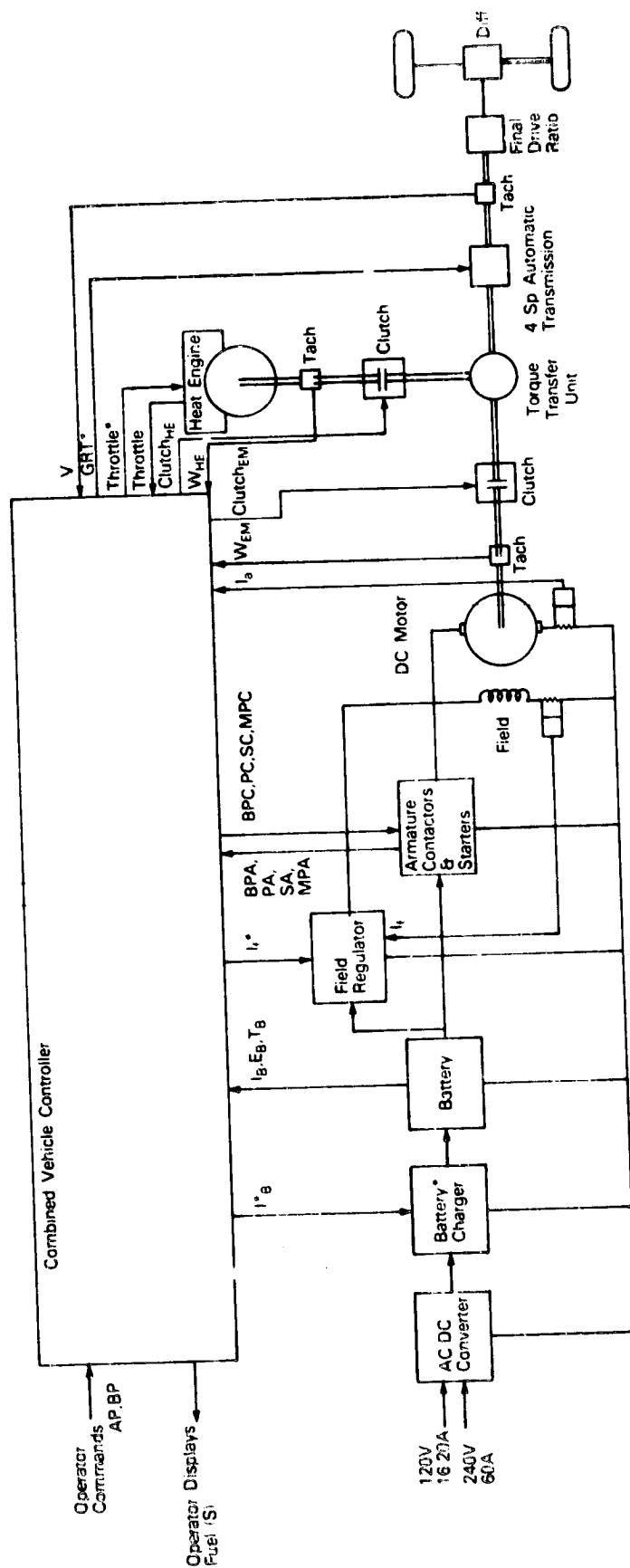
VEHICLE PARAMETERS

Subsystem	Input		Output	
Operator	AP	Accelerator Pedal		
	BP	Brake Pedal		
Battery	I_B	Battery Current	Fuel	Battery State Of Charge
	E_L	Battery Voltage	I^*_B	Battery Charge Command
	T_B	Battery Temperature		
Electric Motor	I_a	Armature Current	I^*_f	Field Current Command
	I_f	Field Current		
	W_{EM}	Electric Motor Speed		
Heat Engine	TP	Throttle Position	TP^*	Throttle Pos. Command
	T_{HE}	Heat Engine Temp.		
	W_{HE}	Heat Engine Speed		
Vehicle	V	Vehicle Speed	GRT^*	Transmission Gear Ratio

LOGIC

Input	Output
Operator Input Signals	Warning Status Signals
BPA Bypass Acknowledge	BPC Bypass Contactor
MPA Main Power Acknowledge	MPC Main Power Contactor
PA Parallel Acknowledge	PC Parallel Contactor
SA Series Acknowledge	SC Series Contactor
	$Clutch_{EM}$
	$Clutch_{HE}$
	$Start_{HE}$

Figure III-1. Hybrid Vehicle Propulsion System Block Diagram
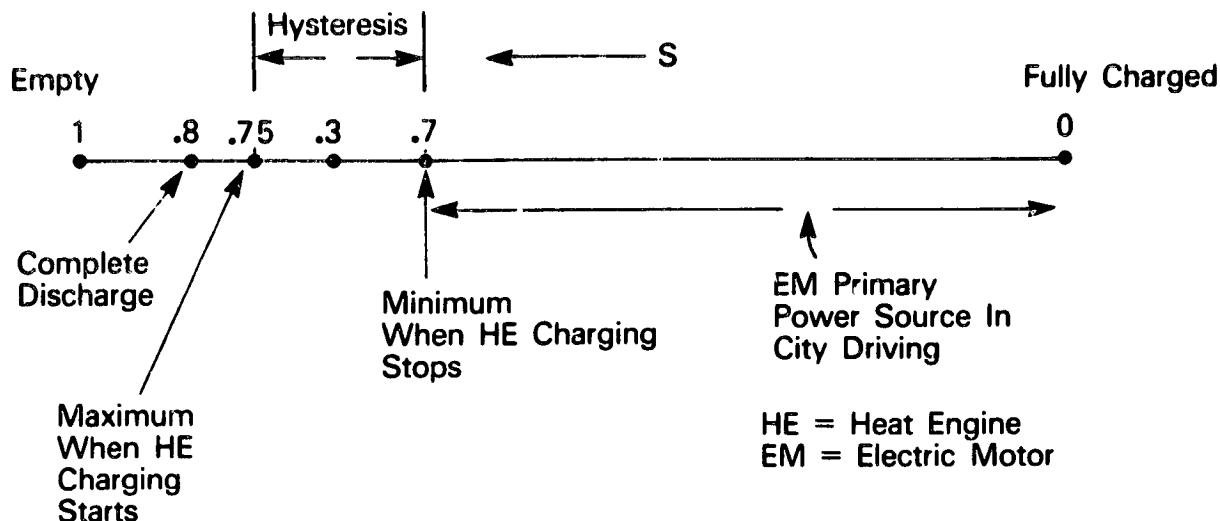
Figure III-2.   Battery State-of-Discharge Diagram

Figure III-3 shows the armature current profile when the motor is started by the battery switching method. The field current is assumed to be at the rated value (I_{fr}) during the entire startup transient. Initially, $0.5\ E_b + R_s$ is impressed in the armature circuit. When the current (I_a) falls to 170 A as speed rises, only $0.5\ E_b$ is switched on. At 430 A, $E_b + R_s$ is impressed and then at 250 A the full E_b is applied. Under all transient conditions, the peak armature current is limited within 480 A. With full E_b, the motor can operate at peak power which corresponds to 480 A for 60 seconds or at rated loads (rated current = 213 A) continuously. Figure III-4 shows the torque-speed characteristics of the motor. During battery switching, the field current is constant and therefore the torque is proportional to armature current. However, during field control, the torque-speed curves have the shape of a rectangular hyperbola. Figure III-5 shows the motor power-speed characteristics which have been derived from Figure III-4. Figure III-6 shows the relation between motor developed power and the armature current limit. With the rated current of 213 A, the motor can develop 19 kW whereas the peak power output - 35 kW - corresponds to armature current of 480 A.

Figure III-7 shows the motor efficiency-speed curves with full battery voltage. At the rated output (18 kW), the efficiency falls but the peak efficiency remains near 2000 rpm. With the reduced output, the efficiency first increases and then decreases, and the peak efficiency point shifts to a higher speed. Figure III-8 shows the similar efficiency speed curve at half battery voltage. Figure III-9 compares the efficiency curves at $0.5\ E_b$ and E_b. For the same output power the efficiency is higher with E_b above a critical speed. The critical point shifts to the right as the power output decreases.
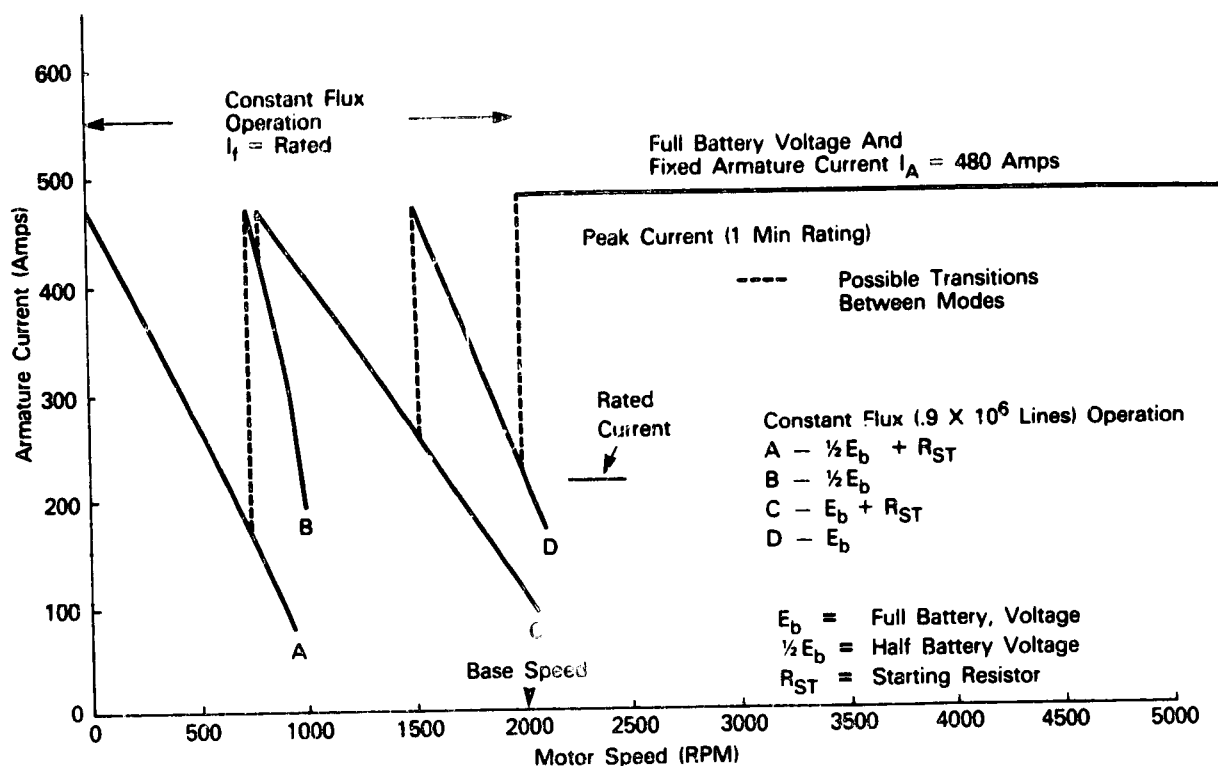
Figure III-3. Armature Current Profile at Starting by Battery Switching Method
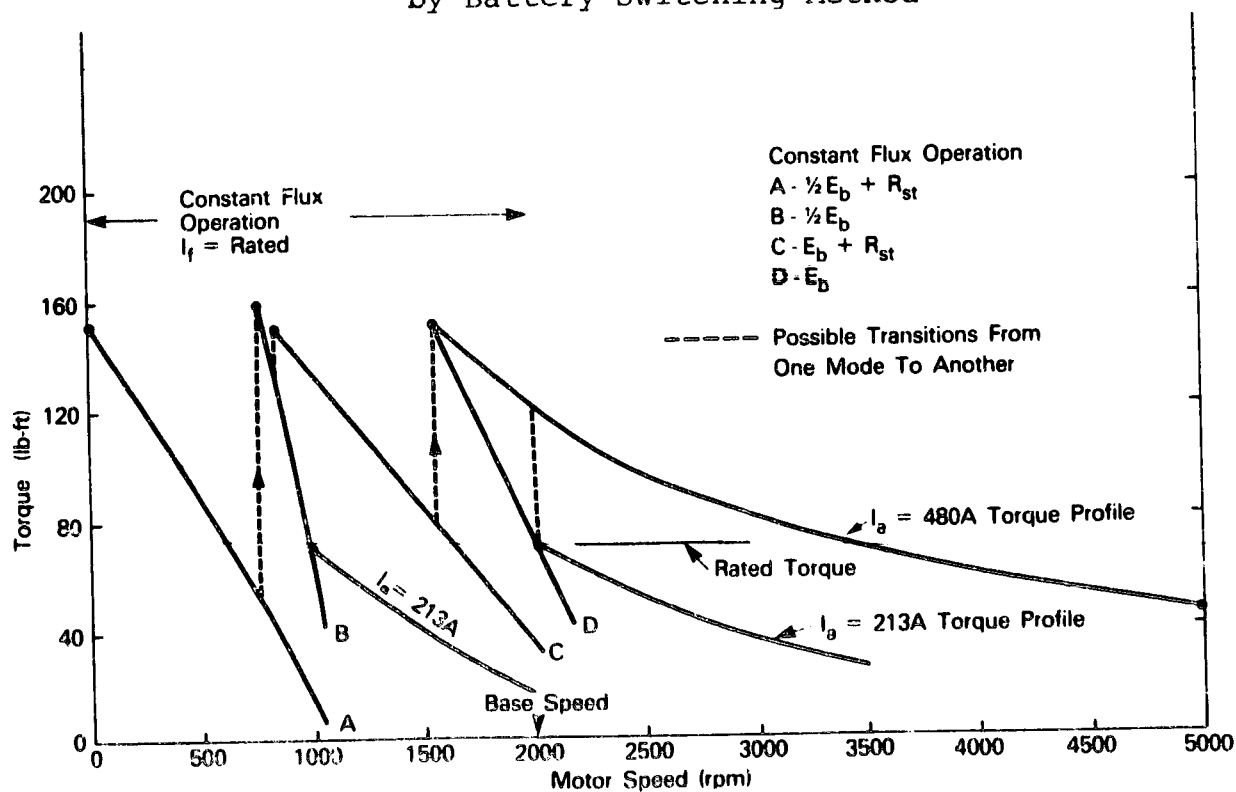
Figure III-4. Torque-Speed Curves of DC Motor
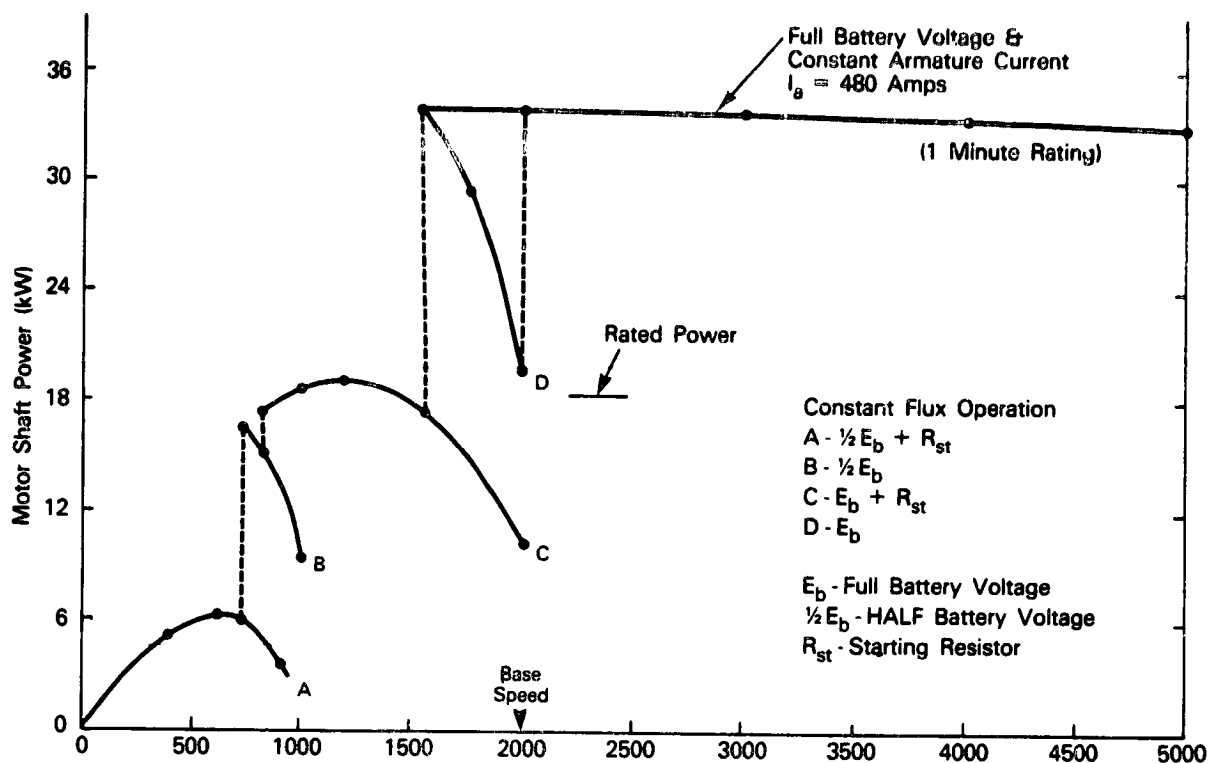
III-5

Figure III-5. Power-Speed Curves of DC Motor
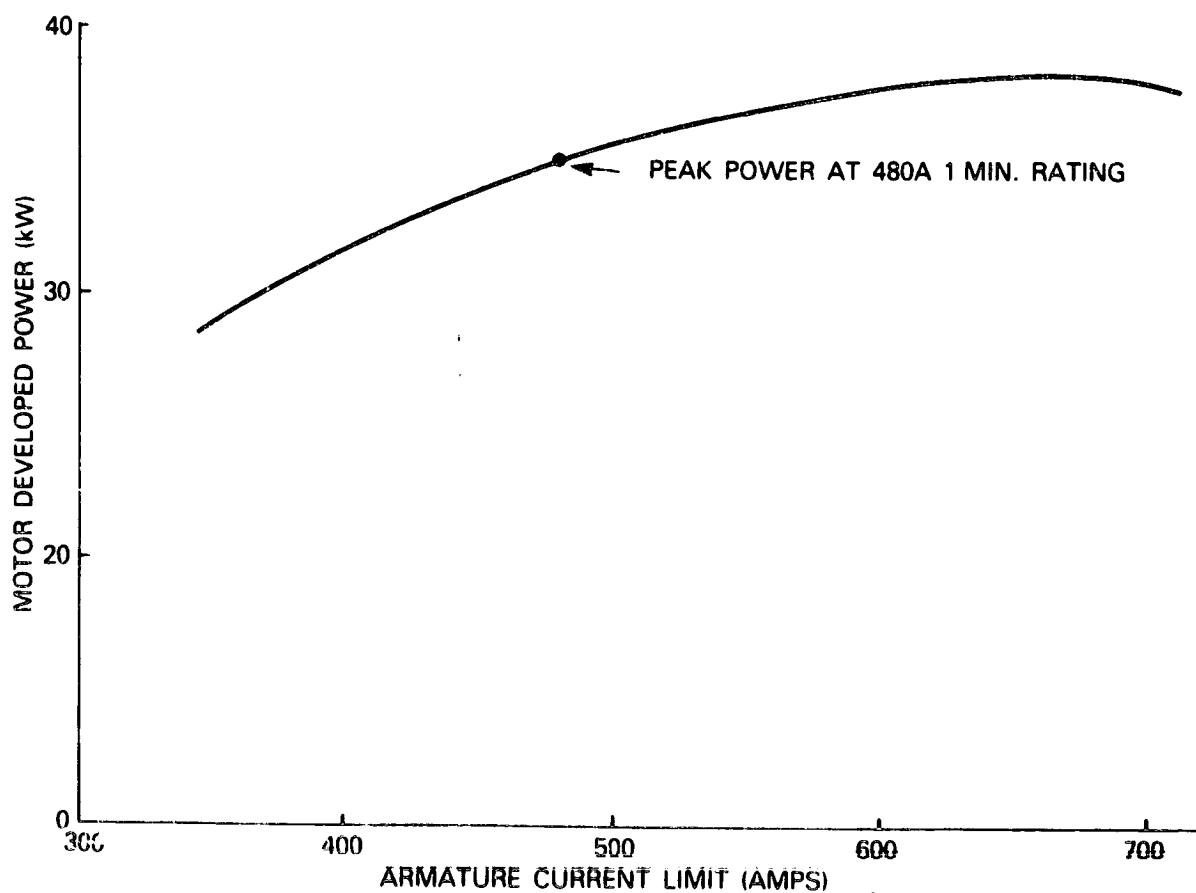
Figure III-6. Relationship Between Motor Developer Power
and Armature Current Limit of Motor
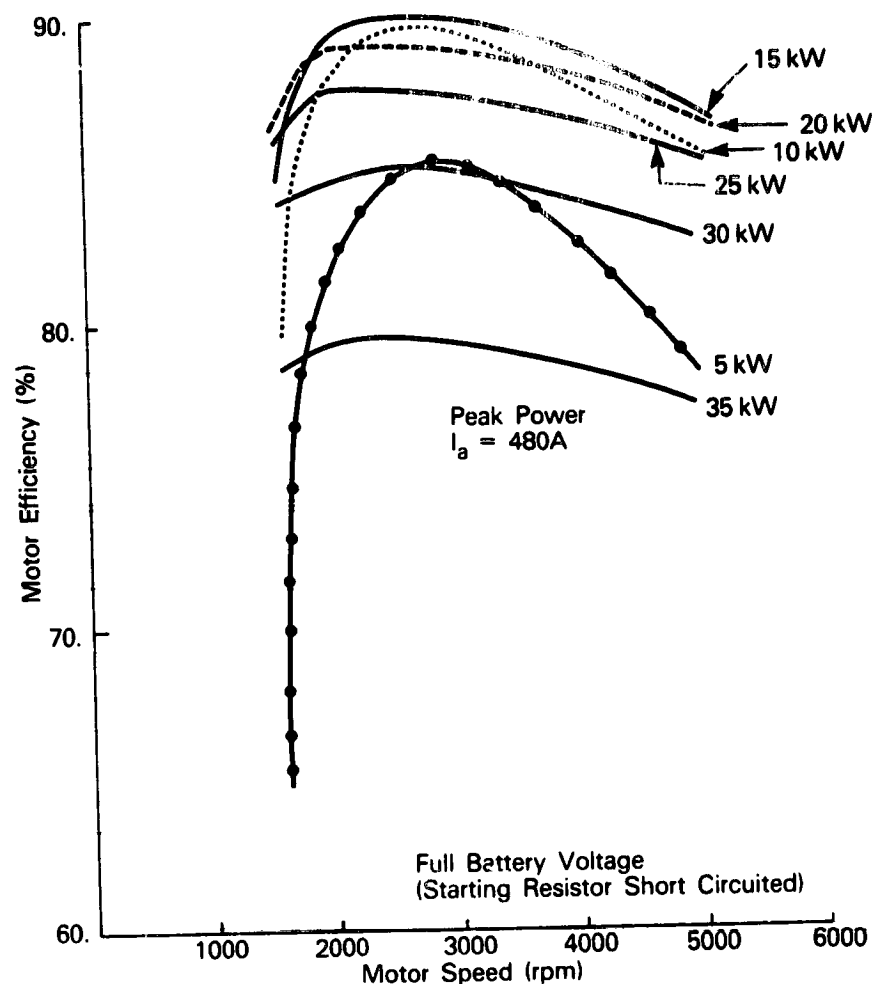
Figure III-7. Efficiency Curves of Motor at Full
Battery Voltage

III.2.1.2 Zones of Operation

The electric motor (or the heat engine or the combined drive)
can operate with either of the four gear ratios, and the torque-
speed curves of Figure III-4 can be translated to vehicle torque-
speed curves corresponding to each of the gear ratios as shown in
Figure III-10. Since the vehicle always starts with first gear,
the battery switching transients are translated for this gear
ratio only. For a constant power operation in the field control
region, the operation remains on the constant power curves for all
gear ratios. The peak power curves corresponding to 0.5 E_b and
E_b operation are also shown in Figure III-10. If the vehicle op-
erates between zero and 6 mph, the motor is always operated at
0.5 E_b and 1000 rpm, and the slipping clutch provides the required
speed. However, when the vehicle speed falls below a specified
value during a deceleration or when standing before a traffic
light, the primary drive clutch is disengaged (opened).

Between 6 to 12 mph the vehicle is operated with 0.5 E_b only.
Below the rated power line (with 0.5 E_b), steady state operation
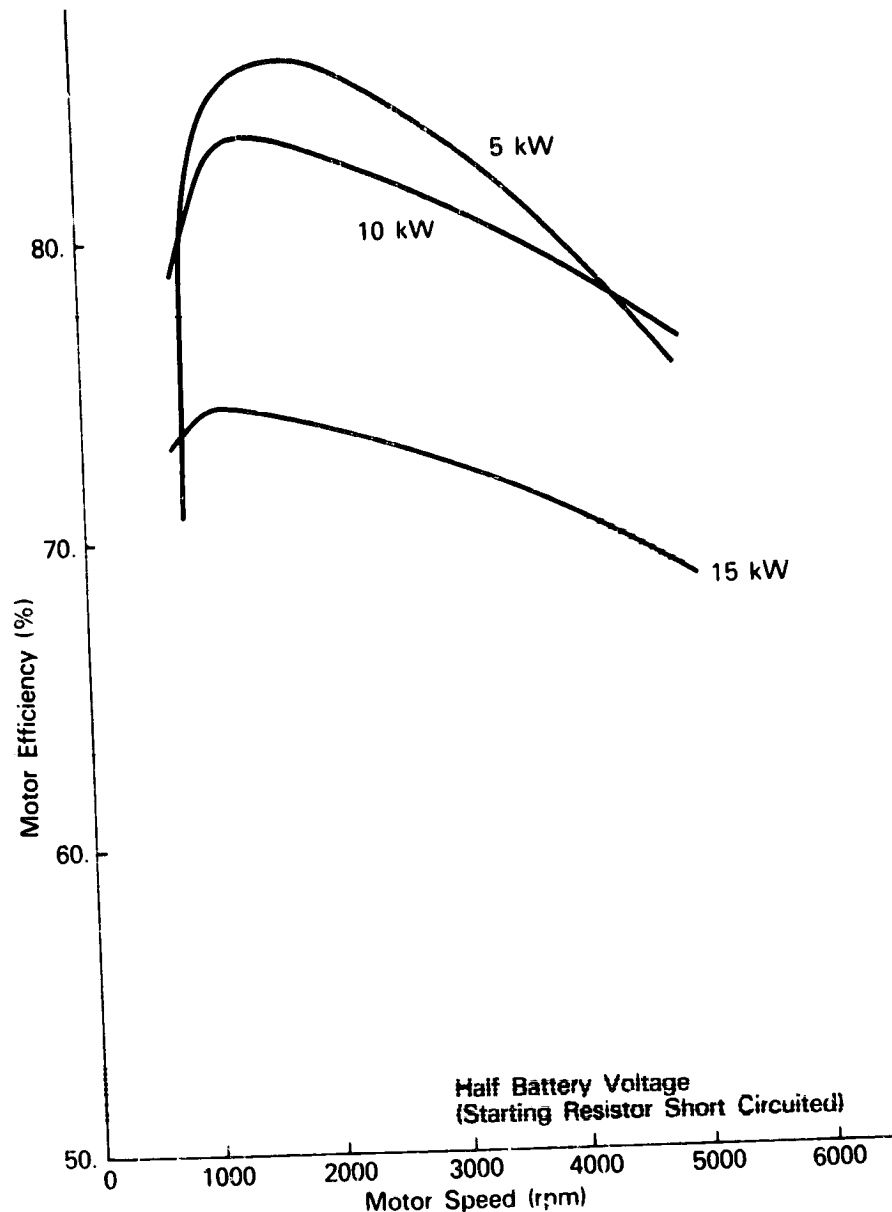
Figure III-8. DC Motor Efficiency Curves at Half Battery Voltage (Parallel Operation)

is possible at any point by control of field current. In the region above the rated power line but below the constant rated torque, T_r, transient operation is permissible with the peak armature current (i.e., 480 A). Above 12 mph the vehicle is operated in field-controlled E_b mode. Steady state operation is possible if the operating point lies below the rated power line, whereas transient operation is permissible in the region between the rated power and peak power lines.

III.2.1.3 Control Block Diagram

The driver essentially controls the propulsion command torque by pressing the accelerator or brake pedal. The accelerator pedal
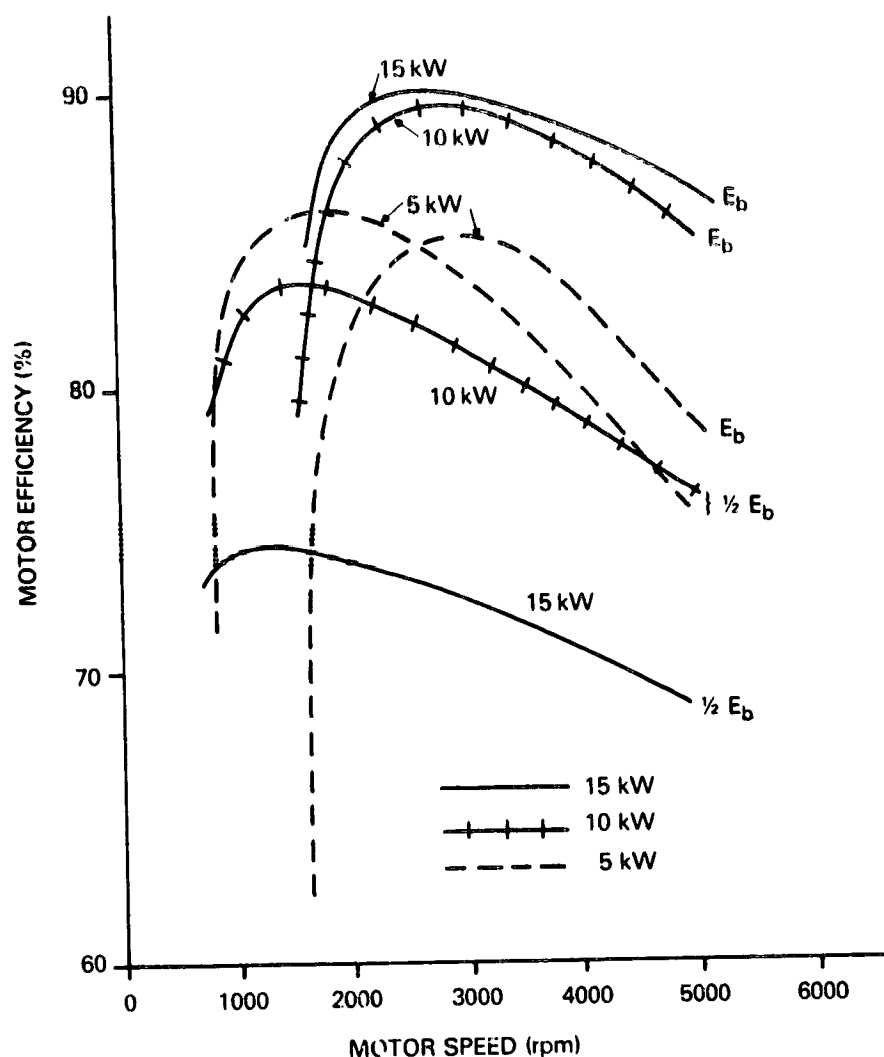
Figure III-9.   Comparison of Efficiency-Speed Curves of DC
Motor for Full and Half Battery Voltage

commands the positive torque which is developed by electric motor
and heat engine, but the negative torque commanded by brake pedal
can be developed by the electric motor only in the regenerative
mode of operation. A simplified block diagram of the motor torque
control system is shown in Figure III-11. The total command torque
$T^* = T^*_{EM} + T^*_{HE}$, where T^*_{EM} = command torque assigned to electric mo-
tor and T^*_{HE} = command torque to heat engine. The optimum distri-
bution of T^*_{EM} and T^*_{HE} depends on a special algorithm which will
be described later. $T^*_{HE} = 0$ indicates motor operation only.

The feedback torque control loop system has an inner armature
current control loop. The error in the current control loop weakens
the field current to establish the desired armature current. Under
the condition of battery state of discharge S > .75 and $T^*_{EM} = 0$,
the heat engine will be required to charge the battery by the com-
mand current $-I_{CH}$. $-I_{CH}$ will depend on the excess engine capacity
available that is subjected to a maximum limit. The actual current

III-9
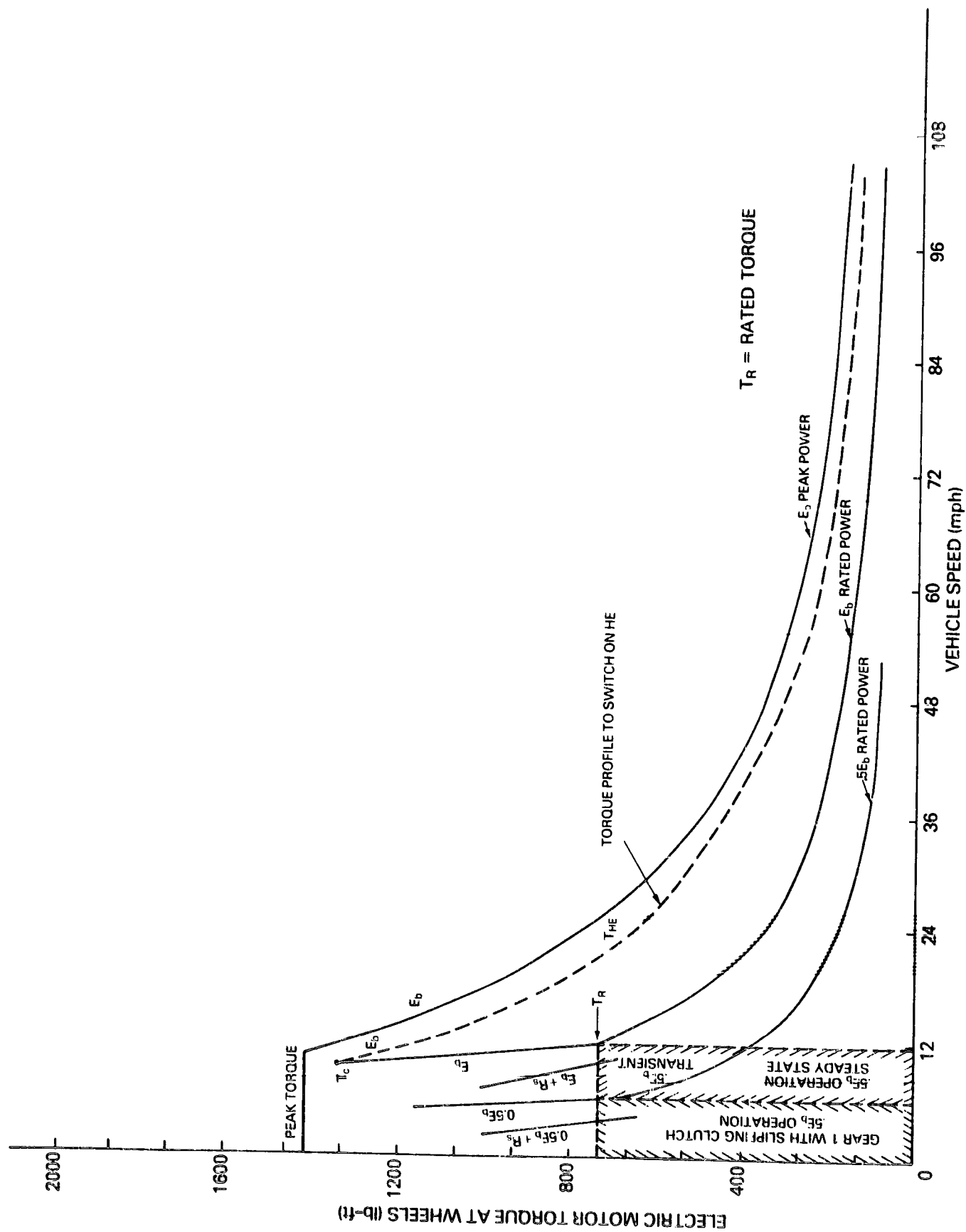
Figure III-10. Vehicle Torque-Speed Curves with Electric Motor Drive
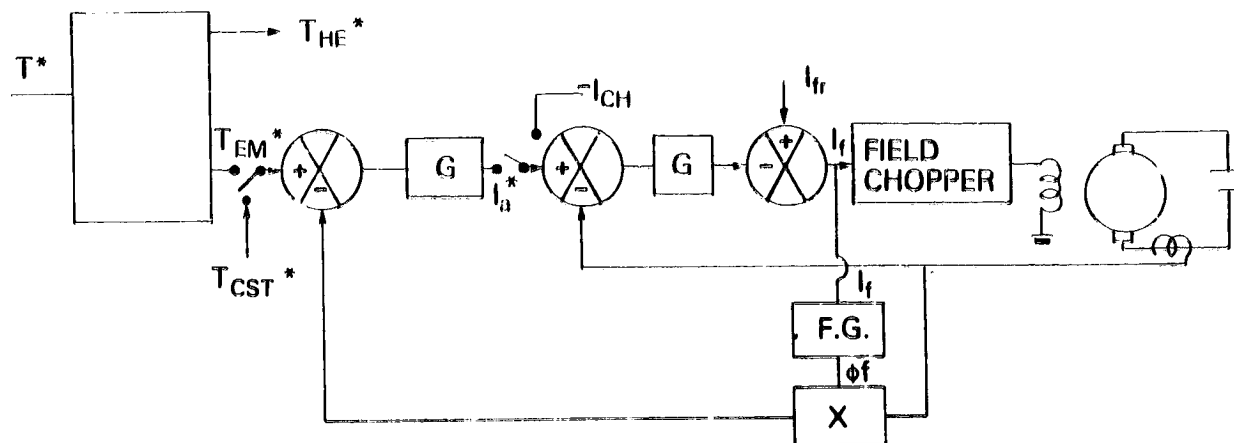
Figure III-11.   Motor Control Block Diagram

limit will be set after consultation with the battery manufacturer.
Feedback torque is not available through a transducer and will be
computed by the relation $T = K\emptyset_f I_a$. The coast down torque, T_{cst},
holds true when both accelerator and brake pedals are released
and corresponds to a fixed amount of regeneration.

III.2.1.4 Gear Changing Strategy

The gear ratio at any vehicle speed is determined by the de-
sire to attain the optimum efficiency condition of the electric
motor. The motor efficiency is highest near the base speed (2000
rpm).

The strategy of gear changing is illustrated by the sequence
diagram in Figure III-12 and the operating points are shown in the
vehicle torque-speed curves in Figure III-13. Regardless of .5 E_b
E_b mode of operation, the motor always starts from standstill in
first gear (GR1) and as the speed increases, the motor goes to
second gear (GR2) at 3567 rpm so that the speed after shifting is
2000 rpm. The same principle is followed for GR2 to GR3 and GR3
to GR4 transitions. As the car slows down from high speed, the
reverse transitions occur at the same operating points.
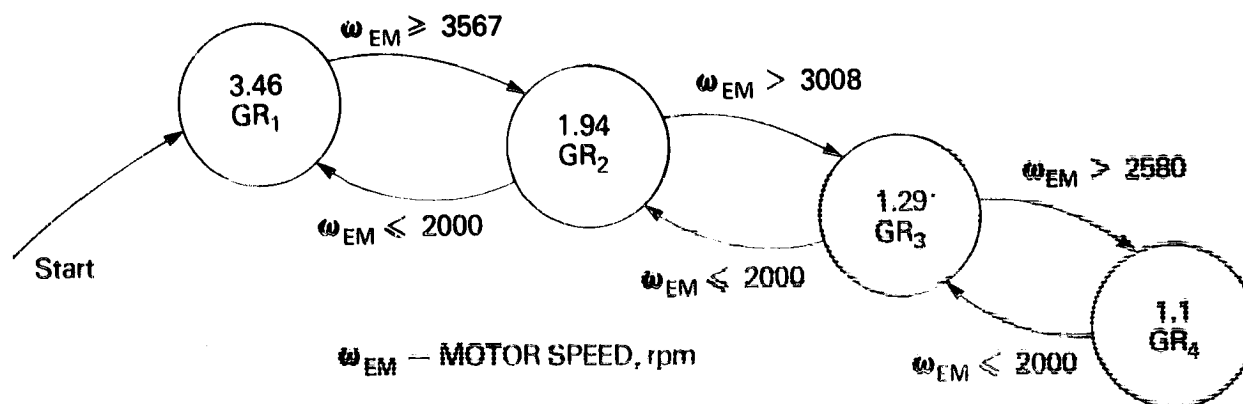
Figure III-12.   Motor Gear Changing Sequence Diagram

III-11
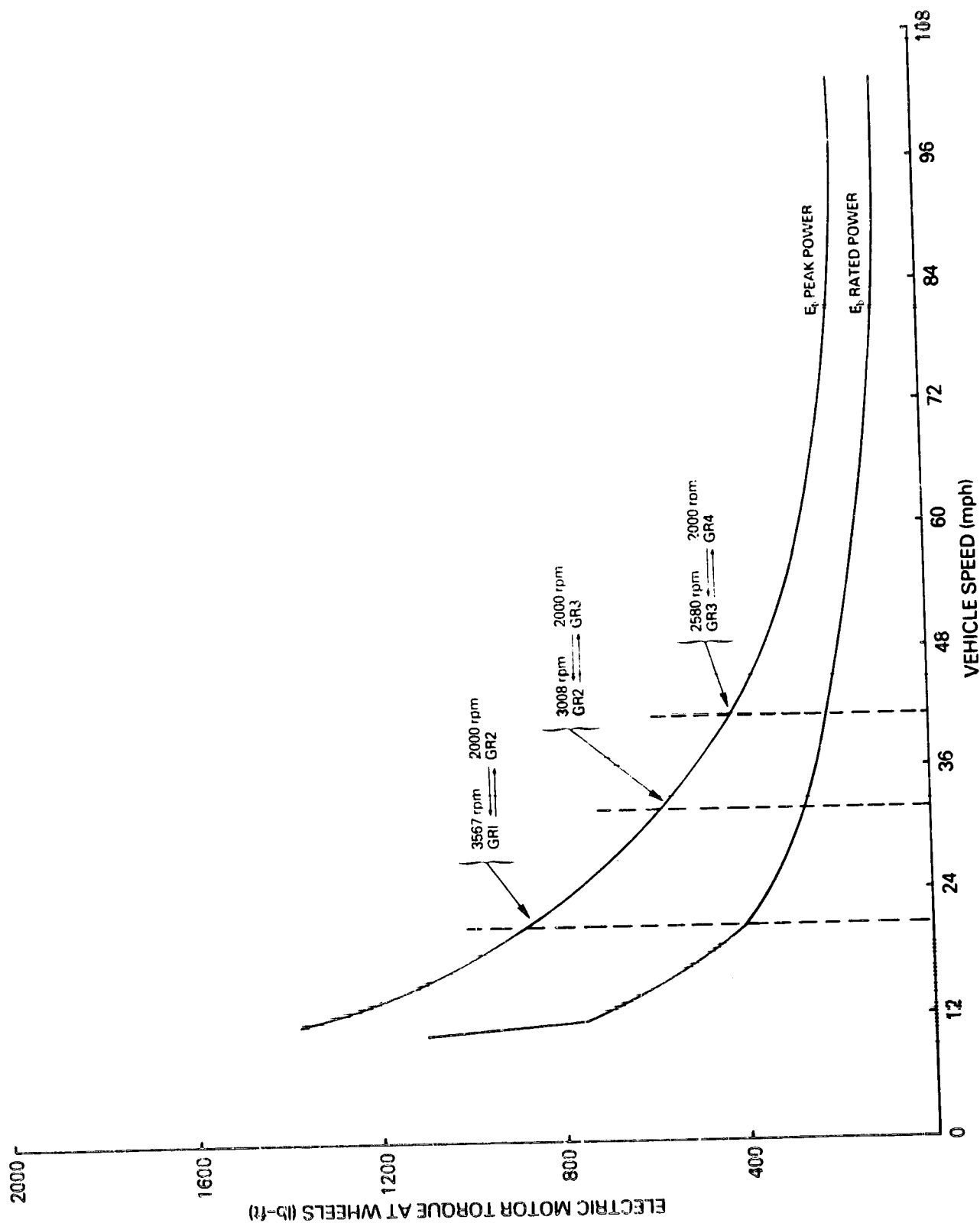
Figure III-13. Electric Motor Torque-Speed Curves Showing Points of Gear Changes

III.2.1.5 Startup Sequencing

Figure III-14 shows the startup sequencing flow chart. As mentioned previously, regardless of which propulsion unit is primary in the drive system, the vehicle always starts with the electric motor. Soon after the start from rest, the sequencing has to take one of the following branches:

(1) If the demand torque is less than rated motor torque, T_r, and vehicle speed is below 12 mph, 0.5 E_b mode of operation is desired. However, in this mode if motor speed is above 2000 rpm (vehicle speed = 12 mph) or armature current exceeds 430 A, conditions are established for going to E_b mode.

(2) If during steady operation in 0.5 E_b mode the battery state-of-discharge becomes greater than 0.7, the vehicle is run with the heat engine as the primary propulsion unit.

(3) If the initial command torque is greater than T_r, and the battery state of charge permits, the transition to E_b mode of operation occurs. However, if the condition $S > 0.7$ is detected, the heat engine is started and used as the primary propulsion unit. On the other hand, if $T^* > T_c$, the heat engine is started for load leveling purposes. The heat engine is always started using the vehicle drive shaft until its speed reaches 500 rpm and then the heat engine is fired.

III.2.1.6 Regeneration Mode Sequencing

For the active regeneration mode, the same block diagram as seen in Figure III-11 holds true except that the command torque is negative. In this mode the battery is charged by the motor acting as a generator. The regeneration mode flow chart is shown in Figure III-15. As the speed slows down in the E_b mode and the field current rises to the rated value, .5 E_b + R_s is applied to the armature circuit. As the current falls below critical value I_{ac}, .5 E_b is switched on and regeneration is continued until $I_f = I_{fr}$. Then the vehicle stop is completed by applying mechanical brakes. Several other possible entry points are also shown in the flow chart.

III.2.2 PROPULSION WITH HEAT ENGINE ONLY

The heat engine is the primary source of power in highway driving when the vehicle speed is typically above 30 mph or if the battery state of discharge becomes greater than 0.7.

III.2.2.1 Performance Characteristics

The operating characteristics of the heat engine which are important for control strategy development will be briefly reviewed. Figure III-16 shows the maximum engine power and torque
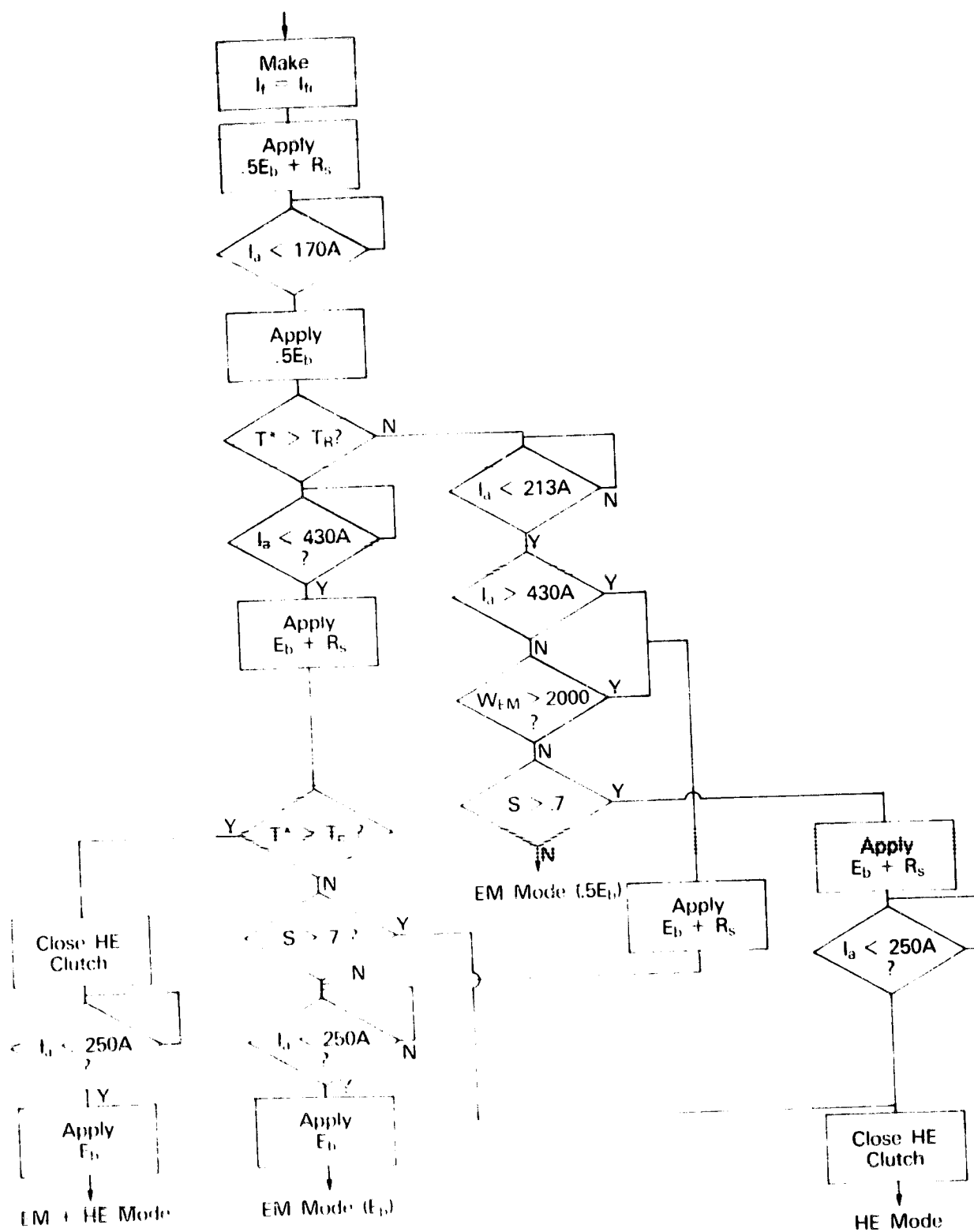
Figure III-14. EM Startup Sequencing Flow Chart
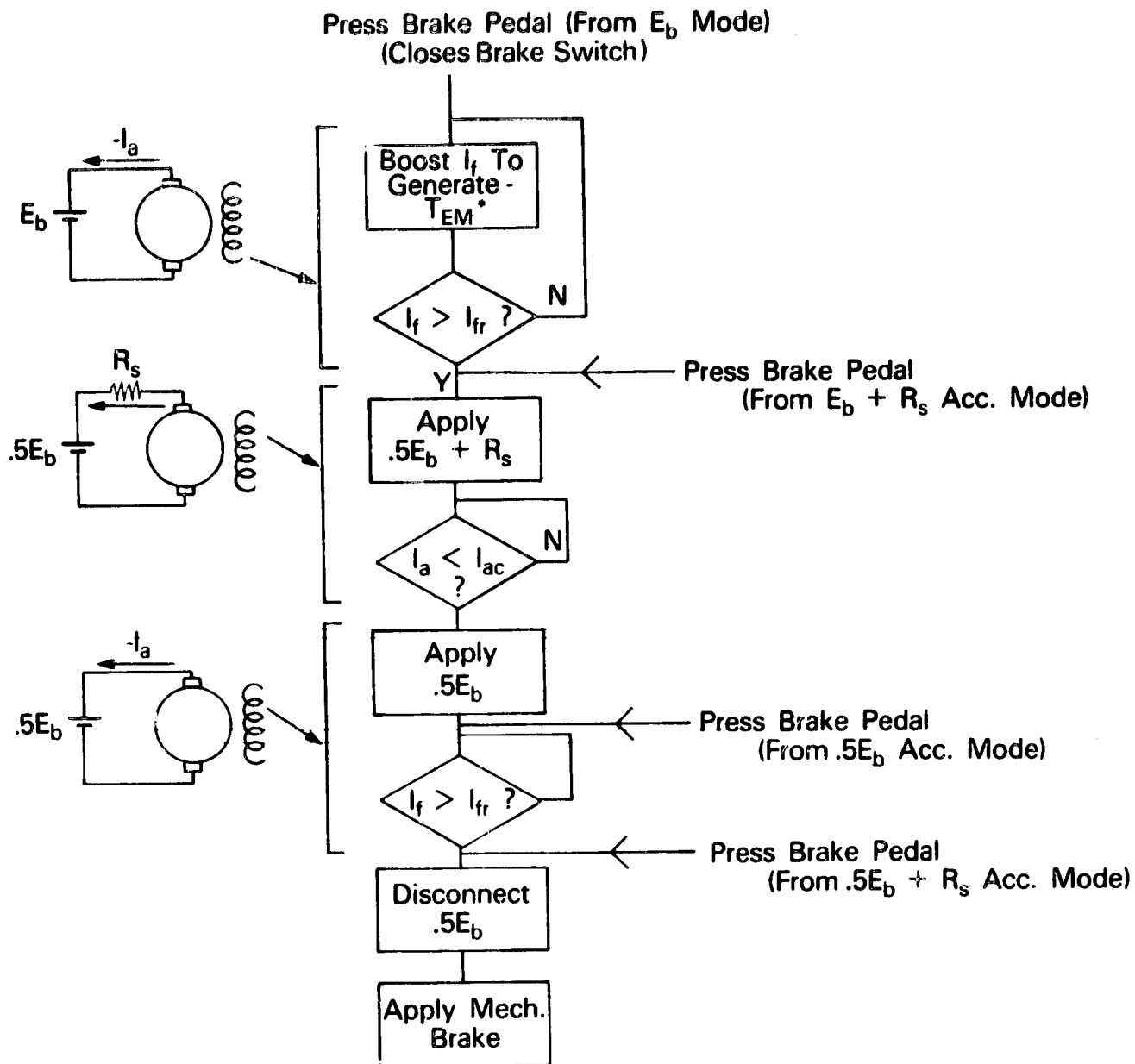
Figure III-15.   Regeneration Mode Flow Chart

available for various speeds (rpm) under maximum throttle opening.
Figure III-17 shows the fuel consumption at different power frac-
tions (P_f) under different engine speeds. As shown in the figure,
the fuel consumption is lowest for the 2000-3000 rpm curve. Again
as P_f decreases below typically 40%, fuel consumption increases
rapidly. Similarly, emissions become high if the engine is run
above 86% power fraction. Though transient operation is permit-
ted at any operating point, the control will attempt to restrict
the operation to the high-efficiency region bounded by the effi-
ciency/emission limit curves. Figure III-18 shows the normalized
torque vs. throttle angle curves at different engine speeds. Fig-
ure III-19 shows the torque vs. speed curves with different throt-
tle angles which have beed derived from Figures III-16, 17, and 18.
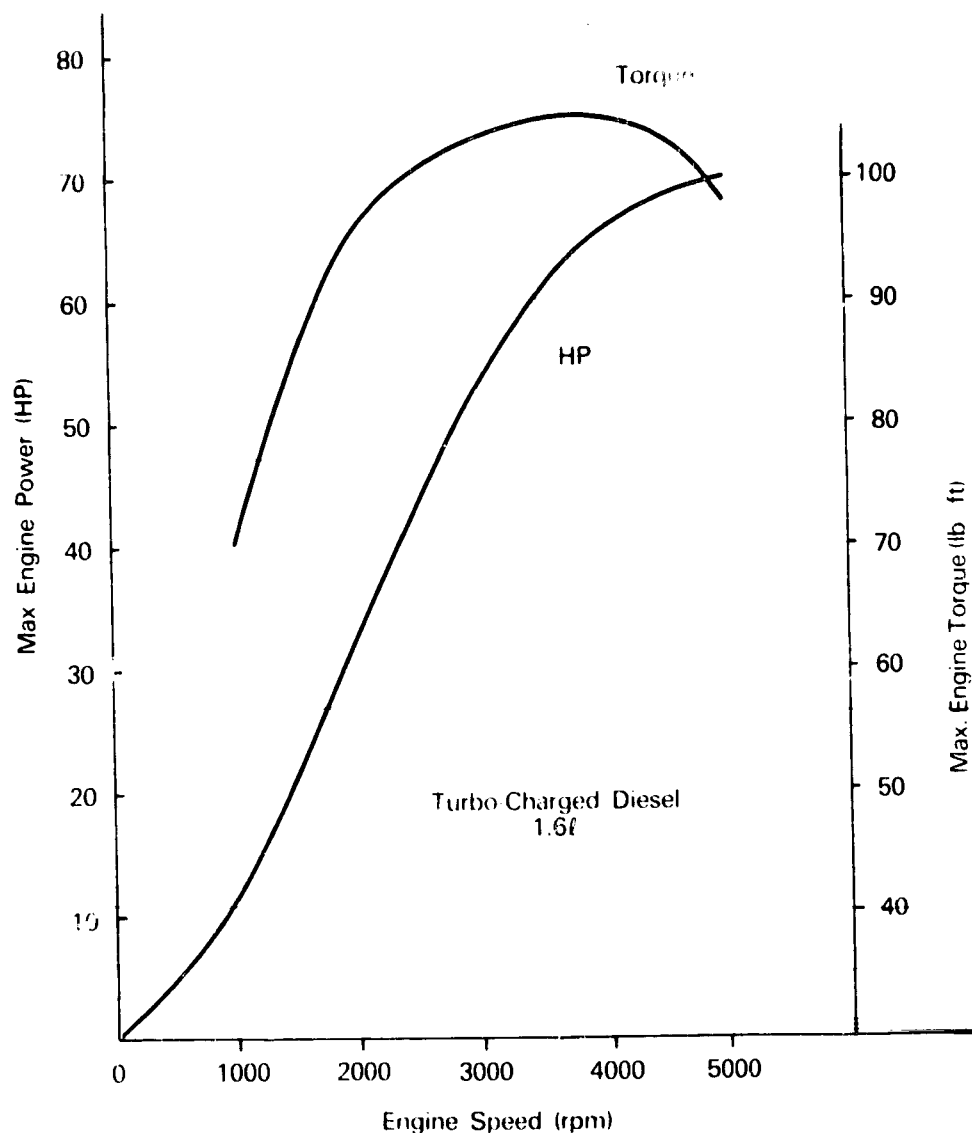
Figure III-16. Maximum Engine Power and Torque vs Speed

The torque corresponding to 86% (T_{CH}) and 40% (T_{CL}) power outputs
are also shown in the figure. The throttle angle is the main con-
trol variable when the heat engine is in operation. The throttle
angle relationships used in the present study are for the diesel
engine, but they are typical for a fuel-injected gasoline engine.
Further system controller development in Phase II would use throt-
tle angle relationships for the 1.6 ℓ gasoline engine supplied by
VW.

III.2.2.2 Zones of Operation

The torque-speed curves of the heat engine given in Figure III-16
can be translated to vehicle drive torque vs speed curves for each
gear ratio. Figure III-20 shows such a plot of maximum torque-speed
curves corresponding to a throttle opening of 60°. The 86% and 40%
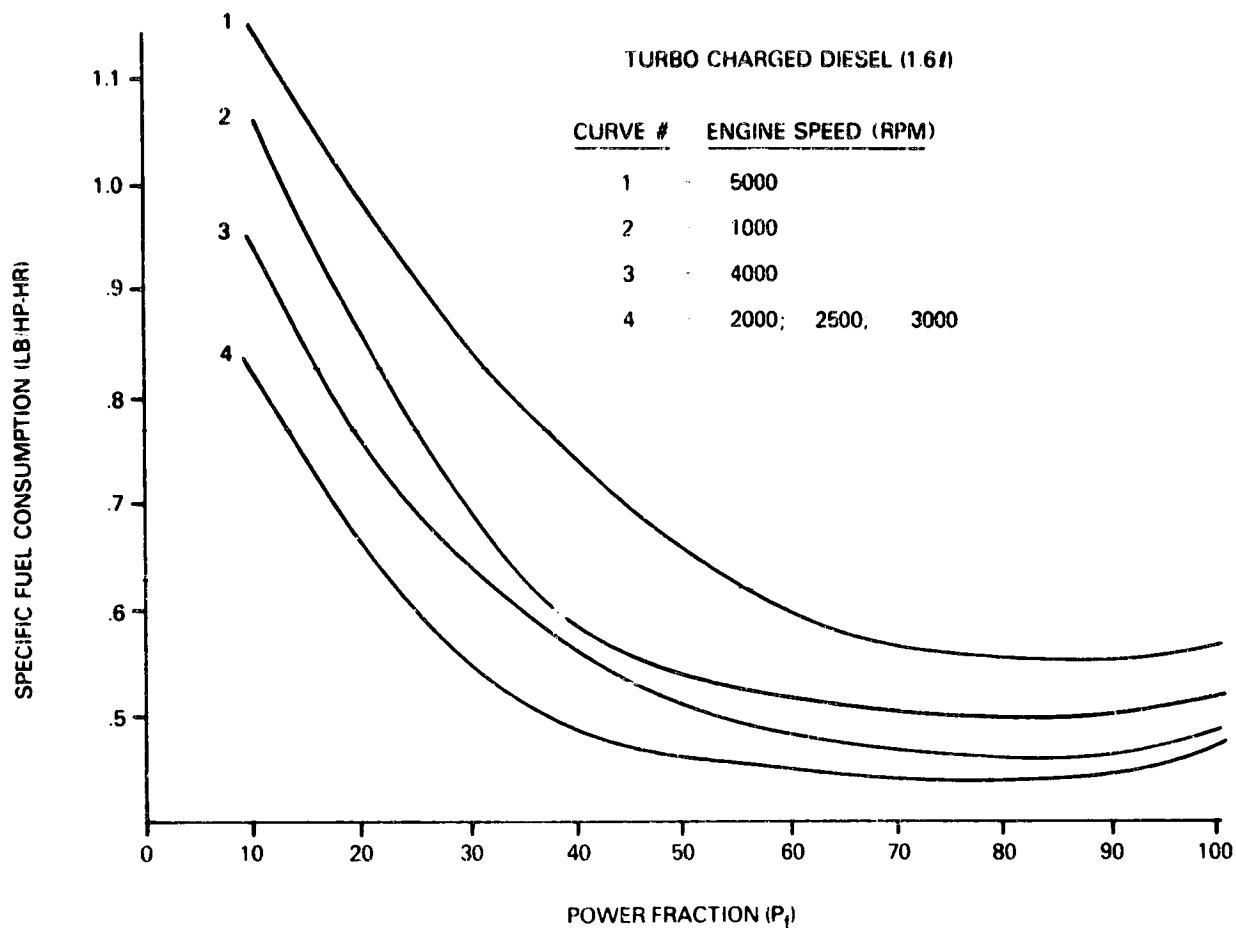
Figure III-17. Engine Fuel Consumption at Different Speeds

curves are also plotted for each gear ratio. Since the power trans-
mitted is essentially unaffected by the change of gear ratio, the
operating points described by a constant speed (in rpm) lie on a
constant power hyperbola. The envelope bounded by the maximum
torque-speed curves in Figure III-20 describe the zone of operation
by the heat engine.

III.2.2.3 Heat Engine Startup

The heat engine is always started off the vehicle driveshaft.
This procedure means, in essence, that the electric motor acts as
the starter. Figure III-21 shows the transient when the heat en-
gine is coupled with the power train. Assume that HE clutch is
closed at A which lies on a constant power profile $P_{HE}(P_{HE} < P_{PK})$.
Momentarily, the motor speed will fall from ω_1 to ω_2 resulting in
an armature current overshoot. The locus of P_{HE} should be such
that the resulting current peak does not exceed the profile of peak
power P_{PK}. Eventually the field current will respond to return the
armature current to the original value. The heat engine might be
required to start early during battery switching because of peak
load requirements or battery state of discharge becoming greater
than .75. Under these conditions, the engine clutch may be closed
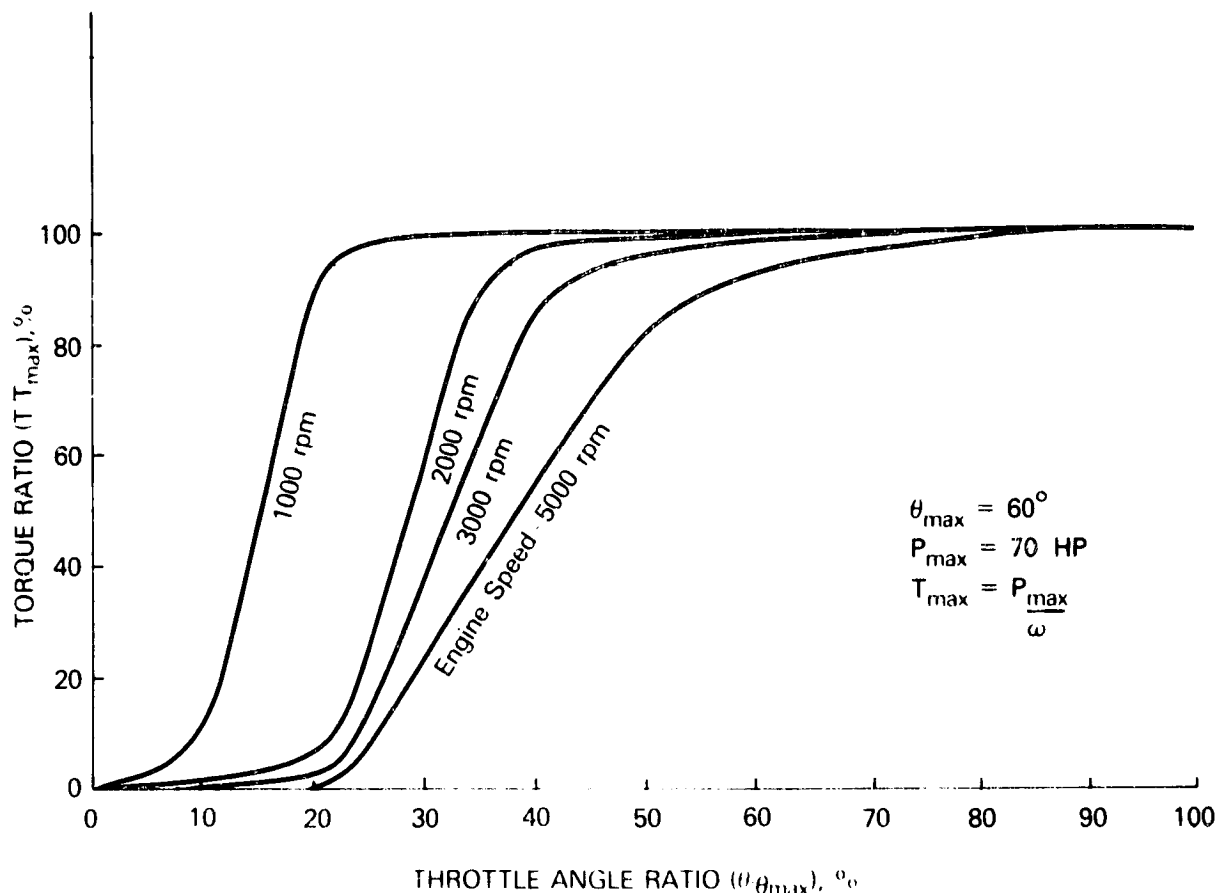
Figure III-18.   Normalized Torque-Throttle Angle Curves

in the 0.5 E_b mode so that the engine speed would be about 1000 rpm
and the peak current would be limited to 480 A.   This procedure is
shown in Figure III-10 and explained in the flow chart (Figure III-14).

III.2.2.4   Control Block Diagram

The control block diagram of heat engine operation is shown
in Figure III-22.   It is a torque controlled system similar to that
of electric motors where the command torque T_{HE}^* is assigned by the
torque distribution algorithm.   The error in the torque loop gener-
ates the throttle angle command θ^* and the corresponding error in
the angle control loop drives a step motor to set the angle.   Since
no torque transducer is used, torque will be derived by computation
from θ and ω_{HE} signals.   The torque relationship will be supplied
by VW based on tests of the 1.6 ℓ EFI-L engine.

III.2.2.5   Gear Changing Strategy

The optimum regions of operation with different gear ratios
are shown in Figure III-23 and the gear changing sequence diagram
is shown in Figure III-24.   The transition from GR1 to GR2 occurs
if the speed exceeds 5000 rpm or the speed is greater than ω_1 with
torque falling below the T_{CH} curve of GR2.   The down-shifting tran-
sitions will be initiated if the speed falls below 1000 rpm or speed
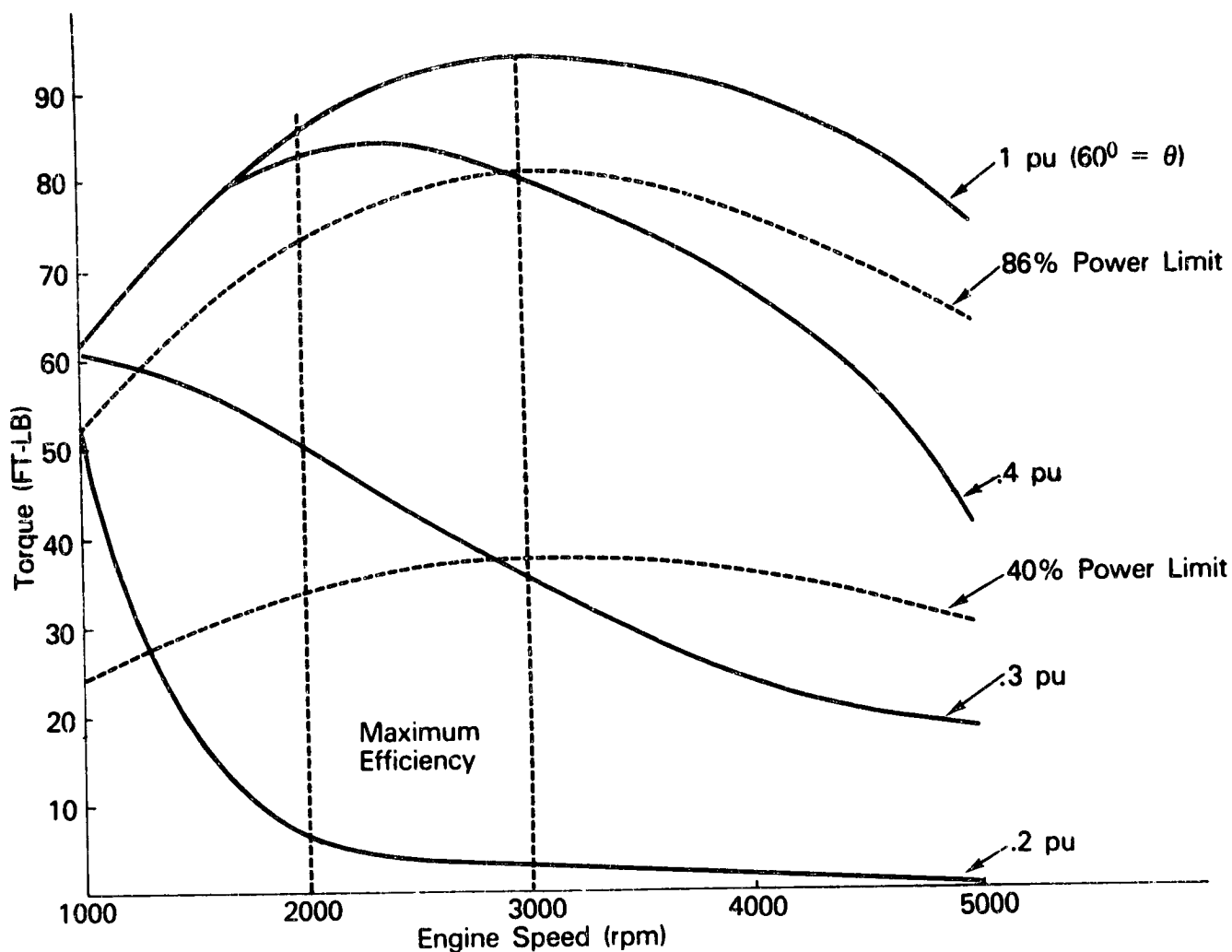
Figure III-19. Torque-Speed Curves at Different Throttle Angles

is less than ω_2 with torque exceeding the T_{CH} curve. Similar transitions in the higher gear ratios in Figure III-24 are described with the help of the Boolean Functions.

III.2.3 PROPULSION WITH ELECTRIC MOTOR AND HEAT ENGINE COMBINED

The electric motor and the heat engine will be required to operate simultaneously under the following conditions:

(1) When the heat engine or the electric motor is running alone and the commanded propulsion torque is beyond the capability of the primary propulsion unit, combined operation will be demanded. In this combined operation, when the total commanded torque falls within the capability of the primary unit, the system reverts back to the original condition (i.e., one unit operating).

(2) Electric motor starts the vehicle from rest. If, after the initial start-up operation of the vehicle, the battery state-of-discharge is greater than 0.70, the motor and the engine run together for a short period until the engine begins to function as the primary drive unit.
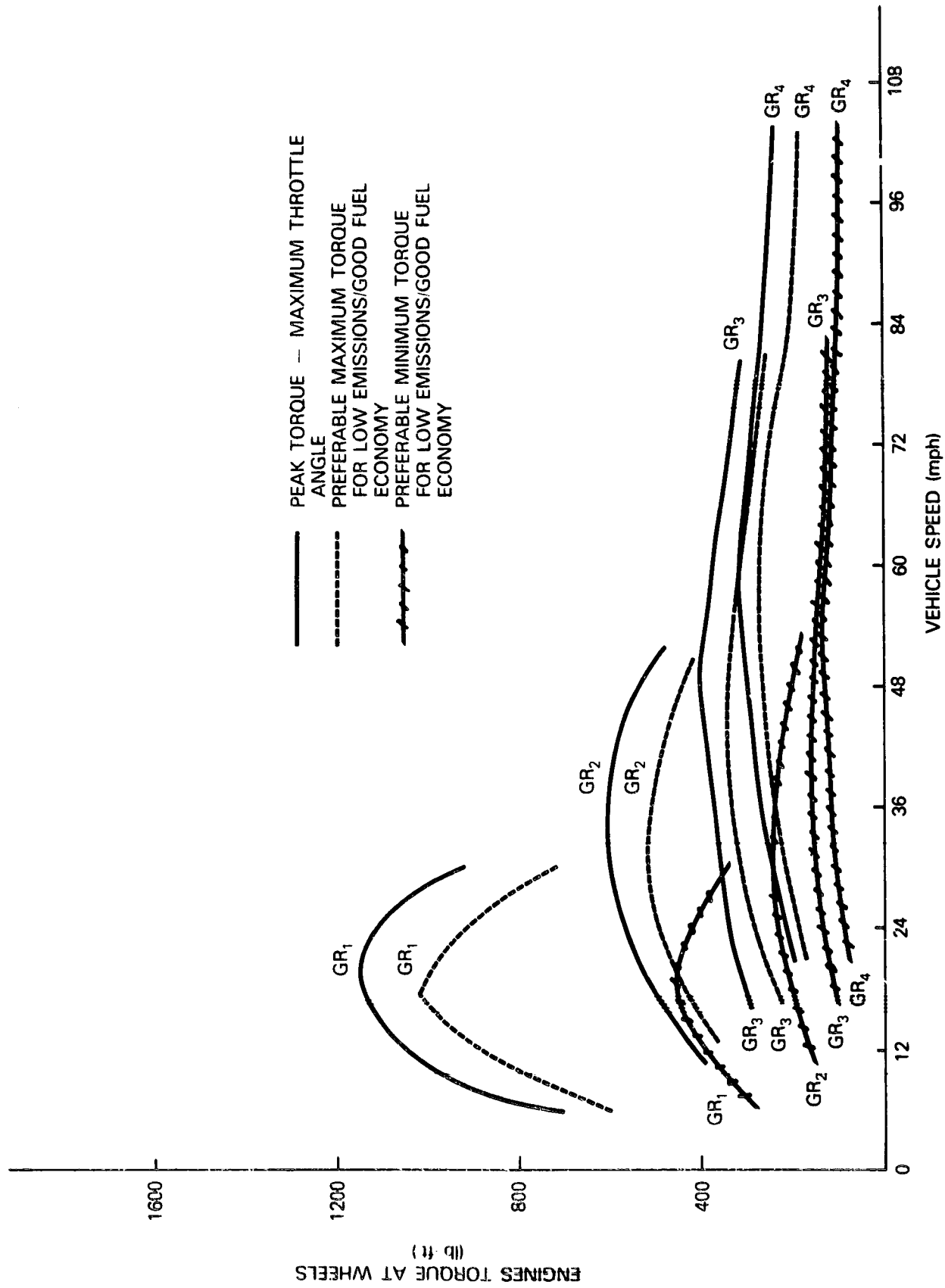
Figure III-20. Torque-Speed Curves of Vehicle with Heat Engine

GENERAL ⚙ ELECTRIC

HE COUPLING TO EM
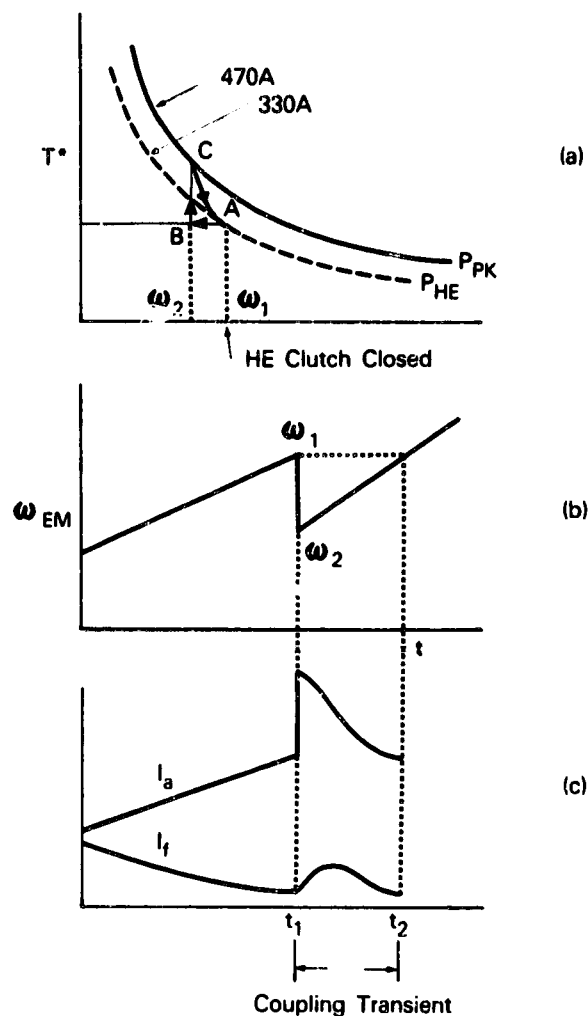
Figure III-21. Motor Transients Due to
Coupling of Heat Engine

(3) The heat engine is required to charge the battery anytime
the state-of-discharge exceeds .75, so that the battery
capacity remains sufficient for starting from rest and
peak load requirements. In this mode of operation, the
motor acts as a generator and it operates in the current
control mode. Since the heat engine acts as the primary
propulsion unit only, its excess power capacity is uti-
lized to charge the battery subject to a maximum current
limit.

III.2.3.1 Gear Changing Strategy

In the combined operation of the heat engine and electric
motor, the total available torque is determined by the addition of
their separate torques. The gear changing strategy is defined such
that the gear ratio falls in the common range of both the drive

III-21
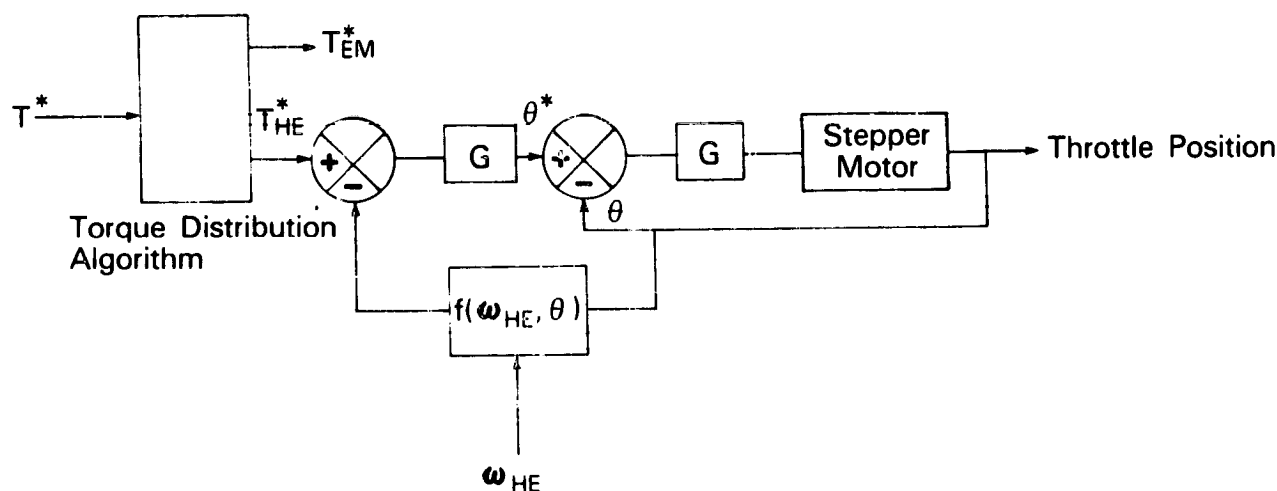
Figure III-22. Heat Engine Control Block Diagram

units. The gear ratio is determined by the operating point on
heat engine torque-speed curves provided the operating speed of
the motor is above the base value (2000 rpm) and below the maximum
speed. Figure III-25 shows the zones of operation of the heat en-
gine for different gear ratios and the corresponding sequence dia-
gram is given in Figure III-26. Parallel operation of motor and
engine is normally restricted to above 12 mph (i.e., 2000 rpm in
GR1). The .5 E_b mode of operation for the motor is permitted with
the heat engine on a temporary basis during a transition from motor
only to heat engine only or vice versa. If the speed in GR1 ex-
ceeds 5000 rpm, shifting occurs to GR2. The down-shifting transi-
tion will occur if speed goes below 2000 rpm or torque is higher
than T_{CH} of GR2 with speed below ω_1. The gear shifting conditions
for different gear ratios are summarized by Boolean functions in
Figure III-26.

III.2.3.2 Torque Distribution Algorithm

In the combined operation of engine and motor, the total com-
manded torque is to be distributed between the propulsion units so
that the overall system operates in an optimum manner. Table III-1
gives the algorithm for torque distribution. The total commanded
torque T^* is determined from the accelerator pedal position and is
identified to be in the range for combined propulsion unit operation
and T_{EM}^* and T_{HE}^* are determined.

III.2.4 PROPULSION UNIT SEQUENCING STRATEGY

The sequencing strategy of propulsion units is summarized in
Figure III-27. The vehicle will start in EM mode and can transition

Table III-1

TORQUE DISTRIBUTION ALGORITHM

$$T_{EMm} + T_{CH} < T^* < T_{max} \qquad T_{EM}^* = T_{EMm}, \; T_H^* = T^* - T_{EM}^*$$

$$T_{EMr} + T_{CH} < T^* < T_{CH} + T_{EMm} \qquad T_{HE}^* = T_{CH}, \; T_{EM}^* = T^* - T_{HE}^*$$

$$T_{cl} + T_{EMr} < T^* < T_{CH} + T_{EMr} \qquad T_{EM}^* = T_{EMr}, \; T_{HE}' = T^* - T_{EM}^*$$

$$T_{mn} + T_{cl} < T^* < T_{cl} + T_{EMr} \qquad T_{HE}^* = T_{cl}, \; T_{EM}^* = T^* - T_{HE}^*$$

$$T_{mn} < T^* < + T_{cl} \qquad T_{EM}^* = T_{mn}, \; T_{HE}^* = T^* - T_{EM}^*$$

$$T^* \le 0 \qquad T^* = T_{EM}$$

The variables used above are defined below:

T_{CH} — maximum preferable heat engine torque for low emission

T_{cl} — minimum preferable heat engine torque for good fuel economy

T_{EMm} — peak motor torque for E_b transient operation

T_{EMr} — rated motor torque

T_{max} — total peak torque for motor and heat engine

T_{mn} — minimum preferable motor torque for good efficiency

to HE mode through the EM + HE mode only. If regenerative braking is commanded, the system always returns to EM mode irrespective of the present mode of operation. During steady operation in any of the modes, the required command torque is determined from the accelerator pedal position and executed by the respective control block diagram. The system transitions are summarized as follows:

EM ⤢ EM + HE

There are two possible paths of transition from EM to EM + HE mode. If the motor is running in the 0.5 E_b mode and the battery state of discharge becomes greater than 0.7, transition will be commanded to EM + HE mode for eventual transfer to HE mode. In this transition, the engine is started from the vehicle driveshaft
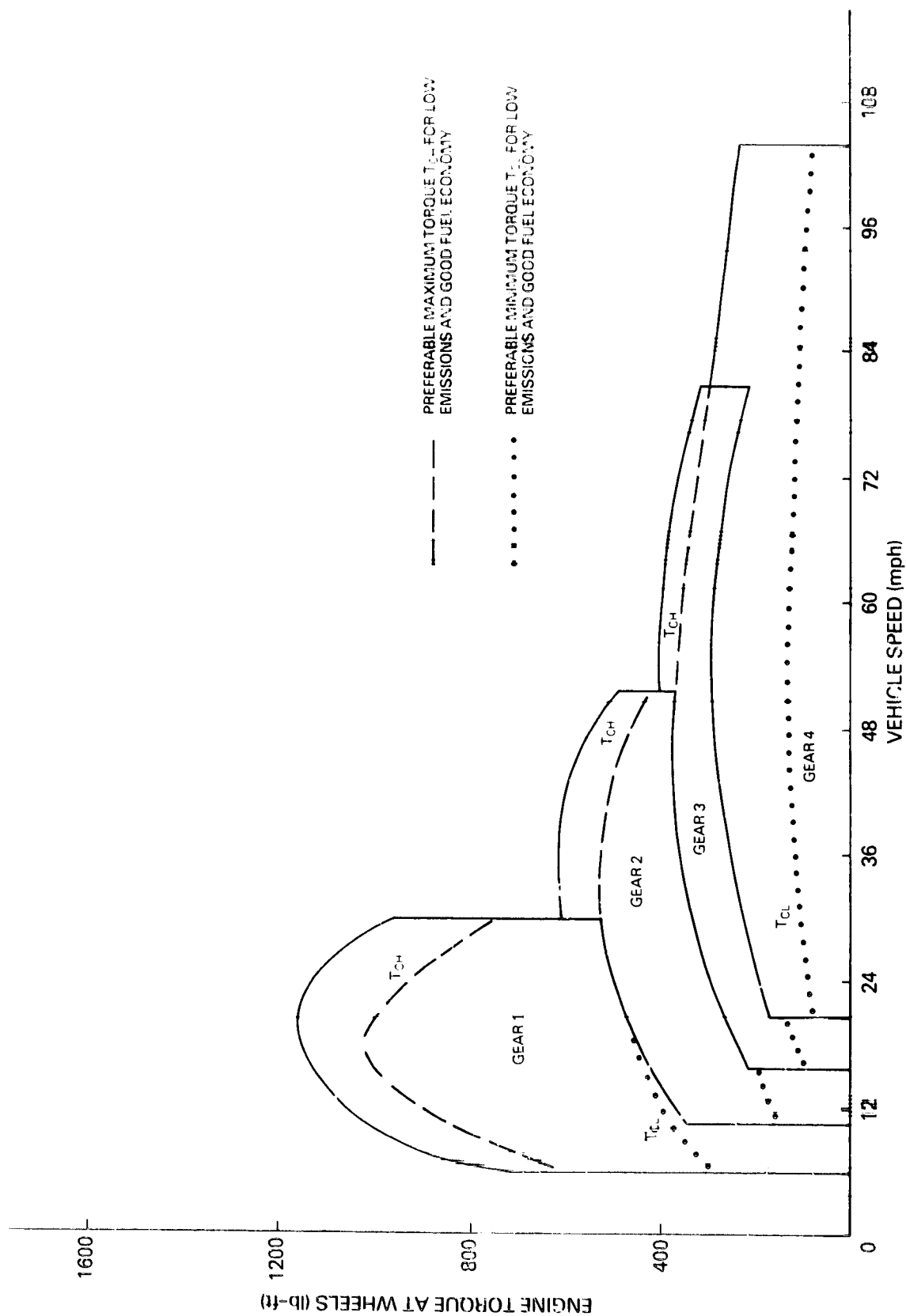
Figure III-23. Engine Operation Regions at Different Gear Ratios

SYMBOL	SPEED, rpm
ω_1	1784
ω_2	1504
ω_3	1290
ω'_1	2803
ω'_2	3325
ω'_3	3876

$(\omega > \omega_1) \cdot (T < T_{CH}$ Of $GR_2)$
$+ (\omega > 5000)$

$(\omega > \omega_2) \cdot (T < T_{CH}$ Of $GR_3)$
$+ (\omega > 5000)$

$(\omega > \omega_3) \cdot (T < T_{CH}$ Of $GR_4)$
$+ (\omega > 5000)$

$(\omega < \omega'_2) \cdot (T > T_{CH}$ Of $GR_2)$
$+ (\omega < 1000)$

$(\omega < \omega'_3) \cdot (T > T_{CH}$ Of $GR_3)$
$+ (\omega < 1000)$

$(\omega < \omega'_4) \cdot (T > T_{CH}$ Of $GR_4)$
$+ (\omega < 1000)$

GR_1 GR_2 GR_3 GR_4

ω - HEAT ENGINE SPEED, rpm
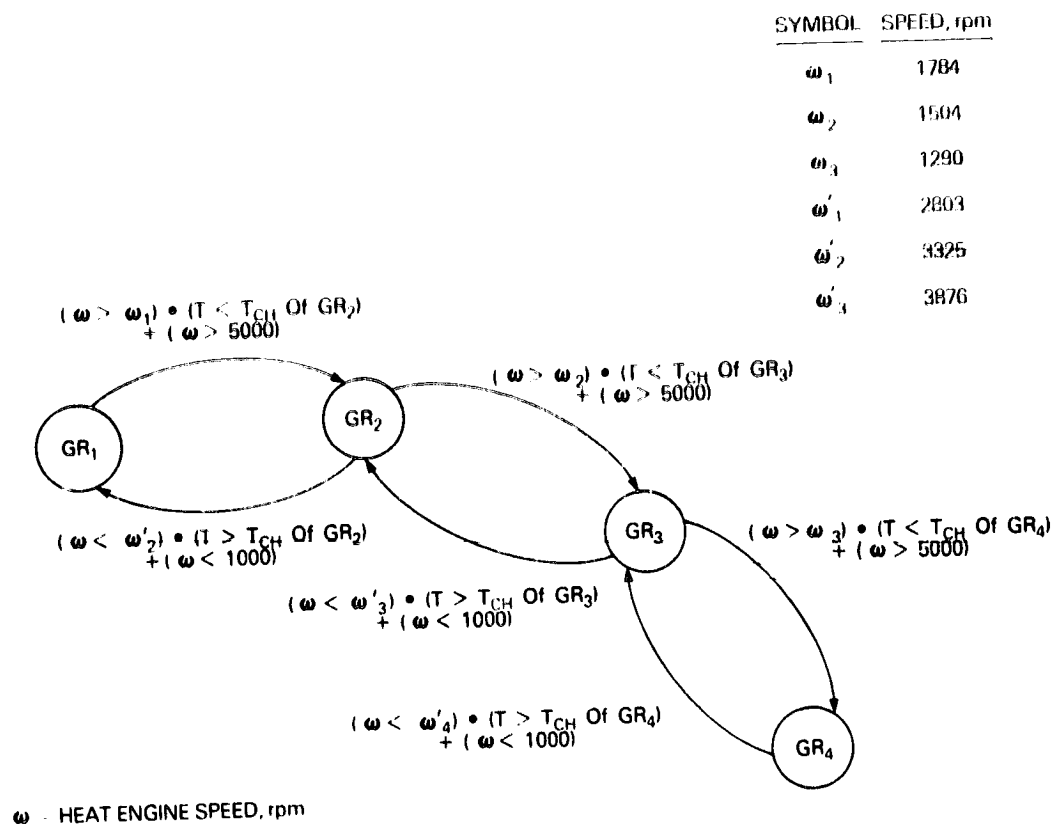
Figure III-24. Engine Gear Changing Strategy

until its speed reaches 500 rpm and then fired. The alternate transition path holds true for a number of conditions which can be summarized as follows:

- In the E_b mode of operation if the battery state of discharge becomes greater than 0.7.

- The torque demand is such that it crosses the critical power profile P_{HE} for time delay Td.

- The initial torque command is above T_C (Figure II-10), and speed above 1000 rpm is detected in 0.5 E_b mode.

- The battery discharge exceeds 0.7 and speed above 1000 rpm is detected in the 0.5 E_b mode.

- Vehicle speed exceeds $30(1-S)^2$ mph for time delay Td.

Under any of the above conditions, the vehicle goes to EM + HE mode after closing the HE clutch.

The transition from the EM + HE to EM mode occurs when the brake pedal is pressed (regeneration required) or the total command torque falls below that corresponding to the P_{HE} curve with the battery state of charge permitting. Under this condition, the command torque is transferred to the motor, HE clutch is opened, and the engine is shut off by setting $\theta^* = 0$.
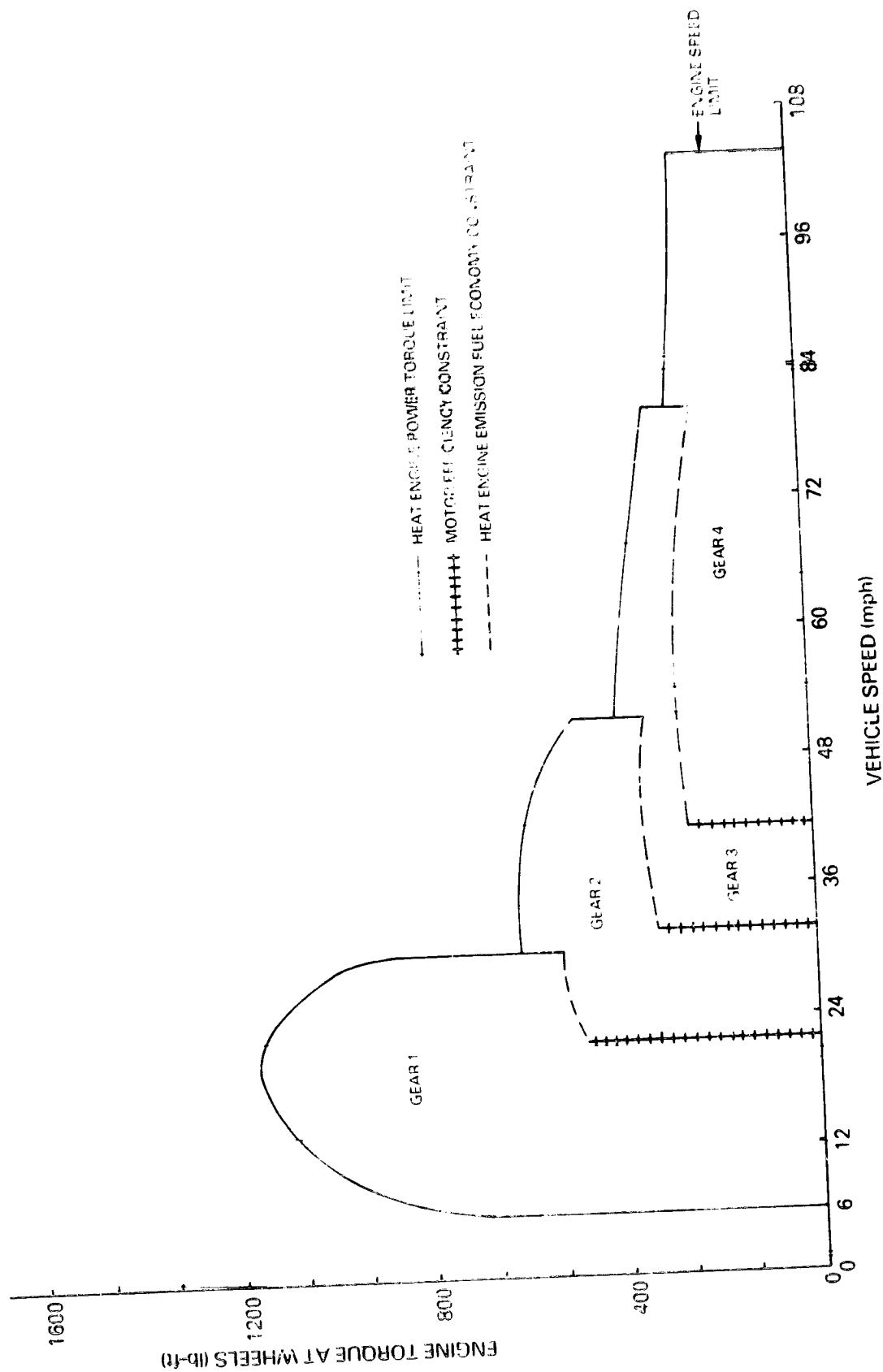
Figure III-25. Gear Ratio Operation Zones in Combined Drive
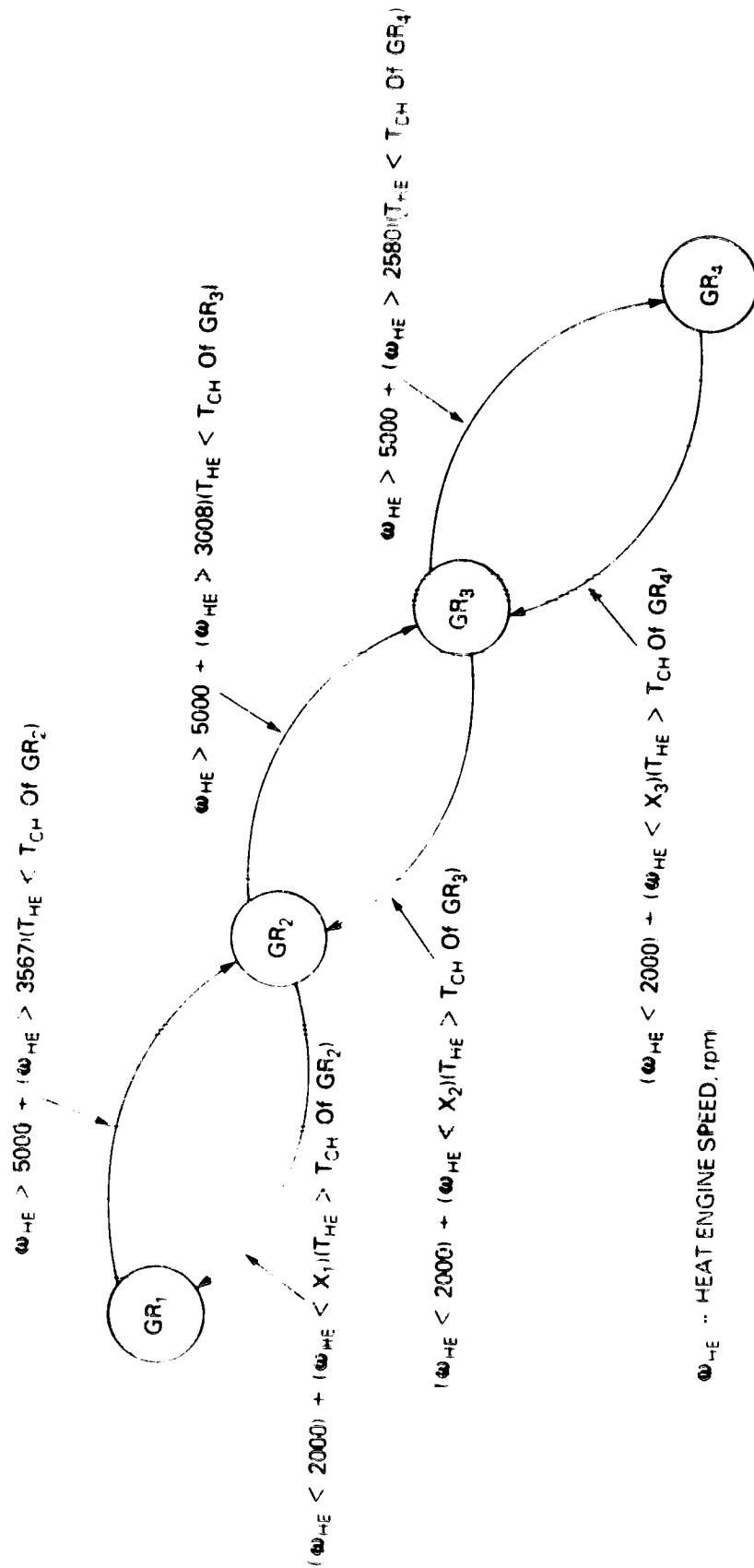
Figure III-26. Combined Drive Gear Changing Strategy

X_1 2603
X_2 3325
X_3 3876

$\omega_{HE} > 2580 (|T_{HE} < T_{CH}$ Of $GR_4)$

$\omega_{HE} > 5000 + (\omega_{HE} > 3608)(T_{HE} < T_{CH}$ Of $GR_3)$

$\omega_{HE} > 5000 + (\omega_{HE} > 3567)(T_{HE} < T_{CH}$ Of $GR_2)$

$(\omega_{HE} < 2000) + (\omega_{HE} < X_1)(T_{HE} > T_{CH}$ Of $GR_2)$

$(\omega_{HE} < 2000) + (\omega_{HE} < X_2)(T_{HE} > T_{CH}$ Of $GR_3)$

$(\omega_{HE} < 2000) + (\omega_{HE} < X_3)(T_{HE} > T_{CH}$ Of $GR_4)$

ω_{HE} - HEAT ENGINE SPEED, rpm

GR_1 GR_2 GR_3 GR_3
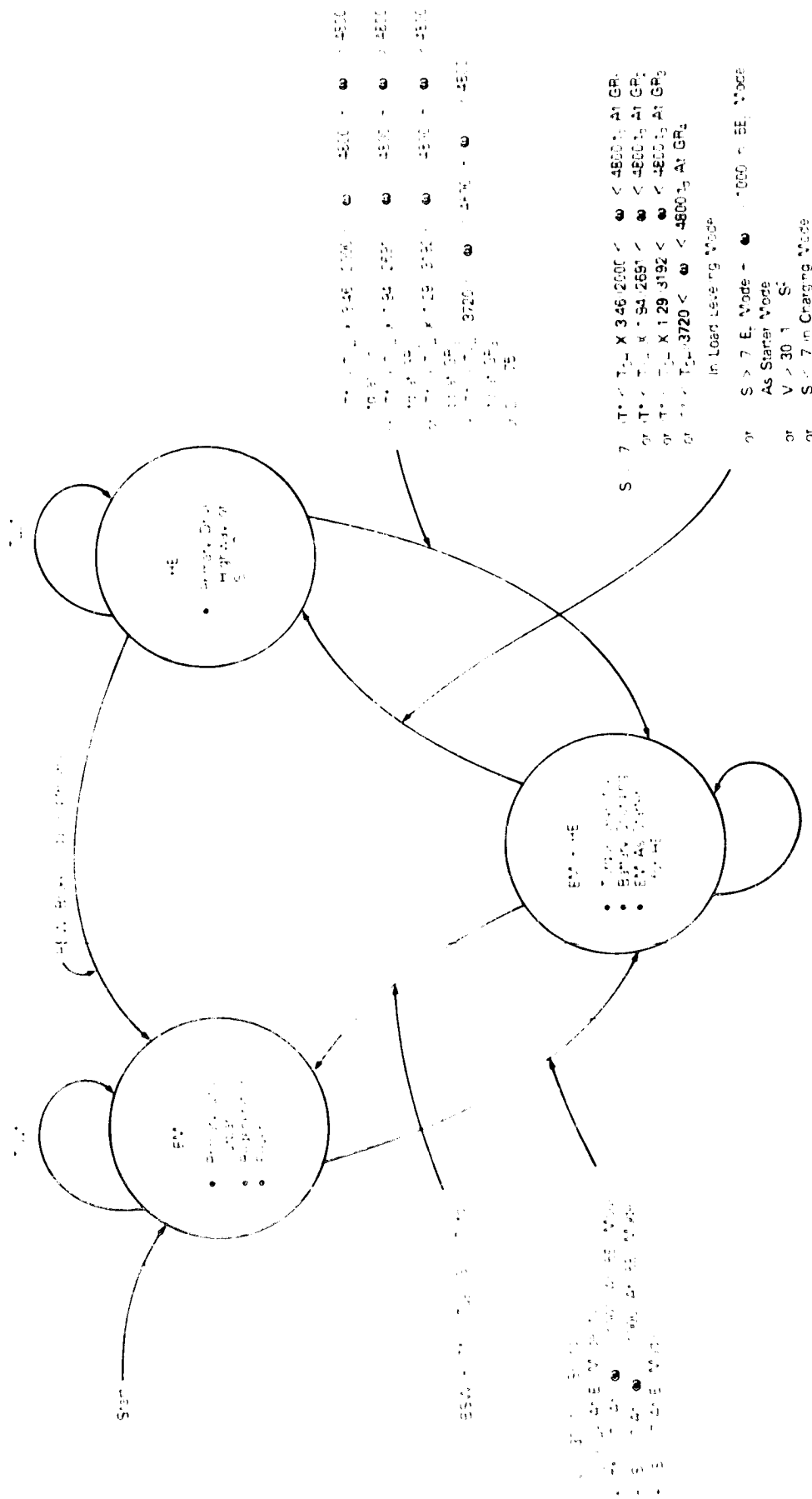
Figure III-27. Propulsion Source Sequencing Strategy

HE ⇄ EM + HE

The transition from HE to EM + HE mode occurs either to meet peak power demands (passing) or as a transition to EM mode of operation. Figure III-28 shows the envelope above which assistance of the motor is required. The profile is placed somewhat below the maximum envelope such that engine operation above TCH is avoided by allowing sufficient time for starting the motor.

In the above transition in highway driving, the motor can be started (i.e., brought up to idle speed) by the battery switching method. It is then brought up to 90% of HE speed before the clutch is closed. This avoids a deceleration of the vehicle during motor starting. In urban driving, the electric motor is always up to speed and it is activated by simply turning on the field current and then closing the main contactors.

The reverse transition to HE mode from the HE + EM mode occurs under the following conditions:

- The command torque falls below the envelope shown in Figure III-28.
- The battery state-of-discharge exceeds 0.75.
- Battery state-of-discharge is greater than 0.7 when engine is charging the battery.
- Vehicle speed exceeds $30(1-S)^2$ mph.

When any one of the above conditions is encountered, the command torque is transferred to the heat engine, the EM clutch and contactors are opened, and motor field is de-energized.

HE ⇄ EM

This simple transition occurs when the brake pedal is pressed. At this command, HE clutch is opened and EM clutch is closed, and the motor counter emf is brought up by the field before the armature contactor is closed.

III.3 MICROCOMPUTER SYSTEM

III.3.1 DESIGN CONSIDERATIONS

The controller is to be designed to perform the following major functions:

- VEHICLE DRIVE TRAIN SEQUENCING
- HEAT ENGINE TORQUE CONTROL
- ELECTRIC MOTOR TORQUE CONTROL
- BATTERY CHARGE/GAUGING
- OPERATOR INTERFACE
- SYSTEM MONITORING AND DIAGNOSTICS
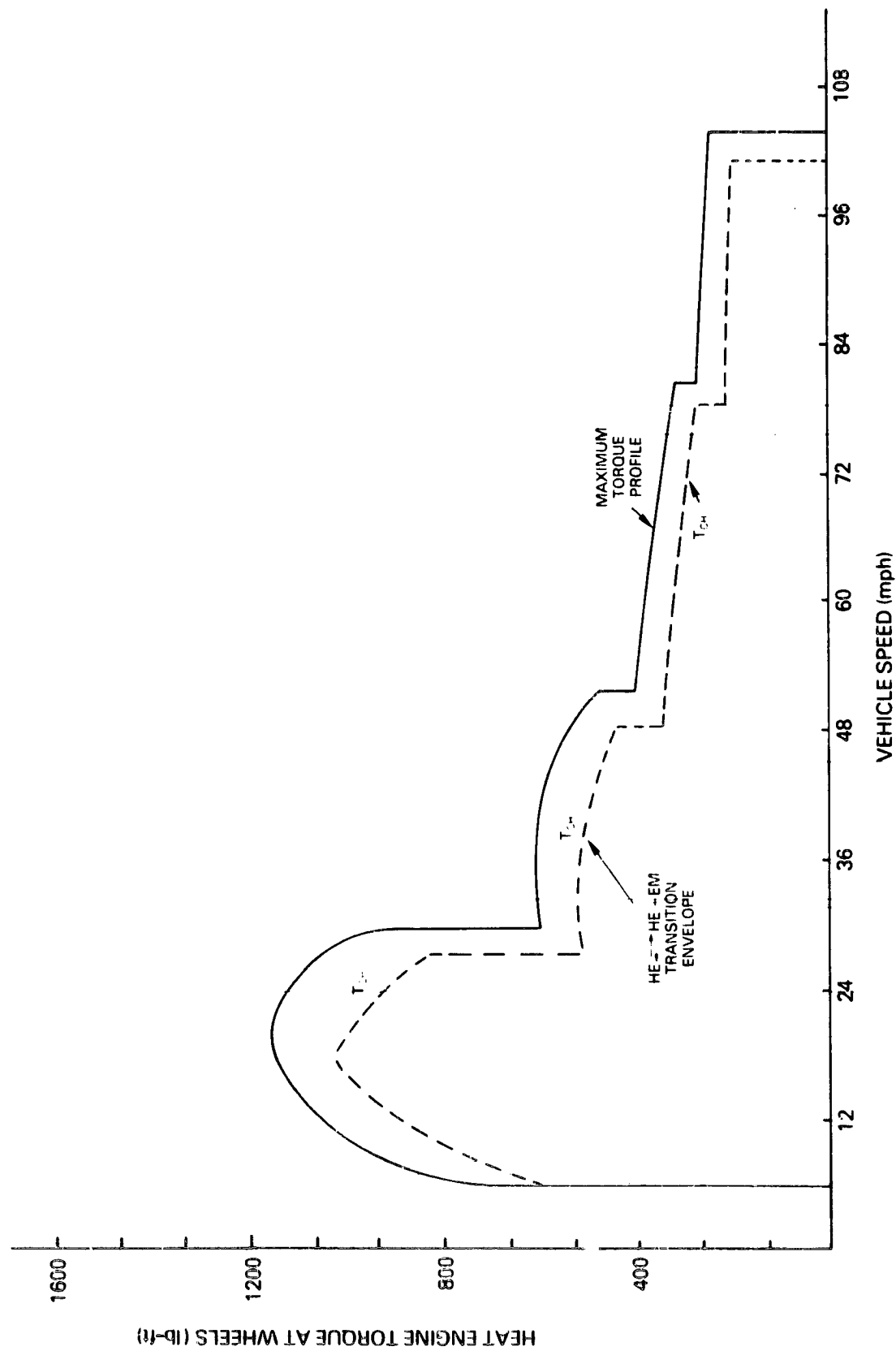
Figure III-28. Engine Torque-Speed Envelope Beyond Which Transition Occurs

The selected implementation must take into account the relative
complexities and sampling intervals necessitated by each function.
The most complex function, VEHICLE SEQUENCING, is slow relative to
the TORQUE CONTROL functions. From previous experience with the
ITV electric vehicle controller, preliminary estimates for the sam-
pling intervals for each function are given in Table III-2.

Table III-2

CONTROLLER FUNCTION CHARACTERISTICS

Function	Complexity	Sampling Interval
Vehicle Sequence	High	100 msec
HE Torque Control	Medium	4 msec
EM Torque Control	Medium	4 msec
Battery Charge	Medium	1 sec
Operator Interface	Low	120 msec

Consider that the ITV controller required about 50% of an INTEL
8080's processing for mainly two functions, motor current control
and electric drive sequencing. For this application, even with a
higher performance CPU (such as the INTEL 8086) the processing re-
quired would probably be much more than 50% and, therefore, would
leave less margin of flexibility. Beyond functional considerations,
the implementation must take into account special requirements as-
sociated with the maintenance and test of the controller and the
hybrid power train. For diagnostic purposes the controller hard-
ware and software has been partitioned into modular functions which
may be tested independently.

III.3.2 HARDWARE DESIGN

The microcomputer based hardware shown in Figure III-29 is
divided into four major parts and is contained on three separate
boards. Each board has a separate microprocessor and exchanges
information with other boards through a common bus.

Board 1, Vehicle Controller

The vehicle controller provides the vehicle drive train se-
quencing and heat engine torque control functions. This board
serves as master and is based upon a 16-bit CPU (such as the INTEL
8086 type).

Board 2, Electric Drive Controller and Operator Interface Unit

The ELECTRIC DRIVE CONTROLLER provides the electric motor
torque control and battery charge current profile functions. In
addition the OPERATOR INTERFACE UNIT would send display information
and receive control inputs from the operator.
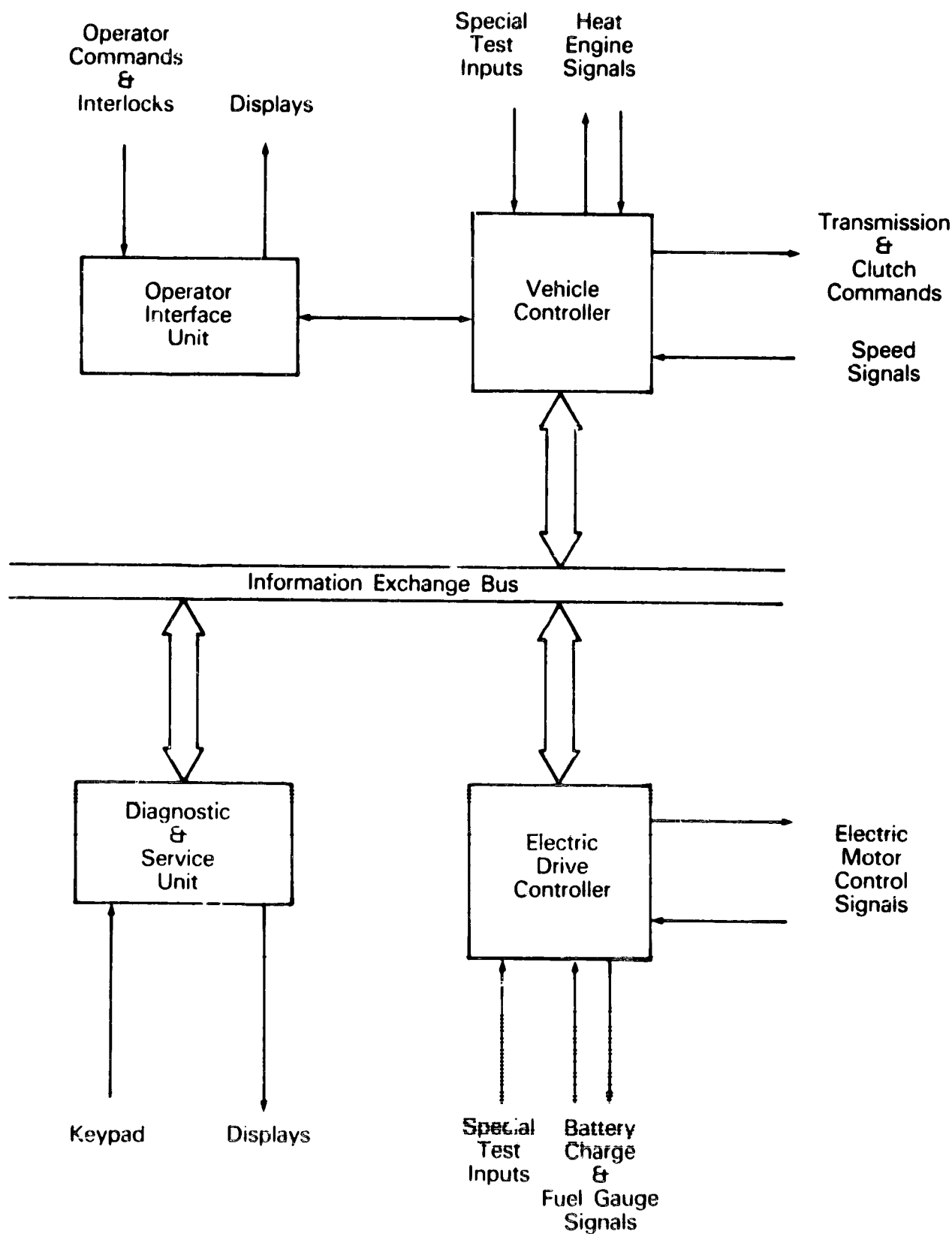
Figure 111-29. Hybrid Vehicle Microcomputer-Based Hardware

Board 3, Controller Monitoring Instrument

The CONTROLLER MONITORING INSTRUMNET enables the on-line monitoring of system parameters within the two controllers and, correspondingly, the hybrid drive train. The unit would serve initially as a means for perfecting the hybrid control system strategy. Later, the same on-line monitoring features might be used for test purposes.

Boards 2 and 3 would be based upon 8-bit CPU's (such as the INTEL 8085). The information exchange bus provides communication between the two controllers and the MONITORING INSTRUMENT. At the time of detailed design, the optimum bus type and communication protocol would be determined. Special test inputs are planned for each controller so that each can be operated independently for debugging of the hybrid drive train.

III.3.3 SOFTWARE DESIGN

The software subsystems for each microcomputer is to be structured top-down into modular units for ease of development and flexibility of design. The software operating system for each microcomputer is to be clock driven for real time operation. Figure III-30 presents a simplified view of the functions implemented in software between the two controllers. Assembly language programming is required for each CPU type in order to meet performance requirements associated with the sampling intervals of the controller functions.
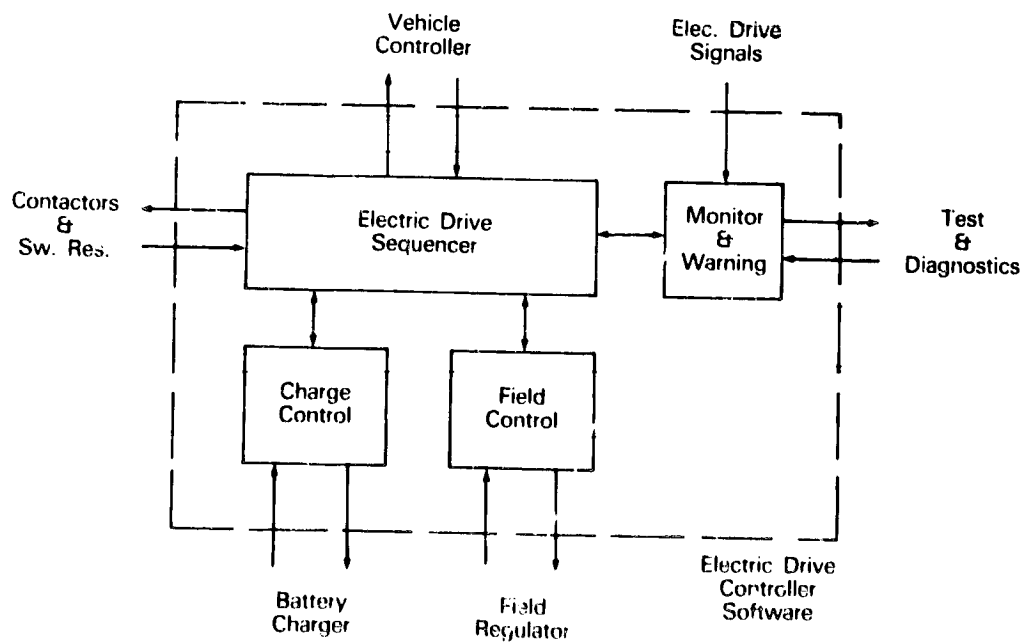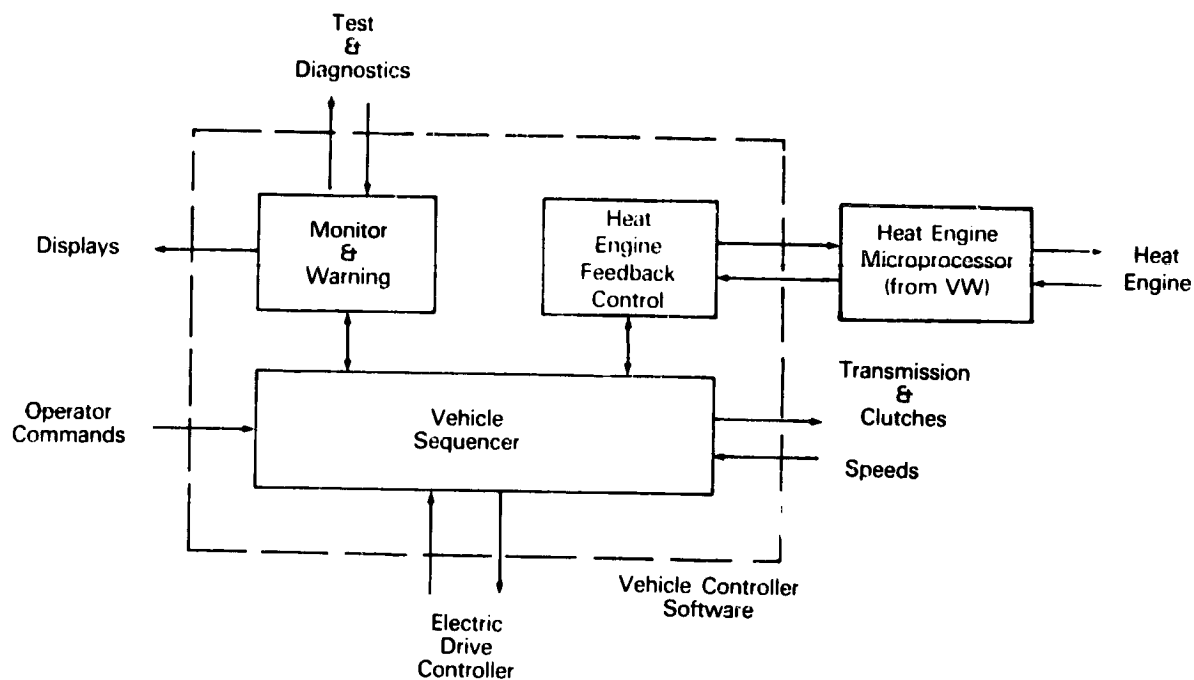
Figure 111-30. Hybrid Vehicle Microcomputer Software Partition

Appendix IV

DESIGN STUDY OF THE BATTERY SWITCHING CIRCUIT FIELD CHOPPER, AND BATTERY CHARGER

Appendix IV

DESIGN STUDY OF THE BATTERY SWITCHING CIRCUIT FIELD CHOPPER, AND BATTERY CHARGER

IV.1 INTRODUCTION

Preliminary design of a battery switching circuit, field chopper and battery charger for the Hybrid Electric Vehicle (HEV) were undertaken in this study. Block diagrams of the circuit implementation, preliminary packaging, and size and weight estimates were desired for each function. Manufacturing cost for production quantities of 100,000 units per year were estimated based on a producibility analysis.

Goals of the preliminary design study include:

- Low-cost but reliable electric propulsion motor controller

- Modular circuits to minimize development time and cost

- Accessible packages, i.e., each function is removable independent of other functions, to simplify debugging, maintenance, and repair.

Figure IV-1 is a functional block diagram of the major components in the HEV electric drive subsystem. Technical and cost details of the microcomputer-based "controller" (above the dotted line) are not included in this study. However, the packages presented are sized to include the microcomputer controller. The propulsion battery is illustrated in Figure IV-1 for clarity only. Remaining functions, including on-board charger power unit, battery charger, battery switching contactors, and field chopper are included in this preliminary design.

The quantitative results of this study are presented in Section IV-2. Design detail and circuit discussions of each function are presented in Section IV-3. Section IV-4 includes details of the preliminary packaging.

IV.2 SUMMARY OF THE DESIGN STUDIES

The preliminary design results for the battery switching circuit, field chopper, and battery charger are summarized in this section. Results are given for manufacturing cost and selling price, size and weight, and recommended packaging for each of the components. The manufacturing cost results presented are appropriate only for the following assumptions:

1) Costs are in first quarter 1979 dollars

2) 100,000 HEV electric drive subsystems are produced per year.

Cost data from the producibility analysis for the Near-Term Electric Vehicle[1] were used for estimating manufacturing costs.
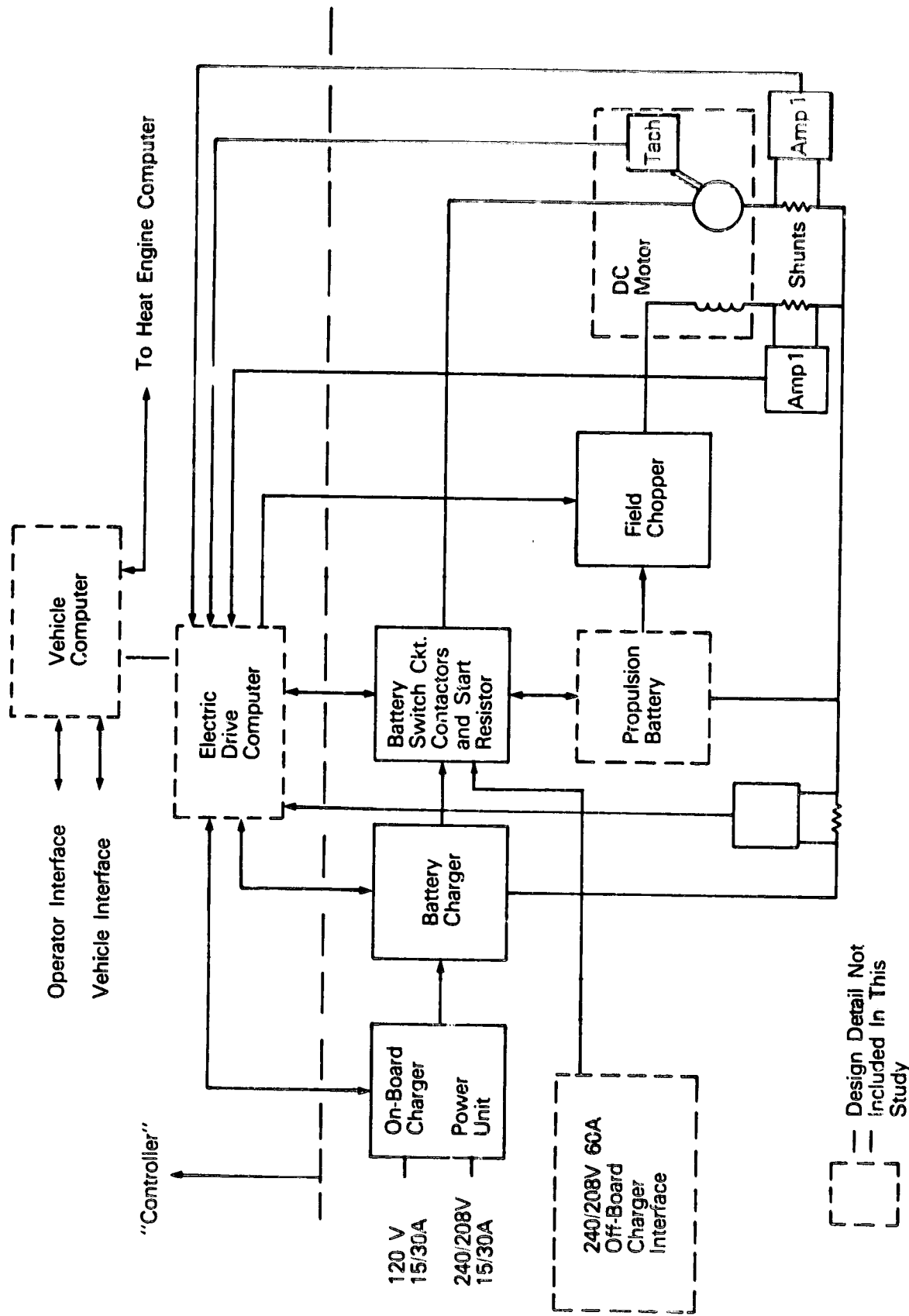
Figure IV-1. Preliminary Hybrid Vehicle Electric Drive Subsystem Block Diagram

Material costs were obtained from vendor estimated quotes for the components in production quantities. Labor estimates are based on typical assembly times for similar General Electric Electronic Systems. Production cost estimates were obtained by applying appropriate factory overhead factors to the base material and labor costs. A functional summary of the estimated manufacturing cost of the propulsion control electronics and the power contactor/starting resistor assembly is given in Table IV-1. The high volume (100 K/yr) selling price estimate of the propulsion control electronics and the power contactor assembly is $829.90 as shown in Table IV-2. The selling price includes profit (10% after taxes) and equipment/development amortization.

Table IV-1

PRELIMINARY PRODUCTION COST ESTIMATES

(Bat. Switch Ckt, Field Chopper, Bat.
Charger and On-Board Chrg. Pwr. Unit)

	Material Cost ($)	Labor (Minutes)	Estimated Mfg. Cost ($), 100 K Qty
Power Contactor Assembly			
Bat. Switch Contactors/ Starting Resistor	173.38	10.0	243.30
On-Board AC Charger Power Unit	58.49	18.0	93.05
Wiring/Enclosure	8.00	10.0	18.38
Propulsion Control Electronics			
Field Chopper	22.00	34.8	57.11
Battery Charger/ Logic Power Supply	137.78	43.0	219.63
Wiring/Enclosure	11.65	29.7	38.12
TOTAL:	412.10	145.4	669.58

A modular circuit board -- Wire Wrap (WW) or Printed Circuit (PC) -- packaging approach is recommended in this study. Each component function is normally mounted on a single board. Function weight estimates, plus approximate circuit board and power supply requirements, are given in Table IV-3.

Recommended packaging requires two enclosures, a power contactor/starting resistor assembly and a propulsion control electronics housing. Functional paritioning and packaging alternatives

Table IV-2

SELLING PRICE SUMMARY
(Power Contactor Assembly and Propulsion Control Electronics)

	Cost/Unit ($)
Manufacturing Cost	669.58
Equipment/Development Amortization	22.00
Profit (10% after taxes)	138.22
TOTAL SELLING PRICE:	829.90

Table IV-3

PRELIMINARY HEV ELECTRIC DRIVE CONTROL PACKAGE SUMMARY

Enclosure/Function	Number of Boards (6"x9")	Power Supply Required	Off-Board Components Required	Function Weight (lbs)
Power Contactor Assembly				
Bat. Switch Contactors/ Starting Resistor	--	$V^+_{Bat.1}$, $V_{Bat.2}$ Bat. Com.	--	18
Shunt Amplifiers	.5	± 15V	--	1
AC On-Board Charger Power Unit	--	$V^+_{Bat.1}$	--	8
Enclosure/Brackets	--	--	--	2
Propulsion Control Electronics				
Field Chopper	1	± 15 V ± 7.5V isolated	20A Darlington +Heat Sink	4
Battery Charger	1		50A Darlington +Heat Sink	4
Microcomputer Controller	2 (available)	+5V	Sensors	5 est.
Logic Power Supply	1	12V DC Input	Fuse	3
Spare Boards	1 (wire wrap) or 2 (Printed Ckt.)	--	--	1
Enclosure/Brackets	--	--	--	2
TOTAL:				48

GENERAL ⚡ ELECTRIC

are presented in Section IV-4. Figures IV-2 and IV-3 illustrate
the packaging recommended based on this preliminary design.

IV.3 PRELIMINARY DESIGN CONSIDERATIONS

Preliminary circuit block diagrams are presented for battery
switching, the field chopper, and the on-board battery charger.
The circuit designs developed present relatively low technical
risk, are highly reliable, and can be produced in large quantities
at low cost.

The relatively simple motor control strategy utilizing field
control and battery switching with a series starting resistor is
justified because the HEV uses a multispeed transmission with slip-
ping clutches. In this control technique, the motor idles at ap-
proximately 1200 rpm when the ignition key switch is initially
turned "on" and the vehicle is not moving. During idle, the two
battery banks are switched to a parallel mode with 60 V applied
to the armature. Motor speeds above 1200 rpm are obtained by
either field weakening or switching the two battery banks in series
(120 V). Transitions from zero rpm to idle or changes in the
battery mode from parallel to series or series to parallel modes
requires the starting resistor to be inserted in series with the
motor armature.

Unique features of the battery switching armature control
with starting resistor include:

- Simplification and increased efficiency of battery
  charging from 120 V or 240 V ac lines

- Extended regenerative braking down to approximatley
  6 mph

- Increased efficiency to drive accessories when the motor
  is idling at 1200 rpm

- Peak battery currents limited during battery mode switch-
  ing by a series starting resistor

- Contactor bounce during battery mode switching cannot
  short batteries

- 120 volt mode requires two contactors to be closed.

Figure IV-4 illustrates the battery switching circuit. Ten
12-V batteries, i.e., two 60-V banks consisting of 5 batteries
per bank, are assumed for the HEV. Single Pole Double Throw
(SPDT) contactors CS/P1 and CS/P2 switch the two battery banks
to either a parallel mode (60 V) or a series mode (120 V). Each
contactor contains a mechanically driven microswitch that is used
to provide return signals to the microcomputer controller to ac-
knowledge contactor closure. Transistorized relay driver modules,
with integrated suppression circuits and optional time delays,
translate logic level contactor commands from the controller.

Figure IV-2. Preliminary HEV Power Contactor/Starting Resistor Assembly

Control Interface Signals	No. Bits (Wires)
Main Disconnect Contactor	1
Resistor Contactor Shunt	1
Series/Parallel Bat. Control	2
Armature Current Shunt Signal	1 Twisted Pair
120/240 AC Line Sense	1
AC Power Disconnect Control	1

MOT⁻

MOT⁺

5"

12"

CONTACTOR
ENCLOSURE

4"

HEAT SHIELD FOR
STARTING
RESISTORS

11"

7"

AC CHARGER
POWER UNIT

B₁⁺ B₁⁻   B₂⁺ B₂⁻

120/240 60 HZ
AC POWER
INPUT

AC POWER
OUTPUT

CONTROL
SIGNALS

FIELD PWR. DASH LIGHTS CONTACTOR DRIVER OUTPUTS

12"

9"

ACCESS COVER
(TO REMOVE
PC BOARDS)

8 "

EXTERNAL
ISOLATED
HEAT
SINK

1"

B_1^+ B_2^+ AC INPUT   +12V   CONTROL I/O

Figure IV-3. Preliminary EPV Propulsion Control Electronics Unit

Two additional Single Pole Single Throw (SPST) contactors, the main disconnect (CMDC) and power resistor shunt contactor (CRS), are required for the battery switching circuit implementation. Normal circuit operation requires the CMDC contactor to open prior to parallel/series battery switching. This allows the SPDT contactors to be switched "dry" without interrupting current. Suppression techniques to prevent arcing and prolong contactor life are required only on the SPST contactors. A freewheeling diode and snubber circuit across the armature allow stored inductor currents to re-circulate during battery current interruptions resulting from contactor switching. The high power nichrome starting resistor is connected in series with the armature whenever the CRS contactor is open (de-energized). This resistor is inserted in the circuit to smooth the transition during battery mode switching and prevent excessive peak currents drawn from the battery.

The battery switching circuit illustrated in Figure IV-4 is packaged along with the on-board charger power unit (OBCPU). Contactors, starting resistor (including a heat shield, if necessary)
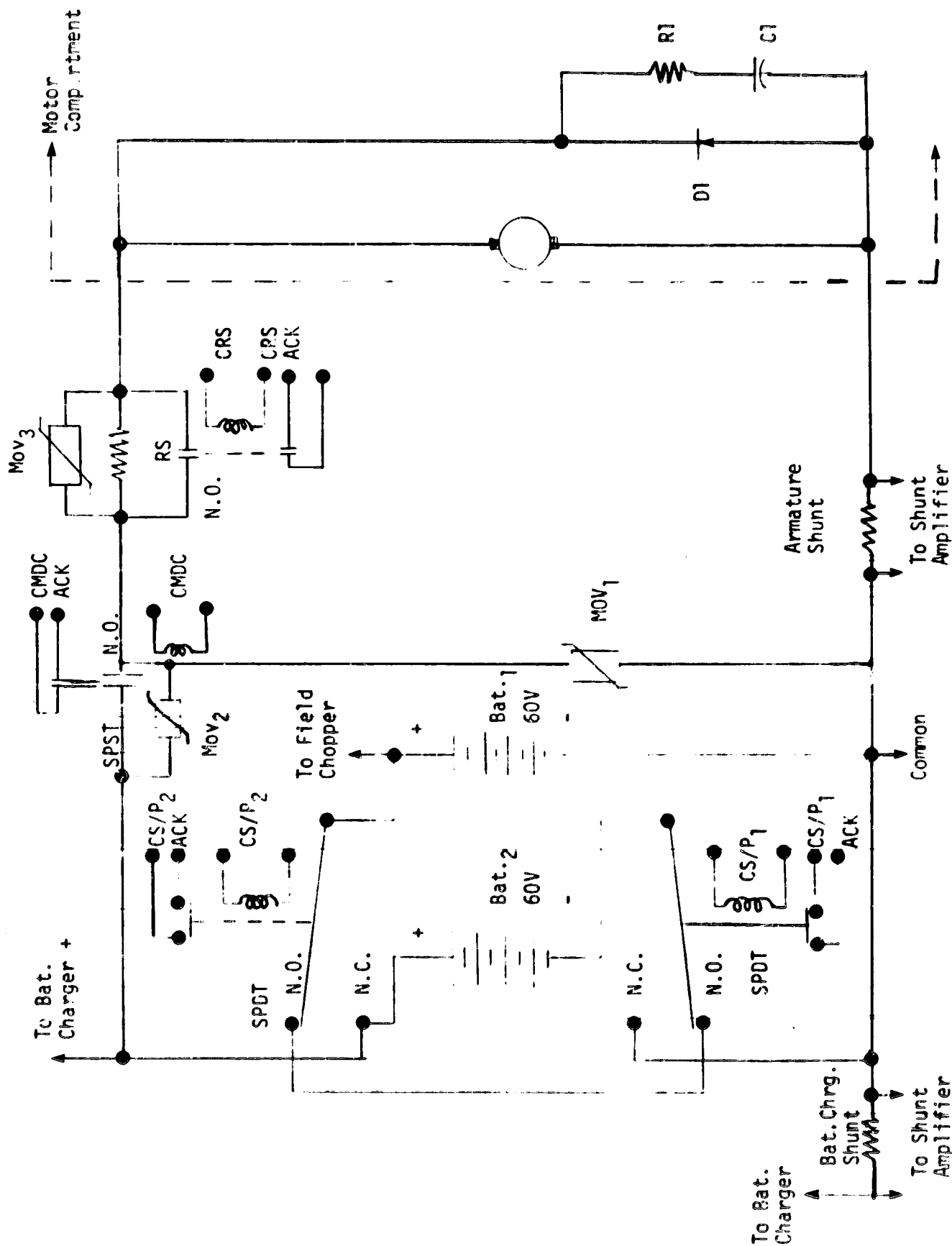
Figure IV-4. Battery Switching Circuit with Series Starting Resistor

along with current shunts and shunt amplifiers are packaged in a
single enclosure and mounted under the hood. Elevated tempera-
tures resulting from the heat engine are not expected to be crit-
ical because there is a minimal amount of electronics contained
in this enclosure

The preliminary design of the field chopper and battery charger
emphasizes high reliability and capability of large volume produc-
tion at low cost. To increase reliability and lower production
costs, circuit designs should include commercially available "off-
the-shelf" components that present moderate technical risks. In
addition, it is desirable to have modular designs that use acces-
sible packaging techniques to simplify debugging, maintenance, and
repair. Modular design, at both the function (board) level and
the sub-function level, reduces circuit development and design
time.

Figures IV-5 and IV-6 illustrate circuit block diagrams of
the field chopper and battery charger. Both functions are "chop-
per" type circuits implemented on single board modules and are
capable of sharing the development cost of several sub-functional
circuits. Table IV-4 illustrates the sub-functional similarities
and differences in the two modular designs.

The field chopper recommended in this preliminary design is
a Pulse Width Modulated (PWM) constant frequency chopper similar
in concept to that currently implemented in the DOE/GE Near-Term
Electric Vehicle. A digital PWM signal from the controller (after
current switch logic and amplification via VMOS base drive circuits)
commands the output power Darlington to turn "on" and "off." In
the event that the instantaneous field current exceeds a predeter-
mined level, the current logic inhibits "on" triggers and hence
turns off the power Darlington until the over current condition
is eliminated. This feature prevents possible damage to the power
Darlington in the event of high level noise, erroneous commands
from the controller, or a defective communication link between the
controller and the field chopper board.

Feedback to the controller concerning both the armature cur-
rent and the field current is used in the computation of the PWM
input command that provides the necessary field regulation and
motor speed control for the given conditions. Preliminary analysis
indicates that an off-the-shelf TRW SVT-6062 NPN power Darlington
(20 A cont., 450 V) is sufficient for the field chopper output
stage. Freewheeling diodes and snubber components prevent ex-
cessive voltage spikes during transistor switching.

Selection of a PWM input from the controller to the field
chopper simplifies and reduces the cost of the current logic, pro-
vides excellent noise immunity, and reduces backplane interface
hardware. All the logic functions of this field chopper are im-
plemented on a single PC board. The power Darlington is mounted
on an external, isolated heat sink. Additional packaging detail
is included in Section IV-4 of this report.

Figure IV-5. Field Chopper Block Diagram
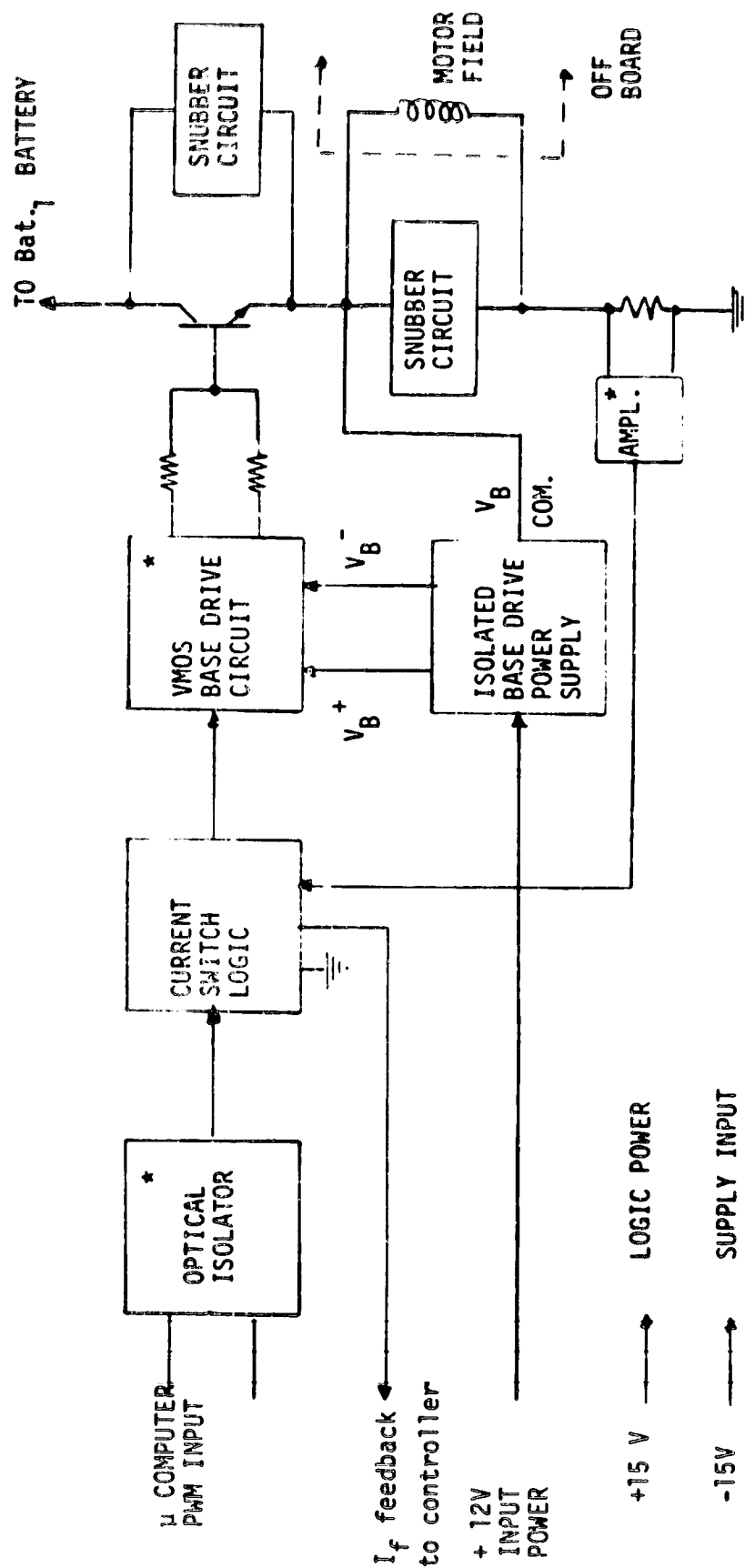
* IDENTICAL MODULE IN BATTERY CHARGER

Figure IV-6.   Battery Charger Block Diagram
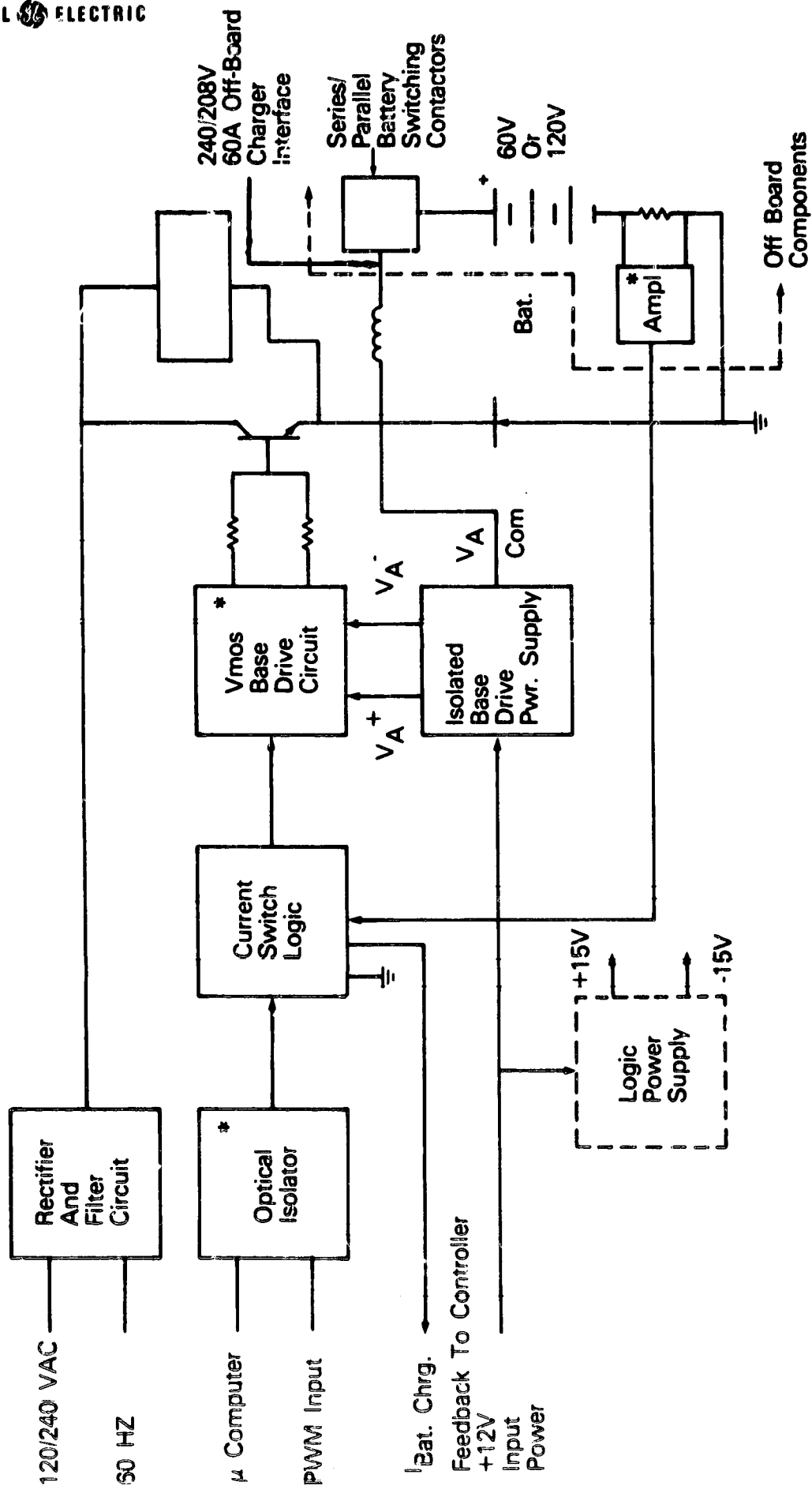
* Identical Module In Field Chopper
  Shared By Other Boards

□

Table IV-4

COMPARISON OF SIMILARITIES AND DIFFERENCES BETWEEN FIELD CHOPPER AND BATTERY CHARGER PRELIMINARY DESIGNS

Similarities	Differences	
	Field Chopper	Battery Charger
Power Darlington output stage microcomputer controlled	Medium power output ($10A_{avg}$, 53V)	High power output ($24A_{avg}$, 150V)
Pulse width modulated (PWM) optical isolation input	Battery input power	Rectified ac (60 Hz) input power
VBEC base drive circuit	Current switch logic (PWM constant frequency)	Current switch logic (peak current limited chopper)
Possibility of sharing common base drive dc-ac converter power supply		
Local on-board current protection		
Operation from same logic power supply		

Unique features of the battery charger for the HEV using battery switching armature control result in increased charging current capability from 120 V ac input power and elimination of the off-board charger.

This battery chopper operates on a "down chopper" technique that effectively supplies current to the battery during intervals when the instantaneous voltage of the full wave rectified input sine wave exceeds the voltage of the battery. When charging from 120 V ac input power, the batteries are configured in the parallel mode (60 V). In this condition, the battery charging duty factor exceeds 70%. In comparison to the battery charger of the Near-Term Electric Vehicle, this charger has improved on power factor and thus improved charging capability from 120-V input power.

Compared to the "on-board" charger, the "off-board" charger normally supplies more power from the ac line and thus it is capable of charging the batteries in a shorter time interval. It is assumed that a future HEV owner who desires a "fast charge" capability will have a 240-V service available. Common household 240-V circuits are 30 and 50 A. An electric clothes dryer is normally operated from a 30-A circuit, and an electric range typically operates from a 50-A circuit.

Assume that the battery charger output Darlington has average and peak current ratings capable of charging two parallel banks of batteries at 60 V from a 120-V, 30-A service. In this

case the maximum average transistor current is approximately twice
the average cell charging current. Also, assume that the voltage
rating of the output power Darlington is sufficient to operate from
240-V input power. For this charging scheme, when the control-
ler senses that 240 V input power is being supplied, it commands
the batteries to be switched to the series mode (120 nominal volts).
Based on the rating of the output power Darlington, and provided
a 240-V, 30-A service is available, the average charge current to
each battery is a factor of 4 greater than it would be with a 120-V,
15-A line, and a factor of 2 greater than it would be with a 120-V,
30-A line. (120-V, 30-A line is the maximum input power specified
for the Near-Term Electric Vehicle, ITV, Reference #2.)

The objective of this discussion is to illustrate that the
recommended battery charger/battery switching technique has the
flexibility to serve double duty as either a low rate or high rate
battery charger. Thus, it may not be necessary to provide an "off-
board" charger, although provision is made to interface with the
higher current off-board 240/208 V charger required by the RFP.
It should also be stressed that the cited example is based only
on the power limits of the output power Darlington and does not
imply that the maximum cell charging current necessarily should
be increased by a factor of 4 without consulting the battery
manufacturer.

For routine battery charging, the battery charger functions
as follows. A one-bit digital PWM input from the system controller,
after low pass filtering, is the battery charger current command.
This input command is compared to the battery charger current.
Current switching logic output, after amplification via the VMOS
base-drive circuit, appropriately pulses the power Darlington to
maintain the battery charger current at the level prescribed by
the system controller. Local current limit feedback protects the
power Darlington from excessive current. Appropriate PWM signals
from the system controller allow the charger to operate as a con-
stant current charger until a predetermined battery voltage limit
occurs. At this point the battery charger current is tapered ac-
cording to an algorithm stored within the system controller. When
the off-board charger is connected to the vehicle, the micropro-
cessor disconnects the on-board battery charger, connects the bat-
teries in the series mode, monitors the state of charge, and trans-
fers charging control to the off-board charger.

For equalization charging, the battery charger functions in
the following manner. Equalization charging is done at a low rate
for an extended time period to allow the state of charge of each
cell to equalize. During the equalization charge mode, the sys-
tem controller commands the batteries to be connected in series
(120 volt) and the charge current to be a specified value (several
amps). This assures that an identical charge current flows through
each cell of the total battery bank. The equalization charge mode
can operate from either 120-V or 240-V ac input power and is done
after the routine charge is completed.

Preliminary analysis indicates that an off-the-shelf Motorola MJ10016 power Darlington (50 A cont., 500 V) is sufficient for the battery charger. A freewheeling diode and an inductor allow stored current to flow into the battery during intervals when the power Darlington is off. All the logic, rectifier, and base drive hardware of the battery charger is implemented on a single PC board. The power Darlington is mounted on an external isolated heat sink. Additional packaging detail is included in Section IV-4 of this report.

The On-Board Charger Power Unit (OBCPU) consists of ac power contactors, Ground Fault Current Interrupters (GFCI), Electromagnetic Interference (EMI) filters, a 120/240 ac input sensor, and safety interlocks. This OBCPU is very similar to its counterpart in the DOE/GE Near-Term Electric Vehicle (ITV) and is often referred to as simply the "AC Box." This unit is packaged in the power contactor assembly and is mounted under the hood of the HEV.

IV.4 ELECTRONICS PACKAGE

Packaging objectives include high reliability, easy access to modular functions, and low cost for high volume production. Accessible packaging allows each function (normally a single board) to be removed independent of other functions. This feature simplifies initial debugging, maintenance, and repair.

Functional packaging, partitioning, and placement depend on interface requirements and the need for protection from extreme ambient temperatures. For example, the system controller (microcomputer) requires considerable operator/display interface. Mounting this controller within the passenger compartment protects the components from the extreme ambient temperatures of the engine compartment and simplifies operator interface. Table IV-5 and IV-6 summarize the functional partitioning. Sketches of the enclosure for the power contactor/starting resistor assembly and propulsion control electronic unit are illustrated in Figures IV-2 and IV-3, respectively, in Section IV.2. Figure IV-7 illustrates a preliminary sketch of board and component placement within the propulsion control electronic unit.

A commercial electronic chassis and backplane assembly is mounted within the enclosure. Access is provided from both end covers. Power Darlingtons are assumed to be mounted to an external isolated heat sink that is fastened to either a removable or hinged cover to provide access. Further thermal analysis is required to determine the heat sink dimension and/or volume of forced air required.

IV.5 SUMMARY

Preliminary designs of a battery switching circuit, field chopper, and battery charger functions for the Hybrid Electric Vehicle are presented in this Appendix. These preliminary designs

Table IV-5

PRELIMINARY HEV POWER
CONTACTOR/STARTING RESISTOR ASSEMBLY CONTENTS

- AC Charger Power Unit

    Ground Fault Current Interrupter, AC Contactor, Relay,
      EMI Filter

- Starting Power Resistors with Heat Shield

- DC Power Contactors

    Series/Parallel Battery Switching

    Main DC Power Disconnect Contactor

    Series Resistor Shunt Contactor

- Power Circuit Wiring and Current Shunts

Table IV-6

PRELIMINARY HEV PROPULSION CONTROL ELECTRONICS UNIT CONTENTS

- Field Chopper

    Printed Circuit (PC) Board

    Power Transistor

- Battery Charger

    Printed Circuit Board

    Power Transistor

- Electric Drive Control

    Microcomputer and Interface PC Board

- Logic Power Supply

    12 Volt Input Power

- One Spare Printed Circuit Board

strive to present a reliable electric motor control system that
has potential capability for high volume production at reasonable
costs. Packaging techniques presented simplify future debugging,
maintenance, and repair efforts.

CONTROL INTERFACE JACK

REMOVABLE OR HINGED COVER

CONTACTOR ASSEMBLY INTERFACE JACK

FIELD CHOPPER DARLINGTON

EXTERNAL ISOLATED HEAT SINK

BAT. CHARGER DARLINGTON

TERMINAL BLOCKS

TERMINAL BLOCKS

12"

LOGIC POWER SUPPLY

μ COMPUTER CONTROLLER BRD #1

μ COMPUTER CONTROLLER BRD #2

SPARE BOARD

FIELD CHOPPER

BATTERY CHARGER

COMMERCIAL CHASSIS
6-1.2" CENTER BRDS OR
11 .6" CENTER BRDS

HEIGHT ≈ 8"

9"

Figure IV-7. Preliminary HEV Propulsion Control Electronics Unit (Top View)

IV.8 APPENDIX IV REFERENCES

1. Producibility Analysis of Electrical Drive Subsystem for Near-
    Term Electric Vehicle, R.D. King, April 2, 1979, Section 4,
    Attachment E; Near-Term Hybrid Vehicle Program Phase I, Vol. 2,
    Deliverable Item 2, Contract No. 955190, General Electric
    Report SRD-79-075, June 8, 1979.

2. Near-Term Vehicle Phase II, Mid-Term Summary Report,
    Contract No. EY-76-C-03-1294, July 1, 1978.

Appendix V

RECENT HYVEC PROGRAM REFINEMENTS AND COMPUTER RESULTS

Appendix V

RECENT HYVEC PROGRAM REFINEMENTS AND COMPUTER RESULTS

V.1 HYVEC PROGRAM REFINEMENTS

As part of the Preliminary Design Task, a number of refinements were made in the HYVEC program to account for power train losses which were neglected in the previous studies and to include the effects of the heater/defroster and a cycling air conditioner. If waste heat from the engine was not sufficient to meet the heating needs, a gasoline burner was used to supply the difference. The additional power train losses included were the following:

- Engine and electric motor friction when either was in a stand-by state

- Transmission pumping losses

- Clutch slip losses

- Energy required to spin up the heat engine before it is turned on when the vehicle is in motion

The HYVEC program was also changed to permit maximum effort accelerations to be run for any specified battery state of discharge.

One of the advanced technology developments considered in the Preliminary Design Task was the continuously variable transmission (CVT). Subroutines were added to HYVEC to handle a CVT in place of the automatically shifted 4-speed gearbox. The CVT was described in terms of a maximum speed reduction ratio, RR, and a maximum overdrive ratio, ODR. Hence using the CVT, the torque input to driveshaft speed ratio can be varied continuously in the range

$$\frac{1}{ODR} \leq \frac{\omega_{input}}{\omega_{driveshaft}} \leq RR$$

With the CVT, the motor and/or engine can be operated at the speed required to attain maximum efficiency as long as the resultant gear ratio falls between the limits indicated and the motor speed is above its base speed. The operating line used for the heat engine (VW 1.6 ℓ gasoline) is given in Figure V-1, and the speed of the electric motor was maintained as close as possible to 1.25 x motor base speed regardless of load. If the required gear ratio is outside the range of the CVT, the gear ratio at the closest limit (RR or 1/ODR) is used. When both the engine and motor are needed to meet the power required, the power is split between the two prime movers in much the same manner as is done with the automatically shifted gearbox (i.e., nearly 50/50).
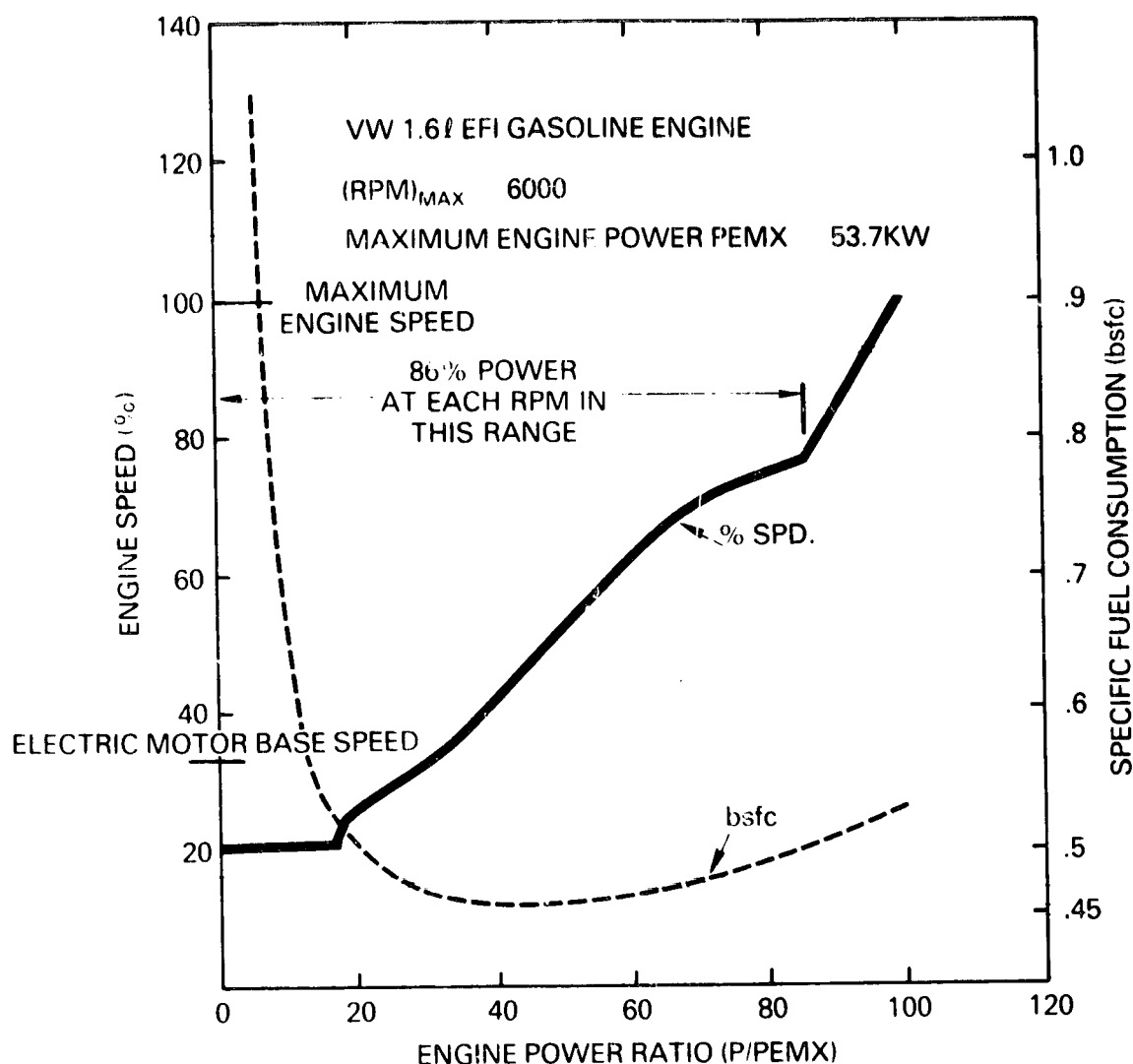
Figure V-1. Operating Line and Specific Fuel Consumption
for the Gasoline Engine Used with a CVT

V.2 HYVEC COMPUTER RESULTS

A number of HYVEC computer runs were made during the Preliminary Design Task. These runs were made to evaluate the effects of component and interface losses which were previously neglected, the influence of operating the heater/defroster and air conditioner, and the effect of changing gear ratios, electric motor rating, and vehicle weight on performance and fuel economy. In addition, the potential advantage of using a continuously variable transmission (CVT) in the hybrid power train, if one were available, was studied.

A summary of the results obtained in the first series of HYVEC runs which dealt with interface losses, accessories, gear ratios, etc., is given in Table V-1. It is clear from the table that the effect of the additional losses included in the refined HYVEC program are significant and reduce fuel economy by as much

Table V-1

SUMMARY OF THE INFLUENCE OF INTERFACE LOSSES, ACCESSORIES, GEAR RATIOS,
AND MOTOR RATING ON HYBRID VEHICLE PERFORMANCE

W_v = 1818 kg, K_p = .05 kW/kg, FE = .6

Gear[a] Ratios	Motor[b] Power Limit (%)	Trans. Pumping Losses	Motor Spinning in Standby	Engine Starting & Clutch Losses	Air[c] Conditioner	Heater/[d] Defroster	Acc. Time 0-100 km/hr Sec.	Fuel Economy (mpg) Urban After First Cycle	Urban After Ten Cycles	Highway
G2	100	N_	No	No	No	No	13.4	81.0	42.7	33.4
Gi	90	No	No	No	No	No	15.7	72.0	37.8	--
G1	90	Yes	No	No	No	No	15.9	70.9	37.0	33.4
G2	90	Yes	No	Yes	No	No	14.9	73.7	33.8	33.4
G3	90	Yes	No	Yes	No	No	14.9	74.2	33.8	33.4
G1	100	Yes	No	Yes	No	No	15.0	74.8	--	--
G1	90	Yes	Yes	No	No	No	15.9	70.2	34.9	33.0
G1	90	Yes	Yes	Yes	No	Yes	15.9	40.1	27.6	32.8
G1	90	Yes	No	Yes	No	Yes	15.9	40.3	28.7	--
G1	90	Yes	No	Yes	Yes	No	17.2	58.6	27.8	30.1

(a) Gear Ratios
   G1 - 2.84/1.6/1.0; AXR = 3.3
   G2 - 2.46/1.94/1.29/1.0; AXR = 3.3
   G3 - 2.84/1.6/1.0/.82; AXR = 4.0

(b) Motor power limit - percent of max. power from a 36 kW motor used.
(c) Air conditioner cycled on/off at 2 min intervals.
(d) Heat required 500 Btu/min corresponding to ambient temp. of 15°F.

as 15%. It is also clear from Table V-1 that when the heater/ defroster heat must be provided primarily by a gasoline burner, the effect on fuel economy is very large. For the example given in Table V-1, the urban fuel economy is reduced from 70 mpg to 40 mpg when 500 Btu/min is needed to heat the passenger compartment (ambient temperature 15 °F). The effect of operating the air conditioner is much less than that of the heater/defroster.

All the HYVEC runs discussed in the Design Trade-Off Studies Report were made using a 4-speed gearbox with gear ratios 3.46/ 1.94/1.29/1.0 in 1st, 2nd, 3rd, 4th gear, respectively. Those ratios are typical for manually shifted synchromesh gearboxes. In the hybrid power train, it is desirable to use a gearbox from an automatic transmission. Those gearboxes typically have only three gears with ratios 2.5/1.5/1.0. The gearbox from the new three-speed automatic transmission in the GM X-body cars has a slightly wider gear range - 2.84/1.6/1.0. That particular gearbox/ transaxle unit appears especially well-suited for the hybrid vehicle design. Hence a series of HYVEC runs were made to compare hybrid vehicle performance and fuel economy using several sets of gear ratios:

G1 : GM X-body Automatic

G2 : Baseline 4-speed manual

G3 : Borg-Warner 4-speed Automatic with overdrive

The results of the simulation runs are given in Table V-1. The effect on acceleration performance is about 1 sec in the 0-100 km/hr acceleration time, and the change in urban fuel economy is only about 5%. The effect on highway fuel economy is much less.

HYVEC runs were also made using a CVT in place of the 3- or 4-speed gearbox. The CVT characteristics used correspond to steel-belt units being developed by Borg-Warner. Those units are not likely to be available before 1985, but it was of interest to determine how they would affect the performance of a hybrid vehicle. The results of the HYVEC calculations for CVTs having overall speed ranges of 4:1 and 5:1 are given in Table V-2 and Figures V-2 and V-3. The use of the CVT yields both better acceleration times and greater fuel economy in urban and highway driving than the gearboxes having 3 or 4 discrete gear ratios. The primary advantage of the CVT is that the high torque of the electric motor near base speed can be better utilized both to attain better acceleration and to almost completely avoid the use of the heat engine at vehicle speeds below VMODE. As indicated in Figure V-2, the fuel economy advantage of using the CVT decreases rapidly for ranges greater than 25 to 30 miles. The CVT-equipped vehicles have a 0-100 km/hr acceleration time of about 1 to 2 seconds less than those using gearboxes for the same size motor and heat engine. Another important advantage of the CVT in a hybrid power train is that it avoids the system transients resulting from gear shifting. This would make control of the hybrid power train less difficult.

Table V-2

HYVEC RESULTS USING A CONTINUOUSLY VARIABLE TRANSMISSION IN THE HYBRID POWER TRAIN

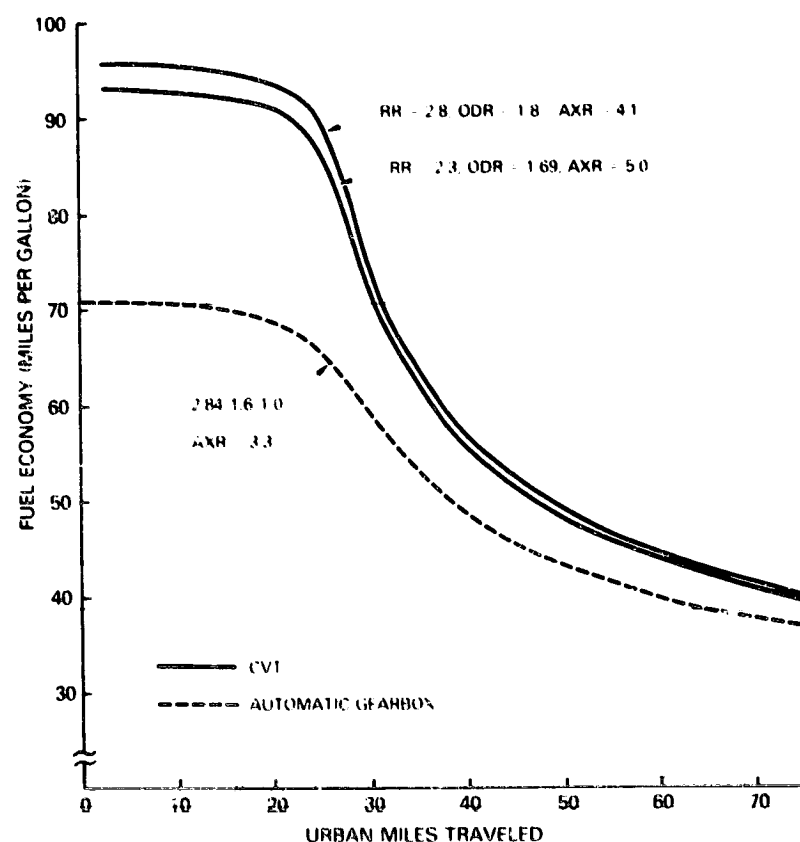| Type		Acceleration		Fuel Economy (mpg)		
				Urban		
		0-50 km/hr	0-100 km/hr	After First Cycle	After Ten Cycles	Highway
Autom. gearbox	Gear ratios: 2.84/1.6/1.0 AXR=3.3	5.4	15.9	70.9	37.0	33.4
Autom. gearbox	Gear ratios: 3.46/1.94/1.29/1.0 AXR=3.3	4.6	14.9	73.7	33.8	33.4
CVT	RR=2.8, ODR=1.8, AXR=4.1	4.5	13.7	95.9	40.3	35.7
CVT	RR=2.3, ODR=1.69 AXR=5.0	4.5	13.7	93.0	39.8	33.9

Figure V-2.   Fuel Economy Using a CVT in the
Hybrid Power Train

During the Preliminary Design Task, detailed discussions
were held with the General Electric DC Motor and Generator De-
partment concerning motor characteristics and with ESB Technology,
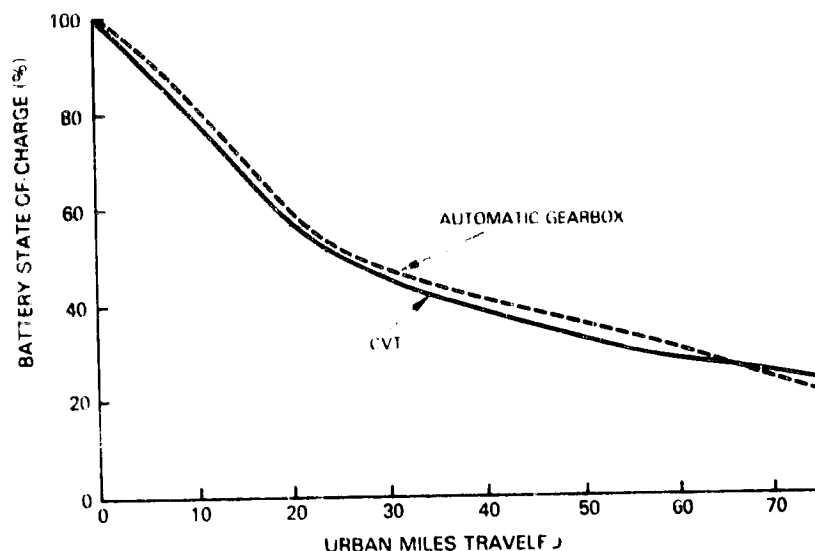
Figure V-3.   Effect of Transmission Type on
Battery State-of-Charge

and with Globe-Union concerning lead-acid battery characteristics.
In each case, inquiry was made as to whether components having
the characteristics assumed in the Design Trade-off Task could be
procured/developed by mid-1981. For both the motor and lead-acid
batteries, it was found that the projected component characteris-
tics were slightly optimistic. In the case of the dc motor, com-
puter design calculations by General Electric indicated that for
a rated horsepower of 24 using the same frame size as the DOE/GE
dc motor, the peak horsepower attainable was 44, which occurs at
a maximum armature current of 600 A. The design goal of 48 hp
could be met using a larger frame size, but the weight of that
motor would have significantly exceeded the 220 lb of the DOE/GE
motor. Based on these considerations, it was decided to reduce
the motor peak horsepower to 44 and use a motor based on a redesign
of the DOE/GE motor with which there was considerable experience.
In the case of the lead-acid batteries, both ESB and Globe-Union
(independently) found that within the volume, cell size, power,
and energy storage constraints of the hybrid vehicle design, the
battery weight would be 750-770 lbs rather than 700 lb used in
Task 2. The reason for this was that the energy density of the
smaller cells (105 AH compared with 170 AH in the electric vehicle
batteries) was about 16.5 Wh/lb rather than the projected value of
17.5 Wh/lb. This increased the hybrid vehicle weight by a corre-
sponding 50-70 lb.

In the HYVEC calculations made in Task 2, a vehicle curb
weight of 3700 lb (1682 Kg) was used. Detailed vehicle weight
studies by Triad Services indicated that a curb weight of 3860 lb,
including 700 lb of batteries, was more likely to result from the
Phase II program. Hence the vehicle curb weight was increased to
3930 lb to account for the increases in battery and chassis weight.
HYVEC calculations were made in Task 3 using the increased vehicle

weight and slightly lower peak electric motor power. In addition, the maximum rating of the heat engine was increased to 80 hp from 73 hp to bring it into agreement with the VW specification for the engine. The inputs for the new HYVEC calculations are:

W_V = 4230 lb (1923 Kg)

K_p = .048 kW/Kg.

FE = .645, FM = .355

The new results for acceleration times and the battery state of discharge, fuel economy, and emissions as a function of urban distance traveled are given in Figures V-4 to V-7. These values were used to update the vehicle specification and energy measure values given in Section 4, Tables 4-2 and 4-4. The present values of acceleration time and fuel economy are less optimistic than those given in reference 1, but it is felt the updated values are more realistic because they more accurately account for interface losses in the power train and for component and chassis characteristics which can be met in Phase II.
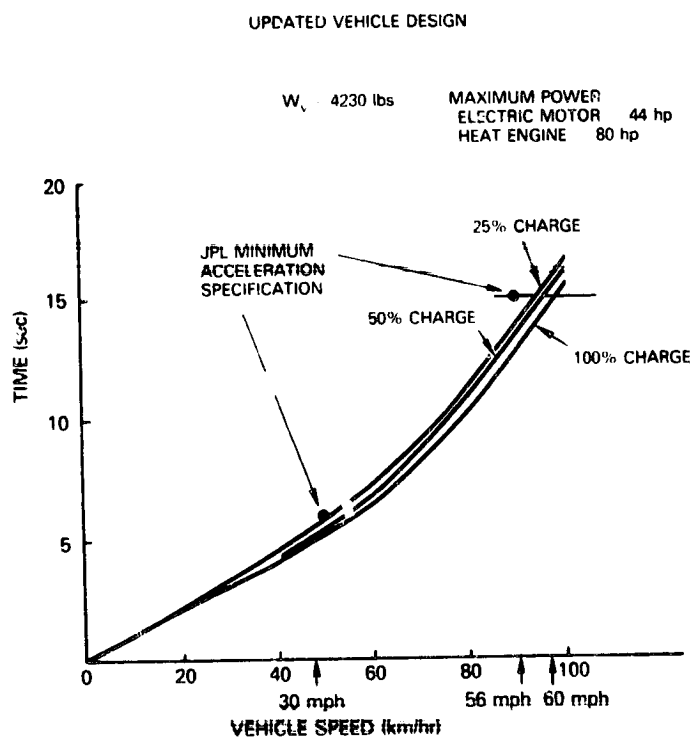
UPDATED VEHICLE DESIGN

Figure V-4. Hybrid Vehicle Acceleration Performance
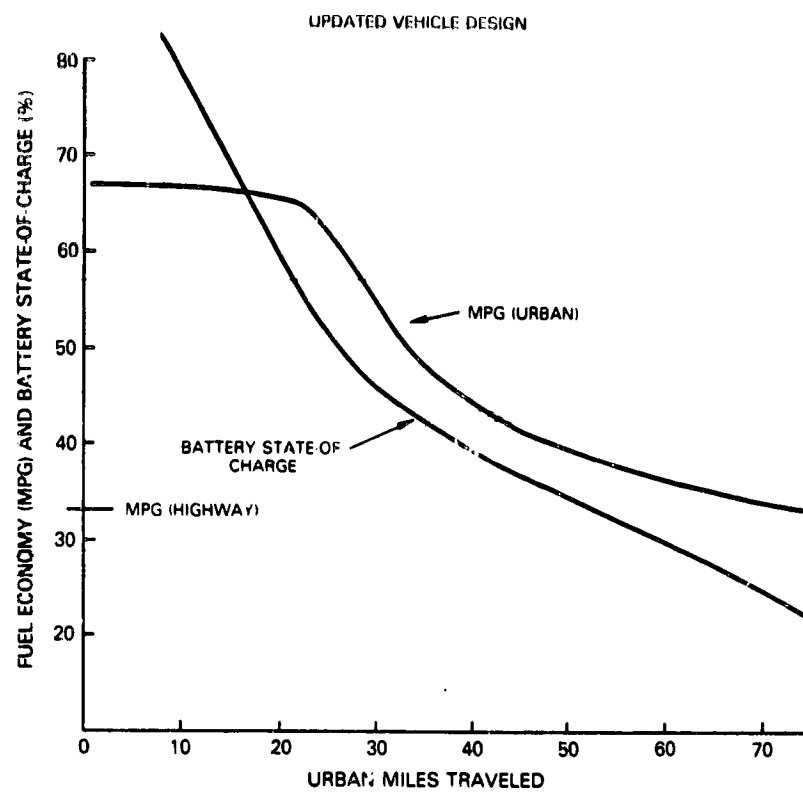
Figure V-5. Battery State-of-Charge and Fuel
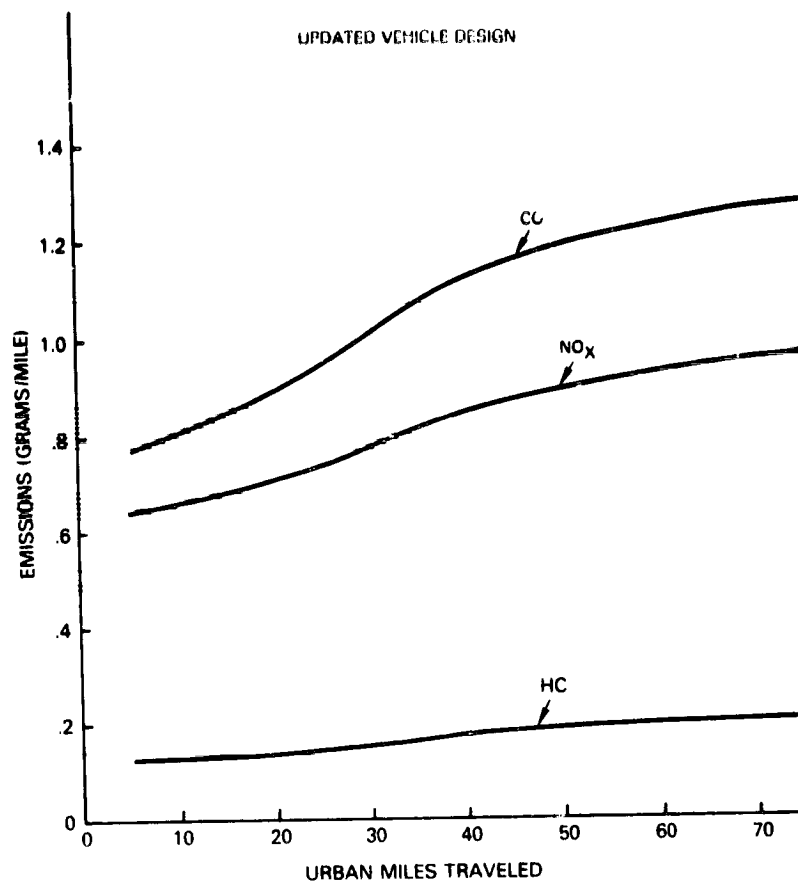Economy for Urban and Highway Driving

UPDATED VEHICLE DESIGN

Figure V-6. Hybrid Vehicle Emission Characteristics
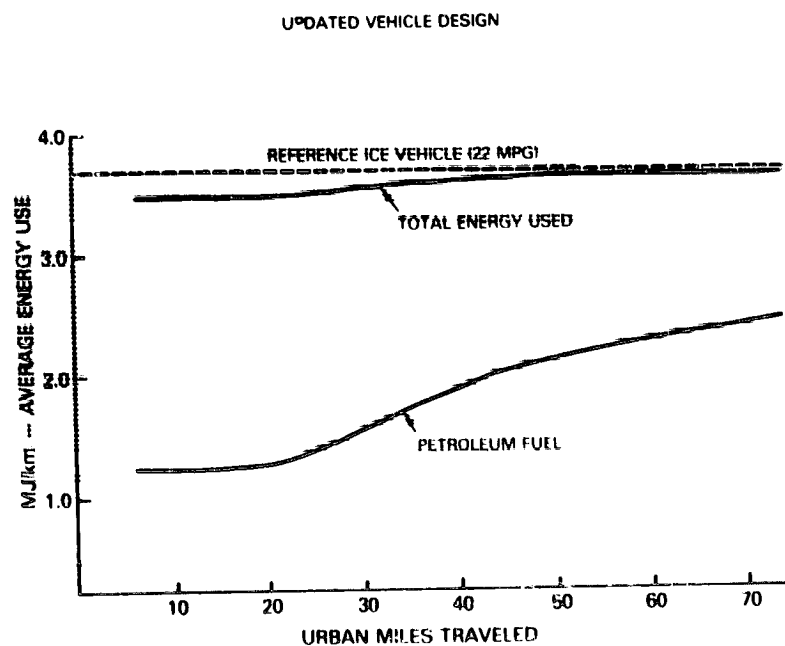
UPDATED VEHICLE DESIGN

Figure V-7. Total Energy and Petroleum Fuel
Usage in Urban Driving